

2020

Role of the schizophrenia-linked gene complement component 4 in prefrontal cortex function in mice

<https://hdl.handle.net/2144/42057>

"Downloaded from OpenBU. Boston University's institutional repository."

BOSTON UNIVERSITY

SCHOOL OF MEDICINE

Dissertation

**ROLE OF THE SCHIZOPHRENIA-LINKED GENE COMPLEMENT
COMPONENT 4 IN PREFRONTAL CORTEX FUNCTION IN MICE**

by

ASHLEY L. COMER

B.S., University of Houston, 2015

Submitted in partial fulfillment of the

requirements for the degree of

Doctor of Philosophy

2020

© 2020 by

ASHLEY COMER

All rights reserved except chapters 2-5 and 7 which are © 2020 *Plos Biology*, chapter 6 which is © 2020 *JoVE*, and chapter 1.4 which is © *Frontiers in Cellular Neuroscience (In Press)* which are all under CC-BY license terms with freedom to copy, adapt and redistribute freely with appropriate credit.

Approved by

First Reader

Alberto Cruz-Martín, Ph.D.
Assistant Professor of Biology

Second Reader

Ian Davison, Ph.D.
Associate Professor of Biology

Third Reader

Tsuneya Ikezu, M.D./Ph.D.
Professor of Pharmacology and Experimental Therapeutics

ACKNOWLEDGMENTS

I would like to recognize the invaluable people that provided assistance, mentorship and support during my graduate education. I owe it to each of you that my research endeavors and scientific training were as productive and well-rounded as they were and that I experienced as much personal growth as I did during this journey. I am forever grateful to everyone that made this undertaking more manageable and memorable.

Much thanks to my advisor, Alberto Cruz-Martín, who allowed me to explore novel scientific questions and embark on a topic that was uncharted territory for both of us. Alberto's enthusiasm for science and dedication to constantly thinking about big picture questions really helped us establish this line of research and enabled us to tackle any road blocks in our research. Thank you for teaching me to think strategically about science.

I would like to thank my other dissertation advisory committee members including Ian Davison, Angela Ho, Michael Hasselmo, Tsyuneya Ikezu, and Dorothy Schafer. Thank you all for the additional mentorship, stimulating conversations about science and for helping me navigate my graduate career. Your words of wisdom and encouragement helped me grow in many ways.

A special thank you to Lisa Kretsge, who helped keep the day-to-day life as a graduate student light-hearted, hilarious and truly enjoyable. Thank you for being such a

great friend and colleague. I am grateful for all of our conversations about science and your valuable input and contributions to this research.

Thank you to all current and former Cruz-Martín lab members and to all of our collaborators including:

My side-kick, Thanh Nguyen, who as an undergraduate research assistant in the lab helped get this research project off the ground and made significant contributions such as performing surgeries and helping with confocal and two-photon imaging experiments. William Yen, an impressive biomedical engineering undergraduate student, who built the lab's two-photon microscope and electroporator and who was an excellent lab manager after graduating. Our postdoctoral fellow Tushare Jinadasa for performing electrophysiological experiments, and to Rushikesh Phadake, Tushare Jinadasa and Yenyu Liu for their contributions to molecular biology and expansion microscopy experiments. Connor Johnson, our current lab manager. All of the lab's undergraduate research assistants, who always impressed me with their thoughtful questions and dedication to science. Jungjoon Lee, Elena Newmark, Frances Hausmann, SaraAnn Rosenthal, and Kevin Liu Kot were a joy to work with and made significant contributions to this work as undergraduates. Giovanna Antognetti and James P. Gilbert for the successful production of an antibody against C4 and for the helpful scientific conversations. Borislav Dejanovic for testing the C4 antibody and for showing that C4 is enriched at synapses when overexpressed- this was a vital piece of evidence in this story; also thank you for stimulating conversations about complement proteins and for useful

feedback on multiple manuscripts. Balaji Sriram for helping analyze behavioral data. Marie-Ève Tremblay and Micaël Carrier for an in progress collaborative project using electron microscopy to observe microglia-neuron interactions with nanoscale resolution and for collaboration on a review paper. Thomas Gilmore for feedback on our manuscripts and helpful conversations about the molecular mechanisms of C4.

Thanks to the Graduate Program for Neuroscience, including Shelley Russek, Sandra Grasso and Nazifa Haque. A special thank you to Shelley Russek who helped me navigate my graduate career and maintain motivation throughout graduate school. Thanks to the Center for Systems Neuroscience directed by Michael Hasselmo. Thanks to both the Biology Department and the Neurophotonics Program including Kim McCall, Helen Fawcett and David Boas.

Thank you to my family for their unyielding support, love and words of wisdom. I'd like to thank my parents, Laura and David Comer, for always encouraging me to carry on and stay strong, and for bringing so much joy to my life even in the challenging moments. I'd like to thank my brother, Austin Comer not only for his scientific advice such as helping me troubleshoot PCR experiments, but also for being one of my best friends. I am grateful for all the times Austin Comer and Taylor Garcia ran practice presentations with me and gave useful feedback. A special thank you to my aunt, Lisa Cherry, for always being a phone call away with motivating words and support. A special thank you to Caitlin Sears, April Frazier, and Jennifer Chittenden for all the happy memories and supportive conversations.

Thanks to all of my dear friends for all the laughter and support during my graduate career. Hana Yeh, Trish Shaw and Sam Shelton made first-year coursework more manageable and were such supportive and compassionate friends from day one of graduate school, thank you for all the great memories. Thank you Sara Erkal for always listening with an empathetic ear and for being such a tough, inspiring feminist and dear friend. A special thanks to Lydia Jeppsen for much needed relaxing yoga dates, Madhura Baxi for the movie nights in with homemade pasta, Margaret Minning for all the coffee dates and Janis Intoy who introduced me to triathlons. I also couldn't imagine graduate school without all the memories made with William Liberti, Adam Vogel and the entire GPN community.

**ROLE OF THE SCHIZOPHRENIA-LINKED GENE COMPLEMENT
COMPONENT 4 IN PREFRONTAL CORTEX FUNCTION IN MICE**

ASHLEY COMER

Boston University School of Medicine, 2020

Major Professor: Alberto Cruz-Martín, Ph.D., Assistant Professor of Biology

ABSTRACT

Schizophrenia is a devastating mental illness characterized by a broad range of clinical manifestations including hallucinations, social cognitive impairments, and disordered thinking and behavior, all of which impair daily functioning. The immune molecule complement component 4 (C4), located in the major histocompatibility locus (MHC) on chromosome 6 in humans, is highly associated with schizophrenia such that specific structural variants and regulatory regions increase the expression of C4 and confer greater risk for this brain disorder. Besides their established role in brain immune defense, complement proteins play a role in various stages of brain development including neurogenesis, migration and synaptic development. However, C4 has never been experimentally upregulated to determine the impact of increased expression of this immune gene on brain development. Here, I study the role of C4 in layer 2/3 pyramidal neurons in the medial prefrontal cortex of mice to study the hypothesis that C4 overexpression causes circuit dysfunction by leading to the pathological elimination of

synapses. Specifically, neuronal connectivity was assayed by measuring dendritic spine density using confocal microscopy and functional connectivity through whole-cell electrophysiology recordings. Additionally, the role of microglia in altering the developmental wiring of the brain was examined by quantifying microglia engulfment in the medial prefrontal cortex. Lastly, complement-induced changes to the prefrontal cortex were accompanied by deficits in social behavior in both juvenile and adult mice. Overall, these studies show that C4 affects brain connectivity by reducing dendritic spine density and excitatory drive through enhanced microglia-engulfment of synaptic material which was sufficient to cause lasting deficits in mouse social behavior.

TABLE OF CONTENTS

ACKNOWLEDGMENTS.....	iv
ABSTRACT.....	viii
TABLE OF CONTENTS.....	x
LIST OF TABLES.....	xvi
LIST OF FIGURES.....	xvii
LIST OF ABBREVIATIONS.....	xx
CHAPTER ONE: Introduction to the pathology and etiology of schizophrenia.....	1
1.1 Clinical features and neuropathology in schizophrenia.....	1
1.2 Major histocompatibility molecules genetically associate with schizophrenia.....	5
1.3 The complement cascade.....	6
1.4 The inflamed brain in schizophrenia: the convergence of genetic and environmental risk factors that lead to uncontrolled neuroinflammation.....	10
1.4.1 Introduction.....	10
1.4.2 Genetic risk factors for schizophrenia that interplay with immunological responses.....	12

1.4.3 Exposure to pollution increases risk for schizophrenia by enhancing inflammatory responses.....	18
1.4.4 The gut-brain axis in schizophrenia.....	22
1.4.5 Maternal immune activation enhances risk for schizophrenia by altering microglia function.....	28
1.4.6 Stress-induced inflammation.....	35
1.4.7 How the peripheral immune system gains access to the CNS in schizophrenia.....	41
1.4.8 Future directions for understanding and targeting the immune system in schizophrenia.....	47
1.5 Linking complement proteins to aberrant circuit development in schizophrenia.....	58
CHAPTER TWO: Materials and methods.....	60
2.1 Ethics statement.....	60
2.2 Animals.....	60
2.3 DNA constructs.....	60
2.4 Antibodies and histology.....	61
2.5 <i>In utero</i> electroporation.....	63
2.6 Imaging.....	64

2.7 Multiples fluorescence <i>in situ</i> hybridization.....	66
2.8 Quantitative polymerase chain reaction.....	67
2.9 Cell culture.....	68
2.10 Isolation of post-synaptic densities.....	69
2.11 Immunoblotting.....	70
2.12 Dendritic spine analysis.....	70
2.13 Electrophysiological recordings and analysis.....	72
2.14 Neuronal morphology analysis.....	74
2.15 Microglial assays.....	75
2.16 Expansion microscopy.....	78
2.17 Maternal interaction task.....	80
2.18 Adult behavior.....	81
2.19 Quantification of transfected cells in behavior brains.....	83
2.20 Statistical analysis.....	84
CHAPTER THREE: Overexpression of C4 and its impact on prefrontal cortex	
development.....	86
3.1 Introduction.....	86

3.2 Results.....	86
3.2.1 Endogenous expression of C4 in the mouse prefrontal cortex.....	86
3.2.2 <i>In utero</i> electroporation is a viable method to increase C4 expression.....	89
3.2.3 C4 overexpression alters developmental synaptic connectivity.....	96
3.2.4 C4 overexpression reduces the functional connectivity of cortical neurons.....	99
3.2.5 Overexpression of mC4 decreased membrane capacitance without altering overall excitability.....	102
3.3 Conclusion and future directions.....	107
CHAPTER FOUR: The role of microglia in C4-induced prefrontal cortical dysfunction.....	
4.1 Introduction.....	110
4.2 Results.....	110
4.2.1 C4 overexpression enhances microglia-neuron interactions during development.....	111
4.2.2 C4 overexpression enhances microglia engulfment of post-synaptic material.....	114

4.2.3 Microglia phagocytose more material in superficial layers of the cortex.....	119
4.2.4 Expansion microscopy confirms that C4 overexpression enhanced microglia-mediated engulfment of synaptic material.....	120
4.3 Conclusion and future directions.....	126
CHAPTER FIVE: Effects of C4 overexpression on mouse behavior across development.....	128
5.1 Introduction.....	128
5.2 Results.....	128
5.2.1 Bilateral <i>in utero</i> electroporation reliably transfects L2/3 excitatory neurons in the frontal cortex.....	129
5.2.2 Complement-dependent alterations in frontal cortical circuitry are sufficient to alter maternal-pup social interactions.....	131
5.2.3 Complement-dependent alterations in social behaviors persist into adulthood.....	134
5.3 Conclusion and future directions.....	139
CHAPTER SIX: A pipeline to study the effect of schizophrenia-associated genes on mouse behavior throughout development.....	140

6.1 Introduction.....	140
6.2 Protocol.....	143
6.2.1 Advance preparation for <i>in utero</i> electroporation.....	143
6.2.2 Surgery preparation and <i>in utero</i> electroporation procedure.....	146
6.2.3 Assaying early and adult social behavior.....	148
6.2.4 Post hoc cell counting to characterize extent of cell transfection.....	151
6.3 Results.....	152
6.3.1 Successful development and implementation of a custom-built electroporator and triple electrode.....	153
6.3.2 Targeting a large population of neurons bilaterally in the frontal cortex of mice.....	154
6.3.3 Social behavior in juvenile and adult mice.....	154
6.4 Discussion.....	156
CHAPTER SEVEN: Concluding remarks and future directions.....	159
BIBLIOGRAPHY.....	170
CURRICULUM VITAE.....	224

LIST OF TABLES

Table 2.1: Antibody table.....	62
Table 2.2: Primers used in cloning and PCR experiments.....	68

LIST OF FIGURES

Figure 1.1: The complement cascade in pathogen recognition and phagocytosis.....	7
Figure 1.2: Overview of the overlap between immune-signaling genes that are altered from pollution and in schizophrenia.....	19
Figure 1.3: Summary of the pathogenic mechanisms of schizophrenia covered in this chapter, which involve microglial alteration induced by neuroinflammation.....	51
Figure 3.1: IUE increased amount of mC4 transcript in neurons.....	87
Figure 3.2: C4 expression is enriched in excitatory neurons.....	89
Figure 3.3: mC4 is expressed in neurons of the medial prefrontal cortex and can be overexpressed using <i>in utero</i> electroporation.....	91
Figure 3.4: PSD synaptosome isolation from PFC tissue.....	93
Figure 3.5: mC4-GFP protein is expressed in transfected HEK cells and L2/3 neurons.....	95
Figure 3.6: C4 overexpression led to dendritic spine alterations in apical arbors of L2/3.....	97
Figure 3.7: C4 overexpression reduced functional connectivity in cortical neurons.....	100
Figure 3.8: Overexpression of mC4 decreased membrane capacitance without altering overall excitability.....	103
Figure 3.9: Overexpression of mC4 did not alter soma size or proximal dendrite width.....	105
Figure 3.10: Dendrite morphology was not altered by mC4 overexpression at P21 ...	106

Figure 4.1: Microglia were in closer proximity to neurons overexpressing mC4 at P21.....	112
Figure 4.2: Microglia density and lysosome size were not altered by mC4 overexpression.....	114
Figure 4.3: Intrabodies against PSD95 label excitatory synapses of L2/3 pyramidal neurons.....	116
Figure 4.4: mC4 overexpression enhanced microglia engulfment of postsynaptic PSD-95.....	118
Figure 4.5: Expansion microscopy (ExM) expanded microglia by ~2.8x.....	121
Figure 4.6: Expansion microscopy confirmed C4 overexpression led to enhanced microglial engulfment of PSD-95.....	123
Figure 4.7: ExM revealed that neuronal mC4 overexpression increased the number of PSD-95+ lysosomes in microglia.....	125
Figure 5.1: Targeting large populations of L2/3 frontal cortex neurons using IUE.....	130
Figure 5.2: C4-dependent alterations in frontal cortical circuitry were sufficient to alter maternal-pup social interactions.....	132
Figure 5.3: mC4 pups had increased grooming occurrences and grooming time compared to controls.....	134
Figure 5.4: C4-dependent alterations in frontal cortical circuitry led to behavior deficits in sociability that persist into adulthood.....	136
Figure 5.5: Adult mice bilaterally expressing mC4 had intact motor abilities.....	138

Figure 6.1: *In utero* electroporation using a custom-built electroporator and a three prong electrode.....154

LIST OF ABBREVIATIONS

AP.....	action potential
ASD.....	autism spectrum disorder
BBB.....	blood-brain barrier
C1q.....	complement component 1 subunit q
C3.....	complement component 3
C4.....	complement component 4
C4 KO.....	C4b knock-out
CaMKII α	calcium/calmodulin-dependent protein kinase type II subunit alpha
CD.....	cluster of differentiation
CDH5.....	cadherin-5
CNS.....	central nervous system
CR3.....	complement component 3 receptor
CRP.....	C-reactive protein
CSF-1R.....	colony stimulating factor 1 receptor
CSMD.....	CUB and sushi multiple domain
DI.....	discrimination index
DISC1.....	Disrupted-in-Schizophrenia 1
E.....	embryonic day
ELS.....	early life stress
ExM.....	expansion microscopy
EZM.....	elevated-zero maze

GABA.....gamma aminobutyric acid

GFP.....green fluorescent protein

GI.....gastrointestinal

GWAS.....genome-wide association study

hC4.....human C4

HEK.....human epithelial kidney

HPA axis.....hypothalamic-pituitary-adrenal axis

Iba1.....ionized calcium binding adaptor molecule 1

IEI.....interevent interval

IFN- γinterferon gamma

IL.....interleukin

IRF3.....interferon regulatory factor 3

IUE.....*in utero* electroporation

L.....layer

LPS.....lipopolysaccharides

mC4.....mouse C4

mEPSC.....miniature excitatory postsynaptic current

mg.....microglia

MIA.....maternal immune activation

mIPSC.....miniature inhibitory postsynaptic current

M-FISH.....multiplex fluorescent *in situ* hybridization

MHC.....major histocompatibility complex

MI1.....	maternal interaction task 1
MI2.....	maternal interaction task 2
mPFC.....	medial prefrontal cortex
NDD.....	neurodevelopmental disorder
NMDAR.....	<i>N</i> -methyl-D-aspartate receptor
nPM.....	nanoparticulate matter
OCLN.....	occludin
OF.....	open field
P.....	postnatal day
PFC.....	prefrontal cortex
poly(I:C).....	polyinosinic:polycytidylic acid
PPAR γ	peroxisome proliferator-activated receptor gamma
PSD.....	postsynaptic density
qPCR.....	quantitative PCR
RFP.....	red fluorescent protein
SCFAs.....	short-chain fatty acids
SCZ.....	schizophrenia
TGF.....	transforming growth factor
TIB.....	total integrated brightness
TLR.....	toll-like receptor
TNF.....	tumor necrosis factor
TRAP.....	traffic-related air pollution

TSPO.....translocator protein

CHAPTER ONE

Introduction to the pathology and etiology of schizophrenia

1.1 Clinical features and neuropathology in schizophrenia

Schizophrenia (SCZ) is a chronic developmental disorder that affects more than 21 million people worldwide (Kessler et al. 2010). SCZ is usually diagnosed in adolescence or early adulthood when prefrontal cortex (PFC) networks mature and individuals experience their first episode of psychosis. Almost all cases of this disorder are both chronic and progressive yielding a grim prognosis for diagnosed individuals (Zhang et al. 2005). Ten years after initial diagnosis, fifty percent of affected individuals are unable to live independently, fifteen percent are hospitalized and ten percent die of suicide (World Health Organization 2017). It is clear that this disease is genetic- a monozygotic twin of an affected individual has a 50% chance of developing SCZ, compared to an occurrence of only 1-2% in the general population (Gottesman & Shields 1976). Scientists have focused on understanding deletions of larger sections of DNA that have been found to be disrupted or deleted in a subset of SCZ cases, yet these sort of studies yield limited success in identifying specific genetic links to SCZ (Kim et al. 2011, Sigurdsson et al. 2010). A limited understanding of the pathogenesis of SCZ has stunted the development of more effective treatments, leaving many affected individuals chronically hospitalized or homeless. More basic research of the underlying pathogenesis in SCZ must be conducted so that novel treatments can be developed.

Individuals afflicted with SCZ experience symptoms that can be categorized into three clusters: positive, negative and cognitive symptoms. Positive symptoms include psychosis, paranoia, and disordered thought (American Psychiatric Association 2013). Negative symptoms include depression, anhedonia, suppressed speech and social withdraw (Lieberman et al. 2005). Cognitive symptoms include a wide range of deficits in social cognition, working memory, attention, and executive function that together leads to a decreased ability to comprehend and manage information to guide thought and decision making (Ellevåg & Goldberg 2000, Piskulic et al. 2007). Treatment of SCZ usually relies on symptom management, such as antipsychotic medication to treat psychosis. However, treating symptoms does nothing to help cure the underlying disease, and patients are frequently not compliant with medication regiments (American Psychiatric Association 2013, Green 2006). Cognitive impairments, including social deficits, are the most common predictor of prognosis, including employment status, relapse and living dependence, but there are currently no available treatments that effectively target cognitive symptoms (Ellevåg & Goldberg 2000, Green 2006).

Among the many clinical traits of SCZ are deficits in social cognition such as social cue perception and emotion regulation, which suggest dysfunction of the PFC (Green 2006). Moreover, patients with SCZ exhibit abnormal activity in the PFC during affective face perception and cognitive reappraisal (Morris et al. 2012, Taylor et al. 2012, Delvecchio et al. 2013). These results are not surprising given the well-established role of the PFC in social behaviors (Yizhar 2012, Grossmann 2013, Vita

et al. 2012). Although the mechanisms that cause social deficits in SCZ are unclear, evidence suggests that dysfunction in the PFC correlates with symptom onset and severity (Vita et al. 2012). In fact, a neurological hallmark of SCZ is a reduction of gray matter in the PFC due to a loss of neuronal processes and synapses (Glantz & Lewis 2000, Thompson et al. 2001). Therefore, it has been hypothesized that pathology in SCZ arises in part due to deficits in the pruning of cortical synapses, thus producing aberrant circuitry (Glantz & Lewis 2000, Thompson et al. 2001).

In line with this, current research suggests that deficits in neuronal connectivity and plasticity, present across multiple brain areas, underlies the diverse disruptions in information processing and cognition (Glausier & Lewis 2013, Glantz & Lewis 2000). Individuals diagnosed with SCZ have decreased cortical volumes prior to, during and after the first episode of psychosis when compared to age and sex-matched healthy samples (Lawrie & Abukmeil 1998, Steen et al. 2006, Levitt et al. 2010). This loss in brain matter is progressive with the most significant losses found in gray matter neuropil, consisting of dendrites and spines, of the prefrontal and temporal cortices (Dazzan et al. 2012, Giedd & Rapoport 2010, McIntosh et al. 2011). Interestingly, the density of cortical neurons is unchanged in these brain regions despite the loss of gray matter (Thune et al. 2001), suggesting a decrease in synaptic density and/or dendritic branching (Glausier & Lewis 2013, Selemon & Goldman-Rakic 1999, Glantz & Lewis 1997). Importantly, these changes in brain structure can be detected in humans before the first episode of psychosis, before patients have begun taking antipsychotic medications, which are known to alter

brain connectivity (Anticevic et al. 2015).

The over pruning of synapses has been suggested to alter multiple neurotransmitters including glutamate and dopamine, with suspected links to a disrupted immune system. The loss of gray matter observed in human SCZ post mortem tissue correlates with a loss of excitatory synapses therefore leading to a decrease in glutamatergic transmission (Bustillo et al. 2014, Glantz and Lewis 1997). Moreover, glutamate levels in the PFC negatively correlated with psychotic symptoms such that greater decreases in glutamate levels were found in SCZ cases with more severe psychotic symptoms (Bustillo et al. 2014). Additionally, inflammatory abnormalities, such as increased expression of SERPINA3, TNF α , IL1 β , IL6, and IL6ST, have been observed in the ventral midbrain in post mortem SCZ tissue, and these results were also replicated in a maternal immune activation (MIA) mouse model (Purves-Tyson et al. 2019). Importantly, these differences in immune markers from SCZ tissue could be accounted for by a subset of cases, including about 45% of high inflammatory cases. The ventral midbrain houses the majority of dopamine-releasing neurons in the brain, therefore MIA might contribute to SCZ pathology by disrupting immune-mediated wiring of dopaminergic circuits (Purves-Tyson et al. 2019). These findings are important because they link SCZ-associated neuroinflammation to dopaminergic abnormalities, which is a hallmark of this disorder.

Alterations in the brain structure of individuals diagnosed with SCZ are accompanied by physiological abnormalities that can be detected with functional

magnetic resonance imaging and electroencephalogram recordings (Volk & Lewis 2010, Cho et al. 2006). Although antipsychotics do help 25% of diagnosed patients (Kessler et al. 2010), current clinical options are limited. Sadly, the majority of individuals diagnosed with SCZ are not able to function as independent members of society with currently available treatments. Thus, there is a tremendous need to develop new treatments. To do this, we must understand how these diverse neurological hallmarks arise based on genetic and environmental risk factors.

1.2 Major histocompatibility molecules genetically associate with schizophrenia

Recent genetic studies have provided insight that enable a greater understanding of the underlying pathology in SCZ and could ultimately lead to novel, more effective therapeutic interventions. Genetic studies conducted using human tissue show that the strongest genetic association to SCZ is contained in a region on chromosome 6 known as the major histocompatibility complex, or MHC locus (Shi et al. 2009, International Schizophrenia Consortium 2009, Ripke et al. 2013, Stefansson et al. 2009, Schizophrenia working group of the Psychiatric Genomics Consortium 2014). The MHC locus encodes genes that are involved in the recognition and elimination of pathogens. However, the MHC locus contains megabases of DNA, including over 200 genes, complicating the identification of candidate genes that could be important in the pathogenesis of SCZ (Carroll et al. 1984, Horton et al. 2004).

A recent study focused on a single gene from the MHC locus, called complement component 4 (C4), because it has a strong association to SCZ in both its coding region

and regulatory regions (Sekar et al. 2016). C4 is a member of a larger family of proteins called the complement cascade family, which are important in the recognition and destruction of pathogens using nonspecific yet rapid defense mechanisms, referred to as innate immunity (Carroll et al. 1984). Human C4 contains two distinct genes, or isotypes, C4A and C4B (Carroll et al. 1984). C4A has been shown to strongly bind protein-antigen complexes, whereas C4B more effectively binds antibody-coated red blood cells to tag pathogens for destruction by macrophages (Law et al. 1984). Importantly, alleles for C4 that generate greater protein expression correlate with increased risk of developing SCZ; C4A expression correlates with 1.4 times the odds risk for SCZ (Sekar et al. 2016). Since complement proteins have previously been studied in the context of immunity, new research has been aimed at understanding alternative roles for this protein in the brain to understand its implication in SCZ.

1.3 The complement cascade

The complement cascade protein family is an intricate network of over 50 membrane-bound and circulating proteins that serve as the first-line of defense against pathogens in innate immune responses. The complement system is divided into 3 proteolytic pathways: the classical pathway, the lectin pathway and the alternative pathway (Morgan & Gasque 1997). When initiated, one or more of these pathways are activated *via* a series of proteolytic cleavages that stimulates either engulfment of the invader material by macrophages, known as phagocytosis, or membrane destruction *via* a

cell-killing complex called the membrane attack complex (Morgan & Gasque 1997). In the classical pathway, complement component 1q (C1q) initiates the classical cascade by recognizing and binding to a pathogen which causes a proteolytic cascade that activates the cleavage of complement component 3 (C3) (Morgan & Gasque 1997). Cleaved C3 (C3b) is then recognized by C3 receptors (CR3) on macrophages, which initiate phagocytosis (Figure 1.1).

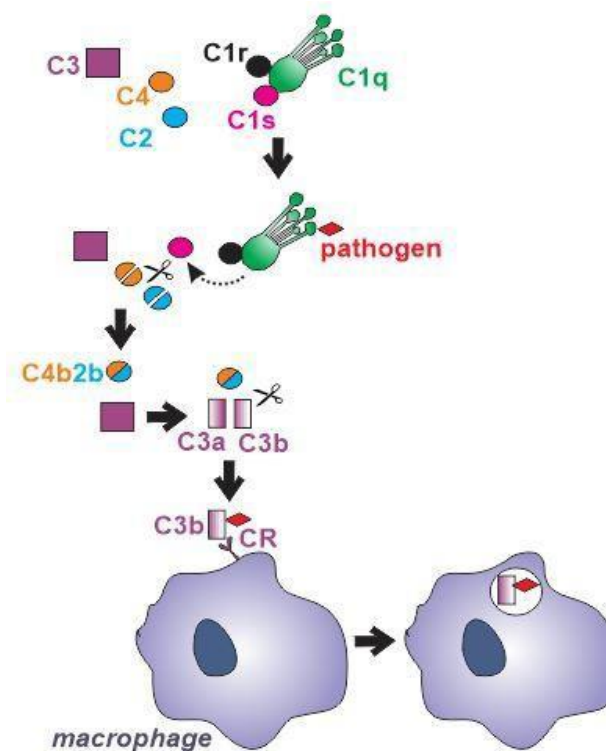


Figure 1.1: The complement cascade in pathogen recognition and phagocytosis. C1q, C1r and C1s form a complex. When C1q recognizes a pathogen, a conformation change allows C1s to dissociate. C1s then initiates a proteolytic cascade that leads to the cleavage of C3 into C3a and C3b. C3b is able to bind the pathogen and is then bound by C3Rs contained on macrophages. The recognition of C3b by macrophages initiates phagocytosis of the pathogen. Note: Figure made by Ashley Comer. Figure not previously published.

The liver produces most of the complement proteins in the body (Morgan & Gasque 1997). After being synthesized in the liver, complement proteins are then released to freely circulate in the blood, ready to respond to an immune insult. Complement proteins, similar to many immune defense molecules, cannot pass the blood-brain barrier (Veerhuis et al. 1998). However, complement proteins are present in the brain, so they must be produced locally (Gasque et al. 1995). Neurons and glial cells, including microglia and astrocytes, have been found to synthesize a wide range of complement proteins including C1q, C3, and C4, among others (Stephan et al. 2013, Veerhuis et al. 1998, Lévi-Strauss & Mallat 1987, Gasque et al. 1995, Walker et al. 1995, Shen et al. 1997, Comer et al, 2020). Additionally, microglia express complement receptors C1qR, C2R, C3R, C4R and C5aR and astrocytes express C1qR (Woodruff et al. 2010). The finding that glia produce much of the brain's complement proteins is consistent with their well-described role in immune defense (Nimmerjahn et al. 2005, Dong & Benveniste 2010, Yang et al. 2010). Microglia play an important role in immune defense since they are the brain's resident macrophage; they physically survey the brain as scavengers that phagocytose both foreign material, such as infectious particles, and neural material such as apoptotic cells and synaptic material (Nimmerjahn et al. 2005, Schfaer et al. 2012). Additionally, when microglia or astrocytes are activated, they produce and secrete complement proteins (Veerhuis et al. 1999). The function of neuronal-derived complement proteins is not as well-defined, and it is unknown if complement derived from different cell-types have slightly different functions. However, one line of evidence suggests that neuron-derived C1q might underlie the pruning

phenotype in the visual system thalamic nucleus, the lateral geniculate nucleus (Bialas et al. 2013).

Recent work shows that complement proteins are implicated in various processes besides immune defense in the brain (Sekar et al. 2016, Stevens et al. 2007, Schafer et al. 2012). Complement proteins play a role in the developmental wiring of the brain. Specifically, microglia engulf synaptic material in the developing brain, but mice deficient in either C3 or the microglial receptor CR3 lose this ability, which leads to aberrant circuit formation in retinogeniculate synapses (Schafer et al. 2012). Further, C3 plays a role in neuronal migration through the lectin pathway C4 (Gorelik et al. 2007). C1q also modulates neurite outgrowth both *in vitro* and *in vivo* in spinal cord regeneration after injury (Peterson et al. 2015). Interestingly, the effect of complement proteins on synaptic pruning might be circuit specific, as there is evidence that certain brain regions, including the visual and barrel cortex, do not depend on complement proteins for proper synaptic pruning (Welsh et al 2020, Gunner et al. 2019). Although there is evidence for microglia-mediated synapse loss in multiple neurological diseases, there is evidence that complement proteins aren't always involved in this process and alternative pathways are being studied such as STAT1 and CCL2 signaling (Lobsinger et al, 2013, Di Liberto et al. 2018). This suggests that complement-dependent wiring might exert differential effects on different brain regions. Together, these studies suggest novel roles of complement signaling in wiring the central nervous system, however little is known about the mechanisms of complement-mediated synapse alterations.

1.4 The inflamed brain in schizophrenia: the convergence of genetic and environmental risk factors that lead to uncontrolled neuroinflammation

1.4.1 Introduction

Schizophrenia (SCZ) is a prevalent mental illness without satisfactory treatment options. Approximately 20 million people worldwide are afflicted by this chronic and debilitating mental disorder (American Psychiatric Association. 2013, Whiteford et al. 2013). SCZ is characterized by a broad range of clinical manifestations including hallucinations, social and cognitive impairments, as well as disordered thinking and behavior that impair daily functioning (American Psychiatric Association. 2013). Current treatment options do not improve cognitive or negative symptoms, both of which contribute more significantly to the long-term prognosis of SCZ than positive symptoms (Lieberman et al. 2005, Green 2006). More effective therapies for SCZ have lagged due to a lack of understanding of its underlying mechanisms.

Genome-wide association studies (GWAS) have identified novel susceptibility loci that confer greater risk for SCZ (Ripke et al. 2013, Li et al. 2017). These breakthroughs have enabled the characterization of genes that may shed light on the pathophysiology of SCZ. In addition, much progress has been made in preclinical studies focusing on environmental risk factors for SCZ and other neurodevelopmental disorders (NDD) that alter brain development such as psychosocial stress, maternal immune activation (MIA), and exposure to pollution (Gomes, Zhu and Grace 2019, Bergdolt and Dunaevsky 2019, Horsdal et al. 2019). Although there are a multitude of genetic and

environmental factors conferring increased risk for SCZ, recent work suggests that these factors converge by altering immune processes, which are known to play an essential role in shaping brain development (Müller and Schwarz 2010, Kroken et al. 2018, Stephan, Barres and Stevens 2012). Indeed, elevated immune function is found in SCZ and therapeutics that target immune function have shown some success in symptom reduction (Sommer et al. 2014, Kroken et al. 2018). Nevertheless, it is still unclear how immune molecules regulate synaptic wiring during normal brain development and contribute to synaptic pathology in neuropsychiatric disorders. Causal links between specific immune molecules and altered synaptic connectivity within circuits implicated in neuropsychiatric disorders are currently lacking (Elmer and McAllister 2012).

Microglia are central nervous system (CNS) phagocytes that, among their other roles, orchestrate innate immunity in the brain. Microglia have well-described roles in rapidly responding to inflammatory insults through dynamic surveillance of the CNS parenchyma (Nimmerjahn, Kirchhoff and Helmchen 2005, Liu et al. 2019b) and clearing debris and apoptotic cells through phagocytosis (Galloway et al. 2019, Ayata et al. 2018). Recent studies have begun to uncover the diversity of microglia, which can have significantly different gene expression patterns across brain regions, in health and in pathological states, and at different developmental time points (Tan, Yuan and Tian 2020, Hammond et al. 2019, Sankowski et al. 2019, Tay et al. 2017a). These complex cells contribute to normal brain development and function by supporting the neuronal circuitry through synapse addition, elimination, maintenance, and plasticity (Hammond, Robinton and Stevens 2018, Bohlen et al. 2019). Despite variability in the findings of several

studies, there is evidence of microglial dysfunction in SCZ (Bayer et al. 1999, Hercher, Chopra and Beasley 2014, Uranova et al. 2020, Bloomfield et al. 2016, Sellgren et al. 2019, Trépanier et al. 2016, De Picker et al. 2017). A key element to understand the pathogenesis of SCZ is to discern how genetic and environmental risk factors intersect to alter microglial function. Furthermore, outstanding questions that remain to be answered are at what stage(s) of disease progression microglial function ameliorates or contributes to the pathology of SCZ, and what are the particular subtypes or phenotypes of microglia that could be targeted for therapeutic intervention.

In this chapter, I discuss the genetic and environmental risk factors for SCZ and how they converge to alter microglial function in response to systemic and central inflammation. Additionally, we highlight how these risk factors alter the indispensable functions of microglia during development, adolescence and adulthood. Limitations of the current knowledge are also addressed, and key future experiments are proposed. Understanding how the heterogeneous genetic and environmental risk factors for SCZ interact to reach a disease threshold and determine its progression is necessary for the development of more effective therapeutics.

1.4.2 Genetic risk factors for schizophrenia that interplay with immunological responses

SCZ is driven by genetic factors, as the risk for developing this disorder increases from 1% in the general population to 50% in individuals with a diagnosed twin (Cardno and Gottesman 2000, Stefansson et al. 2009). Recent ground-breaking genome-wide

association studies (GWAS) have made progress in discovering loci throughout the genome that are associated with SCZ (Dennison et al. 2019, Li et al. 2017, Ripke et al. 2013, Consortium 2011, Schizophrenia Working Group of the Psychiatric Genomics Consortium 2014). These studies reveal that SCZ has a heterogeneous etiology, with genes likely conferring risk across the entire genome. This heterogeneity, in combination with environmental factors, has made it difficult to pinpoint which genes contribute to the disease pathology. Although the genetic determinants for SCZ are not well understood, evidence suggests that immune dysfunction and inflammation contribute to its pathophysiology (van Kesteren et al. 2017, Trépanier et al. 2016).

The major histocompatibility (MHC) locus is located on chromosome 6 and has the highest association to SCZ compared to any other loci across the genome (Schizophrenia Working Group of the Psychiatric Genomics Consortium 2014, Shi et al. 2009, Stefansson et al. 2009). This region encodes genes that are involved in innate immunity. For instance, complement component 4A (C4A), located in the MHC locus, is highly associated with SCZ: specific structural variants and regulatory regions that increase the expression of C4A confer a greater risk for SCZ (Sekar et al. 2016). The complement cascade is part of the innate immune system that recognizes foreign pathogens and apoptotic cells, and tags them for destruction, such as through phagocytosis by macrophages (Veerhuis, Nielsen and Tenner 2011). Besides their established role in immune defense, complement proteins play a role in various stages of brain development including neurogenesis, cellular migration and synaptic development (Lee, Coulthard and Woodruff 2019, Veerhuis et al. 2011). Ground-breaking work in the

last 5-10 years have linked complement proteins to microglia-mediated pruning of synapses, suggesting that C4A could directly contribute to SCZ pathology (Hong et al. 2016, Schafer et al. 2012, Stevens et al. 2007).

In line with this, it was recently shown that increased expression of the mouse homologue of human C4A, called C4b in mice, in medial prefrontal cortex (mPFC) layer (L) 2/3 pyramidal neurons led to a marked reduction in connectivity and decreased sociability in juvenile and adult mice, both of which mirrored the deficits seen in SCZ (Comer et al. 2020). These results suggest that C4A might contribute directly to pathology in SCZ. Although, the molecular mechanisms that link increased C4 expression to synaptic loss remain unclear, overexpressing this neuroimmune gene led to increased localization of the postsynaptic protein PSD-95 to microglial lysosomes, suggesting upregulated microglia-dependent synaptic engulfment (Comer et al. 2020). Additionally, variation in C4 structural alleles increases risk for autoimmune diseases and indicate that sex-differences in the C4 gene might explain greater vulnerability to SCZ in males (Kamitaki et al. 2020). In another study, C4 serum levels were assessed at baseline and in a 1-year follow-up in a cohort of twenty-five patients with first episode psychosis that were taking either olanzapine or risperidone (Mondelli et al. 2020). Compared with responders to antipsychotic medication, non-responders showed significantly higher baseline C4 levels, suggesting that baseline expression of this immune gene can predict clinical outcome (Mondelli et al. 2020). Since this study focused on a limited number of markers, it is not clear how psychosis progression correlates with levels of other immune genes. Lastly, the gene called “CUB and sushi multiple domains 1” (CSMD1) is an

important regulator of C4 that is expressed during early postnatal development (Kraus et al. 2006). Genetic variants located in the CSMD1 and CSMD2 genes have been linked to SCZ (Håvik et al. 2011) and their dysregulation led to deficits in general cognitive ability and executive function (Athanasios et al. 2017), both of which are affected in SCZ. Conversely, a recent study showed that CSMD1 levels in the blood are decreased in SCZ, while antipsychotic treatment resulted in up-regulation of CSMD1 and improved cognitive symptoms (Liu et al. 2019a).

Transcriptomic and genomic studies have implicated alterations in key cytokines with SCZ, including increases in interferon regulatory factor 3 (IRF3) (Li et al. 2015), which is a major transcription factor in viral infection, and interferon gamma (IFN- γ), an important regulator of viral propagation (Paul-Samojedny et al. 2011). In support of neuroimmune genes altered in SCZ, other studies have found changes in pro-inflammatory interleukin 1 (IL)-1 α (Katila, Hänninen and Hurme 1999), IL-1 β (Sasayama et al. 2011, Katila et al. 1999), IL-6 (Frydecka et al. 2015, Kalmady et al. 2014) and anti-inflammatory IL-10 (reviewed in (Gao et al. 2014)). Several studies also investigated circulating C-reactive protein (CRP), IL-6, IL-1 β , TNF- β and TGF- β , which are also elevated at the mRNA level in people with SCZ, to determine their reliability as peripheral biomarkers (Kroken et al. 2018). However, other studies reported limited immune gene enrichment in SCZ (Pouget et al. 2016), highlighting the genetic complexity of the disease, in addition to possible variability between cohorts and confounding factors such as medication, among other challenges with GWAS.

Several GWAS have revealed that multiple immune receptors are associated with SCZ including the MHC receptors and Toll-like receptors (TLRs) (Stefansson et al. 2009, Shi et al. 2009, Schizophrenia Working Group of the Psychiatric Genomics Consortium 2014, Purcell et al. 2009, Consortium 2011). TLRs play a role in the recognition of microbe-derived molecular signals by innate immune cells including microglia (reviewed in (Wright et al. 2001, Lehner 2012)). In addition to their established role in innate immunity, TLRs regulate early brain development (Chen et al. 2019, Mallard 2012) via their effects on synaptic plasticity and neurogenesis (Barak, Feldman and Okun 2014). Other groups have shown alterations in TLR2 (Kang et al. 2013) and TLR4 (García-Bueno et al. 2016, MacDowell et al. 2017) in either the blood or post-mortem brain tissue of people with SCZ. Overall, these data have linked MHC signaling and other immune receptors pathway with the pathology of SCZ, However, the molecular underpinnings of their contribution to SCZ are not yet clear. It is also still not understood how disruption in particular immune pathways contributes to specific cellular and behavioral hallmarks of this disorder, such as decreased gray matter volume.

To identify robust peripheral biomarkers that can predict SCZ pathology, researchers have compiled an architecture of genes observed in patients from multiple GWAS. A subset of overlapping genes from these studies identified candidates including CD14, Clusterin, Dipeptidyl peptidase 4, Early Growth Response 1, Heat Shock Protein Family D Member 1, C4 and MHC genes (Pouget et al. 2016). Despite the identification of these candidate biomarkers, other studies highlight that the current literature does not provide sufficient evidence that increased inflammation is a hallmark of all SCZ cases

(Kroken et al. 2018). Some studies have identified markers that are related to antigen presentation and immune activity (Pouget et al. 2016), whereas others have revealed changes in inflammatory cytokines (Kroken et al. 2018, Hudson and Miller 2018). These studies together indicate that some cases or stages of SCZ may involve the innate and/or adaptive immune system. However, genetics only explains part of the susceptibility and pathophysiology of SCZ, which provides further support that environmental risk factors are also required to trigger the disease in most cases (Knuesel et al. 2014).

Lastly, SCZ-associated genes with diverse functions in the brain have also been implicated in inflammation (Brandon et al. 2009). For example, the gene Disrupted-in-Schizophrenia 1 (DISC1) was first found in a Scottish family with SCZ (St Clair et al. 1990) and subsequently in other populations worldwide (Chubb et al. 2008). Interestingly, the disruption of DISC1 protein in mice led to dysregulation of an immune-related network of genes that are perturbed in SCZ (Trossbach et al. 2019), suggesting that non-immune genes can modulate the expression of inflammatory gene networks. In support of this, in a dual-hit genetic-environmental mouse model of SCZ, where Disc1 mutation was combined with MIA, transient administration of minocycline, an anti-inflammatory antibiotic drug, rescued electrophysiological and structural deficits during early postnatal development, as well as cognitive abilities in juvenile mice (Chini et al. 2020). It is clear that the expression of hundreds of genes is altered in SCZ, although it remains to be determined how the interaction between immune and non-immune pathways is implicated in this disorder. Overall, growing evidence suggests that immune

gene dysfunction and inflammation both contribute to the pathophysiology of SCZ (van Kesteren et al. 2017, Trépanier et al. 2016).

1.4.3 Exposure to pollution increases risk for schizophrenia by enhancing inflammatory responses

The environment is becoming increasingly polluted from multiple sources and has been found to correlate with increased prevalence of SCZ (Horsdal et al. 2019). Traffic-related air pollution (TRAP), such as diesel exhaust (Bolton et al. 2017, Inoue et al. 2006, Hartz et al. 2008, Block and Calderón-Garcidueñas 2009), is the result of the combustion of fossil fuels and can be modeled in the lab using elemental carbon (Newman et al. 2013) (Newman et al. 2013) or by taking the finest particles (<200 nm) from TRAP and re-aerosolizing them into nanoparticulate matter (nPM). nPM is the most toxic component of TRAP, in terms of its impact on the brain (Davis et al. 2013). By-products of TRAP, such as ozone (O₃), which can be generated from nitrogen oxide, can also be changed photochemically after their release from motor vehicles (Mumaw et al. 2016). Altogether, multiple paradigms are currently used in animal models to study the effects of air pollution on brain development (Davis et al. 2013, Newman et al. 2013, Woodward et al. 2017). This work is particularly relevant when considering the epidemiological studies that link air pollution to SCZ pathogenesis (Horsdal et al. 2019). Indeed, many of the genes altered in SCZ overlap with genes that are affected by exposure to air pollution

(Figure 1.2). Interestingly, immune genes, including those expressed by microglia, are at the center of this interaction (Peters et al. 2006, Genc et al. 2012).

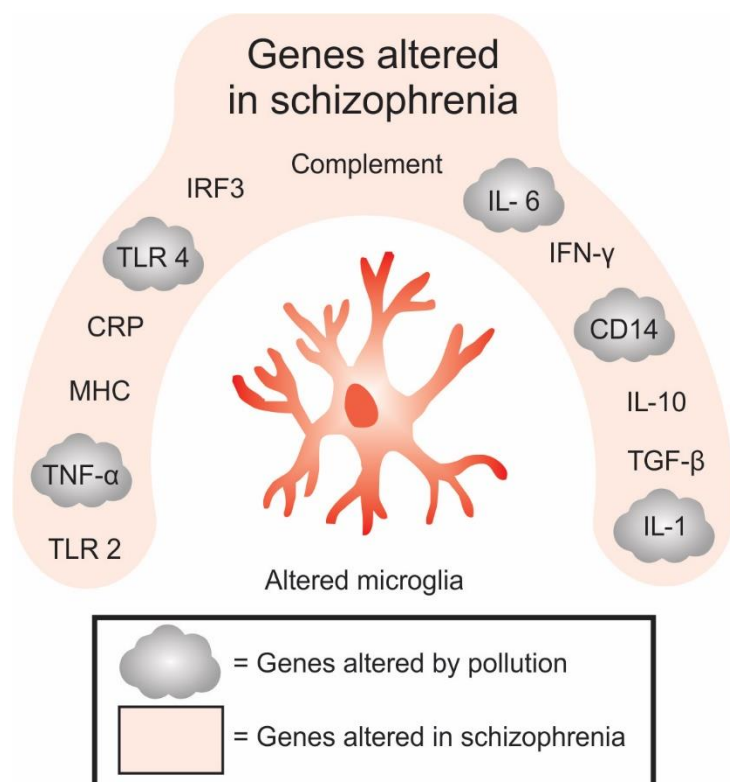


Figure 1.2: Overview of the overlap between immune-signaling genes that are altered from pollution and in schizophrenia.

Of the immune genes that are associated with SCZ, many are also found to be altered either in humans or animals exposed to pollutants, offering a novel hypothesis for the cause of cytokine-induced neuroinflammation observed in people with SCZ. The inflammatory genes including TLR2, TNF- α , MHC, CRP, TLR4, IRF3, complement pathway, IL-6, IFN- γ , CD14, IL-10, TGF- β are altered in SCZ, while TNF- α , TLR4, IL-6, CD14 and IL-1 are altered in SCZ and after exposure to air pollution. Note: Figure made by Micael Carrier as part of Comer et al., *Frontiers in Cellular Neuroscience*, in press.

While the mechanisms involved in SCZ pathogenesis are still unclear, exposure to air pollution has been found to increase the expression of multiple inflammatory genes in

humans and mouse models. Children exposed to TRAP have elevated circulating levels of pro-inflammatory cytokines, including IL-6, IL-1 β , CD14 and TNF- α , compared to children living in less-polluted cities (Gruzieva et al. 2017, Calderón-Garcidueñas et al. 2008, Calderón-Garcidueñas et al. 2015). Additionally, nPM from air pollution induced a similar inflammatory cytokine signature in the circulation of healthy young adults, characterized by an elevation of IL-6, together with an increased density of inflammatory cells and microparticles, suggesting the occurrence of endothelial injury (Pope et al. 2016). In line with this, TRAP exposure in rodents increased IL-1 α , IL-6 and TLR4 expression in the brain (Bolton et al. 2017, Bos et al. 2012). Pollution exposure especially impacted microglial TLR4 signaling in multiple mouse models involving TRAP (Woodward et al. 2017, Woodward et al. 2018), O₃ (Mumaw et al. 2016), or diesel exhaust particle (Bolton et al. 2017, Bai et al. 2019) exposure, by upregulating TLR4 in a MyD88-dependent pathway (Woodward et al. 2017). Male offspring were especially susceptible to these deleterious effects, showing greater changes in microglial TLR4 signaling that were accompanied by behavioral deficits in anxiety-like behavior, contextual and auditory cue fear conditioning and the forced swim test (Bolton et al. 2012, Bolton et al. 2013, Bolton et al. 2017). Prolonged exposure to inflammatory molecules, such as IL-6, additionally led to neuroadaptive effects such as altered synaptic plasticity (Gruol 2015). Therefore, exposure to pollution could alter brain development and function by causing increased expression of pro-inflammatory markers, a feature on which MIA models of SCZ rely on (Girgis, Kumar and Brown 2014).

TRAP alters brain development and increases the risk for SCZ (Woodward, Finch and Morgan 2015, Pedersen et al. 2004), however it is unclear if pollution-mediated changes in brain development or inflammatory signaling directly contribute to pathology. Recent work has studied the effects of chronic nPM exposure using a double-hit model where cortical neuronal cultures from exposed mice were re-exposed in culture. A double exposure to nPM reduced neurite outgrowth (Davis et al. 2013) while resulting in an inflammatory transcriptomic profile (Solaimani et al. 2017) in neuronal cultures. Another group showed that TRAP can reduce hippocampal neurogenesis by 70% in rats, which correlated with behavior deficits in object recognition, food-seeking behavior, and in the forced swim test (Woodward et al. 2018). These phenotypes were reproduced in mice using elemental carbon exposure (Morris-Schaffer et al. 2019). In the mouse brain, nPM exposure induced neuroinflammation evident through a microglia-mediated increase in TNF- α (Cheng et al. 2016). Furthermore, exposure to nPM led to altered microglia morphology and elevated levels of C5, C5a and CD68 proteins, indicative of increased phagocytic activity, in the corpus callosum (Babadjouni et al. 2018) a region that is particularly reduced in volume in SCZ patients (Kubicki et al. 2005). Other work has highlighted the neurotoxicity of ultrafine particles (UFP), which induced pro-inflammatory signaling and lead to a long-lasting reduction of corpus callosum volume (Allen et al. 2017). Overall, neuroinflammation induced by pollution appears to have a substantial impact on the brain by altering axonal myelination (Cole et al. 2016). However, it is still unclear to what extent pollution-driven inflammation, compared to other risk factors, drives myelination deficits in SCZ. Taken together, the inflammatory

state caused by exposure to air pollution has been shown to alter microglial function and neuronal development, as well as axonal myelination, thus affecting several processes of neurodevelopment that have been linked to SCZ pathogenesis.

1.4.4 The gut-brain axis in schizophrenia

The CNS communicates bi-directionally with the gastrointestinal (GI) system to maintain homeostasis, for instance by regulating hunger and digestion processes at steady state (Konturek et al. 2004). There has been extensive study of the reciprocal gut and CNS interactions, which communicate through the enteric nervous system and vagus nerve, and via alternative pathways involving the immune and neuroendocrine systems (Sampson et al. 2016, Singh et al. 2016, Sudo et al. 2004) or through direct secretion by gut microbes of neurotransmitters (Yano et al. 2015) and metabolites (De Vadder et al. 2014, Sherwin et al. 2019). However, the importance of the gut in mediating brain function and behavior was ignited by the discovery that germ-free mice, which are devoid of microorganisms, have heightened stress responses (Sudo et al. 2004). In more recent work, the microbiota has been shown to influence complex behaviors such as social behavior, depression, and anxiety which are directly relevant to SCZ and other neuropsychiatric disorders (Sherwin et al. 2019, Desbonnet et al. 2014). Additionally, 19% of people with SCZ are comorbid for irritable bowel syndrome, which has a known inflammatory etiology (Gupta et al. 1997) compared to an occurrence rate of only 2.5% in the general population. Studying the role of the microbiota in disease states is

challenging since it is highly sensitive to environmental changes. Therefore, most of the environmental risk factors for SCZ also impact the microbiota (Franklin and Ericsson 2017), making it difficult to determine causation. However, recent work suggests a causative role for the microbiota in neuropsychiatric disorders and highlights the role of the immune system in linking the brain and gut in pathological conditions (Castro-Nallar et al. 2015, Yolken et al. 2015, Schwarz et al. 2018, Zheng et al. 2019, Zhu et al. 2019).

The microbiota not only plays a key role in regulating host metabolism but also modulates inflammatory responses and neural function. Germ-free mice have multiple deficits in nervous system function including heightened hypothalamic-pituitary-adrenal (HPA) axis responses (Sudo et al. 2004), altered anxiety-like behaviors (Neufeld et al. 2011), increased motor activity (Diaz Heijtz et al. 2011), and impaired memory (Gareau et al. 2011), and social behaviors (Desbonnet et al. 2014). The microbiota of people with SCZ has been found to contain more of the bacterial species *Lactobacillus* compared to healthy controls, and levels of this bacterium correlate with psychosis severity (Castro-Nallar et al. 2015, Yolken et al. 2015, Schwarz et al. 2018). In a recent study, gut microbiota from SCZ patients was transferred into germ-free mice to test whether SCZ-relevant behavioral phenotypes were transmissible via their gut microbiome. Germ-free mice receiving fecal transplants from these patients had lower levels of glutamate and higher levels of glutamine and GABA in the hippocampus, and these mice exhibited locomotor hyperactivity and decreased anxiety-like and depressive-like behaviors, as well as increased startle responses relative to control mice that received fecal transplants from healthy subjects (Zheng et al. 2019). Additionally, transplantation of the gut microbiome

from drug-free individuals with SCZ into antibiotic-treated mice caused SCZ-related phenotypes such as impaired learning and memory as well as increased psychomotor behaviors, while also leading to increased PFC dopamine and hippocampal serotonin levels compared to mice receiving microbiota transplants from healthy controls (Zhu et al. 2019). Microbes are able to produce or aid in the production of multiple neurotransmitters, including serotonin, dopamine and GABA, but it is still unclear how the gut production of these neurotransmitters affects CNS function (Yano et al. 2015, Strandwitz 2018). Additionally, gut microbiome transplantation or treatment with probiotics has been shown to, at least partially, reverse MIA-associated phenotypes in rodents, including deficits in anxiety-like, stereotypic and sensorimotor behaviors (Hsiao et al. 2013). The reversal of these phenotypes seems to be mediated through the normalization of gut permeability and microbe dysbiosis (Hsiao et al. 2013), suggesting that the gut microbiota can directly modulate immune responses even between a dam and its embryo. This is not surprising given that the microbiota has a well-studied role in inducing and maintaining the function of the host immune system.

The gut-brain axis links multiple environmental risk factors for SCZ, specifically through immune signaling. MIA is a risk factor for SCZ that depends on maternal immune signaling relayed to the fetal brain through the placenta. Maternal gut microorganisms have been found to play an important role in MIA-mediated deficits. A ground-breaking study showed that MIA phenotypes in exposed offspring are dependent on the presence of segmented filamentous bacteria in the maternal gut which promote Th17 cell differentiation, leading to increased IL-17 α production (Kim et al. 2017). MIA

phenotypes, including deficits in cortical development and behavioral abnormalities, depend on gut microbiome-mediated increases in IL-17 α , as these phenotypes were diminished in mice deficient for IL-17 α (Kim et al. 2017, Shin Yim et al. 2017). These data show that maternal microbe-induced immune signaling impacts fetal brain development with long-term consequences. Intriguingly, adult mice that have been exposed to lipopolysaccharides (LPS) *in utero* display improvement of their social deficits in later life upon re-exposure to LPS, which promotes gut microbiome production of IL-17a (Reed et al. 2020). Together, these findings suggest that prenatal inflammatory insults can prime the gut-immune-brain axis, thus leading to altered CNS responses to immune challenges later in life.

The gut microbiome can affect the integrity of the blood-brain barrier (BBB), which facilitates increased neuroinflammation. The presence of gut microbes is necessary for the proper formation of the BBB during early development. Mice from germ-free dams have disrupted BBB maturation, which is evident by decreased tight junction expression both prenatally and postnatally. The hyperpermeability of the BBB in germ-free mice persists into adulthood, but can be rescued by microbiota transplantation from controls or through the administration of bacteria that produce short chain fatty acids (SCFAs) (Braniste et al. 2014), which are known to have anti-inflammatory effects and promote BBB integrity (Hoyles et al. 2018). As mentioned previously, the gut plays an important role in the differentiation of Th17 cells. Interestingly, the gut also promotes the infiltration of Th17 cells into the brain through the meninges where these cells secrete IL-17, which further promotes immune cell infiltration (reviewed in (Cipollini et al. 2019)).

BBB endothelial cells express TLRs and therefore are able to respond to gut microbe components such as LPS, which can alter tight junction expression and promote immune cell infiltration into the CNS (Tang et al. 2017). The BBB and microbiome are both disrupted in SCZ; this works thus highlights the potential for crosstalk between these systems that might act synergistically to further contribute to neuroinflammation in SCZ.

Gut microbes produce metabolites that can cross the BBB and inhibit the function of mitochondria in the CNS (Hulme et al. 2020). A decrease in mitochondria density and altered structure has been observed in post-mortem SCZ brain tissue across multiple regions including the anterior cingulate cortex (Flippo and Strack 2017, Roberts 2017). This finding raises the intriguing possibility that gut microbe metabolites can contribute to SCZ pathology. While the identity of the CNS cell(s) affected by gut metabolites remains unclear, the dysfunction of mitochondria in microglia has been shown to alter cytokine production and inflammatory responses in the brain (reviewed in (Culmsee et al. 2018)). MIA, which increases the risk for SCZ, has been shown in mice to alter the structure of mitochondria in a disease-associated microglial subtype known as dark microglia, among the hippocampus (Hui et al. 2018). Taken together, these studies suggest that there is extensive interplay between risk factors for SCZ, such that signaling from the gut-brain axis and exposure to an early immune insult can alter the function of microglia and CNS mitochondria. Future studies could aim to target the gut microbiome to dually control BBB integrity and reduce neuroinflammation.

Gut microbiota dysbiosis can alter the maturation and function of microglia in the CNS, thus contributing to neuroinflammation (Thion et al. 2018, Erny et al. 2015). Germ-

free mice have microglia with an immature morphology and gene expression profile in adulthood (Erny et al. 2015), suggesting that the microbiota impacts the maturation of microglia. The absence of microbes was found to not only affect microglial function but also impair innate immune responses, which were partially recovered by colonization with a more complex microbiome or by supplementation with SCFAs, which are a byproduct of certain gut microbes (Erny et al. 2015). SCFAs might affect CNS function through their interactions with BBB endothelial cells (Braniste et al. 2014) or directly with the CNS considering that they do not require receptors to bypass the BBB (Frost et al. 2014). The lack of SCFAs could additionally lead to increased peripheral and central inflammation considering their well-known anti-inflammatory functions (Li et al. 2018a, Vinolo et al. 2011).

Microglia also show sex-dependent differences in response to gut microbe sterility. Microglia from germ-free male mice displayed altered expression of immune genes and a more immature phenotype at juvenile stages whereas microglia from female mice were more affected in adulthood (Thion et al. 2018). These findings suggest that the maternal microbiome can regulate microglial function in the offspring brain (Thion et al. 2018), notably in the context of MIA exposure (Kim et al. 2017, Shin Yim et al. 2017), in a sexually dimorphic manner. Sex differences in microglial response to microbiome challenges are intriguing as they could partially explain the earlier onset of SCZ in males compared to females (Ochoa et al. 2012). MIA models also display sexual dimorphism in microglial properties and behavioral outcomes (Hui et al. 2018). However, much work is needed to understand whether microglia-induced sex differences are present in SCZ.

Without a doubt, the gut microbiome influences the development and maintenance of the immune and nervous systems, with significant crosstalk. In the context of SCZ, the metabolites and diversity of gut microbes may impact multiple disease symptoms. The microbiome links multiple risk factors for SCZ, including stress responses, by promoting immune activation and BBB disruption (Figure 1.3). Innate immunity of the brain, including microglial function, is sensitive to gut dysbiosis, making the gut microbiota an interesting target in SCZ. Probiotics and microbiome transplants should be further explored to improve symptom severity in people with SCZ. Additionally, precautionary steps could be taken in pregnant mothers to improve diversity of gut microflora, considering its profound impact on brain development. Future work should further explore the role of SCFA-producing microbes, considering that they exert anti-inflammatory effects and improve brain function and behavior. Taken together, gut microbes are positioned to alter immune responses to environmental challenges by regulating neuronal function, behavior, and microglial responses, all of which are altered in SCZ.

1.4.5 Maternal immune activation enhances risk for schizophrenia by altering microglial function

It has become increasingly clear that immune challenges occurring during pregnancy increases offspring risk for varied neurodevelopmental and neuropsychiatric disorders, including SCZ. Specifically, maternal exposure during pregnancy to bacterial

(Sørensen et al. 2009) or viral infections such as influenza, rubella or herpes (Brown and Derkits 2010, Pearce 2001) leads to lasting changes in offspring brain function and behavior (Estes and McAllister 2016). Maternal infection has been extensively studied using animal models of maternal immune activation (MIA), which have provided a substantial amount of causative evidence for how early immune insults disrupt brain development and function (Knuesel et al. 2014, Estes and McAllister 2016). MIA can be induced by exposing pregnant dams to immunogens that mimic an infection. The most common immunogens used to model MIA include polyinosinic:polycytidylic acid (poly(I:C)) and lipopolysaccharide (LPS) which mimic viral or bacterial infections, respectively. These agents elicit immune responses that enable cytokines to pass through the placental barrier, activating placental and embryo macrophages, and leading to increased inflammation in the developing offspring (Wu et al. 2017). Although work is needed to normalize MIA protocols, particularly on the temporal level, and to understand the variability in reported results (Kentner et al. 2019), this animal model has provided insight into how maternal infection enhances the risk for various disorders. Here, we focus on progress that has been made in understanding prenatal immune challenges in mice and humans.

MIA impacts brain function in a circuit-specific manner and interacts with other risk factors for SCZ. These early immune insults can elicit a vast array of phenotypes in mice that are relevant to SCZ and autism spectrum disorder (ASD), including abnormalities in ultrasonic vocalization and sociability, increased repetitive behaviors, motor dysfunction, and deficits in sensorimotor gating and cognitive abilities such as

working memory (Fernández de Cossío et al. 2017, Pendyala et al. 2017, Shin Yim et al. 2017, Knuesel et al. 2014). Some of these behavioral effects are sex-dependent (Haida et al. 2019). MIA-induced behaviors were accompanied by changes in specific brain areas such as altered hippocampal volume and cortical thickness, and changes in synaptic density and proteins (Fernández de Cossío et al. 2017, Estes and McAllister 2016), which are also observed in SCZ (Glantz and Lewis 2000, Onwordi et al. 2020, Hui et al. 2018). Alterations in amygdala-cortical circuitry have been implicated in SCZ (Benes 2010) and a recent study showed that MIA enhances glutamatergic neurotransmission between these circuits by increasing synaptic strength in the exposed offspring (Li et al. 2018b). An exciting development in this field showed that MIA-induced deficits in neurodevelopment depend on inflammatory signaling through the maternal microbiome (Kim et al. 2017). MIA via LPS also disrupts BBB function by increasing its permeability, thus promoting neuroinflammation (Simões et al. 2018, Estes and McAllister 2014). However, there is also evidence for no change in BBB permeability after MIA induced via poly(I:C) in mice (Garay et al. 2013), suggesting immunogen-dependent effects. These differences also emphasize the variability of MIA animal models and the need for experimental standardization.

Given that microglia are the primary innate immune cells of the brain, they provide rapid responses to immune insults and are greatly affected by systemic inflammation. MIA exerts its effects on neurodevelopment largely by disrupting microglial function and by priming them for altered responses later in life. Changes in the density of microglia are found in early postnatal MIA offspring in multiple cortical and

subcortical regions including the anterior cingulate cortex, striatum and hippocampus (Zhang et al. 2018). Microglial involvement in MIA effects is evident through an increase in cytokine and chemokine signaling, in mouse hippocampus and basal forebrain, during late fetal development in response to either LPS (Schaafsma et al. 2017) or poly(I:C) (Pratt et al. 2013). A recent study showed that an MIA mouse model induced at embryonic day 9.5 with poly(I:C) led to an increased density of a pathological microglial subtype, called dark microglia, in the hippocampus of male versus female offspring (Hui et al. 2018). Dark microglia are almost exclusively observed in disease states or in aged animals, and exhibit greater levels of oxidative stress and hyper-ramified processes in closer proximity to synapses than typical microglia (Bisht et al. 2016). These studies highlight the ability of MIA to alter microglial state and function.

Moreover, MIA in mice alters the transcriptome and phagocytic activity of microglia in offspring (Mattei et al. 2017). Specifically, hippocampal microglia from male poly(I:C) mice displayed a downregulation of genes that encode cell surface receptors associated with phagocytosis (P2ry6, Sirpa, Siglece, Cx3cr1, Fcgr1, Itgav) (Mattei et al. 2017). These receptors are important components of the microglial 'sensome', which contribute to the regulation of microglia-neuron interactions and are important for the engulfment of neuronal material (Mattei et al. 2017). Inflammatory abnormalities, such as increased levels of Serpin Family A Member 3, TNF α , IL-1 β , IL-6, and IL-6ST, have been observed in the ventral midbrain in post-mortem SCZ tissue, and these results were also replicated in an MIA mouse model (Purves-Tyson et al. 2019). Importantly, these differences in immune markers from SCZ tissue could be

accounted for by a subset of cases, including about 45% of high inflammatory cases. The ventral midbrain houses the majority of dopamine-releasing neurons in the brain, therefore MIA might contribute to SCZ pathology by disrupting immune-mediated wiring of dopaminergic circuits (Purves-Tyson et al. 2019). These findings are important because they link SCZ-associated neuroinflammation to dopaminergic abnormalities, which is a hallmark of this disorder.

Multiple studies targeting microglial signaling pathways were able to reverse MIA-associated neuropathology, suggesting that microglia are the main culprit in inducing neurological dysfunction in response to immune challenges. For example, a study that targeted colony stimulating factor 1 receptor (CSF-1R), which plays a role in microglial proliferation, was successful in reversing some MIA-induced phenotypes (Ikezu et al. 2020). Depleting and repopulating microglia by inhibiting CSF-1R was protective in mice exposed to poly(I:C) prenatally (Ikezu et al. 2020). Specifically, once the microglial population was renewed, not only were the deficits in repetitive and social behaviors reversed, but normal neuronal connectivity and microglia-neuron interactions were also restored (Ikezu et al. 2020). Another successful approach to restore typical microglial function targeted the peroxisome proliferator-activated receptor gamma (PPAR γ) signaling pathway. PPAR γ signaling is activated by fatty acids and reduces myeloid cell-induced inflammation via suppressing their production and/or secretion of inflammatory molecules (Bernardo and Minghetti 2006). Agonists of PPAR γ have been found to be protective in the context of MIA by inhibiting microglial expression of pro-inflammatory cytokines and surface antigens (Bernardo and Minghetti 2006), suggesting

that targeting microglial PPAR γ signaling could be beneficial in offspring exposed to MIA (Zhao et al. 2019). In support of this, a recent study showed lower serum levels of PPAR γ in patients with SCZ while levels of this biomarker decreased further with disease progression (Yüksel et al. 2019). Treatment with minocycline, a broad-spectrum anti-inflammatory and antibiotic drug that generally restores microglial functions, also reversed changes in microglial transcriptome and phagocytic activity in mouse offspring exposed to MIA (Mattei et al. 2017). Lastly, there is evidence that deep brain stimulation in rats can prevent some of the behavioral deficits associated with MIA specifically by reducing microglial pro-inflammatory responses (Hadar et al. 2017). Taken together, these data suggest that microglia play a critical role in MIA-induced brain dysfunction and that targeting microglia is a potential therapeutic approach to reverse MIA-induced phenotypes.

MIA is an important model that has increased our understanding of how immune insults occurring during embryonic development can alter brain development. Although there is variability in data obtained using mouse models of MIA, notably due to differences in immunogen manufacture (molecular weight, endotoxin contamination, etc.), timing of immunogen administration, dosage, route of administration, housing conditions, timing of cage changes and mouse strain used (Kowash et al. 2019, Careaga et al. 2018, Kentner et al. 2019), understanding what causes these differences could aid in understanding the mechanisms underlying vulnerability versus resiliency to MIA (Meyer 2019). In humans, only a subset of pregnant mothers who are exposed to a viral or bacterial infection have offspring who later develop SCZ (Estes et al. 2019). This is to be

expected since immune activation is only one of the many risk factors for SCZ. Therefore, the variability in mouse models of MIA might be exploited to elucidate why certain sub-populations of individuals are at greater risk for SCZ. Since some mouse strains are resilient to MIA, the genetic differences between mouse strains could be used to identify protective versus susceptibility genes (Schwartz et al. 2013). Overall, future work aimed at understanding such variability will likely be valuable in discovering how only a subset of subjects is vulnerable to MIA.

It is interesting that MIA is a risk factor for both SCZ and ASD, since some of the neurological deficits observed in these disorders appear to be opposing. For example, SCZ is characterized by a significant loss of gray matter resulting in hypoconnectivity between the anterior hippocampus and PFC (Vita et al. 2012, Blessing et al. 2019), on which the neonatal ventral hippocampal lesion rodent model of SCZ is based (Joseph, Bhardwaj and Srivastava 2018), whereas ASD is associated with hyperconnectivity (Supekar et al. 2013). How could the same risk factor play a role in such opposing phenotypes? We propose that the underlying genetic background and the time of exposure are important factors that determine the effects that MIA exerts on brain development. For example, SCZ is associated with genetic variation in the C4 gene that led to enhanced C4 expression (Sekar et al. 2016) whereas C4, C3 and C1q were found to be downregulated in ASD (Fagan et al. 2017). Differences in certain genes, such as complement genes, which have an established role in synaptic pruning (Schafer et al. 2012, Sekar et al. 2016, Stevens et al. 2007, Comer et al. 2020), could explain how MIA differentially contribute to disease phenotypes. Alternatively, the expression of TLR3 and

TLR4, which directly respond to poly(I:C) and LPS (Zhou et al. 2013, Lu, Yeh and Ohashi 2008), respectively, could differ between mouse strains with varying susceptibility to MIA and in humans predisposed to different NDDs. Lastly, it is not clear how recently emerging viruses, such as the coronaviruses that cause “Severe Acute Respiratory Syndrome” and “Middle East Respiratory Syndrome”, might contribute to NDDs (Gretebeck and Subbarao 2015, Fauci, Lane and Redfield 2020). It is also unknown whether the severe acute respiratory syndrome coronavirus 2, which caused the COVID-19 pandemic, leads to lasting consequences on brain development and behavior while preliminary data suggest that passive transfer of antibodies from mother to embryo is possible (Zeng et al. 2020).

1.4.6 Stress-induced inflammation

Exposure to psychological stress or traumatic life events prenatally and during childhood or adolescence results in an increased risk for SCZ (Holtzman et al. 2013, Read, Bentall and Fosse 2009, Kessler et al. 2010, Weinstock 2008). Specifically, during critical periods of development, certain stressors, such as physical or mental abuse, socioeconomic disadvantage, living in an urban environment and neglect, all confer greater risk for SCZ (Popovic et al. 2019, Quidé et al. 2017, McGrath et al. 2004). Additionally, people with SCZ have altered physiological responses and increased vulnerability to stressful stimuli (Schifani et al. 2018). Thus, increased exposure and vulnerability to psychosocial stress, especially during critical periods of brain

development, represents a significant challenge. However, cellular and molecular mechanisms that link early life stress (ELS) with increased risk for SCZ are still unclear. Nevertheless, evidence suggest that psychosocial stressors contribute to SCZ pathology by in part increasing neuroinflammation.

Individuals with SCZ have altered physiological stress responses (van Leeuwen et al. 2018, Schifani et al. 2018, van Venrooij et al. 2012). Exposure to stress stimulates the sympathetic nervous system causing the secretion of epinephrine and norepinephrine, and increased HPA axis function which leads to the release of stress hormones, such as cortisol, into the blood (reviewed by (Chrousos 2009)). These stress hormones alter an organism's physiology to promote activities that combat the stressor, such as increased cardiac function and glucose availability, while decreasing less urgent processes including digestion, reproduction, and immune function (Chrousos 2009). In healthy individuals, cortisol led to the suppression of adaptive immunity and an increase in innate immunity due to the effects of glucocorticoids on inflammation (Barnes 1998). Although cortisol has some anti-inflammatory effects, its ability to regulate inflammatory responses is altered in SCZ. In healthy individuals, an acute stressor led to increased salivary levels of cortisol and a decrease in IL-6; however, in individuals with SCZ, an increase in cortisol was shown to be accompanied by an increase in IL-6 (Chiappelli et al. 2016). Additionally, chronic and ELS, which are risk factors for SCZ, are linked to increased immune activation (Chiappelli et al. 2016), as well as abnormal sensitivity and levels of glucocorticoids and their receptors (do Prado et al. 2017, Webster et al. 2002, Sinclair et al. 2012), disrupting the ability of cortisol to regulate inflammation (Miller and Chen

2010). In this sense, stress-induced release of cortisol might increase inflammatory responses in people with SCZ instead of having anti-inflammatory effects such as seen in healthy individuals.

Although multiple studies have found an increase in HPA axis function in people with SCZ (Chiappelli et al. 2016, Mondelli et al. 2010a, Walder, Walker and Lewine 2000), others have reported a decrease in cortisol levels compared to controls in response to a stressor (Glassman et al. 2018, Ciufolini et al. 2014, Lange et al. 2017). The inconsistencies between these findings could be due variation including differences in stressor intensity, duration, time point of exposure (Lange et al. 2017), or administration of antipsychotics, which have been shown to alter cortisol stress responses (Houtepen et al. 2015). Despite these discrepancies, HPA axis dysfunction has been observed in first-episode psychosis prior to antipsychotic treatment (Mondelli et al. 2010a, Mondelli et al. 2010b, Ryan et al. 2004). Additionally, recent work has shown that regardless of differences in cortisol responses to acute stressors among people with SCZ, those with decreased cortisol responses to social stress had lower measures of social functioning (Tas et al. 2018). Therefore, understanding differences in cortisol responses and its relationship to immune function in SCZ could provide insight into the role of psychosocial stress on disease progression.

Prenatal psychological stress is associated with an increased risk of SCZ (Pugliese et al. 2019, Weinstock 2008, Kofman 2002). In mice, prenatal stress increased placental expression of several pro-inflammatory genes including IL-6, IL-1B, and TNF α specifically in males, and these changes were partially rescued by maternal

administration of a nonsteroidal anti-inflammatory drug (Bronson and Bale 2014). Additionally, studies in mice have shown that male offspring exposed to prenatal stress displayed behavioral deficits including anhedonia and changes in stress responses that coincided with altered placental gene expression in males but not females, affecting PPAR α , the growth factor IGFBP-1, hypoxia-inducible factor 3 α (HIF3 α), and glucose transporter GLUT4, all of which have been implicated in immune system function (Mueller and Bale 2008). Importantly, the placenta is a regulator of maternal-fetal immune initiation in offspring (reviewed in (Hsiao and Patterson 2012)) and this interaction appears to be crucial given that prenatal dysregulation of the immune system can lead to altered immune responses postnatally (Pedersen et al. 2018, Bilbo and Schwarz 2009). Maternal restraint stress resulted in offspring with altered microglial morphology and density in the cortical plate at embryonic stages and in neocortex at adulthood, and these prenatal-induced changes were reversed by blocking IL-6 (Gumusoglu et al. 2017), confirming that increased maternal expression of IL-6 can cause neuroinflammation in embryos by crossing the placenta (Dahlgren et al. 2006). Nevertheless, the role of maternal stress-induced inflammation and the specific involvement of the placenta in mediating its consequences are not fully understood.

Early life stress (ELS), such as childhood abuse or neglect, is a major risk factor for SCZ, however the mechanisms by which ELS induces changes in neuronal circuitry is not clear. Mounting evidence suggests that dysfunction of the immune system and microglia, especially, can contribute to brain miswiring and behavioral deficits after ELS (Na, Jung and Kim 2014, Johnson and Kaffman 2018). In humans and mice, ELS

increases multiple blood pro-inflammatory markers including CRP, IL-1 β , IL-6, IL-8, TNF- α (Hepgul et al. 2012, Marsland et al. 2017, Réus et al. 2017) while suppressing the anti-inflammatory cytokine IL-10, leading to depressive-like behaviors in mice (Réus et al. 2017). In line with these findings, ELS resulted in altered microglial gene expression, density, morphology and phagocytic activity during maturation in particular brain regions including the mPFC, striatum, anterior cingulate cortex and hippocampus (Banqueri et al. 2019, Réus et al. 2019, Bollinger et al. 2017, Wang et al. 2017, Cohen et al. 2016, Delpech et al. 2016). Chronic stress also altered microglial function by activating the P2X7 receptor, which induced the NLRP3 inflammasome thus increasing levels of mature IL-1 β within the brain (Pan et al. 2014, Yue et al. 2017).

Since microglia play vital roles in brain development and homeostasis including neurogenesis, synaptic formation and elimination (Tay et al. 2017b, Salter and Beggs 2014, Hong et al. 2016), their dysfunction could explain some of the neurological deficits observed after exposure to stress. Studies using RT-PCR from isolated microglia show that steroid hormone receptors, such as the glucocorticoid receptor, are abundant in microglia (Sierra et al. 2008), suggesting the possibility that stress could directly impact microglial function through glucocorticoid signaling. Indeed, a line of evidence suggests that stress can impact microglial proliferation, while blocking corticosterone synthesis or glucocorticoid receptor activity restored normal microglia density in mice (Nair and Bonneau 2006, Duque and Munhoz 2016). There is evidence that stress later in life can also induce changes in microglia, especially when these cells are primed by an environmental insult either prenatally or during early postnatal development (Catale et al.

2020). For instance, mice that were susceptible to repeated social defeat had microglial transcriptomes that were enriched for markers of phagocytosis, pro-inflammatory responses and reactive oxygen species compared to mice that were either resistant or not exposed to stress (Lehmann et al. 2018). Additionally, mice that were sensitive to repeated social defeat showed an increase in markers for extracellular matrix remodeling and BBB leakage, which coincided with an enhanced permeability of the BBB to a fluorescent tracer, and correlated with increased microglial phagocytosis of neuronal material (Lehmann et al. 2018, Stankiewicz et al. 2015). Additionally, microglial depletion by the CSF1R antagonist PLX5622 in a repeated social defeat mouse model protected against the behavioral abnormalities and prevented an increase in reactive oxygen species in the mPFC, nucleus accumbens and paraventricular nucleus (Lehmann et al. 2019). Together, these data support that microglia play a vital role in stress-induced neuropathology by becoming more phagocytic, inducing the inflammasome and engulfing neuronal material.

Psychosocial stress might be more preventable than the other risk factors for SCZ. Reducing psychosocial stress in expecting mothers and young children or combating stress with exercise, nature exposure, yoga, or therapy could be used in individuals at risk for or diagnosed with SCZ (Vancampfort et al. 2011, Brannigan et al. 2019, Entringer et al. 2009). Some lines of evidence show that environmental enrichment can protect against or reverse many effects of stress, including ELS, by rescuing behavioral phenotypes, inflammatory responses, microglial function, and oxidative stress, notably in the mPFC (Dandi et al. 2018, González-Pardo et al. 2019, do Prado et al. 2016, McCreary and Metz

2016), a region implicated in SCZ (Glantz and Lewis 2000, Barch et al. 2001). However, there is conflicting evidence concerning the ability of environmental enrichment to rescue these phenotypes in severe cases of ELS (Mackes et al. 2020). Alternatively, future studies could determine if treatment with anti-inflammatory medications can protect against stress-induced neuroinflammation since microglial depletion has been shown to be protective (Lehmann et al. 2019).

1.4.7 How the peripheral immune system gains access to the CNS in schizophrenia

The link between BBB dysfunction and SCZ was first established when epidemiological studies revealed that about two-thirds of SCZ cases are diagnosed with comorbid conditions associated with deficits in endothelial cell function, such as metabolic syndrome and cardiovascular disease (Burghardt, Grove and Ellingrod 2014, Israel et al. 2011). Capillary wall endothelial cells form tight junctions with one another and are an integral component of the BBB along with pericytes, astrocytic endfeet, microglia, and the extracellular matrix that forms the basement membrane (Abbott et al. 2010, Lassmann et al. 1991, Joost et al. 2019, Bisht et al. 2016). The BBB restricts the passage of molecules between the blood and the brain to protect sensitive neural tissue from pathogens and immune molecules while allowing the passage of vital molecules such as glucose (Abbott et al. 2010). This allows the BBB to isolate the brain from peripheral immune responses; however, it has become increasingly clear that in

pathological states the ability of the BBB to isolate the CNS from harmful immunological responses is disrupted (Najjar et al. 2017, Bechter et al. 2010).

Claudin-5, expressed in brain endothelial cells, forms a major component of the BBB barrier-forming tight junctions (Greene, Hanley and Campbell 2019, Morita et al. 1999). Claudin-5 maps to a region on chromosome 22 where small deletions cause the 22q11 deletion syndrome, which is found in 30% of SCZ cases (Murphy 2002, Motahari et al. 2019). People with this syndrome are haploinsufficient for claudin-5 and have increased odds of developing SCZ (Fiksinski et al. 2018, Greene et al. 2018). A recent study showed that during acute versus chronic inflammation, levels of claudin-5 are differentially expressed (Haruwaka et al. 2019). It is still unknown if microglial phagocytosis of tight junctions is also involved in SCZ, although this finding suggests that BBB dysfunction could be mediated through a decrease of molecules involved in tight junctions or BBB permeability.

Indeed, post-mortem mPFC tissue from SCZ individuals show changes in the endothelial cell gene expression of molecules involved in tight junctions and BBB permeability. People with SCZ can be divided into subgroups based on their extent of brain and serum inflammatory markers (Fillman et al. 2016). Cases of SCZ that have higher serum pro-inflammatory markers, which include about 40% of affected people (Fillman et al. 2016), also have greater gray matter loss in the mPFC, which is thought to underlie multiple symptoms of SCZ (Zhang et al. 2016). Compared to healthy controls, SCZ cases, especially high-inflammatory cases, have increased expression of the intercellular adhesion molecules ICAM-1 and VCAM-1 in endothelial cells from the PFC

(Kavzoglu and Hariri 2013, Nguyen et al. 2018, Cai et al. 2018). ICAM-1 and VCAM-1 interact with receptors on leucocytes to allow monocyte infiltration into the brain (Hermand et al. 2000). In endothelial cell cultures, ICAM-1 expression can be induced in a dose-dependent manner by the pro-inflammatory cytokine IL-1 β (Cai et al. 2018). ICAM-1 expression has also been found to correlate with the expression of the macrophage marker CD163, and CD163-positive macrophages were found in close association with neurons in the frontal cortex of high-inflammatory SCZ cases (Cai et al. 2018). In this study, proteins that form endothelial cell tight junctions, including cadherin-5 (CDH5) and occluding (OCLN), were also upregulated in the frontal cortex (Cai et al. 2018), which highlights a compensatory mechanism to regain BBB integrity. Conversely, multiple studies have found a decreased expression of CDH5 in the PFC of SCZ individuals, while genetic knockdown of CDH5 in mouse PFC led to BBB disruption and changes in behavior including deficits in learning, memory, sensorimotor gating, and anxiety-like behavior (Greene et al. 2018, Nishiura et al. 2017). The expression of tight junction genes could differ depending on the time point during SCZ progression, such that compensatory mechanisms could be elicited in later disease stages. In addition, the conflicting evidence for a leaky BBB in SCZ suggest that the BBB is compromised in only a subset of SCZ cases. The finding of subgroups of people with SCZ showing variable levels of systemic inflammation support this hypothesis. Together, these findings reveal the importance of studying subgroups of SCZ patients, based on systemic inflammation, to gain a more comprehensive understanding of the disease pathogenesis.

In addition to endothelial cells, pericytes and astrocytes have also been implicated in BBB dysfunction during systemic inflammation (Nishioku et al. 2009, Fabry et al. 1993, Banks, Kovac and Morofuji 2018, Chen et al. 2017). There is some evidence that pericytes can exit the perivascular space in response to LPS-induced inflammation in mice, while the extent of pericyte detachment correlated with microglial reactivity (Nishioku et al. 2009). Pericytes secrete cytokines, including IL-1 and IL-6, which are capable of disrupting endothelial cell tight junctions (Fabry et al. 1993). Disruption of the BBB in several mouse models of neuropsychiatric or inflammatory diseases has been shown to affect microglial function, while dynamic neuroimmune interactions were described at the BBB in both health and diseased states (Borjini et al. 2019, Merlini, Davalos and Akassoglou 2012, Haruwaka et al. 2019). Although causal evidence is needed, multiple studies have found that microglial reactivity worsens BBB integrity in pathological states and that administration of the anti-inflammatory drug minocycline can improve BBB function (Shigemoto-Mogami, Hoshikawa and Sato 2018, Yenari et al. 2006, da Fonseca et al. 2014). More work is still needed to understand whether or how the interplay between BBB dysfunction and microglia abnormalities contribute to the pathogenesis of SCZ. Complex cytokine signaling between the pericytes, endothelial cells, astrocytes and microglia is crucial for the development and maintenance of BBB integrity (Banks et al. 2018, Chen et al. 2017). Lastly, it was suggested that PFC hypoconnectivity in SCZ might result from altered blood flow regulated by pericytes, together with abnormalities in the structures of capillaries and astrocytic end feet (Uranova et al. 2010). As such, understanding the complex interactions between cell-

types of the neurovascular unit and how they might be altered in response to inflammation in SCZ will likely be important.

Abnormal activity in multiple brain networks and regions are observed in SCZ (Uhlhaas 2013). There is clear evidence that excitatory circuits are altered in SCZ (Uhlhaas 2013, Glantz and Lewis 1997, Glantz and Lewis 2000). Blockade of N-methyl-D-aspartate receptors (NMDARs) in healthy subjects leads to psychotic symptoms and cognitive deficits that resemble those observed in SCZ (Balu 2016). Additionally, both mRNA and protein levels of the NMDA subunits NR1 and NR2C are decreased in post-mortem SCZ brain tissue (Weickert et al. 2013). Recent evidence suggests that NMDAR function might be inhibited in SCZ by autoantibodies, which are produced against an organism's own tissue and are implicated in autoimmune disorders such as lupus (Becker et al. 2019). Circulating autoantibodies against glutamate and NMDARs were found to be present in approximately 20% of psychotic SCZ patients (Jézéquel et al. 2017). An increased BBB permeability might alter neuronal function by allowing the entry of autoantibodies against NMDARs into the brain, which have been shown in mouse models and neuronal culture experiments to suppress glutamatergic activity by altering the organization of NMDARs and their anchoring molecule ephrin-B2 (Jézéquel et al. 2017, Kannan et al. 2017, Kayser and Dalmau 2016). Studies that interrogate specific cell-type and neural circuit responses will allow greater understanding of the impact of BBB permeability on brain function and open new opportunities to therapeutically modulate these pathways.

Beyond the BBB, peripheral inflammatory responses can gain access to the CNS via the meninges, the multi-layered protective tissue that surrounds the brain and spinal cord (reviewed in (Rustenhoven and Kipnis 2019)). Cytokines can accumulate in the dural CSF and cross into the brain, passing between endothelial cells that lack tight junctions (Louveau et al. 2015). Additionally, cytokine signaling specifically within the meninges has been shown to alter neuronal function by binding directly with receptors on neurons in frontal cortical regions and altering cognitive and social behaviors in mice (Derecki et al. 2010, Filiano et al. 2016). Meningeal T-cell production of multiple inflammatory molecules, including IL-17, IL-4, and INF- γ , have been shown to alter both excitatory and inhibitory circuitry and modulate cognitive function and social behavior (Ribeiro et al. 2019, Derecki et al. 2010, Filiano et al. 2016). Lastly, the CNS meningeal lymphatic system also offers a route for peripheral-central immune crosstalk. Since the brain does not contain a resident lymphatic system, waste removal is facilitated by cerebrospinal fluid draining through the meninges into the deep cervical lymph nodes, where interactions between CNS immune molecules and peripheral immune cells can occur (Louveau et al. 2015, Louveau et al. 2018). In this manner, the peripheral immune system can gauge central immune status. In the aging brain, dysfunction of the meningeal lymphatic vessels leads to accumulation of harmful amyloid beta-protein toxicity and increase Alzheimer's pathology (Da Mesquita et al. 2018). Longitudinal imaging studies have shown that progressive brain matter loss is consistent with accelerated aging in patients with SCZ (Schnack et al. 2016). It remains to be determined whether therapeutic agents that boost lymphatic function by either increasing the diameter of the lymphatic

vessels or cerebral spinal fluid drainage (Da Mesquita et al. 2018) could improve the cognitive and social deficits observed in SCZ.

1.4.8 Future directions for understanding and targeting the immune system in schizophrenia

There is growing evidence from both human and animal studies that many of the risk factors for SCZ converge on their ability to promote neuroinflammation, and that these effects are mediated in part by microglia. However, is there a pro-inflammatory phenotype in SCZ? Post-mortem and clinical studies show an increase in pro-inflammatory markers in people with SCZ compared to controls (Sekar et al. 2016, Fillman et al. 2016, Boerrigter et al. 2017, Goldsmith and Rapaport 2020, Pedraz-Petrozzi et al. 2020, Lesh et al. 2018). Moreover, there is evidence for elevated levels of cytokines in blood samples from people with SCZ, whether they are medication-naive or receiving antipsychotic treatment, during episodes of psychosis (Mondelli et al. 2020, McKernan et al. 2011, De Picker et al. 2019, Steiner et al. 2020). Thus, such studies suggest that inflammation might contribute to the development of SCZ and also drive its progression and cyclic nature.

SCZ cases can be sub-divided using either serum or post-mortem brain tissue levels of pro-inflammatory cytokines, which reveal that about 40% of SCZ cases have a high inflammatory expression signature (Boerrigter et al. 2017, Fillman et al. 2016, Cai et al. 2018). Although these studies suggest there are subtypes of SCZ patients, they do not

provide information on their inflammatory states earlier in the disease development nor do they assay inflammation in the brain, which could differ from blood or CSF biomarkers of inflammation. There has been some success in longitudinal PET imaging studies that measure expression of translocator protein (TSPO), a non-specific marker of pro-inflammatory microglia, in the brain (Selvaraj et al. 2018). These studies show that SCZ is characterized by increased TSPO expression, which correlated with greater gray matter loss (Selvaraj et al. 2018). However, there have been mixed results concerning PET measurements of TSPO with some studies showing increased TSPO binding in SCZ (Doorduyn et al. 2009, Bloomfield et al. 2016) and others showing no correlation (Di Biase et al. 2017, Notter et al. 2018). Additionally, recent work revealed that neuronal activity can also drive the expression of TSPO (Notter et al. 2020). It is thus not clear if TSPO is a reliable marker for neuroinflammation (Sneeboer et al. 2020). The identification of more specific *in vivo* markers for neuroinflammation would be useful. Ideally, additional work should be done to specifically interrogate the extent of neuroinflammation in SCZ, in addition to peripheral inflammation, to determine if increased inflammation correlates with all or only a percentage of SCZ cases.

Given that SCZ is a highly heterogeneous disease, it is not surprising that there are different disease subtypes. Studies that have divided individuals with SCZ based on inflammatory markers have found more severe symptomology in those with higher levels of pro-inflammatory markers. Specifically, there is evidence for greater gray matter loss and poorer performance in language tasks (Fillman et al. 2016) and increased depressive symptoms (Bossù et al. 2015) in SCZ cases characterized by high inflammatory state.

Consistent with this, therapeutics that reduce inflammation provide the greatest symptom improvement in neuropsychiatric cases associated with high inflammation. For example, inhibition of TNF was shown to improve symptoms in people with major depression, but only in those with heightened immune biomarkers (Weinberger et al. 2015, Raison et al. 2013). Additionally, various anti-inflammatory agents including aspirin, estrogen, N-acetylcysteine, COX-2 inhibitors, minocycline and fatty acids (Sommer et al. 2014) have been shown to improve symptom severity in SCZ, but there are some mixed findings of the efficacy of these therapeutics. Minocycline has been shown to reduce microglia and complement-dependent synapse removal in an in vitro model from patient-derived neuronal cultures while decreasing the risk for SCZ when administered to young adults (Sellgren et al. 2019), suggesting that targeting synaptic pruning via neuroinflammation would be therapeutic for SCZ and might directly target the disease process. Nevertheless, it is possible that there are discrepancies concerning the ability of some of these drugs to improve symptoms in SCZ because they might only be effective in high-inflammatory cases. Future work aiming to elucidate the differences between subtypes of SCZ could potentially allow for the development of more effective and targeted therapeutics. Although people with SCZ can be divided based on extent of inflammation, there is no denying the role of the immune system in this complex disease.

In line with this, microglia are significantly altered in SCZ and contribute to neural dysfunction by responding and contributing to neuroinflammatory signaling. In SCZ post-mortem tissue, microglia have been noted to have altered morphologies and densities in brain regions known to contribute to the symptomology of SCZ. Microglia

engulfment of synaptic material is essential for the normal wiring of the brain and can contribute to pathological states when mis-regulated (Filipello et al. 2018, Vainchtein et al. 2018, Weinhard et al. 2018, Tremblay, Lowery and Majewska 2010, Wake et al. 2009, Paolicelli et al. 2011, Schafer et al. 2012, Comer et al. 2020, Dejanovic et al. 2018).

There is also evidence that microglia contribute to synapse formation during development, adolescence and into adulthood (Akiyoshi et al. 2018, Weinhard et al. 2018, Miyamoto et al. 2016, Parkhurst et al. 2013). Additionally, a two-photon in vivo imaging study in awake mice has shown that microglial contacts with synapses increase synaptic activity thus enhancing neuronal network synchronization (Akiyoshi et al. 2018). In this study, when MIA was induced with poly(I:C), microglia became reactive while neuronal synchronization decreased (Akiyoshi et al. 2018), suggesting that microglia contribute to network function and that their role in this process can be easily disrupted by immune responses.

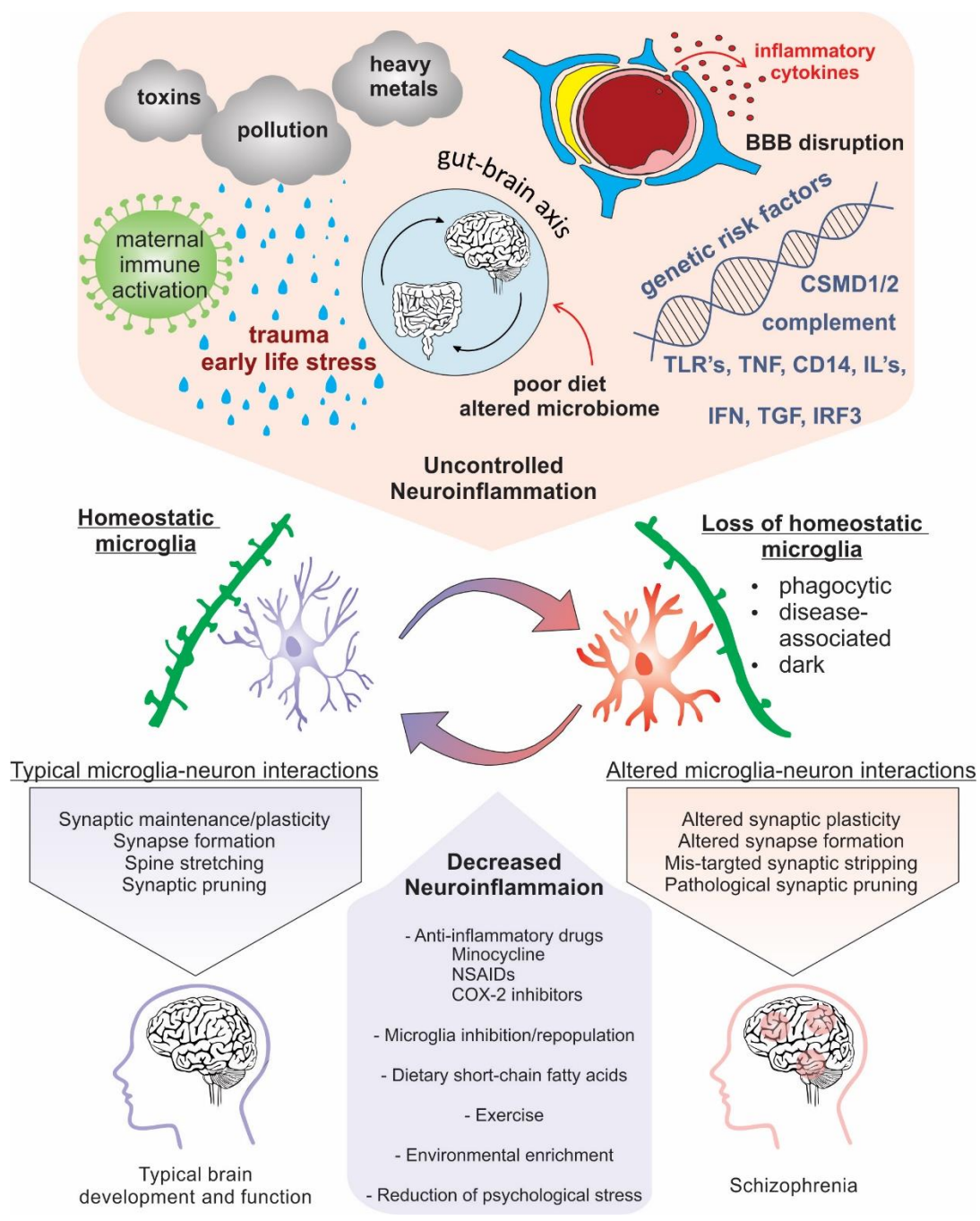


Figure 1.3: Summary of the pathogenic mechanisms of schizophrenia covered in this chapter, which involve microglial alteration induced by neuroinflammation

Risk factors for SCZ that enhance neuroinflammation include pollution, nutrition induced gut-brain axis dysbiosis, viral infection, maternal immune activation, genetic predisposition and cytokine secretion. The increase in neuroinflammation leads to changes in microglial function. In their homeostatic state, microglia perform their immune sentinel role by interacting with neurons to guide circuit wiring during development. In an increase inflammatory milieu, there is a loss of microglial homeostasis where microglia-neuron interactions are disturbed, causing altered plasticity, as well as synaptic formation, synaptic stripping, and pruning. In turn, therapeutic approaches that reduce neuroinflammation via anti-inflammatory drugs, microglial inhibition and repopulation, improved nutrition, environmental enrichment and/or prevention of psychological stress, which promote the return of microglia to their homeostatic roles, could be potentially exploited to limit SCZ-associated exacerbations. Note: Figure made by Ashley Comer as part of Comer et al., *Frontiers in Cellular Neuroscience*, in press.

Although there is evidence that microglia contribute to excessive synaptic pruning in SCZ, it is not clear if microglia-dependent synapse formation is also altered. Since much of the data collected from individuals with SCZ is from post-mortem samples, it is difficult to discern what is occurring on the synaptic level earlier in development. Recent studies suggest that more immature spine types can be differentially targeted in SCZ (Comer et al. 2020, MacDonald et al. 2017), therefore, it is possible that synapse formation mediated by microglia is also altered in SCZ. In a prenatal ventral hippocampus lesion model for SCZ, microglia displayed altered density, morphology and ultrastructure, together with increased expression of multiple complement genes including C1q and C3 (Hui et al. 2019). This increase in microglial expression of complement proteins coincided with an increase of synaptic pruning in the PFC and behavioral deficits in rats, but was reversed by administration of minocycline (Hui et al. 2019). These studies highlight the necessary role exerted by microglia in normal brain

development but also show their ability to drive neuroinflammation and contribute to pathology in disease states.

Indeed, there are multiple disease-associated microglial subtypes such as those seen in neurodegenerative disorders (Deczkowska et al. 2018) and dark microglia which were recently observed in SCZ post-mortem brain samples (Uranova et al. 2018). More work is needed to fully understand microglial subtypes that are more prevalent in disease states and how they contribute together to pathology, however data suggest they partially contribute to disease by enhancing synaptic pruning (Stratoulis et al. 2019). Future studies should also aim to develop more translational animal models so that in vivo studies can be performed to gain greater understanding into how microglia functionally impact synaptic development and circuit function in pathological states.

Although there is no doubt that the immune system plays a critical role in shaping brain development and contributes to disease states when dysregulated, there is a need to understand which specific circuits and neuromodulatory systems in particular are most impacted by abnormal immune signaling. It is clear that complement proteins facilitate the removal of synapses (Stevens et al. 2007) and that the upregulation of complement proteins contributes to circuit miswiring (Comer et al. 2020). However, SCZ is also characterized by alterations in inhibitory circuits (Dienel and Lewis 2019), neuromodulatory systems such as dopamine (Howes et al. 2017) and glutamate (Uno and Coyle 2019), and changes in the connectivity between brain regions such as the hippocampus and PFC (Sigurdsson and Duvarci 2015). Do inflammatory responses alter specific neurotransmitter systems and networks differentially?

There is evidence that inflammatory responses target specific neuromodulatory systems and brain circuits. For example, changes to the gut microbiome driven by inflammation can alter the production of serotonin (Rogers et al. 2016), which is known to be disrupted in SCZ. Interestingly, MIA in rats has been found to increase the levels of dopamine in both the nucleus accumbens and mPFC (Luchicchi et al. 2016) of offspring, which is well-known to play a role in the positive symptoms of SCZ (Kesby et al. 2018). Additionally, MIA initially triggers hyperinhibition and neuronal miswiring, before leading to a reduced inhibitory drive (Thion et al. 2019). ELS in mice was shown to alter HPA circuitry development, in addition to hippocampal and PFC function (Brenhouse, Danese and Grassi-Oliveira 2019). In addition, ELS is known to have an impact on inhibitory connectivity (Ohta et al. 2020, Goodwill et al. 2018), and previous work suggests that oxidative stress and/or neuroinflammation might underlie the changes in parvalbumin interneurons in response to ELS (Brenhouse et al. 2019, Holland et al. 2014). There is evidence for parvalbumin interneuron dysfunction in SCZ, as they have altered density in the frontal cortex of individuals with SCZ (Kaar et al. 2019). Interestingly, the meninges modulate cortical interneuron migration during development (Borrell and Marín 2006); future work could interrogate whether changes in meningeal signaling, such as immune molecule signaling, could contribute to alterations in interneuron migration in SCZ. Although these studies suggest that risk factors for SCZ can exert specific effects on different CNS circuits, more work is needed to fully understand the mechanisms by which inflammation alters specific neuromodulatory systems and circuits. Studies that combine mouse models of SCZ and inflammation with

whole-brain or mesoscopic imaging could shed light into how specific neuronal networks are impaired in SCZ (Grandjean et al. 2020, Boido et al. 2019, Sofroniew et al. 2016).

It is well-established that spine dysfunction is present in SCZ and is at least partially mediated by reductions in excitatory synaptic connectivity and plasticity (Berdenis van Berlekom et al. 2020, Glantz and Lewis 2000, Glausier and Lewis 2013). However, most of the work in this field has relied on human post-mortem tissue, so there is limited knowledge of what could be occurring earlier in development to drive these synaptic alterations. Recent work has highlighted the fact that the immune system works closely with the CNS to establish and refine neural circuits in healthy states as a part of normal development (Tay et al. 2017b, Hammond et al. 2018, Paolicelli et al. 2011). However, when this process is dysregulated, it can lead to pathology and the miswiring of the brain through synaptic loss (Schafer et al. 2012, Comer et al. 2020), which occurs in SCZ.

How are certain synapses selectively removed while others are protected? In the developing brain, there is a period of intense synaptogenesis followed by critical developmental periods characterized by experience-dependent refinement of synapses (Trachtenberg et al. 2002, Holtmaat and Svoboda 2009). Synaptic elimination driven by sensory experience refines brain circuitry by optimizing connections between neurons. In SCZ, this process is thought to be dysregulated, thus leading to a loss of both excessive and necessary synapses, causing aberrant brain connectivity. Recent data suggest that more immature spine types, such as filopodia and thin spines (Cruz-Martín, Crespo and Portera-Cailliau 2012), are lost while larger, more established spines remain intact in

SCZ (MacDonald et al. 2017). A similar phenotype was seen in mice overexpressing the mouse homologue of the SCZ-associated gene C4. In this in vivo model, synaptic loss observed in the PFC was specifically due to a loss of smaller spine-types while mushrooms spines were unaffected (Comer et al. 2020). This evidence is in line with previous work showing that complement-dependent synapse removal is activity-dependent and that connections with less activity are more likely to be eliminated (Schafer et al. 2012). Small spines were also shown to be preferentially contacted and eliminated upon microglial contact in vivo (Tremblay et al. 2010). Additionally, it has been suggested that immune signaling is able to protect more mature spines. There is increased expression of the “don’t eat me” signal CD47 at synaptic inputs that are more active (Lehrman et al. 2018). In this way, the immune system would guide synaptic wiring by tagging synapses for removal while protecting other connections that are essential to the function of a circuit. However, more work is needed to support this idea and understand the mechanisms by which the immune system contributes to synapse-specific elimination versus stabilization.

It is also possible that in SCZ, spine loss is driven by the inability of circuits to produce “appropriate” connections. Therefore, the subsequent excessive pruning that occurs in SCZ could be due to the fact that neurons fail to produce adequate connections in the first place. This is relevant in the context of microglia since they regulate synaptogenesis (Miyamoto et al. 2016). Since most of the data obtained from people with SCZ is limited to post-mortem tissue, our information about what is happening on the circuit and synaptic level during development is limited. In this scenario, using mouse

models to understand the role of microglia and immune signaling in synapse formation during the first weeks of postnatal development, when most synaptogenesis occurs (Cruz-Martín, Crespo and Portera-Cailliau 2010), is key. Future advances in the resolution and capabilities of in vivo human imaging studies notably through specific markers could help answer this question. It is encouraging that previous studies show a similar phenotype in mice that is seen in humans in terms of weaker synapses preferentially being eliminated (MacDonald et al. 2017, Comer et al. 2020). This could allow for studies in mice that more readily translate to humans. Understanding the mechanisms of complement-mediated circuit wiring is a worthwhile area of future study given it is both a mechanism of normal brain development and is implicated in multiple neurodevelopmental and neurodegenerative diseases. Lastly, enthusiasm has grown over the last decade to study marmosets in neuroscience research and an increase in the feasibility of genetic manipulations could provide a more relevant model to study how abnormal neuroimmune signaling contributes to SCZ (Okano et al. 2016, Servick 2018).

Here, I have highlighted the diverse risk factors for SCZ and how they impact the CNS by altering immune signaling. Likely, these risk factors act additively on certain signaling pathways to push vulnerable individuals past a certain threshold into a disease state. This field would benefit from future studies that aim to elucidate how the immune system regulates specific circuits and neuromodulatory systems to drive the diverse phenotypes observed in SCZ. Additionally, an in-depth understanding of the specific signaling networks compromised in SCZ may enable the restoration of typical immune-

driven neurodevelopment after exposure to the various genetic and environmental risk factors described in this section.

1.5 Linking complement proteins to aberrant circuit development in schizophrenia

Despite significant progress in this field, it is still not clear how reciprocal interactions between neurons and microglia contribute to the maturation and refinement of developing cortical circuits (Tremblay et al. 2010, Hoshiko et al. 2012, Miyamoto et al. 2016). Mouse studies investigating the role of C4 and other complement proteins in synaptic refinement have relied on loss-of-function manipulations (Sekar et al. 2016, Stevens et al. 2007, Schafer et al. 2012, Martinelli et al. 2016), whereas SCZ is linked to increased C4 expression (Sekar et al. 2016). Additionally, previous studies have focused on the role of complement proteins in the visual system (Sekar et al. 2016, Stevens et al. 2007, Schafer et al. 2012) rather than interrogating their role in more SCZ-relevant brain regions, such as the PFC. Thus, overall, it is not known how increased C4 expression impacts the development of cortical microcircuits, which are commonly altered in neurodevelopmental disorders (Meredith 2015, Del Pino et al. 2018).

Herein, the role of the immune system in the pathophysiology of SCZ is detailed, describing how environmental and genetic risk factors converge to cause uncontrolled neuroinflammation in this neurodevelopmental disease. To systematically study the effects of an overactive immune system on brain

development, I investigated the effects of C4 overexpression on developing networks in layer (L) 2/3 of the mouse medial prefrontal cortex (mPFC), a cortical region where gray-matter loss is most prominent in SCZ (Glantz & Lewis 2000, Thompson et al. 2001). I show that C4 overexpression induced transient structural and functional changes to L2/3 excitatory neurons in the mPFC. Additionally, I interrogated the role of microglia in complement-induced wiring deficits in the mPFC by measuring microglia engulfment of synaptic material. The relationship between C4-induced PFC circuit dysfunction and abnormalities in rodent social behavior was examined. Lastly, a technical pipeline is described to enable the study of novel disease-associated genes in rodents without the reliance on genetic animal lines, which can be costly and time-consuming to create. Taken together, these results link C4 overexpression to neural and behavioral deficits relevant to SCZ and identify a critical window in which the trajectory of brain development might be able to be therapeutically targeted in SCZ.

CHAPTER TWO

Materials and methods

2.1 Ethics statement

All experimental protocols were conducted according to the National Institutes of Health (NIH) guidelines for animal research and were approved by the Boston University Institutional Animal Care and Use Committee (IACUC; protocol #17–031).

2.2 Animals

All mice were group housed on a 12-hr light and dark cycle with the lights on at 7 AM and off at 7 PM and with food and water ad libitum. Offspring were housed with dams until weaning at postnatal day 21 (P21). For spine density and morphology, microglia engulfment, electrophysiology, and behavior experiments, wild-type CD-1 mice of both sexes from age 7 to 70 d were used (CD-1 IGS; Charles River; strain code: 022). For in situ hybridization, C4b knockout (KO) mice in a C57BL/6 genetic background (The Jackson Laboratory, stock number: 003643) and wild-type C57BL/6 mice of both sexes at age P30 were used (Charles River; strain code: 027). Males and females were used for all experiments, and no differences were found between sexes.

2.3 DNA constructs

For control conditions, we used a plasmid containing EGFP under the CAG promoter (pCAG-EGFP, Addgene plasmid #11150) (Matsuda & Cepko 2004). DNA sequences containing mC4b (NM_009780.2, synthesized by Genescript) and hC4A (RC235329, Origene) were subcloned (InFusion Kit, Clontech) into the pCAG backbone to produce pCAG-mC4 and pCAG-hC4A, respectively (See Table 2.2 for primers used to subclone). Endogenous PSD-95 was fluorescently labeled *in vivo* using PSD95-FingR (EF1a-PSD95.FingR-RFP) which tags endogenous PSD-95 protein using a Fibronectin scaffold with mRNA display which acts as an antibody-like protein to tag a specified target (Gross et al. 2013). For electroporations with RFP and fusion C4-GFP, pCAG-mRFP was obtained from Addgene (Addgene plasmid #28311) (Manent et al. 2009), and C4-GFP was made by inserting GFP from the pCAG-GFP plasmid C terminus to C4 using a GSSGSS linker (subcloned by Genescript). All plasmid DNA was purified using the ZymoPureII (Zymo Research) plasmid preparation kit and were resuspended in molecular biology grade water.

2.4 Antibodies and histology

Mice were administered a lethal dose of sodium pentobarbital (250 mg/kg; IP) before being transcardially perfused with PBS and then 4% paraformaldehyde (PFA) solution. After brains were dissected and postfixed for 24 hr in 4% PFA solution, they were transferred to a 30% (w/v) sucrose solution and stored at 4°C. Coronal sections were cut on a sliding microtome (Lecia SM2000) at different thicknesses appropriate for

each experiment (see specific methods). For immunostaining, tissue was blocked and permeabilized in 10% donkey serum with 0.25% TritonX100. Sections were incubated with primary antibodies (see antibody table for dilutions) overnight at 4°C on a shaker and with secondary antibodies for 2 hr at room temperature. After incubation periods and between each step, sections were rinsed three times with PBS for 10 min. Depending on the experiment, the following primary antibodies were used: guinea pig anti-Iba1 (Synaptic Systems, 234004), rat anti-CD68 (Bio-Rad, MCA1957GA), rabbit anti-RFP (Rockland, 600-401-379), mouse anti-PSD95 (BioLegend, clone K28/43), guinea pig anti-Synaptophysin 1 (Synaptic Systems), rabbit anti-C4 (Biogen, 931–946), and Beta-Actin HRP-conjugate (Sigma, clone AC-15). The following secondary antibodies (see antibody table) were used: donkey anti–guinea pig Alexa Fluor 594 (Jackson Laboratories, 706-545-148), donkey anti–guinea pig Alexa Fluor 488 (Jackson Laboratories, 706-585-148), donkey anti-rabbit Alexa Fluor 647 (Jackson Laboratories, 711-605-152), llama anti–guinea pig Atto 647 (Progen: 80308), donkey anti-rat 488 (Invitrogen: A21208), donkey anti-rabbit 594 (Jackson Laboratories, 711-585-152), and donkey anti–guinea pig 647 (Jackson Laboratories, 711-605-152). Brain sections were subsequently mounted onto microscope slides (Globe Scientific) using Fluoromount-G mounting medium with DAPI (Thermo Fisher Scientific).

Antibody	Supplier	Dilution
guinea pig anti-Iba1	Synaptic Systems: 234-004	1:500
rat anti-CD68	Bio-Rad: MCA1957GA	1:500
rabbit anti-RFP	Rockland: 600-401-379	1:1000
mouse anti-PSD95	BioLegend: K28/43	1:1000
rabbit anti-C4	(House made) Biogen: 931–946	1:500-1:1000

guinea pig anti-Synaptophysin 1	Synaptic Systems: 101-004	1:500-1:1000
Beta-Actin HRP-conjugate	Sigma: AC-15	1:1000
donkey anti-guinea pig Alexa Fluor 594	Jackson Laboratories: 706-545-148	1:1000
donkey anti-guinea pig Alexa Fluor 488	Jackson Laboratories: 706-585-148	1:1000
donkey anti-rabbit Alexa Fluor 647	Jackson Laboratories: 711-605-152	1:1000
llama anti-guinea pig Atto 647	Progen: 80308	1:1000
donkey anti-rat 488	Invitrogen: A21208	1:1000
donkey anti-rabbit 594	Jackson Laboratories: 711-585-152	1:1000
donkey anti-guinea pig 647	Jackson Laboratories: 711-605-152	1:1000

2.5 In utero electroporation

L2/3 progenitor cells in the mPFC were transfected via *in utero* electroporation (IUE) (Szczerkowska et al. 2016). pCAG-EGFP was electroporated in the control condition, and pCAG-EGFP plasmid was co-electroporated with either pCAG-mC4 or pCAG-hC4A plasmids for the mC4 or hC4 groups, respectively. Prior to surgery, all tools were sterilized by autoclaving. Aseptic techniques were maintained throughout the procedure, and a sterile field was prepared prior to surgery using sterile cloth drapes. Animals were weighed, and a combination of buprenorphine (3.25 mg/kg; SC) and meloxicam (1–5 mg/kg; SC) was administered as a preoperative analgesic. Timed-pregnant female CD-1 mice at E16 were anesthetized by inhalation of 4% isoflurane and maintained with 1%–1.5% isoflurane via mask inhalation. The abdomen was sterilized with 10% povidone-iodine and 70% isopropyl alcohol (repeated 3 times) before a vertical

incision was made in the skin and then in the abdominal wall. The uterine horn was then exposed to allow injection of 0.5–1.0 μl of DNA solution (containing 1 $\mu\text{g}/\mu\text{l}$ plasmid and 0.1% Fast Green) into the lateral ventricles using a pressure-injector (Picospritzer III, Parker Hannifin) with pulled-glass pipettes (Sutter Instrument, BF150-117-10). To target L2/3 progenitor cells in PFC for imaging and electrophysiological experiments, a custom-built triple electrode probe (Szczyrkowska et al. 2016) was placed by the head of the embryo, with the negative electrodes placed near the lateral ventricles and the positive electrode placed just rostral of the developing PFC. For bilateral IUEs used in behavioral experiments, plasmid DNA (1 $\mu\text{g}/\mu\text{L}$) was injected into both lateral ventricles by positioning the glass pipette at a 90° angle relative to the midline of the embryo's head and injecting 2–4 μl of DNA solution. These modifications ensured that the DNA solution would travel to the lateral ventricle contralateral to the injection site. Next, four square pulses (pulse duration: 50 ms, pulse amplitude: 36 V, interpulse interval: 500 ms) were delivered to the head of the embryo using a custom-built electroporator (Bullmann et al. 2015). Embryos were regularly moistened with warmed sterile PBS during the surgical procedure. After electroporation, the embryos and uterine horn were gently placed back in the dam's abdominal cavity and the muscle and skin were sutured (using absorbable and nonabsorbable sutures, respectively). Finally, the dams were allowed to recover in a warm chamber for 1 hr and then returned to their cage.

2.6 Imaging

Fluorescence images were collected using an inverted laser scanning confocal microscope (Nikon Instruments, Nikon Eclipse Ti with C2Si+ confocal) controlled by NisElements (Nikon Instruments, 4.51) including four laser lines (405, 488, 561, and 640 nm). For M-FISH and microglia experiments, confocal images were taken with a 60X Plan Apo objective (Nikon Instruments; Plan Apo, NA 1.4, WD: 0.14 mm, oil objective) using $1,024 \times 1,024$ pixel scans (pixel size = $0.27 \times 0.27 \mu\text{m}$). For dendritic spine imaging, images from P7–9, P14–16, P21–23, and P55–60 brain tissue were taken using a 40X Plan Apo λs objective (Nikon Instruments; Plan Apo, NA 1.3, WD: 0.2 mm, water objective) using $1,024 \times 1,024$ pixel scans (pixel resolution = 0.12). We imaged apical dendritic tufts in L1 and basal dendrites in L2/3. For dendritic spine imaging and neuronal reconstructions, we collected ROIs that consisted of stacks of images (approximately 20–40 optical sections, z-step = $0.3 \mu\text{m}$ and $1 \mu\text{m}$, respectively). The area and diameter of neurons were analyzed in 40X images from the brightest z-plane of the soma. Brain sections from behavior mice were imaged using an upright wide-field microscope (Nikon Instruments, Nikon Eclipse Ni) controlled by NisElements (Nikon Instruments, 4.20) using a 10X objective (NA: 0.3, WD: 16 mm). DAPI and GFP-transfected cells in behavior brains were imaged using fluorescence filters for BFP (excitation: 370–401, dichroic: 420) and GFP HC (excitation: 470/40, dichroic: 495). Images in all conditions were collected using the same imaging conditions and exposure settings. Imaged stacks were imported in TIFF format into ImageJ (NIH). For confocal image analysis, we only measured neurons and glia in the anterior cingulate cortex and

prelimbic, infralimbic, and medial orbital divisions of the mPFC. For behavior brain analysis, all GFP-positive cells were counted to quantify the extent of electroporation.

2.7 Multiples fluorescence in situ hybridization

For M-FISH experiments, P21 and P30 brains were collected and immediately fresh-frozen on dry ice in O.C.T. compound (Fisher HealthCare, 23-730-571). Tissue was cut on a cryostat (Leica CM 1800) at 15- μ m thickness, and M-FISH experiments were completed by using a commercial assay (RNAscope, Advanced Cell Diagnostics). In situ fluorescent probes were used to detect mC4 (#445161-C1), EGFP (#400281-C2), and CaMKII α (#445231-C3). M-FISH assay and all reagents were obtained from Advanced Cell Diagnostics. All M-FISH experiments had N = 3 mice per condition. For in situ analysis, we quantified fluorescent signal from L2/3 CaMKII α ⁺ cell bodies of transfected GFP⁺ cells and their untransfected neighbors in mC4 conditions from single z-planes of 60X confocal images. This approach allowed us to control for variability of transcript expression between mice. We use the DAPI signal to identify the cell's nucleus, and all quantification of in situ signals was performed in the soma's brightest focal plane. CaMKII α signal was used to delineate the perimeter of the cell body of L2/3 excitatory neurons in the mPFC and this ROI was used for analysis. Transfected cells were identified by presence of GFP mRNA, and nontransfected cells were GFP (-). Next, fluorescent signals from GFP and C4 transcripts were thresholded and binarized. The binarized signal was then used to calculate the percentage of soma area covered by GFP

or C4 mRNA. We used the same binarization threshold and analysis procedure for both conditions.

2.8 Quantitative polymerase chain reaction

Animals at P21 or P60 were anesthetized with 4% isoflurane/oxygen (v/v). Brains were rapidly extracted following transcardiac perfusion using NMDG slicing solution: 92 mM NMDG, 2.5 mM KCl, 1.25 mM NaH₂PO₄, 30 mM NaHCO₃, 20 mM HEPES, 25 mM glucose, 2 mM thiourea, 5 mM Na-ascorbate, 3 mM Na-pyruvate, 0.5 mM CaCl₂·2H₂O, and 10 mM MgSO₄·7H₂O. Sections (200 μm) were cut on a vibratome (LEICA VT1000 S) and kept in the NMDG slicing solution bubbled with 95% O₂/5% CO₂ (295–305 mOsm). The sections were trimmed under a wide-field microscope to isolate the transfected region (containing GFP⁺ cells) of the tissue. Each trimmed piece was flash frozen in dry ice. RNA was extracted from these tissue using Zymo Microprep kit (R1050), and cDNA was synthesized with Azuraquant cDNA synthesis kit (AZ-1997). RNA and cDNA were quantified using a Thermo Fisher Scientific NanoDrop One Spectrophotometer. Primer sets for qPCR were designed using NCBI primer blast (NIH) and were synthesized by Integrated DNA Technologies. Primer sets (Table 3.1) were verified to produce a single product following PCR amplification using Apex Taq RED Master Mix, 2.0X (Genesee Scientific 42–138) on a Bio-Rad T100 thermocycler. qPCR was carried out on an Applied Biosystems ABI 7900 Real Time PCR machine using AzuraView Greenfast qPCR Blue Mix HR (AZ-2401). All qPCR results were normalized

to three biologically diverse internal reference genes (GAPDH, beta-Actin, and HPRT). These references were amplified in parallel with the target genes of interest and all samples were performed in triplicates. Dissociation curves were verified for every reaction, and only dissociation curves yielding single products were used in subsequent analysis.

Gene	Primer	Sequence	Purpose
<i>GAPDH</i>	Forward	5'-CCACCCAGAAGACTGTGGAT-3'	Internal Control qPCR
	Reverse	5'-CACATTGGGGGTAGGAACAC-3'	
<i>Beta Actin</i>	Forward	5'-CCTTCC TCTTGGGTATGGA-3'	Internal Control qPCR
	Reverse	5'-TGCTAGGAGCCAGAGCAGTA-3'	
<i>HPRT</i>	Forward	5'-GGCCAGACTTTGTTGGATTT-3'	Internal Control qPCR
	Reverse	5'-CAGATTCAACTTGCGCTCAT-3'	
<i>C4b</i>	Forward	5'-ACCCCCAGTACTTGCTGGAC-3'	Mouse C4b qPCR
	Reverse	5'-ACCCTGTAGAGCAGAGCCTCTAA-3'	
<i>hC4</i>	Forward	5'- CCCGGATCCACCGGTGATCCGGTA CCGAG GAGATCTG-3'	In fusion reaction (to create pCAG-hC4)
	Reverse	5'- CATGGTGGCGACCGGTCTATTCTGA GATGA GTTTCTGCTCGAGC-3'	
<i>mC4</i>	Forward	5'- CGGGCCCGGGATCCACAGCCATGCG GCTCCT CTG-3	In fusion reaction (to create pCAG-mC4)
	Reverse	5'- CATGGTGGCGACCGGCACCTGGCAC CCCCGG-3'	

2.9 Cell culture

HEK293T cells were maintained in complete media: DMEM (HyClone) supplemented with 10% fetal bovine serum, penicillin (100 units/ml), and streptomycin

(100 $\mu\text{g/ml}$). Cells were maintained at 37°C and 5% CO₂ in a Thermo Scientific HERAcell 150i incubator. Either pCAG-GFP, pCAG-mC4, pCAG-hC4, or pCAG-mC4-GFP (5 μg each) was transfected into HEK293T cells (approximately 70%–80% confluent) grown in 10-cm culture dishes using 2.5 μL of GeneGlide (BioVision, Cat#: M1081) using serum-free media. After 4–6 hr, the transfection media was removed and replaced with complete media. Forty-eight hours after transfection, cells were imaged live in phenol red-free DMEM at room temperature using an Olympus BX51WI upright microscope with a 10X UPlanFL N (NA = 0.30) objective.

2.10 Isolation of post-synaptic densities

Post-synaptic density (PSD) fractions were isolated as described (Dejanovic et al. 2018, Wu et al. 2019) with minor modifications. Briefly, the electroporated region of the PFC was dissected and snap frozen and kept at -80°C until further processing. Pieces of brain tissue were homogenized using a Teflon homogenizer. After 1,400g, 10-min centrifugation, the supernatant was transferred to a new tube and the pellet was rehomogenized and pelleted at 1,400g, 10 min. Supernatants were combined and centrifugated at 13,800g, 10 min. The pellet was resuspended in 0.32 M Tris-buffered sucrose and ultracentrifuged into 1.2, 1.0, 0.85 M sucrose gradient at 82,500g for 2 hr. The synaptosome fraction was collected, solubilized with 0.5% Triton X-100, and then centrifuged at 32,800g for 20 min to yield the PSD fraction. Samples from individual mice were isolated separately and pooled for immunoblot analysis.

2.11 Immunoblotting

Immunoblotting was performed as previously described (Dejanovic et al. 2018) with minor modifications. Briefly, transfected HEK293 cells were directly lysed in the dish with 0.5% SDS in PBS, supplemented with complete protease inhibitor cocktail (Roche) and Benzonase Nuclease (Sigma). All protein samples were boiled in reducing SDS loading buffer and separated on Bolt Bis-Tris Plus gels (Thermo Fisher). After transfer to nitrocellulose membranes (Thermo Fisher), membranes were incubated with the following primary antibodies overnight: mouse anti-PSD-95 (clone K28/43, BioLegend), guinea pig anti-Synaptophysin 1 (Synaptic Systems), rabbit anti-C4 (in house, Biogen 931–946), Beta-Actin HRP-conjugate (clone AC-15, Sigma). HRP-conjugated secondary antibodies were from GE Healthcare. Immunoreactivity was detected on ChemiDoc XRS+ (Bio-Rad) and analyzed with Image Lab software. mC4 levels were quantified by normalizing to the loading control, vinculin.

2.12 Dendritic spine analysis

For the dendritic spine developmental time-course experiments in control, mC4, and hC4 conditions, we analyzed dendritic spines at multiple postnatal days (P7–9, P14–16, P21–23, P55–60). For all groups, we analyzed 20 dendrites from 7 mice (from multiple litters). Confocal image z-stacks (40X) were background subtracted and median filtered (radius 0.25 μm), and the presence or absence of a protrusion was determined by

visually inspecting the entire z-stack of images. Dendrites were selected if the entire length to be analyzed was constricted within about 15 μm in the z-plane; this typically included from the tip of the branch to the bifurcation (for apical tufts). Brightest dendrites were selected from each image to ensure that dim protrusions, such as filopodia, were reliably identified. To reliably identify spines of a given dendrite, we analyzed GFP+ dendrites that were not occluded by other nearby cell processes. Dendrite selection and all following spine analysis were conducted blindly. For a dendritic protrusion to be counted, it had to clearly protrude out of the shaft by at least 3 pixels (approximately 0.36 μm). Dendritic protrusions were quantified from either apical dendritic tufts in L1 or secondary/tertiary basal dendrites in L2/3. Spine density was calculated by dividing the number of counted spines by the total dendritic length analyzed (50–80 μm long shafts). Since GFP brightness is monotonically related to the volume in each protrusion (Holtmaat et al. 2005), we quantified the fluorescent intensity (TIB [a.u.]) of dendritic spines in apical tufts. To obtain a TIB value, the mean gray value of the dendritic spine was measured at the brightest focal plane and was divided by the mean fluorescence intensity of the adjacent dendritic shaft to normalize for varying imaging conditions. We sorted dendritic spine types into large mushroom/stubby (TIB > 75%), medium-size spines ($25\% \leq \text{TIB} \leq 75\%$), and thin-spine/filopodia (TIB < 25%) intensity groups based on percentile cutoffs determined from TIB distribution values of dendritic spines. We previously showed that this is a reliable, unbiased approach for classifying dendritic spine types (Cruz-Martín et al. 2010).

2.13 Electrophysiological recordings and analysis

Mice (P18–25) were anesthetized with 4% isoflurane-oxygen mixture (v/v) and perfused intracardially with ice-cold external solution containing the following: 73 mM sucrose, 83 mM NaCl, 26.2 mM NaHCO₃, 1 mM NaH₂PO₄, 22 mM glucose, 2.5 mM KCl, 3.3 mM MgSO₄, 0.5 mM CaCl₂ and were bubbled with 95% O₂/5% CO₂ (295–305 mOsm). Coronal slices (300- μ m thickness) were cut on a VS1200 vibratome (Leica) in ice-cold external solution before being transferred to ACSF containing the following: 119 mM NaCl, 26 mM NaHCO₃, 1.3 mM NaH₂PO₄, 20 mM glucose, 2.5 mM KCl, 2.5 mM CaCl₂, 1.3 mM MgCl₂, bubbled with 95% O₂/5% CO₂ (295–305 mOsm). Slices were kept at 35°C for 30 min before being allowed to recover for 30 min at room temperature. All recordings were performed at 30–32°C. We only recorded from transfected neurons in the anterior cingulate cortex and prelimbic, infralimbic, and medial orbital divisions of the mPFC. Signals were recorded with a 5X gain, low-pass filtered at 6 kHz, and digitized at 10 kHz using a patch-clamp amplifier (Multiclamp 700B, Molecular Devices).

Whole-cell voltage-clamp recordings were made using 3–5 M Ω pipettes filled with an internal solution that contained 125 mM Cs-gluconate, 3 mM NaCl, 8 mM CsCl, 4 mM EGTA, 4 mM MgATP, 0.3 mM NaGTP, and 10 mM HEPES (pH 7.3) with CsOH (280–290 mOsm). Series resistance (R_s) and input resistance (R_{in}) were monitored throughout the experiment by measuring the capacitive transient and steady-state deflection in response to a –5 mV test pulse, respectively. For mEPSC recordings, cells were voltage clamped at E_{rev} GABA_A (–70 mV) in the presence of 1 μ M Tetrodotoxin

(Tocris). For mIPSC recordings, cells were voltage clamped at Erev Glu (+5 mV) in the presence of 1 μ M Tetrodotoxin (Tocris). For all groups, we analyzed 10–12 cells from 4 mice (from multiple litters). mPSCs were detected by fitting to mPSC amplitude template using pClamp10 analysis software (Molecular Devices). The peak current of each mPSC was calculated. Next, average mPSC amplitude and IEI was calculated for each cell and then averaged across each condition to determine the population mean and SEM. Bath application of 100 μ M GABA_A inhibitor picrotoxin at Erev Glu and 20 mM CNQX and 50 mM DL-AP5 at Erev GABA_A eliminated mPSCs, thus confirming the identity of the recorded currents. Cells were excluded if R_s varied by more than 20% during a recording. For all recordings, series resistance was close to 10 M Ω (control, 9.39 ± 0.53 M Ω , n = 12; mC4, 9.74 ± 0.44 M Ω , n = 10; p > 0.05) and was not compensated.

In current-clamp recordings, CNQX (20 mM), 50 mM DL-AP5, and picrotoxin (100 μ M) were routinely added to the extracellular solution to block ionotropic synaptic transmission mediated by glutamate and GABA_A receptors, respectively, to assess persistent firing. Neuronal excitability was assessed using the input–output curve measured from the changes in membrane potential (presence of APs) evoked by current steps (from V_{rest}, start = –200 pA, step duration: 300 ms), increasing in increments of 10–15 pA in current-clamp mode. C_m and R_m were calculated in seal-test configuration from the decay and steady-state current of a transient generated in response to a –5 mV pulse test. Rheobase is the minimum current amplitude (300 ms) that resulted in an AP.

2.14 Neuronal morphology analysis

Confocal images of L2/3 GFP-positive neurons in mPFC (P21 and P60) were collected using a 40X objective. z-Stacks for images with a large field of view were taken at z-step of 1 μm through the entire section (about 200- μm thickness), taking care to include the entirety of the dendritic tree. Image stacks of dendritic trees and soma were imported in TIFF format into ImageJ (NIH). Cell somas and dendrites were traced manually to ensure accurate reconstruction. Dendritic arbors that could not be confidently and completely reconstructed were not used in the analysis. Dendritic reconstructions were confirmed by comparing independent reconstructions from two investigators (N = 10 neurons per condition). The dendritic parameters analyzed included the total dendritic length (of all dendrite branches), number of dendritic branches, number of branch points, number of dendritic end tips. Branch order for each dendritic branch was assigned starting at the cell body and increased after each branch point and the maximum branch order quantified. Sholl analysis was performed using Simple Neurite Tracer (SNT, ImageJ plugin, Longair MH, 2011). Each reconstructed neuron was thresholded and binarized, and the skeletons were imported to SNT. Sholl analysis was performed by calculating the number of dendrites that intersected concentric spheres that radiated from the soma in 10- μm radius increments. On some occasions, the dendritic arbor could not be reconstructed for several reasons: dendritic processes extended outside of the acquired field of view (or z-stack); the field of view became too dense with GFP-positive processes from neighboring cells, preventing unambiguous reconstruction; and some dendritic processes were deemed insufficiently bright to allow for unequivocal

reconstruction. Thus, our reconstructions are an underestimate of the entire dendritic arbor. Neuronal soma area and diameter were measured from a single z-plane for each neuron. Soma diameter was measured perpendicular to the apical axis. Analysis was performed at P21 in the mPFC and 315 neurons were analyzed for control (6 ROIs from 3 mice) and 216 cells were analyzed for the mC4 condition (7 ROIs from 3 mice).

2.15 Microglial assays

GFP colocalization with microglia (Iba1) was quantified at P21. Confocal images of mPFC (60X objective) were collected using the same exposure settings between conditions including channels for DAPI, GFP (transfected neurons), and Iba1 (microglia). All images were background subtracted and binarized using the same settings between experimental groups. Analysis was completed for single z-planes. To quantify microglia proximity to GFP⁺ neurons, we first defined the electroporated region (ROI) to be analyzed. We created an ROI for a single z-plane in the mPFC where transfected neurons were located. There were 26 ROIs for each condition. The ROIs of electroporated regions were, on average, 98,000 μm^2 (approximately 280 $\mu\text{m} \times 350 \mu\text{m}$) and contained, on average, 13.6 microglia per ROI. We then identified microglia by tracing around the perimeter of the cell (using Iba1 signal), including the cell body and any proximal processes in the single analyzed z-plane. Microglia cell bodies were confirmed by the presence of DAPI. Colocalized GFP and Iba1 signal was isolated and quantified within the microglia by creating a thresholded mask. Colocalized signal within the microglia

mask was only included in the analysis if it was equal to or larger than 1.23 μm (approximately 3 pixels). GFP-positive puncta within microglia were visually inspected in three-dimensional space by examining multiple z-planes to confirm the containment of the puncta to the microglia cytoplasm. The percentage of colocalized signal was quantified by dividing the area of the mask by the total area of the microglia (GFP/Iba1 colocalization [%] = microglia area colocalized with GFP / total microglia area). Using this analysis, we also calculated the percentage of microglia that were positive for GFP (GFP-positive microglia [%] = total number of GFP-positive microglia / total number of microglia), N = 26 ROIs (ROIs of electroporated regions from 3 mice per condition including 373 control and 334 mC4 microglia).

To quantify engulfment of synaptic material in nonexpanded tissue, we electroporated (E16) a plasmid that labels endogenous PSD-95 (EF1a-PSD95.FingR-RFP) for control and mC4 conditions. Analysis was completed for single z-planes using DAPI, PSD-95-FingR-RFP, Iba1, and CD68 (a lysosomal marker). ROIs of electroporated regions were defined as described in the previous section (Colocalization of GFP and Iba1). Analysis was completed using the same method as in the GFP and Iba1 colocalization analysis, except synaptic material was only counted if it was within the lysosome of the microglia (PSD-95-positive puncta that colocalized with both Iba1 and CD68 signals). For each thresholded mask, the total colocalized area (microglia engulfment area [%] = microglia area colocalized with PSD-95 and CD68 / total microglia area) was quantified. We also quantified the percentage of microglia positive for engulfment (engulfment-positive microglia = [%] total number of positive microglia

/total number of microglia). We also quantified the colocalization of fluorescent signals from PSD-95, Iba1, and CD68 in confocal images that were pixel shifted randomly by 12 μm in four possible directions for each channel, independently. The percent area of each microglia colocalized with CD68 signal was calculated as a measure of microglia reactivity (area of CD68 / microglia area). In a separate analysis, the cortical depth of each engulfment-positive microglia was determined by measuring the distance from the center of the cell body (using DAPI) to the adjacent pia mater. We restricted cortical depth analysis to L1 and L2/3 of the mPFC, where the dendritic spines of L2/3 cortical neurons are localized (depth $\leq 300 \mu\text{m}$). Microglia that did not contain triple-stained puncta (PSD-95/Iba1/CD68) were excluded from correlation analysis. Control: N = 26 ROIs (from 5 mice; 345 microglia); mC4: N = 26 ROIs (from 5 mice; 319 microglia).

Microglia density analysis (P21) was completed using 50- μm z-stack images using DAPI and Iba1 signals. Microglia density was independently calculated for L1 (cortical depth: 0–120 μm) and L2/3 (cortical depth: >120–300 μm) of the mPFC. Density was calculated per ROI (electroporated region) by dividing the number of microglia in the ROI by the total volume of tissue for each ROI. Microglia density was measured in 19 control ROIs (from 5 mice, 2,146 microglia) and 17 mC4 ROIs (from 5 mice, 1,640 microglia) in the superficial layers of cortex, and in each ROI the density was calculated for L1 and L2/3. Microglia cell bodies were confirmed by the presence of DAPI.

2.16 Expansion microscopy

Coronal mouse brain sections (50 μm) were permeabilized as previously described and stained at 4°C for 24 hr with primary antibodies (rat anti-CD68, rabbit anti-RFP, guinea pig anti-Iba1) at a dilution of 1:500 for each. Tissue was subsequently washed three times for 10 min in 1X PBS with 0.025% Triton-100X. The tissue was then incubated with secondary antibodies (anti-rat 488, anti-rabbit Alexa 546, anti-rabbit 594, anti-guinea pig Atto 647, anti-guinea pig Alexa 647) at 4°C for 24 hr. Tissue sections were again washed three times with PBS for 10 min. Sections were then anchored in 0.1 mg/ml Acryloyl-X SE in 1X PBS for 12 hr and polymerized within a polyacrylamide and sodium acrylate gel (Tillberg et al. 2016). The gels were trimmed and subsequently digested with proteinase k (8 units/ml) for 8–10 hr. Following digestion, the sections were transferred into a #1.5 glass-bottom dish, washed three times with 1X PBS, and expanded with milliQ purified water for 15 min twice. Fluorescence images of the expanded tissue were acquired with a Nikon C2Si inverted laser scanning confocal microscope (Nikon Instruments, Nikon Eclipse Ti with C2Si+ confocal) with a 40X Plan Apo λs objective (Nikon Instruments; Plan Apo, NA 1.3, WD: 0.2 mm, water objective). Images of microglia near apical dendrites of L2/3 FingR-PSD95-RFP(+) neurons were acquired with a pixel sampling of (0.155 $\mu\text{m}/\text{pixel}$) and 1- μm z-axis step interval.

The scaling factor for each expanded microglia was determined by comparing pre-expansion measurements of the long and short cross sections of the microglial cell body in a maximum-intensity projection image, and these values were compared to expanded microglia measurements. The scaling factor for each microglia was calculated

based on pre-expansion images. This scaling factor was applied to any measurements made within that expanded image (e.g., lysosomes area) to calculate the original size of the organelles. To determine the number and size of lysosomes, ROIs were manually drawn following the perimeter of the lysosome using the z-axis plane with the brightest CD68 signal. This z-plane was determined first qualitatively and confirmed by a line scan through the approximate center of the lysosome signal, which yielded the largest slope of intensity versus distance. The lysosome ROIs were counted and the cross-sectional areas measured and compared between experimental groups. CD68-positive signals were scored as a lysosome if they were 3×3 pixels, or 7–9 clustered pixels ($0.216 \mu\text{m}^2$ expanded), in size with an average signal intensity of at least two times above local background levels and were present in two consecutive z-planes.

Additionally, each lysosomal ROI was verified for FingR-PSD95-RFP signal using a z-axis profile plot for both CD68 and RFP signal. ROIs that show overlapping peaks between RFP and CD68 were verified for signal within the ROI in comparison to the surrounding local background. Local background was determined by calculating the mean background signal of RFP in a region surrounding each ROI. We considered lysosomes positive for synaptic engulfment if the ROI signal increased by two standard deviations over the local background signal. PSD95-FingR-RFP-positive signal was scored as a PSD-95 internalized puncta if they were 2×2 pixels, or 4–5 clustered pixels ($0.0961 \mu\text{m}^2$ expanded), in size with an average signal intensity of at least two times above local background levels. The data were derived from 5 and 4 mice each for control and mC4 conditions, respectively, and 45 and 41 microglia were analyzed from control

and mC4 conditions, respectively. We analyzed a total of 1,987 and 2,531 lysosomes from control and mC4 conditions, respectively.

2.17 Maternal interaction task

For all juvenile behavior tasks, we used control (N = 15) and mC4 (N = 21) mice that were electroporated bilaterally at E16. Prior to the maternal homing test, dams were acclimated to the behavioral task by placing them in the mesh cup for 5-min periods, for 3 d consecutively. Mice were separated from their dams for 1 hr immediately before testing. The MI task consisted of two phases. In phase 1 (MI1), mice were placed in an OF with home bedding and fresh bedding, and in phase 2 (MI2) mice were placed in an OF with home bedding, and their dam was restrained in a small wire mesh cup and an empty wire mesh cup. Both phases of the behavioral task were run on P18.

For MI1, individual pups were transferred to a homemade acrylic arena ($50 \times 50 \times 30$ cm length-width-height) and placed in a “starting corner.” The arena contained fresh bedding in two neutral corners and nest bedding in the corner opposite from the starting corner. Mice explored for 3 min, and the total time spent in the starting, nest, and fresh corners was measured using a homemade video tracking system written in MATLAB (MathWorks). Grooming occurrences and time spent grooming were annotated by a trained experimenter blind to experimental conditions.

For MI2, two wire mesh cups were placed in opposite corners of a homemade acrylic arena ($50 \times 50 \times 30$ cm length-width-height), one containing the animal's dam and

the other empty, and the start corner contained soiled home bedding. Mice spent 5 min exploring the MI2 environment, and we video-recorded behavior using a Logitech C270 Webcam at 30 fps. Time spent near each cup and other areas was measured using our homemade video tracking system that tracked the centroid of the mouse. Behaviors were recorded under a dim light (approximately 20 lux) positioned over the center zone of the arena. Between trials and mice, the arena was cleaned with 70% ethanol.

2.18 Adult behavior

For all adult behavior tasks, we used control (N = 22) and mC4 (N = 20) mice that were electroporated bilaterally at E16. The same cohort of adult mice was run in all adult behavioral tasks between the ages of P60–70. All behavior was recorded using a Logitech C270 Webcam at 20 fps. All mice were handled for 3 d consecutively prior to any behavioral testing to ensure familiarity to the experimenter. For all behavioral tasks, experiments were recorded under a dim light (approximately 20 lux) positioned over the center zone of the arena. For the open field task (OF), mice were placed in a homemade acrylic arena (50 × 50 × 30 cm length-width-height) and were free to explore for 5 min. For EZM, mice were placed in the closed arm of a homemade elevated-zero maze (EZM) (track diameter = 50 cm, track width = 5 cm, wall height for closed arms = 40 cm, height of track = 61 cm) and were free to explore for 5 min. For OF and EZM, mice were not exposed to the arenas until testing day, since the initial response to the environment is measured. Sociability and object tasks were run in the OF arena. Mice were acclimated to

the OF arena for 3 d prior to behavioral testing (5 min each day). For the novel-object interaction task, mice were placed in the center of the arena that contained a novel object (small plastic toy with smooth, cleanable surfaces) in one corner (corner alternated between mice). Mice were free to explore the arena for 5 min. For novel-object recognition, the arena contained a familiar object (object exposed in novel-object task) in one corner and a novel object in the opposite corner (corners alternated between mice), and mice were free to explore for 5 min. For the sociability task, the arena contained a novel mouse (age, sex, and strain matched) under a mesh wire cup in one corner and an empty mesh wire cup in the opposing corner, and mice were free to explore for 5 min. For all behavioral tasks, the arena was cleaned with 70% ethanol between all trials.

All adult behavior was analyzed using DeepLabCut (Mathis et al. 2018), an open-source software package that uses deep neural networks to automatically track body parts from videos. We confirmed accurate tracking of mice based on this software by close inspection of videos once they had been annotated by DeepLabCut. For all adult behavior position tracking, we used the centroid of the mouse and compared amount of time spent in ROIs. For OF, we calculated the maximum and average velocity and the total distance traveled. For EZM, we compared the time spent in the open arms of the maze. For both novel-object and sociability tasks, we quantified amount of time spent in the corners of interest in the arena (time spent with novel object for novel-object interaction, time spent with novel versus familiar object for novel-object recognition, time spent with novel mouse versus empty cup for sociability).

2.19 Quantification of transfected cells in behavior brains

We counted the number of GFP-positive cells and assessed the extent of cell transfection in brains of animals that were tested in behavioral tasks. Experimental groups included mice from at least two litters (N = 15 mice for control and N = 21 for mC4 condition for juvenile behaviors; N = 22 mice for control and N = 20 for mC4 condition for adult behaviors). Somas were counted by multiple trained, independent experimenters. Coronal sections (50- μ m thickness) from the entire brain were carefully inspected, and the DAPI signal was used to corroborate the presence of cell nuclei. We used a brain atlas (Paxinos & Franklin 2001) to confirm the location of GFP+ cell bodies and to delineate the boundaries of each brain region. Most transfected cells were located in frontal cortical regions, between Bregma +3.0 mm and 1.6 mm. We did not observe transfected cells in caudal cortical regions or subcortical areas.

To estimate the total amount of cells transfected in each brain, cells were counted from 50- μ m sections, including every other section. Since transfections were homogenous across neighboring brain sections, once we obtained the total number of cells per section, we plotted cell counts against their respective Bregma coordinates. We then used a linear interpolation to estimate the cell counts from missing brain sections. In a small number of brains (N = 3), we found no differences in total cell counts when we compared values obtained from counting GFP-positive cells in all transfected brain sections to estimated values obtained using the interpolation approach. In total, including juvenile and adult brains, we counted 174,041 neurons from 78 brains. All control and mC4 brains from mice used in behavioral tasks were GFP+ and had similar rostro-caudal

patterns of transfected neurons. We did not find any differences in total cell counts between groups for juvenile or adult conditions.

2.20 Statistical analysis

For confocal image analysis and electrophysiological recordings, we focused on neurons in the anterior cingulate cortex and prelimbic, infralimbic, and medial orbital divisions of the mPFC. All statistical analysis was completed in GraphPad Prism 8.0, and threshold for significance for all tests was set to 0.05 ($\alpha = 0.05$). M-FISH and qPCR data sets were analyzed with an unpaired t test. Spine developmental data were analyzed using a one- or two-way ANOVA followed by Tukey's posttest. Dendritic spine fluorescent intensity values were sorted based off of percentile cutoffs determined from TIB distribution values of dendritic spines in control conditions, and differences in the density of spine types between groups were tested with a one-way ANOVA followed by Tukey's posttest. Electrophysiological data were analyzed with an unpaired t test, and cumulative distributions were analyzed with a Kolmogorov-Smirnov (KS) test. Microglia data were analyzed using either an unpaired t test or a one-way ANOVA followed by Tukey's posttest. Behavioral data were analyzed with a two-way ANOVA followed by Sidak's posttest and a t test with Welch's correction. Dendrite and soma morphology measurements were analyzed using a t test. Both male and female mice were used, and we did not observe any differences between the sexes among groups. Correlations were determined using Pearson's r correlation and linear regression. Analysis was performed

blind to condition. Soma area/diameter and dendrite measurements were analyzed using GraphPad Prism 8.0 (GraphPad Software). Figures were prepared using CorelDRAW Graphics Suite X8 (Corel Corporation) and ImageJ (NIH). Custom-written routines for behavioral tracking and analysis are available upon request. Data are presented as the mean \pm SEM, unless otherwise noted.

CHAPTER THREE:

Overexpression of C4 and its impact on prefrontal cortex development

3.1 Introduction

It is not clear which cells types or brain regions produce C4 in the mouse brain. Additionally, since C4 has not yet, to our knowledge, been experimentally overexpressed, it is not known how its expression impacts developing cortical networks. Here, we characterize the endogenous expression of C4 in L2/3 neurons using M-FISH. We compare the endogenous expression of C4 between excitatory and inhibitory neurons. A modified, bilateral in utero electroporation method is verified in its ability to experimentally increase the expression of C4 in the PFC, using both qPCR and western blot methods. Lastly, the effects of C4 overexpression on developing mPFC networks are characterized by examining both developmental spine density with confocal imaging and the functional connectivity of neurons using whole-cell patch clamp electrophysiology methods.

3.2 Results

3.2.1 Endogenous expression of C4 in the mouse prefrontal cortex

Using multiplex in situ hybridization (M-FISH), we showed that PFC neurons in postnatal day (P) 30 control mice express low levels of C4b transcript (Figure 3.1), which

was not present in tissue from C4b knock-out (C4 KO) mice (Figure 3.1). Additionally, when comparing the endogenous expression of C4 between excitatory and inhibitory cells, labeled with probes for CaMKIIa and GAD, respectively, we find an enrichment of C4 in excitatory neurons compared to inhibitory neurons in L2/3 of the mPFC (Figure 3.2).

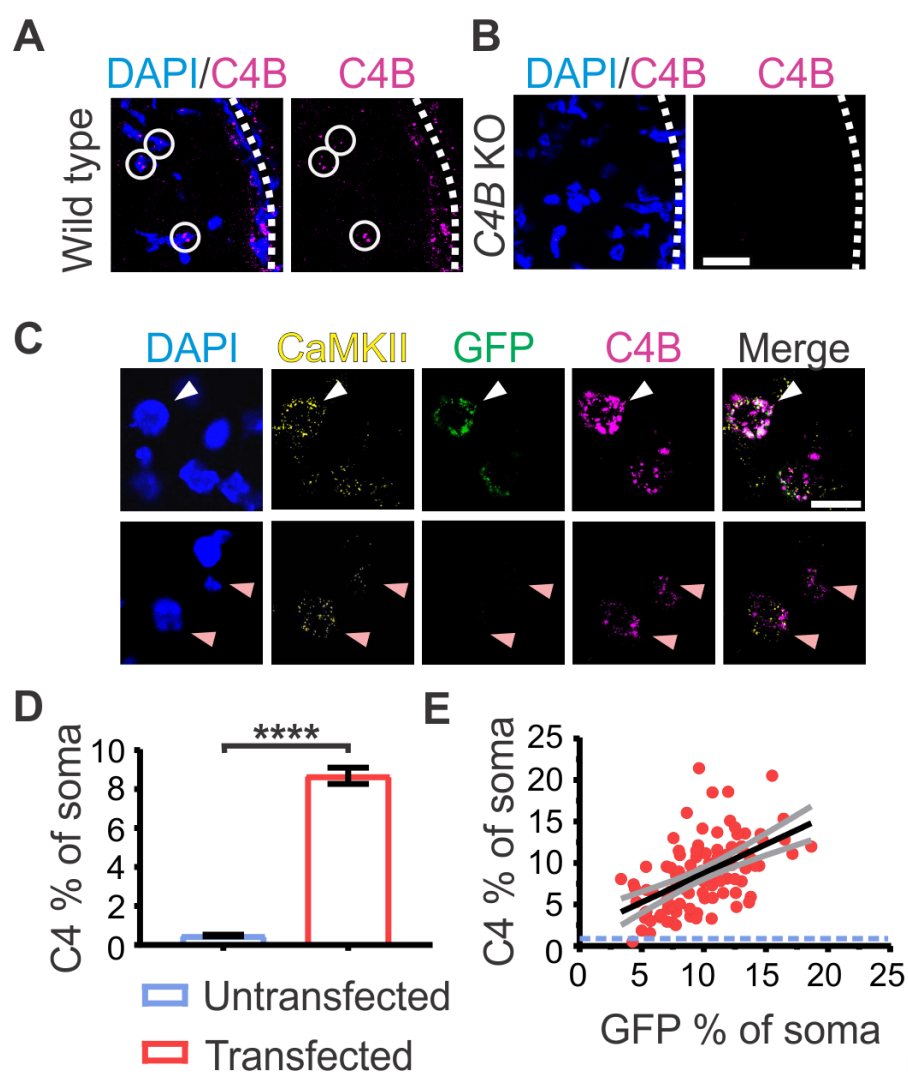


Figure 3.1: IUE increased amount of mouse C4 transcript in neurons.

(A) Representative 60X confocal images of in situ hybridization showing that C4b mRNA is expressed in mPFC superficial layers in P30 WT mice. White dotted line: pia mater. White circles: nuclei with C4 mRNA. (B) Representative 60X confocal images of in situ hybridization showing that C4b mRNA was not expressed in mPFC superficial layers in P30 C4b KO mice. White dotted line: pia mater. (A-B) Confirmed in 3 mice per condition. Scale bar = 60 μm . (C) Representative 60X confocal images at P21 of in situ hybridization from the same coronal section showing CaMKII α ⁺ neurons that were transfected with GFP and mC4 (C4b) (white arrowhead) and untransfected neighbors expressing mC4 (pink arrowhead). Scale bar = 15 μm . (D) IUE reliably increased C4b transcript levels in transfected cells. Percent of soma area positive for C4 transcript in transfected and untransfected neurons. N = 100 neurons (3 mice) per condition. t-test. ****p < 0.0001. Mean \pm SEM. (E) Transcript levels of GFP and mC4 positively correlated in transfected cells. black line: linear fit. gray lines: 95% confidence intervals. blue dotted line: average endogenous C4 expression at P21 in CaMKII α ⁺ mPFC L2/3 neurons. N = 100 transfected neurons (3 mice). Pearson's r correlation and linear regression. r = 0.28. ****p < 0.0001. Note: Experiments performed by Ashley Comer and Lisa Kretsge, data analyzed and figure made by Ashley Comer. Data and figure published in Comer et al., *Plos Biology*, 2020.

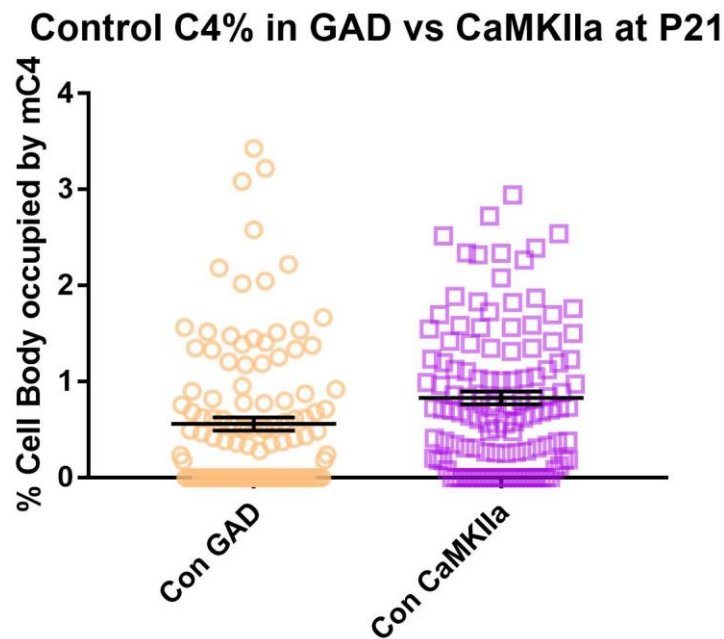


Figure 3.2: C4 expression is enriched in excitatory neurons.

Graph showing the % of each cell body occupied by mC4 transcript expression using M-FISH. Orange: control GAD (+) neurons. Magenta: control CaMK11a (+) neurons. N = 6 mice (200 neurons). Note: Experiments performed and data analyzed by Ashley Comer and Lisa Kretsge. Data and figure not previously published.

3.2.2 *In utero electroporation is a viable method to increase C4 expression*

To target L2/3 mPFC pyramidal neurons for C4 overexpression, we used *in utero* electroporation (IUE) in mice at embryonic day (E) 16 (Figure 3.3) (Szczyrkowska et al. 2016). To overexpress C4, we performed IUE using plasmids with the CAG promoter to coexpress green fluorescent protein (GFP) and mC4b (mC4 condition). Then, we used M-FISH at P21 to quantify the extent of C4 overexpression achieved. Within the same coronal section and cortical layer of the mPFC, we identified excitatory L2/3 neurons that were either transfected (GFP+/calcium/calmodulin-dependent protein kinase type II

subunit alpha [CaMKII α]⁺) or untransfected (GFP⁻/CaMKII α ⁺) and compared the percent of C4 mRNA⁺ cell body areas (Figure 3.1). This allowed us to quantify both endogenous expression of mC4 in pyramidal neurons and the extent of mC4 overexpression in transfected cells at P21.

IUEs reliably increased expression of mC4 at P21 in excitatory CaMKII α ⁺ neurons of the mPFC relative to their nearby untransfected neighbors (Figure 3.1, t test, ****p < 0.0001). Furthermore, we found that 99% of cells expressing GFP had higher amounts of mC4 mRNA relative to the mean transcript levels of nearby untransfected cells (Figure 3.1). To quantify mRNA levels more precisely, we performed quantitative PCR (qPCR) in tissue that was dissected to isolate the transfected region of the mPFC (Figure 3.3, B, right panel) from control (IUE with pCAG-GFP) and mC4 (IUE with pCAG-GFP and pCAG-mC4) animals at P21 and P60. At P21, IUEs reliably increased mC4 transcript by approximately 2.8-fold relative to control (Figure 3.3, C). However, there was not a significant increase of mC4 mRNA at P60 in the mC4 condition (Figure 3.3, D).

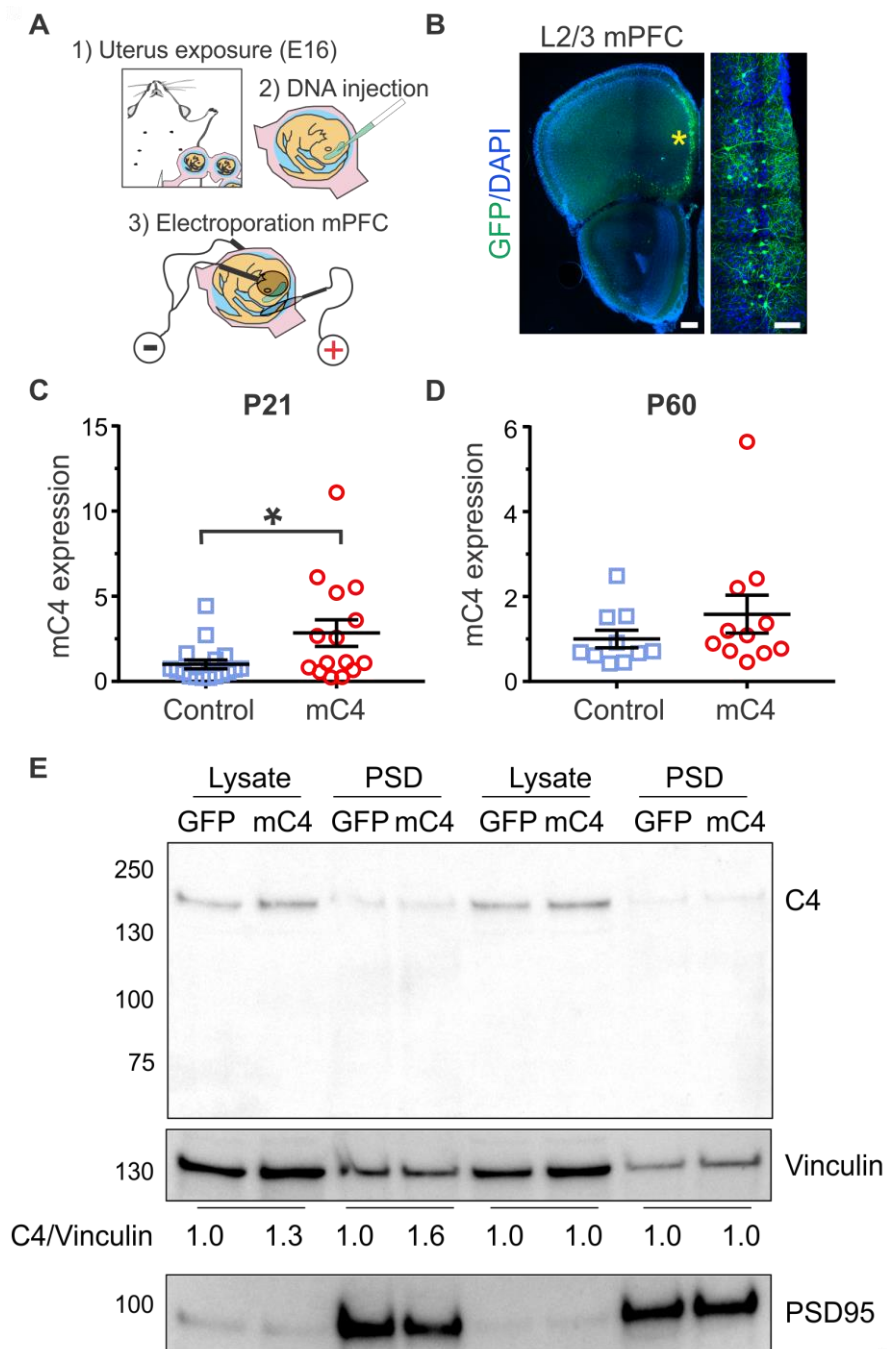


Figure 3.3: mC4 is expressed in neurons of the medial prefrontal cortex and can be overexpressed using in utero electroporation.

(A) Diagram depicting IUE surgery performed in E16 dams. (B) Representative 20X confocal image of IUE with GFP targeted to L2/3 mPFC, the electroporated region. Yellow asterisk: L2/3 GFP+ neurons. Left panel scale bar = 250 μm . Right panel scale bar = 75 μm . (C) IUE increases mC4 expression by 2.84-fold compared to P21 control. N = 18 control mice. N = 15 mC4 mice. t-test with Welch's correction. $p = 0.0392$. (D) mC4 mRNA expression at P60 for control and mC4 conditions. N = 10 control mice. N = 11 mC4 mice. t-test with Welch's correction. $p = 0.2564$. (C-D) qPCR performed from the dissected electroporated region. Control: blue. mC4: red. Mean \pm SEM. (E) Immunoblot (top) and quantification (bottom) of relative mC4 levels in total lysates and isolated PSD fractions from GFP or mC4 conditions from the electroporated region. Since C4 was expressed at relatively low levels, it could only be detected when brains were pooled. Lysates and PSDs from the electroporated region were prepared from the individual mice and pooled for the Western blot analysis. N = 7 mice per group for P21. N = 4 mice per group for P60. Vinculin was used as loading control for lysates and PSD fractions. PSD-95 immunoblot served as a control for successful isolation of PSD fractions. Note: qPCR data collected and analyzed by Rhushikesh Phadke (tissue collection and qPCR), Tushare Jinadasa (tissue collection and qPCR), Yenyu Liu (tissue collection and qPCR), Lisa Kretsge (tissue collection), and Ashley Comer (produced IUE mice and tissue collection). Western blot data performed and analyzed by Borislav Dejanovic. Figure made by Ashley Comer (panels A-D) and Borislav Dejanovic (panel E). Data and figure published in Comer et al., *Plos Biology*, 2020.

We tested multiple commercial antibodies in order to detect mC4 protein.

However, they were either nonspecific and/or not sensitive enough to detect C4 upon transient transfection of human epithelial kidney (HEK) cells. Therefore, we generated an antibody that detected both mC4 and hC4 in HEK cells that were transfected with C4 (Figure 3.4). Using this antibody, we found that C4 protein expression was increased in the mC4 condition approximately 1.3-fold at P21 and was unchanged at P60 in pooled total cell lysates taken from the mPFC (Figure 3.3, E). To test whether C4 is synaptically localized, we isolated postsynaptic density (PSD) fractions from PFC tissue (Figure 3.4). Indeed, we found that C4 protein was present in the PSD fraction in control conditions

and synaptic C4 protein was increased approximately 1.6-fold at P21 and was unchanged at P60 in C4-overexpressing tissue compared to controls (Figure 3.3, E). Since we had to pool isolated PSDs from multiple mice to have enough synaptic material, we were unable to run statistics on this data.

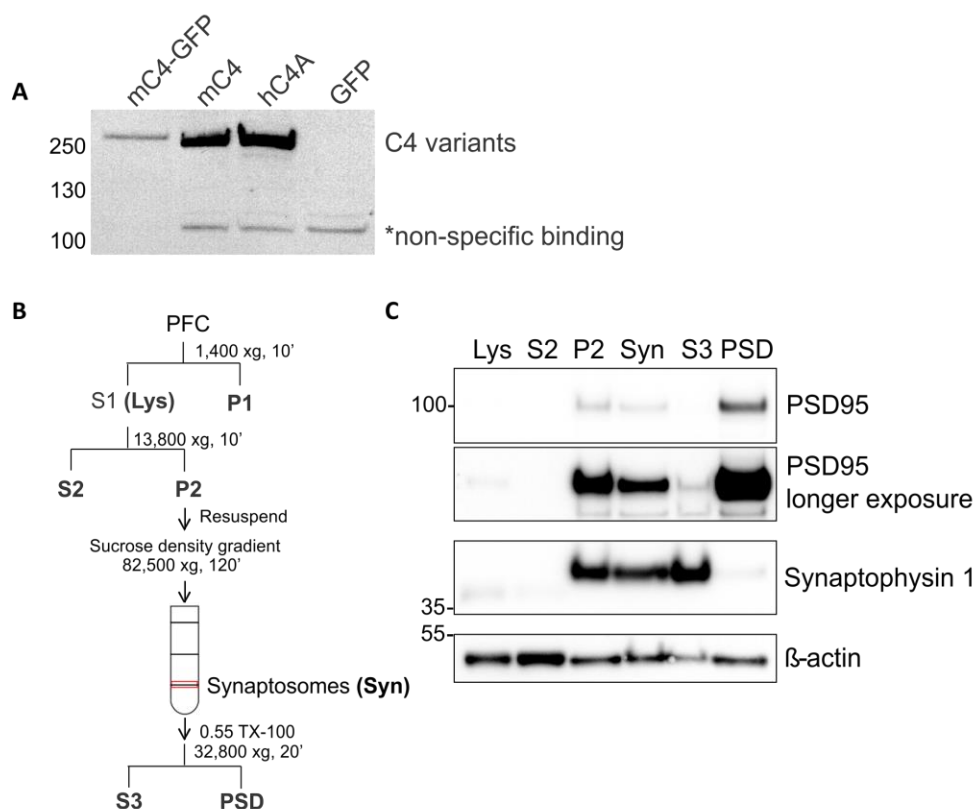


Figure 3.4: PSD synaptosome isolation from PFC tissue.

A) Immunoblot assay showing C4 staining with anti-C4 antibody (clone 931-946). Samples were from HEK293 cells transfected with GFP, hC4A, mC4 or mC4-GFP constructs. We detected C4 variants as ~250 kDa proteins, which is likely the unprocessed protein (predicted molecular weight is 193 kDa) or not fully reduced C4 protein (C4 has disulfide bonds). (B) Fractionation scheme for the preparation of PSDs from mouse PFC region. Fractions that were used for immunoblot analysis are shown in bold. (C) Immunoblot of postsynaptic (PSD-95) and presynaptic (Synaptophysin 1) marker proteins in PSD isolation steps. Synaptosome fraction contains both PSD-95 and synaptophysin 1. Note: Data collected and analyzed and figure made by Borislav Dejanovic. IUE mice provided by Ashley Comer. Data and figure published in Comer et al., *Plos Biology*, 2020.

We were unable to detect either endogenous or exogenous C4 in histological sections using our antibody or other commercially available antibodies. Therefore, we created a C4-GFP fusion protein construct (pCAG-C4-GFP) to visualize exogenous C4 protein expression without the need for antibodies. We confirmed C4-GFP expression in HEK cells using western blot (Figure 3.4, A). In both transfected HEK cells and L2/3 neurons at P21, mC4-GFP protein was expressed (Figure 3.5, A). We found C4-GFP localized to cell bodies and dendrites in L2/3 neurons (Figure 3.5, B, yellow arrowhead). Overall, these results showed that mPFC L2/3 neurons express endogenous mC4, that a subpopulation of C4 is synaptically localized, and that IUE successfully increased mC4 levels at P21.

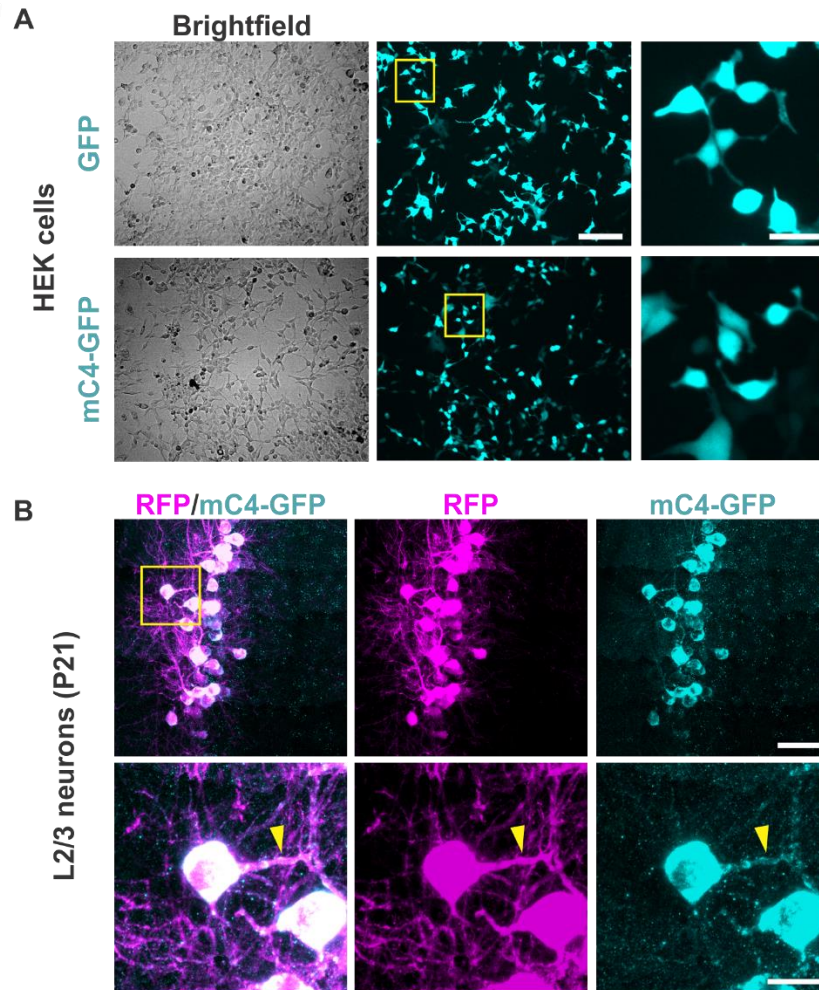


Figure 3.5: mC4-GFP protein is expressed in transfected HEK cells and L2/3 neurons.

(A) Representative 10X wide-field images of HEK cells transfected with either GFP (top panels) or fusion mC4-GFP (bottom panels). Left panel shows brightfield image. Middle and right panels show GFP signal (cyan). Right panel is zoom region of yellow square in middle panel. Scale bar left and middle panels = 100 μm . Scale bar right panels = 25 μm . (B) Representative 40X confocal image of IUE-transfected L2/3 neurons in the mPFC of P21 mice. Neurons co-transfected with pCAG-RFP (magenta) and pCAG-mC4-GFP (cyan). Bottom panels are zoomed region from the yellow square in the top left panel. Yellow arrowheads in bottom panels show C4-GFP signal in the dendrites of a neuron. Scale bar top panels = 50 μm . Scale bar bottom panels = 15 μm . Note: Panel (A) data collected by Rhushikesh Phadke, Tushare Jinadasa and Yenyu Liu. Panel (B) data collected by Ashley Comer. Figure made by Ashley Comer. Data and figure published in Comer et al., *Plos Biology*, 2020.

3.2.3 C4 overexpression alters developmental synaptic connectivity

Since we found C4 in PSD fractions, we wondered whether increased expression of C4 in developing neurons led to structural alterations in dendritic spines. We used IUE to produce control (pCAG-GFP) or C4 overexpression conditions (pCAG-GFP with pCAG-mC4b or pCAG-hC4A, for mC4 and hC4 conditions, respectively). Since early postnatal development is an important period for synaptic maturation and refinement of cortical circuitry (Cohen-Cory 2002), we measured dendritic spine density using confocal imaging of GFP in fixed brain sections collected at P7–9, P14–16, P21–23, and P55–60. Besides control and mC4 conditions, for comparison we also electroporated hC4A, which is highly associated with SCZ (Sekar et al. 2016).

In control conditions, the density of apical tuft dendritic spines was developmentally regulated and increased nearly 8-fold in the 2 wk from P7 to P21 (Figure 3.6, A, Tukey's test, **** $p < 0.0001$). Whereas spine density in mC4- or hC4-overexpressing neurons was similar to that of control conditions at P7 and P14, apical tuft dendritic spine density was approximately 30% lower at P21 (Figure 3.6, A and B). There were no differences in apical tuft protrusion density between any groups at P60 (Figure 3.6, A). These results suggest that overexpression of C4 alters the developmental maturation of dendritic spines and that overexpression of either human or mouse homologues of C4 causes spine loss/dysgenesis in the mouse mPFC.

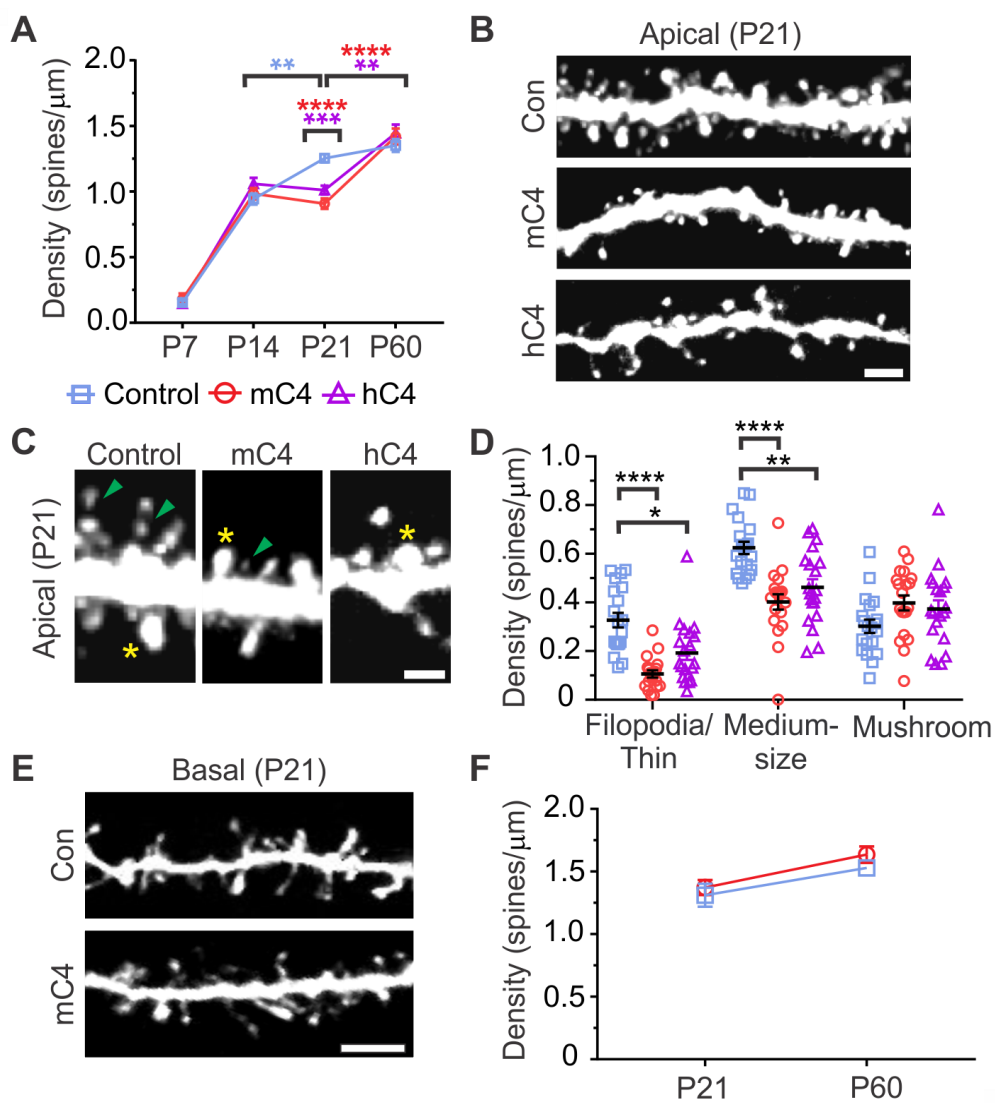


Figure 3.6: C4 overexpression led to dendritic spine alterations in apical arbors of L2/3 mPFC neurons.

(A) Developmental time course of spine density in the mPFC revealed a significant decrease in spine density in neurons overexpressing C4, as compared to controls, at P21-23. $**p < 0.01$, $***p < 0.001$, $****p < 0.0001$. N = 240 dendrites from 84 mice (20 dendrites per each time point; 20 dendrites x 4 time points x 3 conditions). (B) Representative 40X confocal images of P21-23 apical dendritic tufts. Scale bar = 5 μm . (C) Representative 40X confocal images of P21-23 apical dendritic spine types. Yellow asterisk: large mushroom spine (TIB (a.u.) > 75%). Green arrowhead: thin spine/filopodia (TIB (a.u.) < 25%). Scale bar = 3 μm . (D) Spine density (spine/ μm) sorted by spine types reveals a specific reduction of medium-sized and thin/filopodia spine types in the mC4 and hC4 condition. $*p < 0.05$, $**p < 0.01$, $****p < 0.0001$. N = 60 dendrites from 21 mice (20 dendrites per condition x 3 conditions). (E) Representative 40X confocal images of P21-23 basal dendritic spines. Scale bar = 5 μm . (F) Analysis of basal dendritic spine density (spine/ μm) revealed no difference across groups. N = 80 dendrites from 28 mice (20 dendrites per each time point; 20 dendrites x 2 time points x 2 conditions). Two-way ANOVA followed by a Tukey's test for all comparisons. Control: blue, mC4: red, hC4: purple. Mean \pm SEM. Note: Ashley Comer and Thanh Nguyen performed IUEs. Data collected and analyzed by Ashley Comer, Thanh Nguyen, Jungjoon Lee, Frances Hausmann, Meaghan Connolly, Thara Venu and Alberto Cruz-Martín. Figure made by Ashley Comer. Data and figure published in Comer et al., *Plos Biology*, 2020).

Closer inspection of protrusion morphology at P21 revealed a significant reduction of thin spines/filopodia and medium-sized spines in neurons overexpressing either mC4 or hC4, as compared to controls, whereas putative large mushroom spines remained intact (Figure 3.6, C and D; spine types sorted by total integrated brightness [TIB], see Methods). Since dendritic spine volume positively correlates with PSD size and synaptic strength (Arellano et al. 2007, Holtmaat & Svoboda 2009), this result suggests that increased expression of mC4 preferentially alters the development of weaker synaptic connections. Since overexpression of mC4 and hC4 led to similar defects in dendritic spine density at P21, in subsequent experiments we focused on the mouse homologue to investigate the role of C4 in cortical circuit function. In contrast to

the structural alterations we observed in apical tufts, increased expression of mC4 did not significantly alter the density of basal dendritic spines, as compared to control conditions (Figure 3.6, E and F). Taken together, these results demonstrate that increased expression of C4 in developing cortical neurons caused input-specific dendritic spine pathology and that less mature protrusions were preferentially affected, whereas larger mushroom spines remained intact.

3.2.4 C4 overexpression reduces the functional connectivity of cortical neurons

To determine whether the morphological spine deficits observed in C4-overexpressing cells were accompanied by functional connectivity changes, we performed electrophysiological whole-cell voltage-clamp recordings in acute brain slices prepared from mPFC of P18–25 control and mC4 animals. Voltage-clamp recordings demonstrated that overexpression of mC4 caused an approximately 60% decrease in the frequency of miniature excitatory postsynaptic currents (mEPSCs) and an increase in the interevent interval (IEI) (Figure 3.7, A–C). Increased levels of mC4 also caused an approximately 18% reduction in the amplitude of mEPSCs (Figure 3.7, D and E), demonstrating that mC4 modifies not only the density of synaptic connections but also the postsynaptic responses of L2/3 neurons.

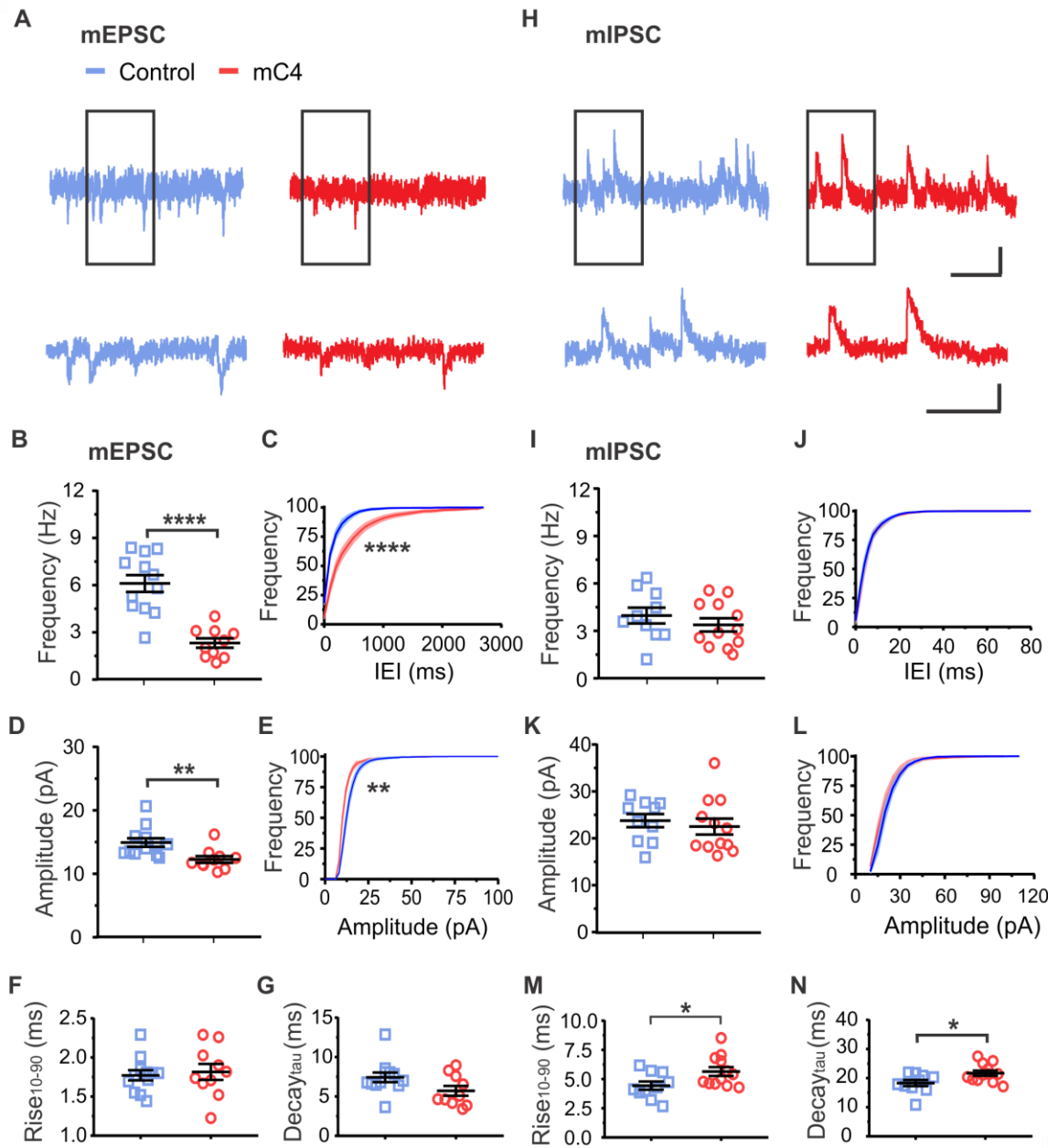


Figure 3.7: C4 overexpression reduced functional connectivity in cortical neurons. (A) Top: Representative whole-cell voltage clamp recordings showing mEPSCs. Top scale bar = 250 ms/10 pA. Bottom: same as top traces but expanded (black rectangle region). Bottom scale bar = 125 ms/10 pA. (B) Increased mC4 expression causes a reduction in mEPSC frequency. t-test. **** $p < 0.0001$. (C) Overexpression of mC4 causes a rightward shift in the distribution of mEPSC interevent interval (IEI). Kolmogorov-Smirnov test. **** $p < 0.0001$. (D) mC4 causes a reduction in mEPSC amplitude. t-test. ** $p < 0.01$. (E) mC4 overexpression causes a leftward shift in the mEPSC amplitude distribution. Kolmogorov-Smirnov test. ** $p < 0.01$. (F) mEPSC Rise₁₀₋₉₀ is not altered by mC4 overexpression. t-test. $p = 0.715$. (G) No changes in mEPSC Decay_{tau} with mC4 overexpression. t-test. $p = 0.07$. (B-G) $N = 12$ control neurons, $N = 10$ mC4 neurons. Mean \pm SEM. Control: blue, mC4: red. (H) Top: Representative recordings showing mIPSCs. Top scale bar = 250 ms/20 pA. Bottom traces are same as (H) top but expanded (rectangle region). Top scale bar = 125 ms/20 pA. (I) No difference in mIPSC frequency between control and mC4 conditions. t test. $p = 0.3726$. (J) Distribution of mIPSC IEIs is not changed by increased expression of mC4. Kolmogorov-Smirnov test. $p > 0.05$. (K) No changes in mIPSC amplitude with increased expression of mC4. t test. $p = 0.5832$. (L) mIPSC amplitude distribution is not changed by increased expression of mC4. Kolmogorov-Smirnov test. $p > 0.05$. (M) mIPSC Rise₁₀₋₉₀ is increased in neurons overexpressing mC4. t test. * $p = 0.0329$. (N) mIPSC Decay_{tau} is increased in neurons overexpressing mC4. t test. * $p = 0.0225$. (I-N) $N = 10$ control neurons, $N = 12$ mC4 neurons. Control: blue, mC4: red. Mean \pm SEM. Note: IUEs performed by Ashley Comer and Thanh Nguyen. Data collected and analyzed by Tushare Jinadasa. Figure made by Alberto Cruz-Martín. Data and figure published in Comer et al., *Plos Biology*, 2020.

Further analysis of postsynaptic current kinetics revealed no differences in mEPSC Rise₁₀₋₉₀ or Decay_{tau} between control and mC4-transfected neurons (Figure 3.7, F and G). Although overexpression of mC4 did not alter the frequency or the amplitude of miniature inhibitory postsynaptic currents (mIPSCs) (Figure 3.7, H–L), it significantly slowed their kinetics (Figure 3.7, M and N, 27% and 19% increase in Rise₁₀₋₉₀ and Decay_{tau}, respectively), suggesting that there could be mC4-dependent changes in the location of inhibitory synapses. Taken together, our data suggest that increased

expression of mC4 alters the developmental wiring of cortical neurons by decreasing their excitatory synaptic drive.

3.2.5 Overexpression of mC4 decreased membrane capacitance without altering overall excitability

We also monitored the electrophysiological properties of L2/3 mPFC neurons to determine whether overexpression of mC4 altered neuronal excitability. To do this, we injected hyperpolarizing and depolarizing current step injections of different amplitudes and recorded the membrane potential (V_m) in control and mC4-overexpressing neurons (Figure 3.8, A and B). Overexpression of mC4 did not alter the number of action potentials (APs) in response to step current injections of incrementally increasing amplitudes (Figure 3.8, C). In agreement with this, we did not see a change in the IEI of APs in response to step current injections (Figure 3.8, D) or the minimal current injection that resulted in AP generation (Figure 3.8, E) in mC4-overexpressing neurons. Together, these results suggest that overexpression of mC4 did not alter the intrinsic excitability of cortical neurons.

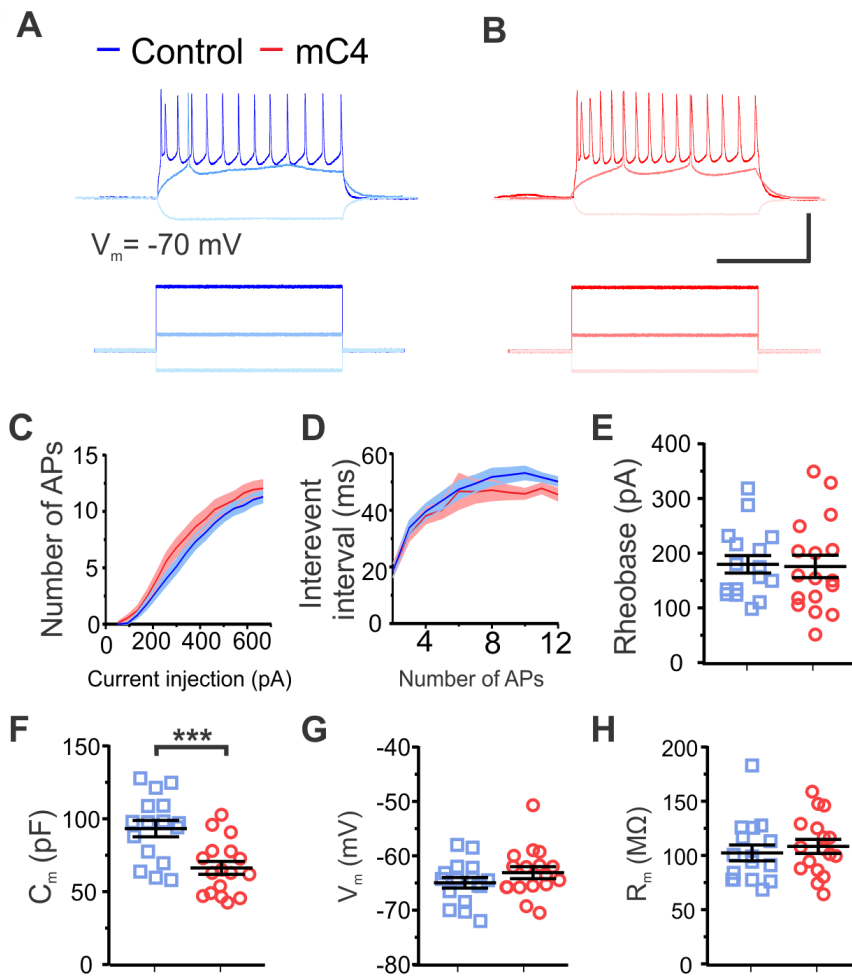


Figure 3.8: Overexpression of mC4 decreased membrane capacitance without altering overall excitability.

(A-B) Representative current clamp recordings from control (A) and mC4 (B) neurons in response to injection of constant-current pulses. Voltage traces (top) shown for response to -220 pA (light blue/pink), 185 pA (medium blue/red) and 685 pA (dark blue/red) current injections (bottom). Scale bar = 500 pA or 50 mV. Scale bar = 250 ms. (C) The number of APs were not different between conditions. Dark blue trace: control mean. Light blue trace: control SEM. Dark red trace: mC4 mean. Light red trace: mC4 SEM. Two-way ANOVA. $p = 0.9989$. (D) Interevent interval was not different between conditions. Dark blue trace: control mean. Light blue trace: control SEM. Dark red trace: mC4 mean. Light red trace: mC4 SEM. Two-way ANOVA. $p = 0.9838$. (E) Rheobase was not altered by the overexpression of mC4. t-test. $p = 0.8795$. (F) mC4 overexpression led to a dramatic reduction in C_m . t-test. $***p = 0.0007$. (G) V_m was not changed by mC4 overexpression. t-test. $p = 0.2166$. (H) R_m was not affected by mC4 overexpression. t-test. $p = 0.5455$. (C-H) Control: N = 16 cells; mC4: N = 17 cells. blue: control. red: mC4. Mean \pm SEM. Note: IUEs performed by Ashley Comer and Thanh Nguyen. Data collected and analyzed by Tushare Jinadasa. Figure made by Alberto Cruz-Martín. Data and figure published in Comer et al., *Plos Biology*, 2020.

In contrast, increased levels of mC4 led to an approximately 29% decrease in the membrane capacitance relative to controls (Figure 3.8, F). This effect on passive membrane properties was specific because increased expression of mC4 did not alter the neuron's resting membrane potential or membrane input resistance (Figure 3.8, G and H). Since membrane capacitance is proportional to a cell's surface area, this result suggests that increased expression of mC4 could affect either the gross morphology of cortical neurons or plasma membrane properties. Further investigation of neuronal morphology showed no difference between conditions in cell body area/diameter or in the width of primary dendrites (Figure 3.9, A-C); there was also no change in dendritic complexity (Figure 3.10), suggesting that gross neuronal morphology was not affected by mC4 overexpression. Besides the mC4-dependent changes in membrane capacitance, increased expression of mC4 did not have an effect on the morphology or intrinsic properties of

transfected cells, thus suggesting that overall neuronal health was not affected by increased expression of mC4 (Figure 3.10).

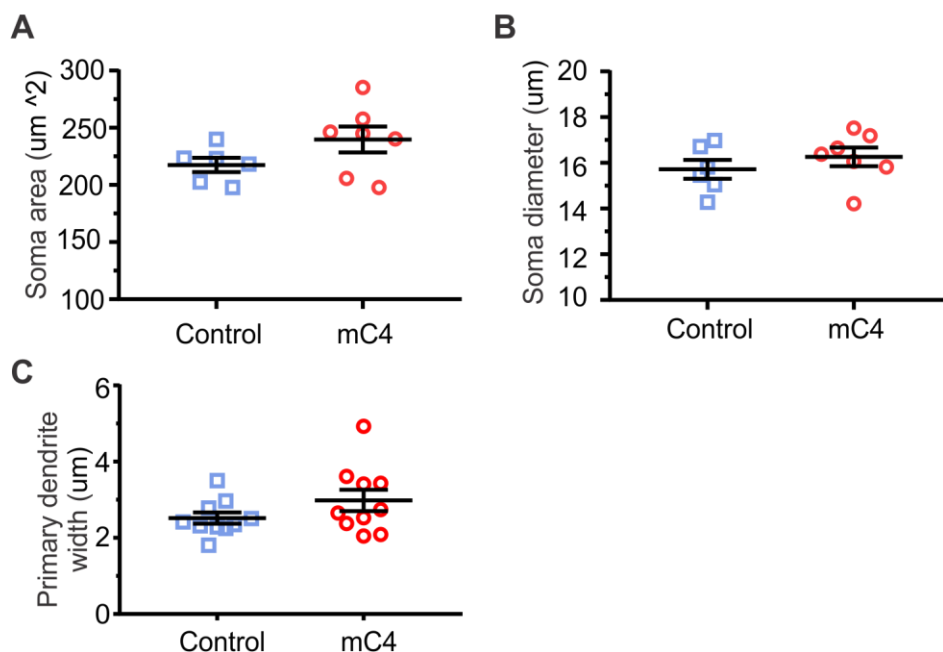


Figure 3.9: Overexpression of mC4 did not alter soma size or proximal dendrite width.

(A) Soma area was not different between control and mC4 conditions. t test. $p = 0.13$. (B) mC4 overexpression did not alter the diameter of neurons. T test. $p = 0.37$. (A-B) Only GFP-positive L2/3 mPFC neurons included in analysis. Data points represent average measures from ROIs containing many neurons from 3 mice per condition. Control: $N = 6$ ROIs (including 316 neurons). mC4: $N = 7$ ROIs (including 216 neurons). (C) Primary dendrite width was not different between conditions. $N = 10$ neurons per condition. Data points represent average primary dendrite width per neuron, including all primary apical and basal dendrites. T test. $p = 0.16$. Mean \pm SEM. Note: IUEs performed by Ashley Comer and Thanh Nguyen. Data collected and analyzed by Frances Hausmann, Alberto Cruz-Martín and Ashley Comer. Figure made by Ashley Comer. Data and figure published in Comer et al., *Plos Biology*, 2020.

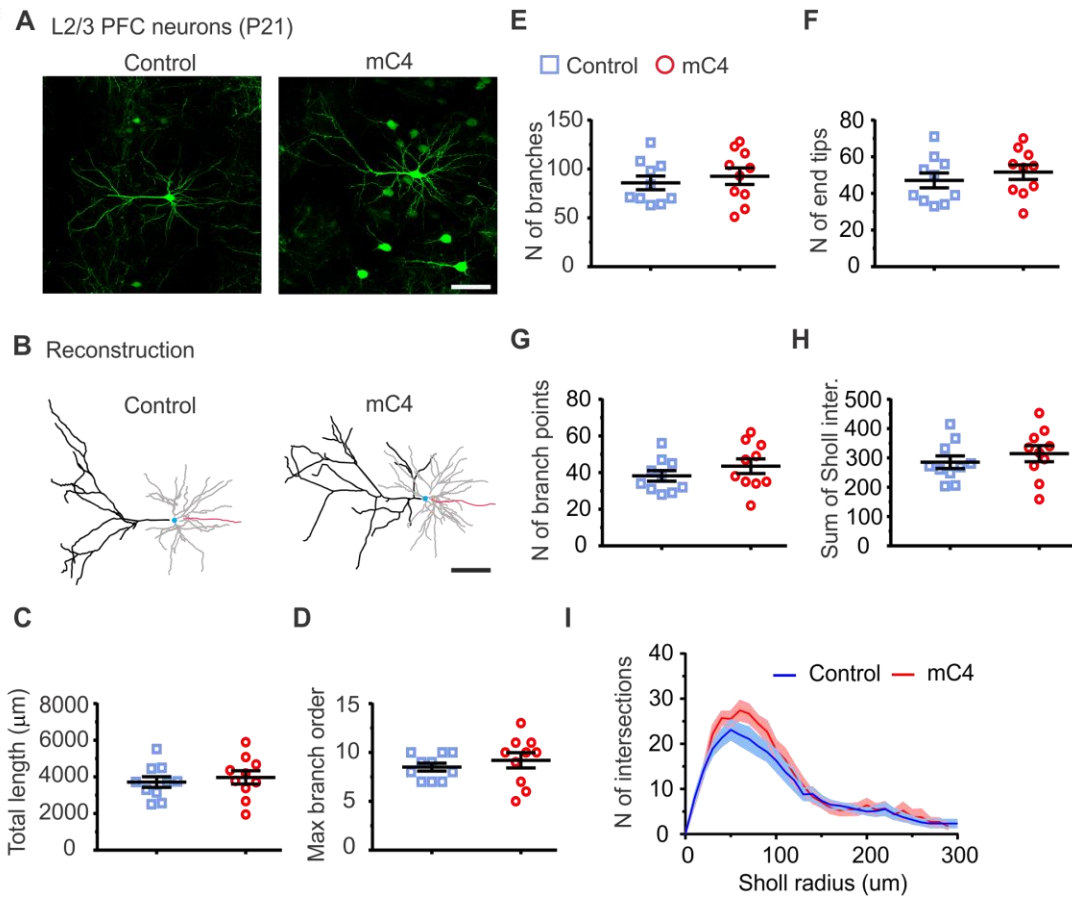


Figure 3.10: Dendrite morphology was not altered by mC4 overexpression at P21. (A) Representative confocal images (40X) of control and mC4 GFP-positive L2/3 neurons in the mPFC at P21. Images are max z-projections. Scale bar = 50 μm . (B) Reconstructions of control and mC4 neurons from (A). Black lines: apical dendrites. Gray lines: basal dendrites. Red line: axon. Light blue: cell body. Scale bar = 50 μm . (C) There was no difference in total dendritic length (μm) between control and mC4 neurons. t test. $p = 0.59$. (D) There was no difference in maximum branch order between control and mC4 neurons. t test. $p = 0.44$. (E) mC4 overexpression did not change the total number of branches in PFC L2/3 neurons. t test. $p = 0.54$. (F) There was no difference in the total number of dendritic end tips between control and mC4 neurons. t test. $p = 0.44$. (G) There was no difference in total number of branch points between conditions. t test. $p = 0.29$. (H) No difference found in the sum of Sholl intersections between control and mC4 neurons. t test. $p = 0.41$. (I) Number of intersections as a function of Sholl radii (μm). Dark blue line: control mean. mC4, Dark red line: mC4 mean. Light blue shade: control SEM. Light red shade: mC4 SEM. (C-I) $N = 10$ neurons per condition. Blue data points: control. Red data points: mC4. Mean \pm SEM. Note: IUEs performed by Ashley Comer and Thanh Nguyen. Data collected and analyzed by Frances Hausmann, Alberto Cruz-Martín, Ashley Comer and Tushare Jinadasa. Figure made by Ashley Comer. Data and figure published in Comer et al., *Plos Biology*, 2020.

3.3 Conclusion and future directions

In both humans and mice, juvenile and early adulthood time points are an important developmental window for PFC development (Marín 2016). Disruption during this critical developmental window can lead to lasting changes in brain connectivity, cognition and behavior (Marín 2016). Here, we show that C4 contributes to miswiring during this critical stage of development. First, we show that mC4 is expressed endogenously in the mouse mPFC in both excitatory and inhibitory neurons. However, C4 expression is enriched in excitatory cells compared to inhibitory cells, suggesting that complement-mediated effects in the brain could be cell-type specific. Using IUE, C4 was experimentally overexpressed in pyramidal neurons. Interestingly, in both control and mC4 overexpression conditions, mC4 was enriched at the synapse, suggesting that C4

might actively be recruited to the synapse. C4 overexpression led to a developmental decrease in spine density at P21, that was then recovered by P60. The recovery of spine density could be either due to the lack of significant overexpression of C4 achieved at P60 or due to active compensation of spine number, or a combination of both. Future studies can answer this question by creating a transgenic mouse model to stably overexpress C4 throughout the lifetime of mice.

For both overexpression conditions, mC4 and hC4, the loss of spines at P21 was due to a loss of filopodia and medium-sized spines, while mushroom spines were intact. Future work will interrogate the factors that protect more mature spines while leaving more immature spine-type vulnerable to complement-mediated spine removal. It is possible that more mature spines express protective factors, such as the protective “don’t eat me signal” CD47 which has been found to protect synapses from microglia-mediated engulfment (Lehrman et al. 2018). Electrophysiological recordings functionally confirm the decrease in excitatory synaptic drive at P21. Interestingly, the excitability of neurons overexpressing C4 was not altered, although the capacitance of these cells significantly decreased. Future work is required to determine the cause behind decreased capacitance which could be due to a change in plasma membrane properties, such as C4-induced changes in lipid composition. Since there are known interactions between complement proteins and cellular membranes, such as C1q, it is possible that changes in complement proteins induce alterations to the plasma membrane (DeLisi & Wiegel 1983). Overall, these data suggest that C4 overexpression drives spine dysgenesis and hypoconnectivity

of the mPFC by decreasing the spine density and excitatory synaptic drive of pyramidal neurons.

CHAPTER FOUR

The role of microglia in C4-induced prefrontal cortical dysfunction

4.1 Introduction

It has been shown that microglia, the brain's resident macrophage, engulf neuronal and synaptic material dependent on the presence of complement proteins (Stevens et al. 2007, Schafer et al. 2012). Microglia are the only cells in the brain that express the complement 3 receptor (CR3), which allows microglia to recognize and phagocytose material tagged by the complement cascade (Stevens et al. 2007, Schafer et al. 2012, Zabel & Kirsch 2013). Microglia-mediated synaptic pruning is necessary for normal development of the brain, but can also contribute to abnormal wiring of circuits and pathology when mis-regulated (Sekar et al. 2016, Paolicelli et al. 2011, Bohlen et al. 2019, Hong et al. 2016, Lui et al. 2016). Despite significant progress in this field, it is still not clear how reciprocal interactions between neurons and microglia contribute to the maturation and refinement of developing cortical circuits (Tremblay et al 2010, Hoshiko et al. 2012, Miyamoto et al. 2016). Here, we investigate the role of microglia in complement-mediated synaptic loss by observing the colocalization of microglia with synaptic material in the mPFC.

4.2 Results

4.2.1 C4 overexpression enhances microglia-neuron interactions during development

Several lines of evidence suggest that microglia contribute to circuit maturation and synaptic refinement through the secretion of effector molecules and direct interactions with neurons (Wu et al. 2015). To determine whether increased expression of mC4 led to closer associations of microglia with neurons at P21, we measured the colocalization of transfected neuronal GFP with microglia (immunostained for ionized calcium binding adaptor molecule 1 [Iba1]) in single z-planes using confocal microscopy (Figure 4.1, A). Using this approach, we found instances of microglia colocalized with GFP+ neuronal processes in both conditions (Figure 4.1, B; white arrowheads), suggesting that microglia were in close proximity with the dendritic processes of transfected L2/3 neurons. Increased expression of mC4 led to an approximately 35% increase in the number of microglia that colocalized with GFP+ L2/3 neurons (Figure 4.1, C) and an approximately 2-fold increase in the area of GFP signal that colocalized with the microglia cell body and proximal processes (Figure 4.1, D). These results suggest that neuronal overexpression of mC4 led to an increase in the number of microglia in close proximity to neurons despite no change in the overall density of microglia in the transfected region (Figure 4.2).

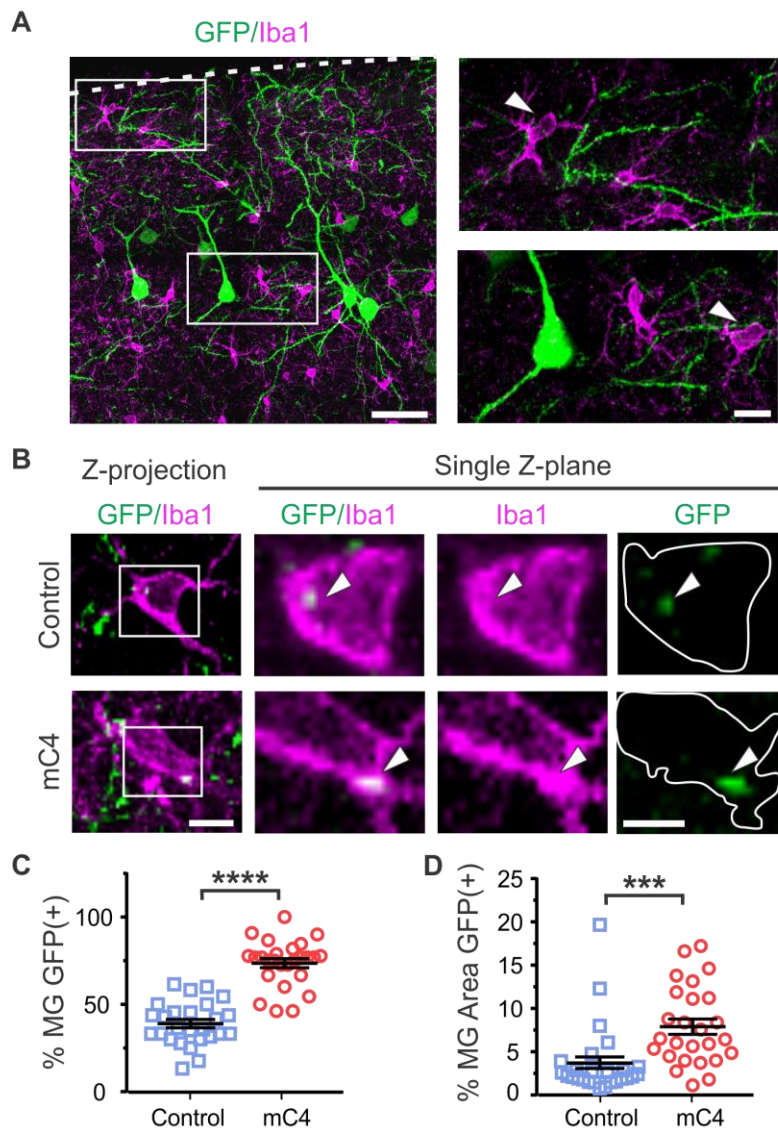


Figure 4.1: Microglia were in closer proximity to neurons overexpressing mC4 at P21.

(A) Representative single z-plane confocal image (60X) showing microglia interacting with processes of electroporated neurons in superficial layers of mPFC (left). White dotted line: pia. Left scale bar = 50 μm . Higher magnification of insets (left) of L1 and L2/3. White arrowhead: microglia (MG). Right scale bar = 10 μm . (B) Representative confocal image (60X) showing microglia (Iba1, magenta) colocalized with neuronal GFP signal in P21 histological sections for control (top) and mC4 (bottom) conditions. White arrow heads: Iba1/GFP-positive puncta colocalized with microglia soma. Left: max z-projection of entire microglia; scale bar: 7 μm . Right: single z-plane; scale bar = 3.5 μm . (C) Overexpression of mC4 in L2/3 neurons increased the number of microglia that colocalized with GFP+ neuronal material (GFP-positive microglia (%)). t test. ****p < 0.0001. (D) mC4 overexpression increased the percentage microglia area colocalized with neuronal material (MG area (%) = Area of MG GFP+ / Total MG Area). t test. ***p = 0.0009. (C-D) N = 26 ROIs (transfected region) from 3 mice per condition (including 373 control and 334 mC4 microglia). Mean \pm SEM. Note: Data collected by Ashley Comer and Thanh Nguyen. Data analyzed and figure made by Ashley Comer. Data and figure published in Comer et al., *Plos Biology*, 2020.

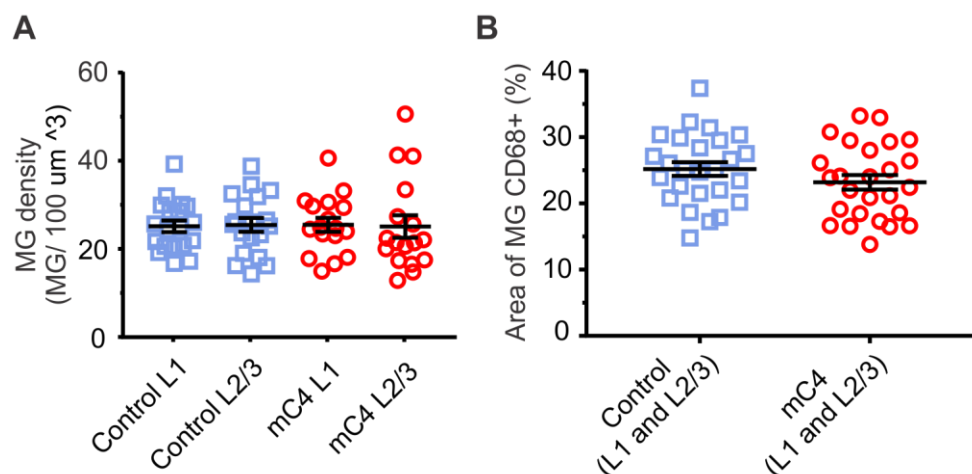


Figure 4.2: Microglia density and lysosome size were not altered by mC4 overexpression.

(A) Microglia density in superficial layers of the mPFC was not affected by mC4 overexpression. Control: N = 19 ROIs (from 5 mice including 2,146 microglia). mC4: N = 17 ROIs (from 5 mice including 1,640 microglia). One-way ANOVA with Bonferroni's multiple comparisons. $p = 0.998$. (B) Microglia lysosomal area, as measured by area of MG positive for CD68, were not different between conditions. Area of MG CD68+ (%) = Area of MG CD68+ / Total MG Area. Control: N = 26 ROIs (from 5 mice including 345 microglia). mC4: N = 26 ROIs (from 5 mice including 319 microglia). t test. $p = 0.19$. Mean \pm SEM. Note: Data collected and analyzed and figure made by Ashley Comer. Data and figure published in Comer et al., *Plos Biology*, 2020.

4.2.2 C4 overexpression enhances microglia engulfment of post-synaptic material

Since increased expression of mC4 led to a decrease in synaptic connectivity (Figure 3.6 and Figure 3.7) and closer association of microglia with transfected neurons at P21 (Figure 4.1), we evaluated whether C4 overexpression also enhanced microglia-dependent phagocytosis of synaptic material. To do this, endogenous PSD-95 was fluorescently labeled in vivo using a plasmid containing PSD95-FingR (EF1a-PSD95.FingR-RFP) (Gross et al. 2013), which labeled only endogenous PSD-95 within transfected neurons with red fluorescent protein (RFP) (Figure 4.3; pseudocolored green).

This approach was preferred instead of using an antibody approach, which would label PSD95 of both transfected and non-transfected cells, or using an overexpression method with PSD95 tagged with GFP because overexpressing PSD95 can alter synaptic properties. Therefore, the advantage of this method is that it allowed endogenous PSD95 protein to be labeled only in transfected neurons. Fluorescent signal from PSD95-FingR was confined to superficial L1 and L2/3 including transfected cell bodies of L2/3 neurons, indicating that expression from this electroporated construct mirrored the expected PSD-95 expression pattern of L2/3 neurons (Hunt et al. 1996, Gray et al. 2006) (Figure 4.3).

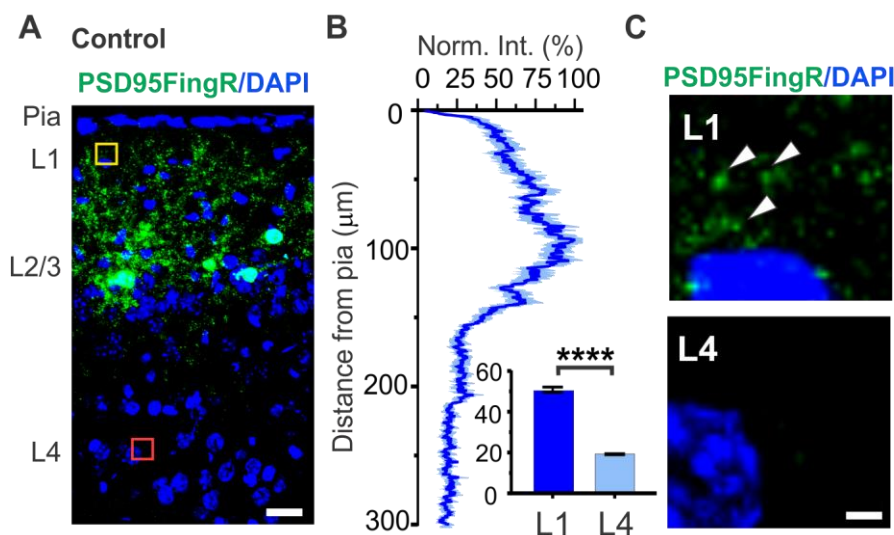


Figure 4.3: Intrabodies against PSD95 label excitatory synapses of L2/3 pyramidal neurons.

A) Representative confocal image (60X) showing cytoarchitecture (DAPI, blue) and labeling of endogenous PSD-95 by FingR (PSD95-FingR-RFP, pseudocolored green) in P21 coronal sections. Scale bar = 25 μm . (B) PSD95-FingR labeling pattern was consistent with endogenous location of synaptic PSD-95 in L2/3 pyramidal neurons. Mean normalized fluorescent intensity (normalized to peak PSD95-FingR signal) as a function of distance from pia (μm). Dark blue line: mean. Light blue shade: SEM. Bar graph: mean normalized fluorescent intensity (y-axis) is greater in L1 (yellow inset) than L4 (red inset). t-test. $p < 0.0001$. (C) Zoomed images from image in (A) showing boxed regions in L1 (yellow inset) and L4 (red inset). White arrowheads: PSD95-FingR puncta. Blue: DAPI (cell nuclei). Scale bar = 5 μm . Note: Data collected and analyzed and figure made by Ashley Comer and Alberto Cruz-Martín. Data and figure published in Comer et al., *Plos Biology*, 2020.

Next, we quantified the colocalization of PSD-95 (identified by PSD95-FingR immunofluorescence) with microglia (Iba1) or microglial lysosomes (CD68) (Figure 4.4). We observed clear instances of PSD-95 colocalized with Iba1 (Figure 4.4, A and C, white arrowheads) and CD68 signal (Figure 4.4, B and D, white arrowheads), suggesting that synaptic material was engulfed by microglia and localized to microglia lysosomes. Furthermore, using orthogonal views, we confirmed that PSD-95 was localized within

microglia soma and lysosomal compartments (Figure 4.4, A–D). We quantified the colocalization of fluorescent signals from PSD-95-FingR with both Iba1 and CD68 to measure postsynaptic puncta within the lysosomes of microglia in control and mC4 conditions. Overexpression of mC4 led to an approximately 2.3-fold increase in the percentage of microglia positive for engulfment (Figure 4.4, E). As a control, we analyzed the same images after pixel shifting (see Methods). In the pixel-shifted data, the percentage of microglia positive for triple-stained puncta dropped to under 3% in both groups (Figure 4.4, E, red dotted line is mean shifted value for both groups), suggesting that the colocalization of signals in microglia did not occur by chance. Lastly, we observed no change in the area of PSD-95-FingR signal within CD68+ structures (Figure 4.4, F). Taken together, these data show that C4 overexpression drives microglia engulfment of synaptic material.

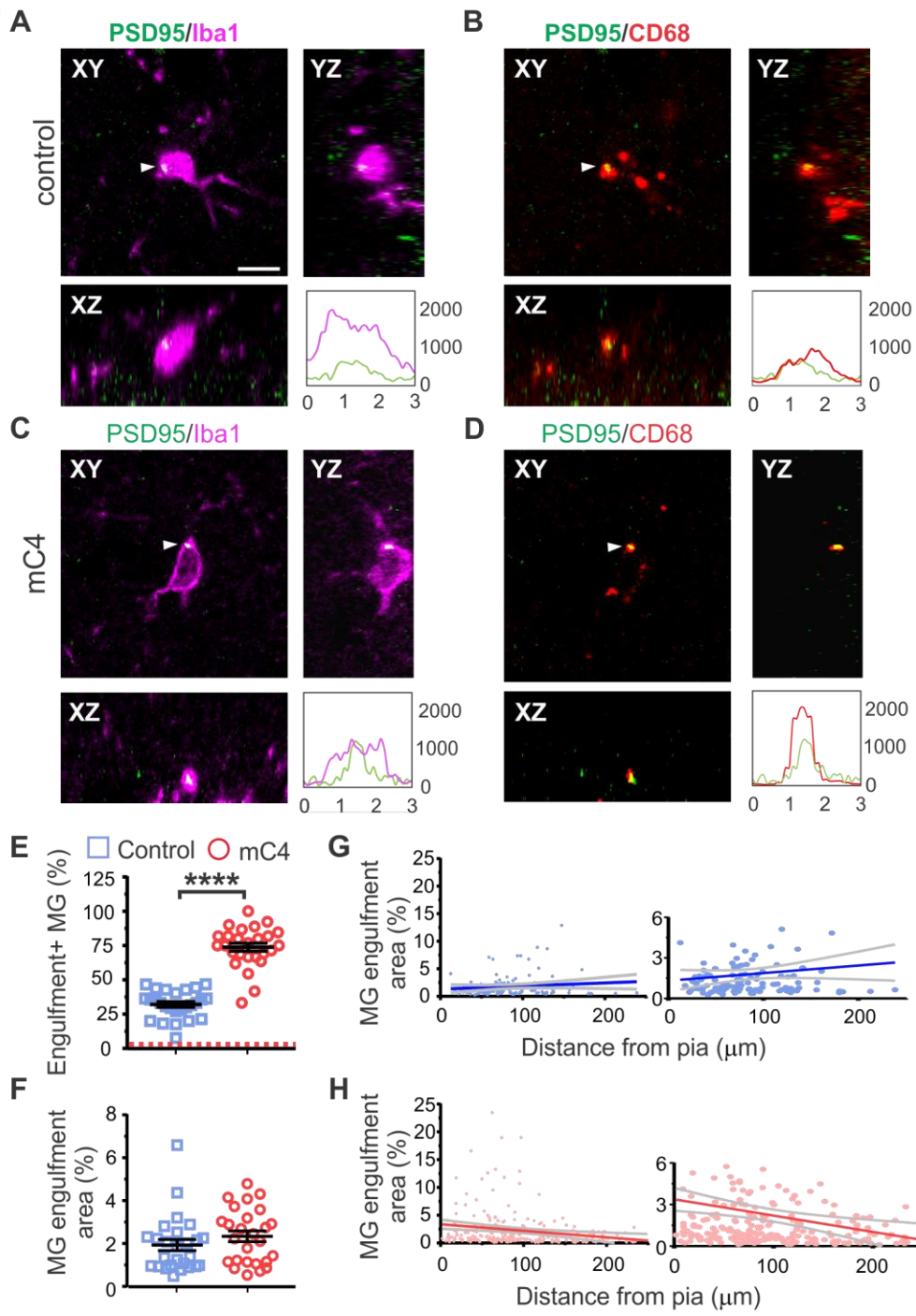


Figure 4.4: mC4 overexpression enhanced microglia engulfment of postsynaptic PSD-95.

(A-D) Representative confocal image (60X) showing PSD-95 located within microglial lysosomes in P21 mice for control (A-B) and mC4 conditions (C-D). Single z-plane shown. Scale bar = 5 μ m. Magenta: microglia (Iba1). Red: lysosomes (CD68). Green: PSD-95 (PSD95-FingR-RFP, pseudocolored green). White arrowheads: indicate colocalization of PSD95 with Iba1 (A and C) or CD68 (B and D). Panels A and C show a representative microglia (for control and mC4, respectively) including Iba1 and PSD95-FingR-RFP signal. Panels B and D show the same z-plane as panels A and C but shows CD68 and PSD95-FingR-RFP signal. Orthogonal views shown. A-D each include a graph (bottom right panel) showing a line intensity scan for each signal (A and C show Iba1 (magenta) and PSD-95 (green); B and C show CD68 (red) and PSD-95 (green)). For line intensity graphs, y-axis shows gray intensity value (a.u.) and x-axis shows length (μ m). (E) mC4 overexpression increased the number of microglia positive for PSD-95 engulfment (PSD95-FingR-RFP signal colocalized with CD68 and Iba1). t test. ****p < 0.0001. red dotted line: average of control and C4 in shuffled pixel analysis. (F) There was no difference in area of PSD95 colocalized with microglia lysosomes between conditions. (MG engulfment area % = area of microglia occupied by PSD95-FingR signal in lysosomes / Total microglia area). t test. p = 0.1927. (E-F) Data points represent averages from transfected region ROIs. Control: N = 26 ROIs (from 5 mice; 345 microglia). mC4: N = 26 ROIs (from 5 mice; 319 microglia). Mean \pm SEM. (G-H) Microglia engulfment area (%) (from (F)) as a function of cortical depth (μ m) for control (G) and mC4 (H). Data points represent individual microglia. N = 345 control and N = 345 microglia. Right graphs are same as left but are zoomed on the y-axis. blue line: control mean. red line: mC4 mean. gray lines: 95% confidence intervals. Pearson's r correlation. Control: r = 0.12. p > 0.05. mC4: r = -0.21. **p < 0.01. Note: Data collected by Ashley Comer and Thanh Nguyen. Data analyzed and figure made by Ashley Comer. Data and figure published in Comer et al., *Plos Biology*, 2020.

4.2.3 Microglia phagocytose more material in superficial layers of the cortex

Since increased expression of mC4 led to specific spine loss in L1 apical tufts with no changes in basal dendrites (Figure 3.6), we tested whether microglia engulfment of synaptic material was more prominent near the apical dendrites of cortical neurons. We measured the distance from the center of each microglia soma to the pia to identify its cortical depth, and this measurement was then compared to the area of microglia-

engulfed PSD-95 signal. This allowed us to determine whether the connectivity deficits in apical tufts were due to altered microglia phagocytosis of synapses in a layer-specific manner. In control conditions, there was no correlation between the amount of PSD-95 colocalized with microglia and cortical depth, suggesting that, during normal development, microglia were not biased toward phagocytosis of PSD-95 in specific layers (Figure 4.4, G). However, we observed a significant correlation in the mC4 condition such that microglia closer to L1, where apical tufts are located, engulfed more PSD-95 material than their counterparts in deeper layers (Figure 4.4, H). To test whether mC4-dependent enhancement of phagocytosis in L1 was due to an increased density of microglia, we quantified microglia density in L1 (cortical depth: 0–120 μm) and L2/3 (cortical depth: >120–300 μm) and found no difference between microglia density between layers in either condition (Figure 4.2). There was also no difference in CD68 area within microglia between control and mC4 conditions (Figure 4.2). In summary, our data support the hypothesis that C4 overexpression drives layer-specific circuit dysfunction through excessive microglia engulfment of postsynaptic material.

4.2.4 Expansion microscopy confirms that C4 overexpression enhanced microglia-mediated engulfment of synaptic material

We used expansion microscopy (ExM), a biological sample–preparation procedure that allows for nanoscale imaging with standard confocal microscopes (Wassie et al. 2019) (Figure 4.5), to confirm colocalization of fluorescent signals from PSD-95

and CD68 located in microglia. Using ExM, we increased the size of microglia soma by approximately 180% (equivalent to approximately $2.8\times$ linear expansion) in control and mC4 conditions at P21 (Figure 4.5, D-F). Microglia cell body size increased similarly along its long and short axis, supporting previous findings that have shown that ExM expands biological tissue linearly (Wassie et al. 2019) (Figure 4.5, D-F). Other than increasing their size, expanded microglia had morphologies similar to cells in pre-expansion conditions (Figure 4.5), suggesting that ExM did not fundamentally alter the structure of these brain-resident macrophages.

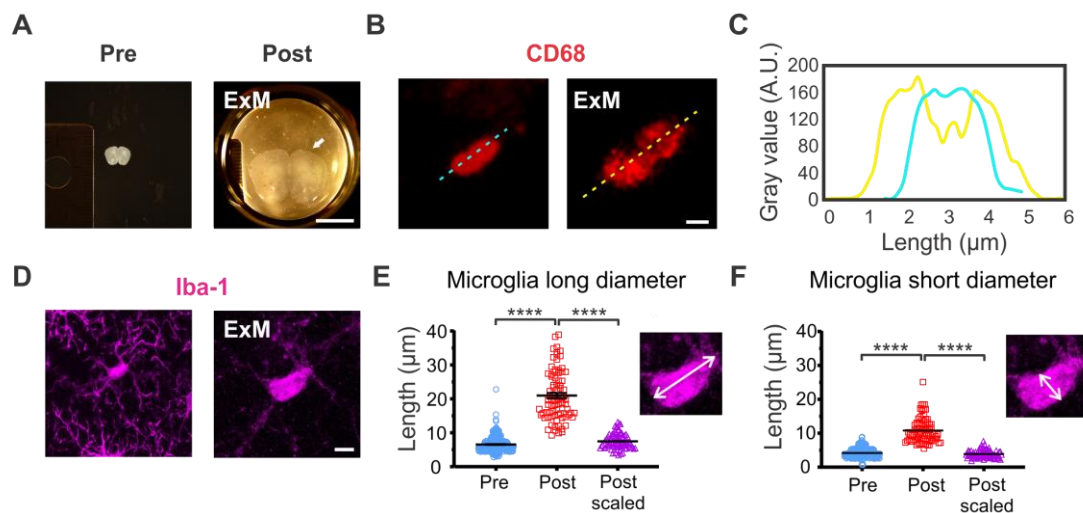


Figure 4.5: Expansion microscopy (ExM) expanded microglia by ~2.8x.

(A) Representative photograph of a coronal PFC brain section before (left) and after (right) expansion. Scale bar = 1 cm. (B) Representative confocal image (40X) of a lysosome (CD68+) before (left) and after (right) expansion. Scale bar = 1 μ m. (C) ExM revealed greater detail of lysosome morphology. Mean gray value line intensity scan (for dotted lines shown in (B)). Blue line: pre-expansion. Yellow line: post-expansion. (D) Representative confocal image (40X) of an Iba+ microglia before (left) and after (right) expansion. Scale bar = 5 μ m. (E) Graph showing the long diameter of each microglia before (blue) and after (red) expansion and after post-scaling (purple). One-way ANOVA with Tukey's. **** $p < 0.0001$. (F) Graph showing the short diameter of each microglia before (blue) and after (red) expansion and after post-scaling (purple). One-way ANOVA with Tukey's. **** $p < 0.0001$. (E-F) The average scaling factor was ~2.78 (control: 2.79 = 0.069; mC4: 2.76 = 0.092). N = 86 microglia (45 control microglia and 41 mC4 microglia). Post-scaled = post / scaling factor (2.78). Inset image of microglia shows the long (E) and short (F) diameter of soma (white line with arrows). The coefficient of variation between pre-expansion, post-expansion and post-expansion scaled microglia sizes was 30.24%, 34.35% and 29.22%, respectively. The variance between the pre-expansion and post-expansion scaled sizes was compared with an F-test and no difference was found between these populations (One-way ANOVA with Tukey's test; $p = 0.4212$). Mean \pm SEM. Note: IUEs performed by Ashley Comer. Data collected and analyzed by Rhushikesh Phadke, Tushare Jinadasa, Shirley Mai, and Connor Johnson. Figure made by Rhushikesh Phadke, Tushare Jinadasa and Ashley Comer. Data and figure published in Comer et al., *Plos Biology*, 2020.

Using ExM, we observed clear examples of PSD-95 colocalized with Iba1 (Figure 4.5 A and C, white arrowheads) and CD68 signal (Figure 4.5, B and D), suggesting synaptic material was localized to microglia lysosomes. Confocal images obtained after ExM show examples of microglia lysosomes that were both negative and positive for PSD-95 in control and mC4 conditions (Figure 4.6). Overexpression of mC4 in L2/3 neurons led to an approximately 3.3-fold increase in lysosomes positive for PSD-95 (Figure 4.5, E). Additionally, microglia in the mC4 condition contained significantly more lysosomes relative to control (Figure 4.5, F, approximately 1.2-fold increase). In contrast, previously we found no change in CD68 reactivity using conventional confocal

microscopy (Figure 4.2, B); this could be due to the enhanced resolution made possible by ExM. For both conditions, lysosomes positive for PSD-95 were approximately 1.5-fold larger than those that were negative for postsynaptic material (Figure 4.5, G).

Additionally, lysosome size did not differ between conditions for PSD-95(+) lysosomes (con[+] versus mC4[+]) or for PSD-95(-) lysosomes (con[-] vs mC4[-]). This suggests that lysosomes positive for PSD-95 were morphologically different than lysosomes without synaptic material for both control and mC4 conditions.

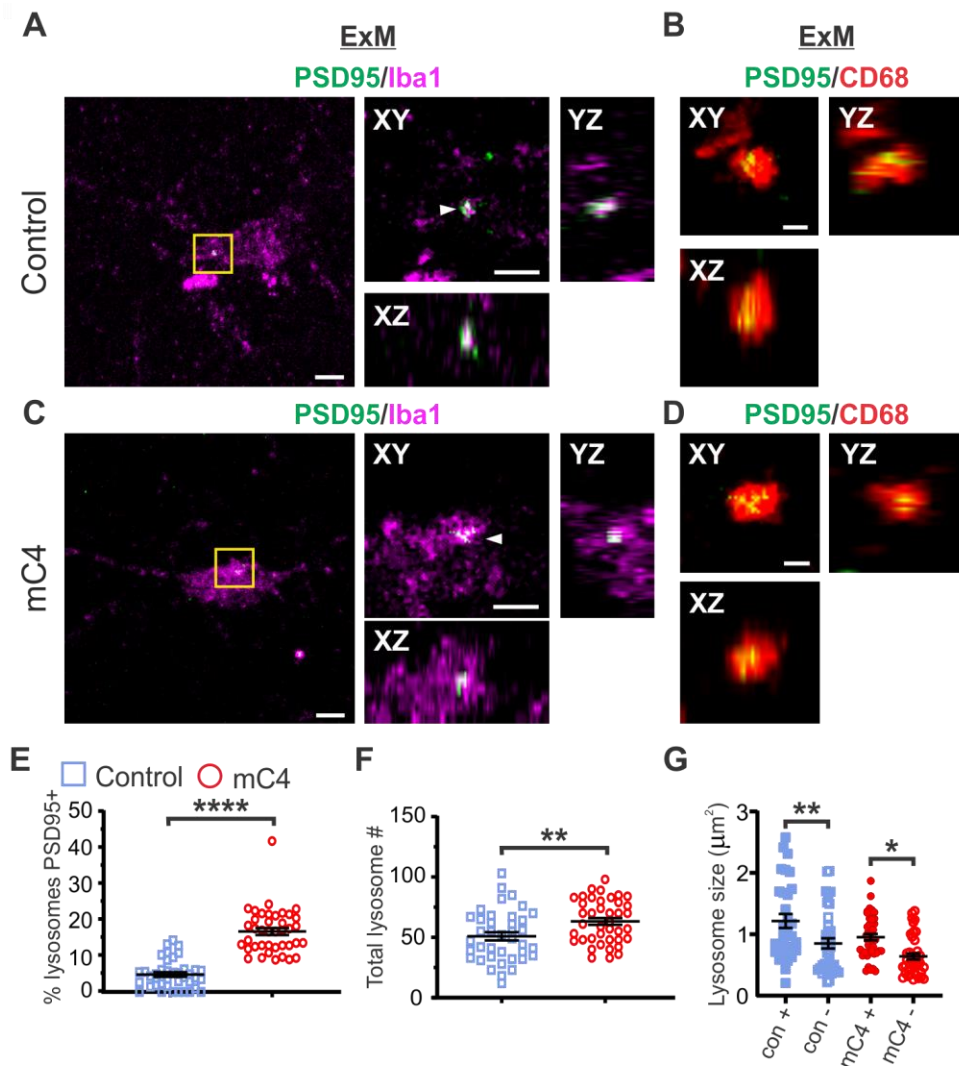


Figure 4.5: Expansion microscopy confirmed C4 overexpression led to enhanced microglial engulfment of PSD-95.

(A-D) Representative confocal images (40X) in expanded tissue showing PSD-95 within microglial lysosomes in P21 mice for control (A and B) and mC4 (C and D) conditions. Panels A and C show a representative microglia (for control and mC4, respectively) including Iba1 and PSD95-FingR-RFP (pseudocolored green) signal. White arrowheads: indicate colocalization of PSD-95 with Iba1 (A and C). Panels B and D show the same z-plane as panels A and C but with CD68 and PSD95-FingR-RFP signal. Orthogonal views shown (XY, YZ and XZ). All images are single z-planes. Magenta: microglia (Iba1). Red: lysosomes (CD68). Green: PSD-95 (PSD95-FingR-tagRFP, pseudocolored green). Yellow box in (A and C) shows zoomed region for orthogonal views. A and C: left scale bar = 5 μm , right scale bar (in XY plane) = 2.5 μm . B and D: scale bar = 1 μm . (E) mC4 overexpression led to an increase of lysosomes that were positive for PSD-95 signal. The percent of lysosomes that were PSD95 positive per each microglia compared between control and mC4. t test. ****p < 0.0001. (F) Number of lysosomes in microglia was increased in the mC4 condition relative to controls. t-test. **p = 0.0064. (G) Lysosomes that were positive for PSD-95 were larger in size compared to PSD-95(-) lysosomes in both control and mC4 conditions. Lysosome size (μm^2) per microglia for control and mC4 conditions separated into lysosomes positive or negative for PSD-95 signal. Control (+) and mC4 (+) are lysosome size for lysosomes positive for PSD95. Control (-) and mC4 (-) are lysosome size for lysosomes that are negative for PSD95. Two-way ANOVA followed by a Tukey's test for all comparisons. Control (+ vs -): **p = 0.0071. mC4 (+ vs -): *p = 0.0150. Control (+) vs mC4 (+): p = 0.0868. Control (-) vs mC4 (-): p = 0.2987. (E-G) blue: control. red: mC4. N = 86 microglia (45 control (from 5 mice) and 41 mC4 (from 4 mice) microglia). Mean \pm SEM. Note: IUEs performed by Ashley Comer. Data collected and analyzed by Rhushikesh Phadke, Tushare Jinadasa, Shirley Mai, and Connor Johnson. Figure made by Tushare Jinadasa and Ashley Comer. Data and figure published in Comer et al., *Plos Biology*, 2020.

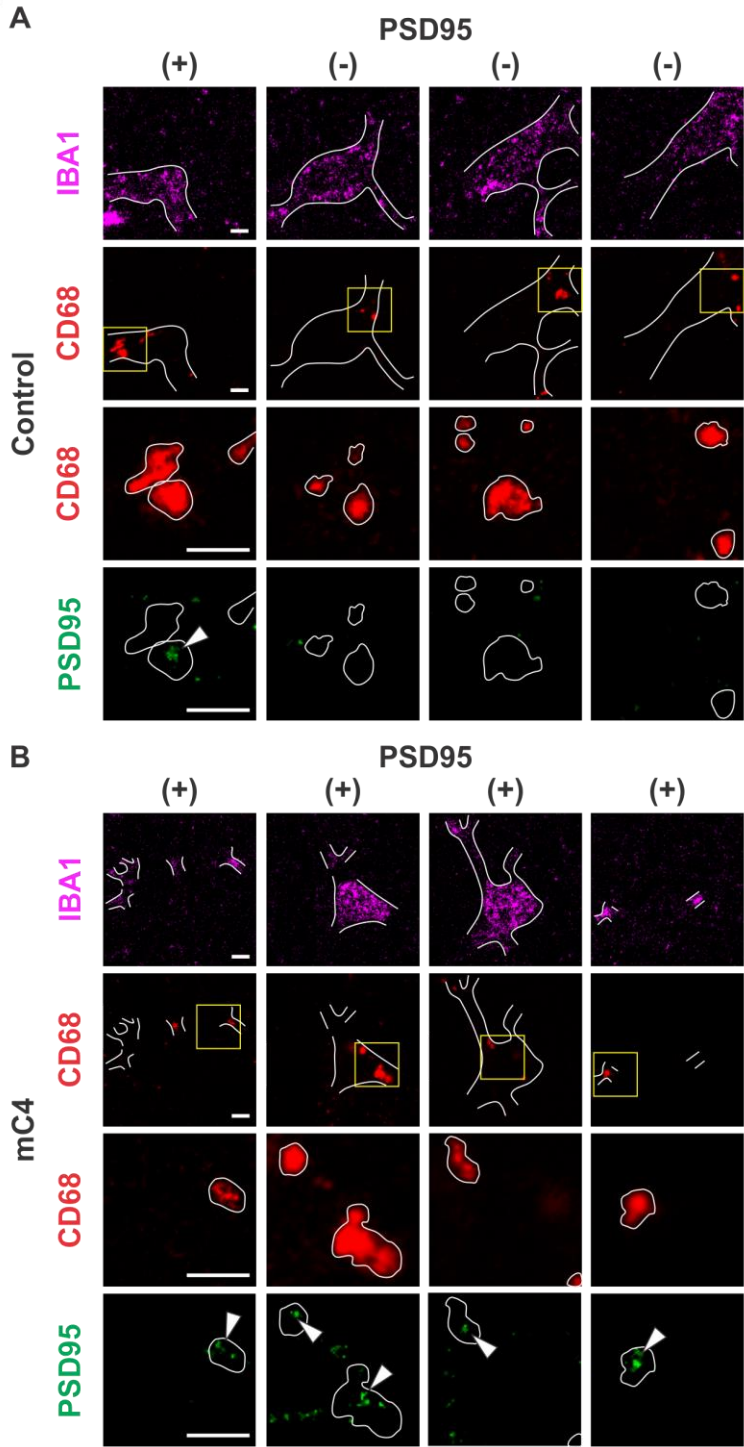


Figure 4.6: ExM revealed that neuronal mC4 overexpression increased the number of PSD-95+ lysosomes in microglia.

(A-B) Representative confocal images (40X) of a single expanded microglia from control (A) and mC4 (B) conditions, respectively. The columns in (A) and (B) show different z-planes of a single microglia in each of the columns that contain lysosomes that were either positive (+) or negative (-) for PSD-95. These images show that mC4 condition microglia contained a greater number of lysosomes positive for PSD-95. The first row shows microglia (Iba1) with a silhouette drawn in white. The second row shows lysosomes (CD68) within the microglia shown in the top panel. The bottom two rows are a zoomed region (yellow inset from row 2) showing lysosomes (3rd row) and PSD-95 (4th row) with a silhouette of the lysosome drawn in white. White arrowheads show PSD-95 within lysosomes. Scale bar (A) = 1 μ m. Scale bar (B) = 1.63 μ m. Note: IUEs performed by Ashley Comer. Data collected and analyzed by Rhushikesh Phadke, Tushare Jinadasa, Shirley Mai, and Connor Johnson. Figure made by Rhushikesh Phadke. Data and figure published in Comer et al., *Plos Biology*, 2020.

4.3 Conclusion and future directions

In summary, our data support the hypothesis that C4 overexpression drives layer-specific circuit dysfunction through excessive microglia engulfment of postsynaptic material. To follow up on this work, in future studies we would like to gain more causative evidence for microglial engulfment of microglia, as opposed to just correlational data showing increased microglia engulfment in mice overexpressing C4. To do this, various microglial receptors that are necessary for microglia-mediated engulfment can be disrupted to see if the phenotype persists when microglia phagocytosis is blocked. For example, CR3 or CX3CR1 could be disrupted using genetic knockout mouse lines. The CR3 is necessary for proper synaptic elimination, as mice deficient for this receptor have excessive synapses compared to wild type mice in the visual thalamus (Schafer et al. 2012). CX3CR1 is a chemokine receptor that is necessary for microglial motility, mice deficient for this receptor also show a lack of synaptic pruning that was

sufficient to alter behavior in mice (Paolicelli et al. 2011). Alternatively, microglia could be depleted using colony stimulating factor 1 receptor antagonists. If the phenotype is reversed when microglia function is impaired, this would be causative evidence that microglia are necessary for synapse loss when C4 is overexpressed. However, since microglia play multiple important roles in development, such as synapse induction, instead of depleting the entire population of microglia, it would likely be best to titer the dosage of CSF1R antagonists to achieve only partial microglia depletion such as a 20-40% reduction in the population. This would potentially avoid secondary effects such as disrupting brain development through altered synapse induction and maintenance.

CHAPTER FIVE

Effect of C4 overexpression on mouse behavior across development

5.1 Introduction

In the developing brain, there is a period of intense synaptogenesis followed by critical developmental periods characterized by experience-dependent refinement of synapses (Trachtenberg et al. 2002, Holtmaat and Svoboda 2009). Synaptic elimination driven by sensory experience refines brain circuitry by optimizing connections between neurons. In SCZ, this process is thought to be dysregulated, thus leading to the loss of both excessive and necessary synapses, thus causing aberrant brain connectivity. If there are pathological change to circuits during these critical periods, the effects on the developing circuitry can be permanent. Therefore, the purpose of this work was to determine if C4 overexpression was sufficient to cause lasting behavioral deficits.

Here, experiments were run to determine whether bilateral C4 overexpression was sufficient to alter behavior in mice. Specifically, we assayed early social behavior in juvenile mice using a maternal interaction task. Behavior was also assayed in adults to determine whether or not the transient spine phenotype at P21 was able to cause lasting behavioral changes, despite the compensation of spines by P60.

5.2 Results

5.2.1 Bilateral in utero electroporation reliably transfects L2/3 excitatory neurons in the frontal cortex

To determine whether overexpression of mC4 in the frontal cortex is sufficient to cause deficits in early (P18) social behaviors, we administered a task that allowed us to measure sensorimotor abilities of mice and maternal–pup social interactions (Zhan et al. 2014). For these experiments, we used a modified IUE method to target large populations of L2/3 neurons in both hemispheres of the frontal cortex. Post hoc analysis of brains from these mice showed that most transfected cells were in prefrontal cortical regions, confirming that we were able to increase mC4 expression in large populations of PFC L2/3 neurons (Figure 5.1). We were able to transfect about 4000 cells per mouse in frontal cortical regions (Figure 5.1, B and D).

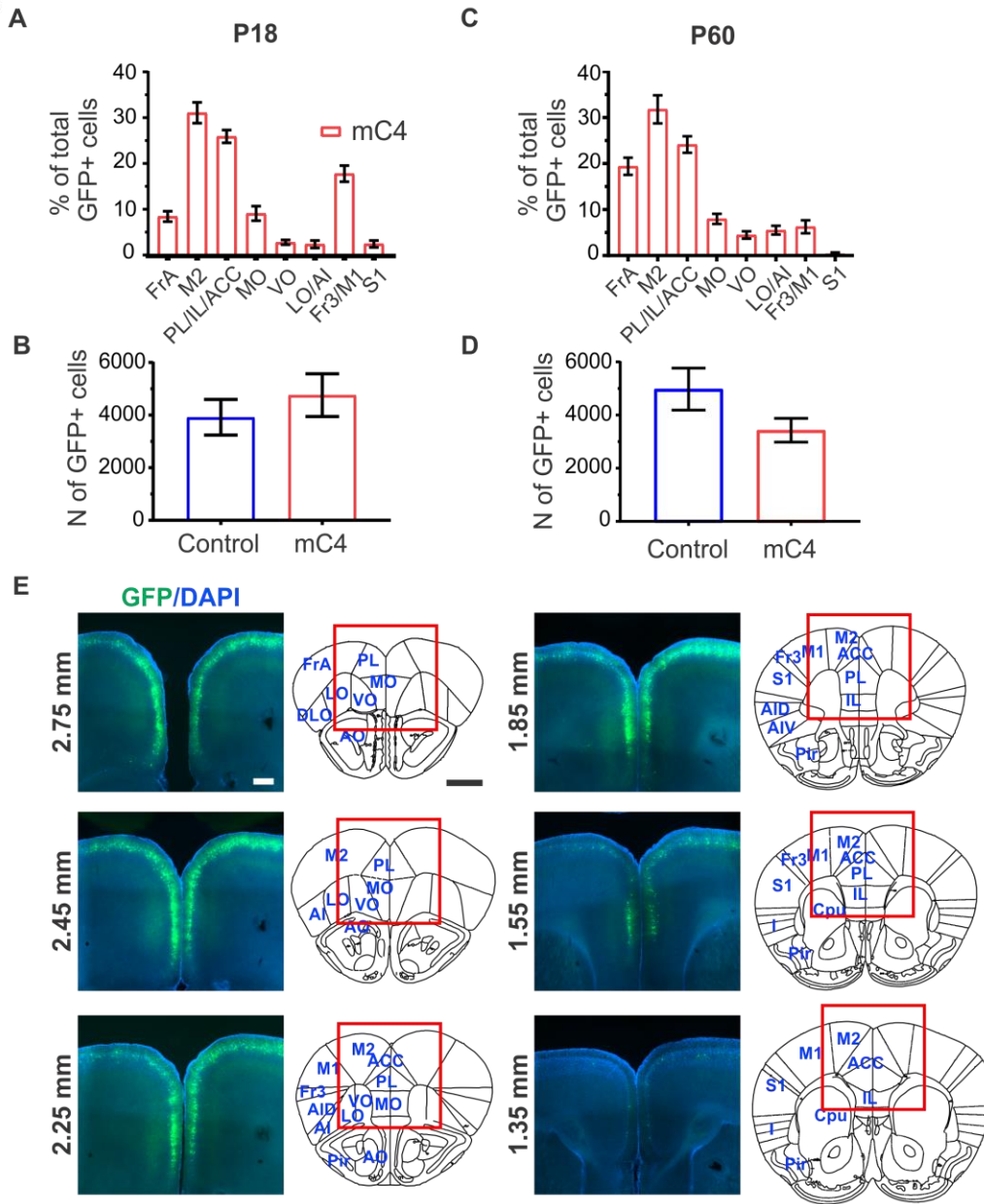


Figure 5.1: Targeting large populations of L2/3 frontal cortex neurons using IUE. (A) Percentage of GFP+ cells per area in juvenile (P18) mC4 mice. N = 21 mC4 mice. (B) Total number of GFP+ positive cells for juvenile mice for control and mC4. N = 36 mice (15 control and 21 mC4 mice). (C) Percentage of GFP+ cells per area in adult mC4 mice. N = 20 mC4 mice. (D) Total number of GFP-positive cells per area for adult mice (P60) for control and mC4. N = 42 mice (22 control and 20 mC4). (E) Representative sections showing rostro-caudal extent of transfections in the frontal cortex. Images in left panels are zoomed areas from the right panels (red square). Frontal association cortex: FrA. Supplementary motor cortex: M2. Prelimbic cortex: PL. Infralimbic cortex: IL. Anterior cingulate cortex: ACC. Medial orbitofrontal cortex: MO. Ventral orbitofrontal cortex: VO. Lateral orbitofrontal cortex: LO. Anterior insular cortex: AI. Frontal cortex area 3: Fr3. Primary motor cortex: M1. Primary somatosensory cortex: S1. Piriform cortex: Pir. Anterior olfactory nucleus: AO. Caudate-putamen: Cpu. Black numbers: Bregma coordinates. Left panel scale bar = 0.5 mm. Right panel scale bar = 1 mm. Mean \pm SEM. Note: IUEs performed and data collected by Ashley Comer. Data analyzed by Ashley Comer, Frances Hausmann, Eli Spevack, Berta Escude, Charlotte Yeung, Thara Venu, Haley Cerretani, Cesar Diaz, and Meaghan Connolly. Figure made by Ashley Comer. Data and figure published in Comer et al., *Plos Biology*, 2020.

5.2.2 Complement-dependent alterations in frontal cortical circuitry are sufficient to alter maternal-pup social interactions

To test sensorimotor abilities (maternal interaction 1 [MI1] task), we transferred P18 pups to an arena that contained fresh bedding in two neutral corners and nesting material from the animal's home cage in the corner opposite to the starting corner, and mice were free to explore the arena for 3 min (Figure 5.2, A). Similar to controls, mC4 mice spent more time exploring the nest corner relative to the neutral corners, suggesting that mC4 mice had normal homing behavior (Figure 5.2, B). Although grooming occurrences of mC4 mice were more frequent and about 4.3-fold longer (Figure 5.3) than in control mice, there was no interaction between experimental group and corner preference (Figure 5.2, B). These results indicate that although mC4 mice engaged in

more repetitive behavior, they were able to explore the arena and interact with their nest bedding to the same extent as control animals. Additionally, these results suggest that increased levels of mC4 in the frontal cortex did not impair overall sensory abilities or cause gross motor deficits in P18 pups.

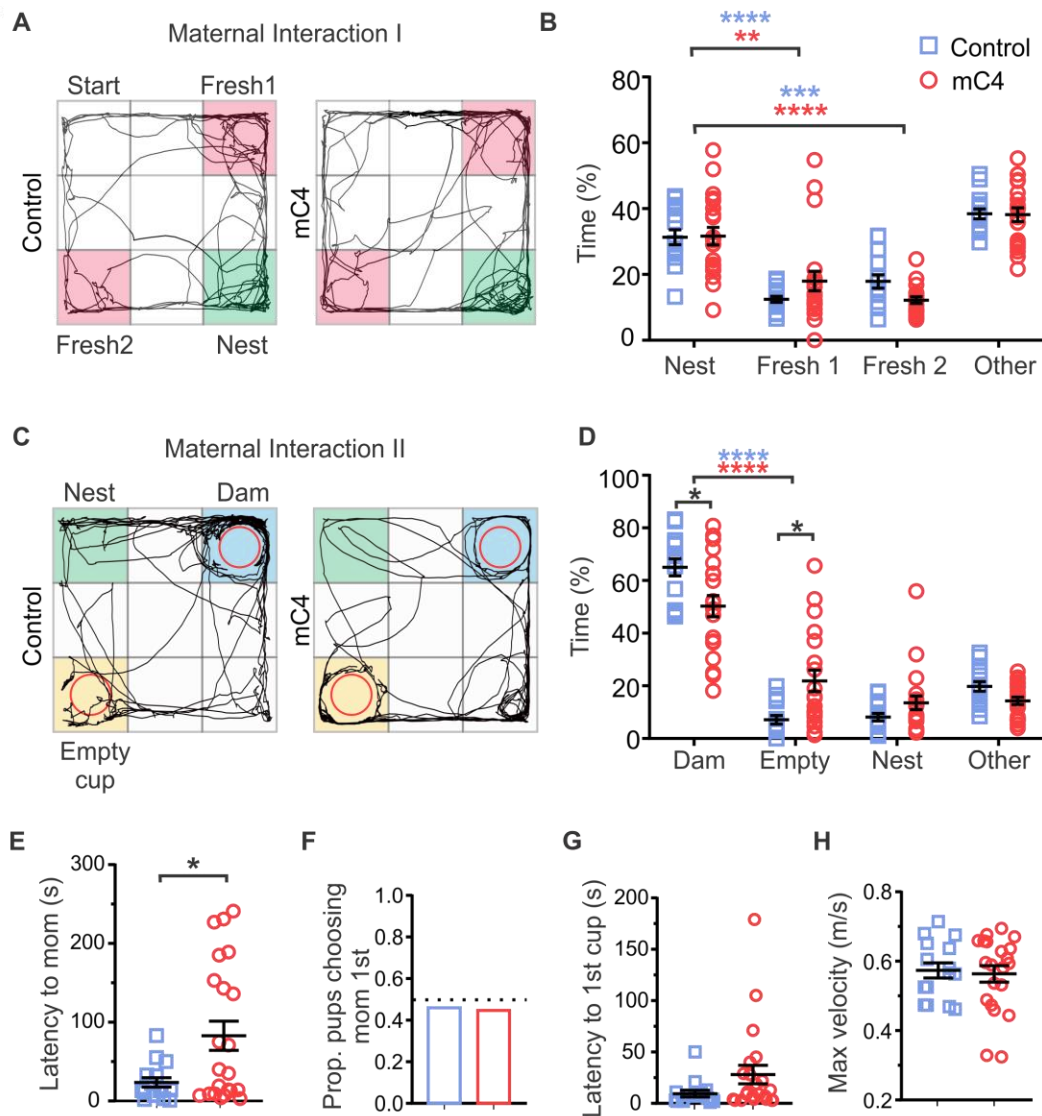


Figure 5.2: C4-dependent alterations in frontal cortical circuitry were sufficient to alter maternal-pup social interactions.

(A) Representative examples of path traveled (black trace) by P18 control and mC4 pups in MI1 task. Fresh bedding corners (fresh 1 and 2, pink) and nest bedding corner (green). (B) Control and mC4 pups spent a similar proportion of time exploring the nest and fresh corners in the MI 1 task, suggesting motor and sensory skills were intact. All mice spent more time in nest bedding than fresh bedding. ** $p < 0.01$, *** $p < 0.001$, **** $p < 0.0001$. Two-way ANOVA and Sidak's post test. Control vs. mC4 time spent in nest: $p > 0.9999$. Control vs. mC4 time spent in fresh 1: $p = 0.3327$. Control vs. mC4 time spent in fresh 2: $p = 0.3138$. (C) Representative examples of path traveled (black trace) by P18 control and mC4 pups in MI 2 task. Dam's cup (dam: blue), Empty cup (empty cup: yellow), Nest bedding corner (nest: green). (D) mC4 pups spent less time interacting with dam and more time near the empty cup compared to controls. Two-way ANOVA and Sidak's post test. * $p < 0.05$. **** $p < 0.0001$. (E) mC4 mice took longer to approach the dam relative to controls (seconds). t-test with Welch's correction. * $p < 0.05$. (F) Control and mC4 pups traveled to dam's cup first ~ 50% of the time, suggesting first choice was random. Fisher's exact test. $p = 0.9999$. (G) Latency to reach first cup (either dam or empty) was not different. t-test with Welch's correction. $p = 0.06$. (H) Control and mC4 pups reached the same maximum velocity (m/s). t test. $p = 0.77$. (B, D-H) $N=15$ control mice and $N=21$ mC4 mice. blue: control. red: mC4. Mean \pm SEM unless otherwise noted. Note: IUEs performed by Ashley Comer. Data collected by Elena Newmark and Ashley Comer. Data analyzed by Tushare Jinadasa, William Yen and SaraAnn Rosenthal. Figure made by Ashley Comer. Data and figure published in Comer et al., *Plos Biology*, 2020.

To test maternal–pup social interactions (maternal interaction 2 [MI2] task), we placed P18 pups in an arena that contained nest bedding, an empty wire mesh cup, and a wire mesh cup containing the pup's dam, and the behavior of each pup was monitored for 5 min (Figure 5.2, C). We found that mC4 mice showed an approximately 23% reduction in time spent exploring the cup containing the dam as compared to control mice (Figure 5.2, D). mC4 mice also exhibited an approximately 2.5-fold decrease in the latency to first approach the dam's cup (Figure 5.2, E). The proportion of pups that approached the dam's cup before the empty cup (at start of trial) was approximately 50% (Figure 5.2, F),

suggesting that pups in both conditions engaged in similar exploratory behavior of the arena before seeking their mother. mC4 and control mice had similar latencies to first reach either the empty or dam's cup (Figure 5.2, G) and similar maximum speeds (Figure 5.2, H). Taken together, these results indicate that mC4 pups had intact motor and sensory abilities but were less motivated or interested in interacting with their mother.

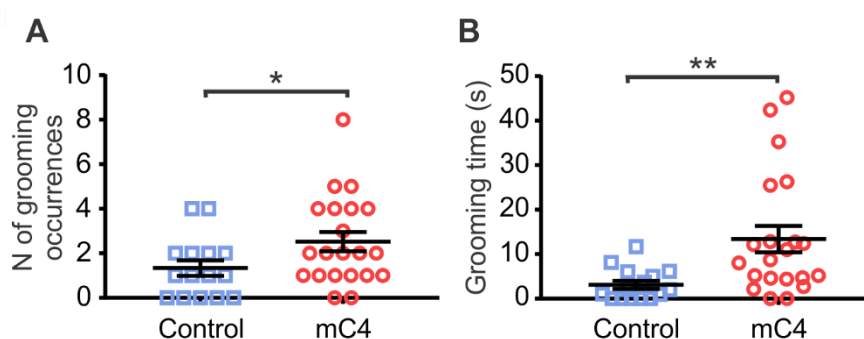


Figure 5.3: mC4 pups had increased grooming occurrences and grooming time compared to controls.

(A) mC4 mice had a greater number of grooming occurrences during the MI 1 task. t test with Welch's correction. * $p < 0.05$. (B) Average time per each grooming occurrence was longer for mC4 mice compared to controls in the MI 1 task. t-test with Welch's correction. ** $p < 0.01$. (A-B) $N = 36$ mice (15 control and 21 mC4). Mean \pm SEM. Note: IUEs performed by Ashley Comer. Data collected by Elena Newmark and Ashley Comer. Data analyzed by SaraAnn Rosenthal. Figure made by Ashley Comer. Data and figure published in Comer et al., *Plos Biology*, 2020.

5.2.3 Complement-dependent alterations in social behaviors persist into adulthood

Although we did not observe changes in dendritic spine density at P60 between conditions (Figure 4.6, A), it is possible that increased C4 expression in adult mice resulted in changes in the function of frontal L2/3 neurons that could not be directly assessed by analyzing the mean dendritic spine density (e.g., miswiring of synaptic

connections or intrinsic excitability). Therefore, we tested whether bilateral overexpression of mC4 in the frontal cortex led to changes in sensorimotor abilities or social behavior in adult (P60–70) mice (N = 22 control mice, N = 20 mC4 mice). We first tested adult mice in a novel-object task to assess whether interest in a novel object was affected by C4 overexpression (Figure 5.4, A). Control and mC4 mice spent similar amounts of time exploring the novel object (Figure 5.4, B). Next, a novel-object recognition task was performed, in which mice were placed in an arena for 5 min with a novel object in one corner and a familiar object in the opposite corner (Figure 5.4, C). The discrimination index (DI) for object interaction ($DI = [\text{time with novel object} - \text{time with familiar object}] / [\text{time with novel object} + \text{time with familiar object}]$) was positive for both control and mC4 mice, indicating that mice in both conditions spent more time exploring the novel object relative to the familiar object (Figure 5.4, D). Additionally, the DI for control and mC4 mice was not different (Figure 5.4, D), suggesting that overexpression of mC4 in the frontal cortex did not alter sensorimotor abilities or general motivation. In support of this, mC4 mice traveled at similar speeds and distances in an open field (OF) arena relative to the control group (Figure 6.4, J; Figure 5.5).

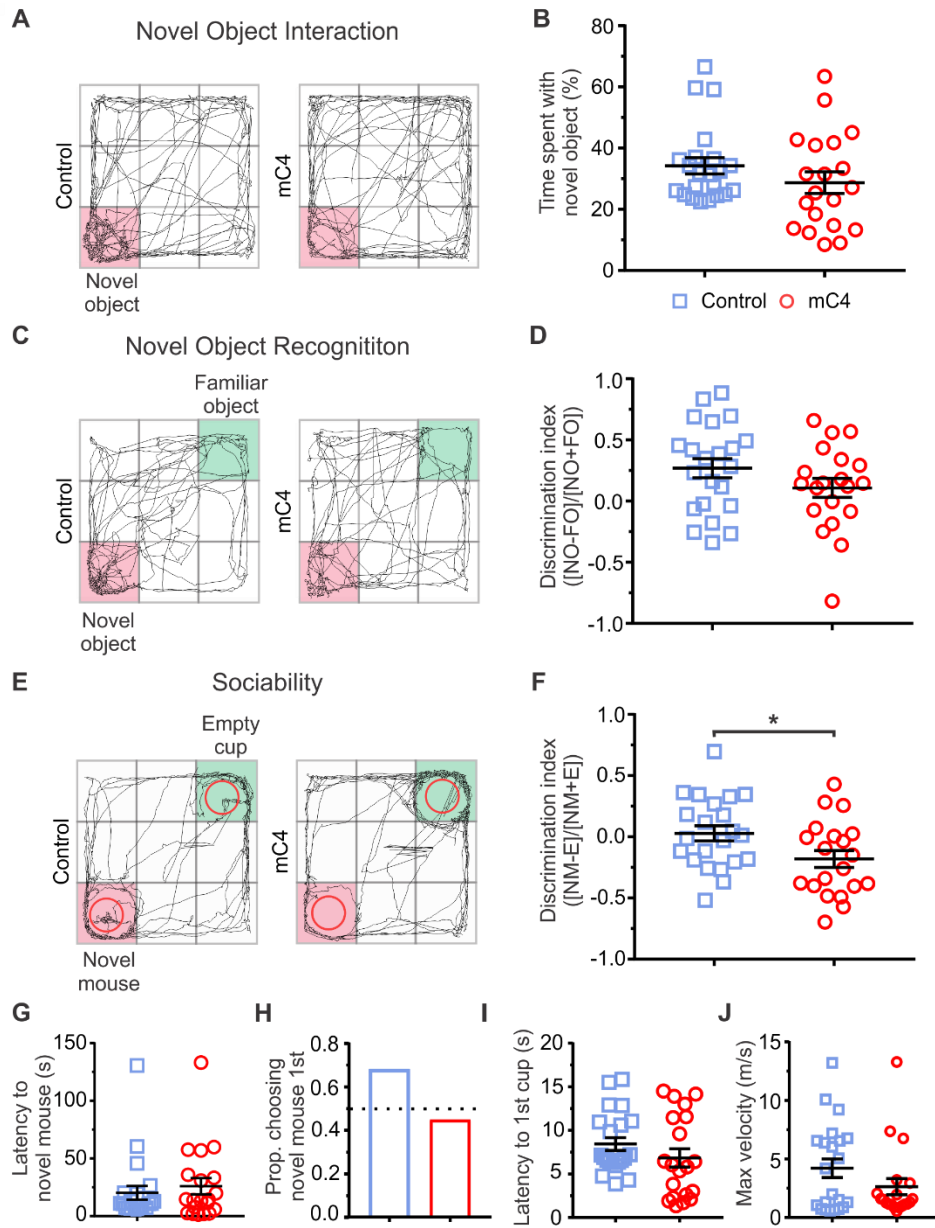


Figure 5.4: C4-dependent alterations in frontal cortical circuitry led to behavior deficits in sociability that persist into adulthood.

(A) Representative examples of path traveled (black trace) by P60 control (left) and mC4 (right) adult mice in novel object interaction task. pink corner = location of novel object. (B) Control and mC4 mice spent a similar amount of time exploring the novel object. Percent time spent in corner with novel object shown. $p = 0.2127$. (C) Representative examples of path traveled (black trace) by P60 control (left) and mC4 (right) adult mice in novel object recognition task. pink corner: location of novel object. green corner: location of familiar object. (D) Novel object recognition was intact in the mC4 condition. Control and mC4 mice had a similar DI ((time with novel object – time with familiar object) / (time with novel object + time with familiar object)). $p = 0.1539$. (E) Representative examples of path traveled (black trace) by P60 control (left) and mC4 (right) adult mice in sociability task. pink corner: location of novel mouse under mesh wire cup. green corner: location of empty mesh wire cup. (F) mC4 overexpressing mice spent less time exploring a novel mouse and more time with the empty cup relative to control. Graph shows DI ((time with novel mouse – time with empty cup) / (time with novel mouse + time with empty cup)). $*p = 0.029$. (G) Control and mC4 mice had a similar latency to first approach the novel mouse (sec). $p = 0.5416$. (H) Control and mC4 mice traveled to the novel mouse cup first at a similar proportion. Proportion of mice that approached the novel mouse cup first. Fisher's exact test. $p = 0.54$. (I) Latency to reach first cup (either novel mouse cup or empty cup) was not different (sec) between conditions. $p = 0.217$. (J) Control and mC4 mice reached the same maximum velocity (m/s). $p = 0.1442$. $N=22$ control and $N=20$ mC4 mice between P60-70. blue: control. red: mC4. t test unless otherwise stated. Mean \pm SEM unless otherwise noted. Note: IUEs performed by Ashley Comer. Data collected by Ashley Comer and Charlotte Yeung. Data analyzed by Balaji Sriram. Figure made by Ashley Comer. Data and figure published in Comer et al., *Plos Biology*, 2020.

Next, we placed either control or mC4 adult mice in an arena that contained an empty wire mesh cup and a wire mesh cup containing a novel mouse (strain, sex, and age matched) in opposing corners, and the behavior of each mouse was monitored for 5 min (Figure 5.4, E). We found that adult mC4 mice showed a significant reduction in social DI, a metric of sociability ($[\text{time spent with novel mouse} - \text{time spent with empty cup}] / [\text{time spent with novel mouse} + \text{time spent with empty cup}]$), as compared to control mice (Figure 5.4, F). This reduction in sociability was not due to an overall increase in

vigilance or anxiety-like behavior in the mC4 condition, because both groups spent similar amounts of time in the open arms of the elevated-zero maze (EZM) (Figure 5.5). We found no difference between control and mC4 mice in latency to approach either the novel mouse or empty cup, or in the proportion of mice choosing the novel mouse first (Figure 5.4, G–I).

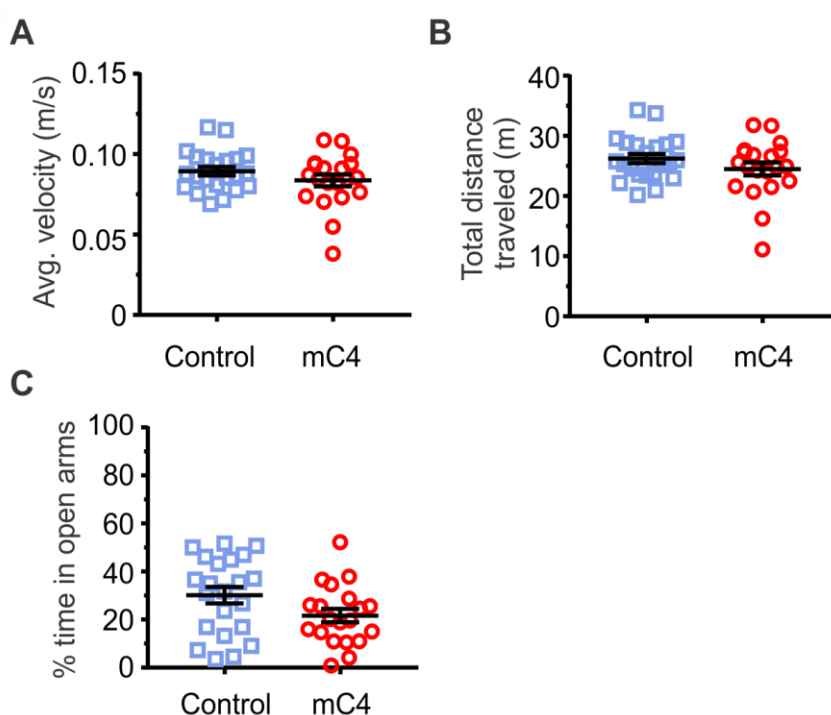


Figure 5.5: Adult mice bilaterally expressing mC4 had intact motor abilities.

(A) Control and mC4 mice (P60) had a similar average velocity in the open field task. t-test. $p = 0.2141$. (B) Control and mC4 mice traveled similar total distances in the OF task. t-test. $p = 0.1986$. (C) Control and mC4 mice spent a similar amount of time exploring the open arms of the EZM task. t-test. $p = 0.0651$ (A–C) $N = 42$ mice (22 control and 20 mC4 mice). Mean \pm SEM. Note: IUEs performed by Ashley Comer. Data collected by Ashley Comer and Charlotte Yeung. Data analyzed by Balaji Sriram. Figure made by Ashley Comer. Data and figure published in Comer et al., *Plos Biology*, 2020.

5.3 Conclusion and future directions

Here, we developed a modified, bilateral in utero electroporation method that allowed for the transfection of larger populations of L2/3 excitatory PFC neurons. Although sensorimotor abilities were intact in both juvenile and adult mice overexpressing C4, their ability to engage in normal social behavior was disrupted. Overall, these results suggest that increased expression of mC4 in frontal L2/3 neurons led to long-lasting alterations in PFC circuitry that were sufficient to cause a reduction in social interactions in both juvenile and adult mice. Since it is known that there are many other behavior deficits observed in SCZ, future studies could elucidate what other behaviors C4 overexpression can impact in mice. For example, the PFC is necessary for normal working memory so future studies could assay mice in tasks such as the delayed alteration T-maze task. We show here for the first time that the overexpression of C4 alters the developmental trajectory of cortical circuits which is sufficient to alter SCZ-related behaviors in mice at both juvenile and adult time points.

CHAPTER SIX

A pipeline to study the effect of schizophrenia-associated genes on mouse behavior throughout development

6.1 Introduction

Genome-wide association studies (GWAS) have driven the discovery of novel candidate genes that are associated with brain pathologies (Yang et al. 2018, Schizophrenia Working Group of the Psychiatric Genomics Consortium, 2014, Howard et al. 2019, Grove et al. 2019). These studies have been particularly beneficial in understanding devastating neuropsychiatric disorders such as SCZ, where the investigation of novel genes has served as a launching point for new lines of research and therapeutic intervention (Comer et al. 2020, Chini et al. 2020). Genes harboring risk for SCZ show biased expression in the prefrontal cortex (PFC) during prenatal and early postnatal development, a region implicated in the pathology of several neuropsychiatric disorders (Clifton et al. 2019). Additionally, mouse models of psychiatric disorders exhibit abnormal activity in prefrontal cortical networks (Chini et al. 2020, Oberlander et al. 2019, Batista-Brito et al. 2019). These results suggest that SZC-associated genes might play a role in the developmental wiring of this region. Further investigation using animal models is required to understand the contribution of these candidate genes to the establishment of connections in the PFC and to determine whether these genes have a causative role in the pathogenesis of neuropsychiatric disorders. Genetic strategies in

mice that allow for the study of gene expression changes on specific neuronal circuits are a promising method to understand the molecular mechanisms that link gene expression changes to PFC dysfunction.

Genetic mouse lines offer a method to study the impact of particular genes on brain development and function. However, relying on transgenic mice can be limiting since there are not always commercially available lines to examine the effects of specific genes on developing neural circuits. Moreover, it can be extremely costly and time consuming to develop custom mouse lines. The use of intersectional genetic manipulation strategies that combine transgenic mice with viral approaches has revolutionized the understanding of the brain (Luo et al. 2018, DeNardo & Luo 2017, Huang & Zeng 2013). Despite much progress, viral strategies come with certain limitations dependent on the viral vector type, including limits in packaging capacity that can restrict viral expression (Wu et al. 2010) and cell toxicity associated with viral expression (Callaway & Luo 2015). Furthermore, in most experimental conditions, robust gene expression using adeno-associated virus (AAVs) requires approximately 2 to 4 weeks (Cruz-Martín et al. 2014), making routine viral strategies unfeasible to manipulate genes during early postnatal development.

In utero electroporation (IUE) is an alternative approach that allows for rapid and inexpensive gene transfer (Saito 2006, Cruz-Martín et al. 2012) that, when coupled with fluorescent labeling and pharmacogenetic or optogenetic approaches, provides a powerful platform to dissect the function of neuronal circuits. Additionally, with the development of CRISPR-Cas9 genome editing genes can be overexpressed or precisely altered through

cell-type specific knock-down or knock-out of specific genes or through the modulation of promoters (Zhang et al. 2016, Strecker et al. 2019). Gene manipulation approaches using IUE are especially advantageous when the effect of genes on neuronal circuits need to be tested during narrow developmental windows (Cruz-Martín et al. 2012). IUE is a versatile technique and overexpression can be easily accomplished by inserting a gene into an expression vector under a specific promoter. Additional control of gene expression can be achieved by driving expression using promoters of different strengths or using inducible promoters capable of temporally controlling gene expression (LoTurco et al. 2009, Kolk et al. 2011). Additionally, IUE allows for the targeting of cells within specific cortical layers, cell types and brain regions, which isn't always feasible using other approaches (Comer et al. 2020, Cruz-Martín et al. 2010). Recent advances in the IUE configuration based on the use of three electrodes, which generates a more efficient electric-field distribution, have expanded the functional repertoire of this method and allowed scientists to target new cell types and increase the efficiency, accuracy, and number of cells that can be targeted (Szczyrkowska et al. 2016, dal Maschio et al. 2012). This technique was recently used to determine the causative role of complement component 4A (C4A), a gene linked to SCZ, in PFC function and early cognition (Comer et al. 2020).

Presented here is an experimental pipeline that combines gene transfer approaches to target large populations of excitatory neurons in the frontal cortex, including the PFC, with behavioral paradigms that not only enables the study of cell and circuit-level changes, but also allows behavior to be monitored throughout early postnatal

development and adulthood. First described is a method to bilaterally transfect large populations of L2/3 pyramidal neurons in frontal cortical regions. Next, tasks to assay social behavior in juvenile and adult mice are outlined. Cell counts can be obtained upon the completion of behavioral tasks to quantify the extent and location of cell transfection. Furthermore, the number of cells transfected can be correlated with behavioral data to determine if a greater number of transfected cells leads to greater perturbations in behavior.

6.2 Protocol

6.2.1 Advance preparation for in utero electroporation

These are the procedures to follow for in utero electroporation. Purchase a commercial plasmid or subclone a gene of interest into plasmid with the desired promoter. Determine the desired promoter based off the level of expression needed. In general, plasmids under the CAG promoter can be used to achieve high levels of the transgene whereas cell-type-specific promoters (e.g., synapsin for neurons) tend to be less active. The experimenter should empirically determine the appropriate expression levels for each plasmid. Transform bacteria and grow stocks in bacterial media with the appropriate antibiotic. Remove commercially obtained competent cells from -80 °C and thaw on ice for 20 min. Mix DNA (100 pg – 100 ng) into 30 µL of competent cells and incubate the mixture on ice for 20 min. Transform the cells with heat shock by incubating in a 42°C water bath for 45 sec and then return the tube back to ice for 2 min. Add 200-

1,000 μL of LB media to the transformed competent cells and grow for 45 min at 37°C on a shaking incubator. Plate 200 μL of the transformed cells into an LB agar plate containing the appropriate antibiotic and incubate the plate overnight at 37°C . The next day, incubate one bacterial colony in 200 mL of LB broth with the appropriate antibiotic at 37°C on a shaking incubator overnight. Purify plasmid DNA using a maxiprep kit. Follow instructions given in obtained maxiprep kit. For elution step, do not elute DNA into elution buffer. Instead, elute DNA using either 200 μL sterile PBS (1X) or molecular grade water. Ensure that the final concentration of the DNA is greater than 1 $\mu\text{g}/\mu\text{L}$. If the plasmid containing the gene of interest does not contain a reporter gene, then also prepare a plasmid to co-transfect with a reporter molecule, such as green fluorescent protein (GFP), to allow for the visualization of transfected cells. Prepare DNA solution for surgery by diluting the plasmid DNA into PBS (1X) so that the final concentration of each plasmid is 1 $\mu\text{g}/\mu\text{L}$. Add fast green dye so that the final concentration in the DNA solution is 0.1%. For bilateral injections, prepare 60 μL of solution per dam (for approximately 10 pups).

In the days and weeks before the surgery, plan to order or breed timed-pregnant mice. If ordering timed-pregnant mice, order mice to arrive on gestation day (E) 13 or earlier to allow the dams adequate time to acclimate to animal housing. This will reduce animal stress and lead to a higher survival rate of the pups. Here, we used CD-1 outbred mice for all experiments since they tend to have more offspring per litter. If breeding timed-pregnant mice, pair female mice with a male overnight, once a week. The presence of a vaginal plug on the following morning is noted as E0.5. Pregnancy can be

determined by monitoring the weight of the female mice. Different mouse strains have different weight increases through pregnancy, so determine typical weight gain for the mouse strain used. Whether ordering or breeding the mice, to reduce stress of the dams, place a nesting pad and mouse house in the cage. Reducing stress can help increase the survival rate of the pups.

Design and assemble the three-prong electrode prior to surgery day and test that it is working. Briefly, to make the three-prong electrode, use grade 2 titanium sheets with a thickness of 0.063 in as stock material for electrode contacts. Using standard machining techniques or precision hand tools, make electrodes with the following dimensions: 20 mm x 5 mm with a rounded tip and grooved back. Remove any rough edges or burrs using fine grit sandpaper. To wire the electrode contacts, wrap 22-gauge stranded copper wire around the grooves of the electrode and secure by soldering. Protect this joint using heat shrink tubing. Then, attach the connected electrode to autoclavable, non-conductive forceps using additional heat shrink tubing to make the two negative electrodes. Attach the single positive electrode to an autoclavable, non-conductive material (such as a toothbrush handle). The open end of the wire can be fitted with a standard banana plug. Test that the three-prong electrode is functioning properly before the start of surgery.

6.2.2 Surgery preparation and in utero electroporation procedure

Prepare for surgery by bringing the pregnant dams to the surgery area at least 30 min prior to surgery to allow stress levels to reduce after transport from the animal facility. Sterilize entire surgery site using sterilizing germicidal wipes and then 70%

ethanol. Sterilize autoclaved tools in a glass bead sterilizer. Prepare sterile PBS (1X) (about 50 mL per dam) in conical tubes and place in water bath heated to 38-40° C. Check the sterile saline temperature with a thermometer. Turn on water heating circulation pump so that it is warmed to 37° C prior to start of surgery. This will maintain the mouse's body temperature for the duration of the surgery. Turn on the pressure-injector and electroporator and ensure proper function prior to surgery. Briefly spin DNA solution on a tabletop centrifuge and place on ice. Pull glass pipettes on a pipette puller so that the tip of the pulled-glass pipette is about 50 µm in diameter. Fill a pulled pipette with 20-40 µL of DNA solution. Set up all necessary items for surgery including hair removing lotion, iodine, 70% ethanol, cotton swaps, eye drops, sutures, gauze, etc. Prepare a surgery sheet and fill out necessary information.

To perform in utero electroporation surgery, weigh the mouse prior to surgery and note this on the surgery sheet. Anesthetize a pregnant mouse (E16) by inhalation in an induction chamber with 4% (v/v) oxygen-isoflurane mixture. Once the mouse has been induced, move to a mask inhalation and maintain isoflurane at 1-1.5% (v/v) and monitor breathing throughout the surgery. Administer preoperative analgesics. Use hair removal cream or carefully use a razor to remove the fur from the abdomen. Sterilize the abdomen by swabbing with povidone-iodine and 70% ethanol and repeat this at least 3 times. Create a sterile field around the abdomen using sterile gauze. Make an incision in the abdominal skin, being sure to lift the skin up with forceps to avoid cutting through the muscle. Then cut through the muscle, again taking care to lift the muscle up to avoid cutting vital organs. Carefully pull the uterine horns out of the dam using ring forceps and

place them gently onto the sterile field, making sure that the uterine horn is supported with padding and isn't tugging too far away from the dam. From this point on, keep the uterine horn moistened throughout the rest of the surgery with the pre-warmed sterile PBS (1X). Position an embryo using either forceps or fingers and carefully insert the pulled glass pipette into the lateral ventricle. Inject about 2-3 μL into each lateral ventricle by either inserting the pipette into one and then the other ventricle (recommended) or by injecting the DNA solution into one ventricle until it passes into both lateral ventricles. Note: The tip of the glass pipette could break during surgery. If this happens, replace the glass pipette, ensuring that the uterine horns are kept moistened while a new pipette is prepared and filled with the DNA solution. To transfect cells bilaterally in the frontal cortex, position the two negative electrodes on the sides of the embryos head just lateral and slightly caudal to the lateral ventricles and position the positive electrode between the eyes, just in front of the developing snout. Ensure the embryo is generously moistened before applying four square pulses (pulse duration: 50 ms, pulse amplitude: 36 V, interpulse interval: 500 ms). Inject and electroporate all embryos, going one-by-one so that each embryo is electroporated immediately after the DNA solution injection. Once all embryos have been electroporated, carefully insert the uterine horns back into the abdominal cavity. The abdominal cavity can be coated in sterile PBS (1X) to aid uterine horn placement. Fill the abdominal cavity with sterile PBS (1X) so that no air pockets remain after suturing is complete. Suture the muscle with absorbable sutures and the skin with silk non-absorbable sutures. Allow the dam to fully recover in a heated chamber for at least 1 hr. In the next 48 hr, check on the dam(s) regularly.

6.2.3 Assaying early and adult social behavior

Perform the maternal homing behavior in postnatal mice born after the IUE surgery. For the maternal interaction I (MI1) task, ensure that cage bedding is not changed in the week before the task will be performed. Obtain or build an open field (OF) arena that can be easily cleaned (acrylic is recommended) with the following dimensions: 50 x 50 x 30 cm (length-width-height). Lighting conditions during performance of behaviors can vary depending on experimental question and can influence levels of arousal and anxiety-like behavior. Record behavioral experiments under a dim light (approximately 20 lux) positioned over the center of the arena. For two days prior to behavior testing, acclimate the dam to the arena by placing it beneath a mesh wire cup (such as a pencil cup) in a corner of the arena for five min per day. On testing day, which can be from postnatal day (P) 18-21, before mice have been weaned, clean the arena thoroughly with sanitizing wipes and 70% ethanol. Set up the arena with two opposing corners both containing clean bedding and one corner containing soiled nest bedding from the pup's home cage. Allow each pup to explore the arena for 3 min, placing each pup in the neutral, empty corner at the start. Record behavior with a video camera at 30 fps. Thoroughly clean the arena between every pup, and replace the fresh bedding. Alternate which corner is the fresh versus nest bedding as a control to avoid corner preference due to other reasons (i.e., ambient noise or light). If running multiple litters across the P18-21 developmental window, run behavioral experiments at the same time between days. Also ensure that during a given day, control and experimental groups are run in parallel.

Perform the maternal social interaction in the maternal interaction II (MI2) task immediately after the MI1 task. Set up the arena so that one corner contains an empty wire mesh cup and the opposing corner contains the dam under a mesh wire cup. If the mice are able to move the cup, weigh the cup down with a weight that can be taped to the top of the cup to prevent movement. Put soiled nest bedding from home cage in another corner. Run the MI2 task. Place the pup in the empty corner and record behavior for five min at 30 fps, allowing the pup to explore. Run each pup separately and thoroughly clean the entire arena and wire mesh cups between every pup.

Follow the following instructions to perform the adult social behavior task. Adult social behavior can be run in the same mice post weaning. Handle the adult mice for 3 consecutive days to allow habituation to the experimenter. Ensure that only experimenters that have been familiarized to the mice run behavior experiments, ideally the same person will run all tasks. Habituate mice to the OF arena for 3 days for 5 min each day. Assay behavior in a novel object recognition task to measure general locomotion and interest in a novel object. This will allow more meaningful interpretation of social behavior if mice have a specific deficit in social interactions. Novel object interaction is performed by placing mice in the arena for 5 min with a novel object (small plastic toy with smooth, cleanable surfaces) in one corner of the arena. Clean the arena thoroughly between mice with 70% ethanol. For novel object recognition, place the previously exposed 'novel object', which is now familiar, in one corner and place a new novel object in the opposing corner. For all tasks, switch the corners between trials as a control. For novel social interaction, ensure that the novel mice are age, strain and sex-

matched and are acclimated to the mesh wire cup for 2 consecutive days for 5 min each day. For each trial, place a novel mouse under a mesh wire cup and in the opposing corner place an empty mesh wire cup. Let the experimental mice explore the arena for 5 min while recording behavior with a video camera. Clean the arena and mesh wire cups thoroughly between each trial.

To analyze behavioral data, we used DeepLabCut (Mathis et al. 2018) to perform basic body part tracking. Detailed notes on how to install and use DeepLabCut can be found on its GitHub page. We also used a custom python-based library 'dlc_utils' (https://github.com/balajisriram/dlc_utils) for further analysis of the data after basic body parts tracking was completed. More details about how to use this library can be found in the GitHub page. Briefly, install DeepLabCut using the anaconda installation process. Install a GUI capable CPU-only version of DeepLabCut as well as the GPU-enabled version for training the network. Follow the instructions to create a project for tracking body parts, choose a sample of frames from our data set, manually mark the relevant body parts in these sampled frames, train the DeepLabCut network to predict the body parts and verify that the trained network performs adequately.

For the purposes of tracking body position and identifying simple interactions in an open field, identify the centroid of the animal, the head (operationally defined as the midpoint between the ears), the left and right ears as well as the snout and the base of the tail. Having multiple body parts tracked allows for appropriate substitution when some body parts are missing in the frame due to occlusion. Apart from animal body parts, track a variety of points related to the environment: such as the edges of behavior boxes. These

allow for repeatable estimation of such points across multiple sessions - even if the position of the camera slightly changes between sessions. After tracking the body parts from the behavioral data, take care to filter the predicted body part locations based on the confidence associated with the prediction on each frame of the video. Low confidence predictions are usually associated with occluded body parts. For such predictions, substitute a given body part with another (if such substitution is appropriate) or use the locations of other body parts to predict where the relevant body part is likely to be. For most open field applications, the centroid of the rodents' body is rarely occluded and can be predicted with high accuracy and precision. Use the predicted location of the centroid as well as the location of the tracked points in the environment to estimate a number of features of the animal's behavior. For example, in the open field data, the time derivative of the position can be used to calculate the speed of the animal. All statistical tests are designed to test an equal number of animals between groups. To avoid bias, perform all experiments “blind” with respect to the experimental group when possible, particularly when there is any subjective element in assessing the results. The effect of sex differences on the main experimental outcomes can be tested by the separating of data into male and female groups.

6.2.4 Post hoc cell counting to characterize extent of cell transfection

The number of cells transfected must be determined per mouse since not all mice will have successful transfection and there will be variation in the number of transfected cells. One method to achieve this involves counting the number of transfected neurons in alternating coronal sections followed by an interpolation to estimate the total number of

transfected cells. For this, image and count every other coronal section (50 μm). For the frontal cortex, count cells within +2.75 and + 1.35 mm from Bregma. These coordinates contain frontal cortical areas and includes part of somatosensory cortex (S1). Using this method, there were no observed transfected cells in more caudal cortical regions or subcortical areas. Be sure to denote the left from right hemisphere, such as marking one hemisphere with a needle hole during sectioning, and count cells bilaterally. Use an automated cell counting software or count cells manually, confirming the presence of a cell body using DAPI.

Once cell counts are obtained, a threshold can be set for inclusion. For example, only include mice that are bilaterally electroporated in analysis. For further analysis, correlate number of cells transfected with behavioral responses to see if there is an association. This technique will target multiple brain areas so it is necessary to provide information on which brain regions have been genetically manipulated. It is possible that manipulating certain genes could alter neuronal migration, specification and/or death. Ensure during cell counting that brain anatomy is examined and each transfected neuron is within the layer that was supposedly transfected (i.e. L2/3). Gross anatomical measurements such as cortical thickness can also be quantified by measuring the distance from the pia to cortical L6.

6.3 Results

6.3.1 Successful development and implementation of a custom-built electroporator and triple electrode

For IUEs, an inexpensive custom-built electroporator was built based on a previously described design (Bullmann et al. 2015) (Figure 6.1, A). A three prong electrode was made (Szczyrkowska et al. 2016, dal Maschio et al .2012) using plastic forceps with 2 negative electrodes attached to the tips of the prongs and the positive electrode was attached to the end of toothbrush handle (Figure 6.1). The electroporator and three prong electrode were tested to ensure proper function. IUE was performed by exposing the uterine horns, injecting plasmid DNA and electroporating each embryo (Figure 6.1, C). The three prong electrode can be held fairly easily in two hands as shown (Figure 6.1, B, right), using the prongs to stabilize the embryo's head. L2/3 PFC pyramidal somas and their processes were labeled with GFP via IUE, thus confirming the success of the gene transfer experiment.

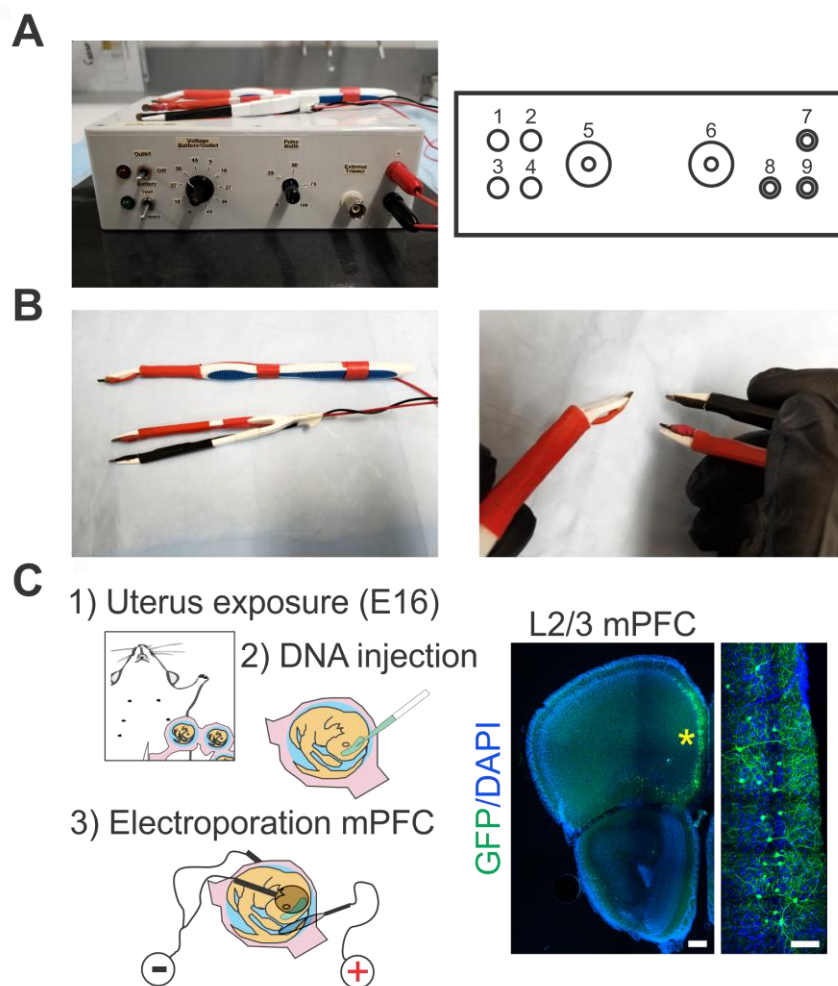


Figure 6.1: In utero electroporation using a custom-built electroporator and a three prong electrode.

(A) Image of the custom-built electroporator (left) and its internal circuit (right). 1: Power Indicator. 2: Power Switch. 3: Pulse Indicator. 4: Test Mode Switch. 5: Voltage Selector. 6: Pulse Width Control. 7: Electrode (+). 8: External Trigger (TTL). 9: Electrode (-). (B) Image of the custom-built three prong electrode (left) and the recommended method to hold the three prong electrode during the IUE (right). (C) Left: Diagram depicting IUE surgery performed in E16 dams. Right: representative 20X confocal image of IUE with GFP targeted to L2/3 mPFC. Yellow asterisk: L2/3 GFP(+) neurons. Left panel scale bar = 250 μ m. Right panel scale bar = 75 μ m. Note: Data obtained and figure made by Ashley Comer. Figures and data adapted from Comer et al., *JoVE*, 2020.

6.3.2 Targeting a large population of neurons bilaterally in the frontal cortex of mice

The total number of transfected cells and the distribution of transfected neurons can be quantified for both juvenile and adult mice⁵. Using this bilateral IUE method, about 4000-6000 L2/3 pyramidal neurons were transfected (Figure 6.1). Additionally, most of these cells were localized to frontal cortical regions including the frontal association cortex, motor association areas, prelimbic and infralimbic cortex and the orbital and anterior cingulate cortex (Figure 6.1). A representative example shows the rostral-caudal distribution of transfected neurons in an adult control mouse (P60, Figure 6.1). This confirms the ability of bilateral IUEs to target and genetically label large populations of L2/3 pyramidal neurons in the frontal cortex.

6.3.3 Social behavior in juvenile and adult mice

The first part of the maternal interaction task tested the ability of control P18 transfected mice (IUE with pCAG-GFP) to find nest bedding (maternal interaction 1 [MI1]). Control mice spent more time exploring their nest bedding than exploring fresh bedding. Thus suggesting that, as expected, these mice have intact sensorimotor abilities and exploratory behavior (Figure 6.2). The second part of the task (MI2) takes advantage of the tendency of mice to be motivated to interact with and be near their mother. In this task, pups spent most of their time near their mother while spending significantly less time exploring the empty cup or nest bedding (Figure 6.2). These results suggest that IUE control mice exhibit normal homing behavior.

Adult control mice (P60) spent approximately 35% of the time exploring a novel object (total time spent in the arena = 5 min, Figure 6.4). When presented with a novel and familiar object, adult mice spent more time exploring the novel object, suggesting intact interest in novelty (Figure 6.4). In the sociability task, control adult mice spent similar amounts of time exploring a novel mouse and empty cup (Figure 6.4). This behavior was automatically tracked using the freely available DeepLabCut software (Mathias et al. 2018). DeepLabCut was also used to determine when mice were rearing by examining the length of the mouse's body, since this distance becomes shorter when the mouse rears.

6.4 Discussion

Herein, a pipeline is described that combines the manipulation of novel genes of interest in large populations of frontal cortical neurons with behavioral assays in mice. Moreover, this pipeline allows for the longitudinal study of behavior in the same mice both during early postnatal development and in adulthood. This technique bypasses the need to rely on genetic animal models that can be costly in terms of time and expenses. The strength of this protocol is that it can be used to study neurodevelopmental and neuropsychiatric disorders for which recent genome-wide association studies have discovered novel genetic associations (Li et al. 2017, Ripke et al. 2013). Although this method provides cell-type specific transfection of excitatory neurons, one limitation is that it is less feasible to target other brain cell types such as interneurons or glial cells.

However, multiple studies suggest a modified approach to target other brain cell-types (De Marco Garcia & Fishell 2014, Borrell et al. 2005). Additionally, by modifying the position of the electrodes relative to the embryo's head and changing the timing of the IUE, other brain regions can be bilaterally transfected including the hippocampus, amygdala, cerebellum, and the visual, somatosensory and motor cortices (dal Maschio et al. 2015, Soma et al. 2009). Additionally, different cortical layers can be targeted by performing IUE at different developmental stages.

Although IUE can have a high success rate, there are critical steps and troubleshooting of the method that is required at times. It is necessary that plasmids are carefully designed and validated in cell lines. As with all cloning, care must be taken to ensure proper gene expression such as confirming the sequence is in frame. Additionally, the effect of gene manipulation (e.g., overexpression or silencing) should be confirmed taking into consideration that expression levels could vary across the developmental time course of the mouse. Western blot and qPCR can be used to determine the extent of genetic overexpression (Comer et al. 2020). It is recommended to co-electroporate a reporter gene, such as GFP, in a separate plasmid since proteins tagged with GFP can be mis-folded or lose their function. Alternatively, if a reporter is not used the experimenter can use in situ hybridization, qPCR or western blot to determine expression levels of the gene of interest (Comer et al. 2020). If plasmids have been verified but there are no animals that appear to be positive for transfection, thoroughly check all equipment, especially the electroporator, to ensure proper function. When delivering voltage pulses to embryos, the uterine horns should be moistened well with warmed saline and the

electrodes should produce bubbles upon generation of the voltage pulse. If no bubbles are present when the voltage is delivered, there is likely a problem with the electroporator. Alternatively, the cDNA might not have been injected properly into the ventricle. When cDNA is injected properly into the lateral ventricle, the fast green dye will be visible in the shape of a crescent. Lastly, the position of the electrodes is important. If the electrodes are positioned slightly incorrectly, cells might not be transfected in the region of interest. Therefore, when checking for successful transfection, save some more caudal brain sections to see if perhaps the wrong brain region was transfected. Once this method has been practiced, an experienced surgeon can expect to achieve a success rate of nearly 90%. This protocol can be modified to target other brain regions of interest. For example, it is possible to target most cortical regions bilaterally and even certain subcortical regions, including the hippocampus (Szczerkowska et al. 2016). It is also possible to further cut down costs by building a custom electroporator, which was used in the data presented here (Comer et al. 2020, Bullmann et al. 2015).

Future studies could make use of this method to understand the role of newly discovered gene candidates in various neurological diseases. The presented pipeline offers a relatively quick assay to test the effects of specific genetic manipulations on early postnatal development and behavior into adulthood. Future efforts using this method have the potential to discover which genes play a causative role in certain brain disorders, including SCZ and autism spectrum disorder.

CHAPTER SEVEN

Concluding remarks and future directions

We showed here that overexpression of C4 in the mPFC can perturb circuit development. We demonstrated that, during normal early postnatal development, excitatory neurons in the mouse mPFC express low levels of C4. Moreover, overexpression of C4 in these cells led to spine dysgenesis that was evident through a transient decrease in filopodia and medium-sized spine density during the third week of postnatal development. We also showed that C4-dependent spine abnormalities were accompanied by a decrease in excitatory synaptic drive onto pyramidal cells in the mPFC. C4 overexpression caused microglia to engulf more PSD-95 from transfected neuron's apical dendrites in L1, where spine loss was observed. Lastly, increased expression of C4 in the frontal cortex was sufficient to reduce social interactions in juvenile (P18) and adult (P60–70) mice. Our findings implicate C4 in shaping the developmental trajectory of cortical circuits and provide a causal link between increased C4 levels and PFC dysfunction. These data show for the first time, to our knowledge, that C4-driven circuit dysfunction in the PFC drives cellular and behavioral phenotypes observed in SCZ rather than merely being a consequence of disease and/or pharmacological treatment.

Our morphological characterization of L2/3 mPFC neurons revealed that C4-mediated connectivity deficits are both circuit and spine-type specific. That is, overexpression of C4 caused a decrease in spine density of apical but not basal dendrites

of L2/3 neurons. These data provide evidence that C4-driven synaptic alterations in the mPFC are cortical layer and/or input specific. Interestingly, previous data have shown that exposure to repeated stress in adolescent rats can reduce connectivity in superficial L1 of the mPFC (Negrón-Oyarzo et al. 2015), suggesting that this layer is susceptible to genetic and environmental perturbations during development. In SCZ, dendritic spine changes are most prominent in L2/3 of the mPFC (Glantz & Lewis 2000); therefore, we focused on how overexpression of mC4 causes anatomical and functional changes in this region. However, imaging studies have reported structural changes in a variety of brain regions in SCZ, including the frontal and temporal lobes and hippocampus (DeLisi 2008). It remains unknown whether mC4 overexpression in other brain regions leads to a decrease in spine density or other abnormalities. This question could be answered by targeting other brain regions using IUE or generating a global mC4-overexpressing transgenic mouse.

When we further investigated which spine types were affected by C4 overexpression, we found a specific loss of filopodia and medium-sized spines, whereas the density of mature mushroom spines were intact. This is in line with previous observations that complement-mediated pruning is activity dependent (Schafer et al. 2012). Large mushroom and stubby spines are also associated with an accumulation of extracellular matrix proteins, which could protect them from synaptic elimination by microglia (Levy et al. 2014). Future studies could shed light on the molecular mechanisms of input-specific plasticity by identifying “eat me”/“don’t eat me” signals (Elward & Gasque 2003, Lehrman et al. 2018) or complement proteins that are

differentially present in large mushroom versus filopodia spine types. For example, the protective “don’t eat me” signal CD47 and its receptor SIRP α have been found to protect synapses from microglia-mediated engulfment and can be regulated by activity to allow for input-specific elimination (Lehrman et al. 2018). Further study of signals that promote or hinder phagocytosis, such as Fc and complement receptors or C-type lectin and phosphatidylserine receptors (respectively) (Galloway et al. 2019), will likely be critical to understand the dynamic and complex role of microglia in synapse elimination.

Major contributors to synaptogenesis are dendritic filopodia, which are thin, specialized postsynaptic structures that orchestrate synapse formation by dynamically sampling potential presynaptic partners, thus optimizing circuit wiring (Bonhoeffer & Yuste 2002, Ozcan 2017). It is possible that C4 contributes to aberrant synaptic wiring by reducing the ability of developing circuits to form appropriate connections. At its simplest, increased levels of C4 may underlie PFC pathology and dysfunction by specifically altering filopodia-dependent synapse formation during early development. This interpretation would suggest that subsequent aberrant synaptic elimination in SCZ is a consequence of suboptimal circuit wiring. Transient deficits in dendritic spines and filopodia are seen in several mouse models of neurodevelopmental disorders (Del Pino et al. 2018). Similar to these models, our data suggest that there are sensitive developmental periods during which cortical circuitry is especially susceptible to altered expression of C4. It is well-established that there are critical windows of development and that alterations through genetic or environmental perturbations during these times can have lasting effects on brain function (Meredith et al. 2012). Certain ages of development

might be more sensitive to perturbations such as increased C4 expression due to increased plasticity of circuits during critical windows and the presence of homeostatic signals. For example, in typical brain development the human prefrontal cortex undergoes significant wiring changes including synaptic elimination and refinement that continues into early adulthood until about age 25 (Meredith et al. 2012). Insults during this time might have the potential to impact circuit development since the cellular machinery and expression profile is already in place to remove synapses. Therefore, the factors that initiate the complement cascade in the brain might only be present or might be present at higher levels during these critical windows of brain development. Notably, the factors that initiate the complement cascade in the brain are still not clear. In the periphery, C1q initiates the complement cascade by recognizing invading pathogens (Dunkelberger and Song 2010). Future work should aim to identify the binding partners of C1q specifically in the brain as this work would likely be valuable in determining the mechanism of complement-mediated synapse removal.

In our experiments, we did not observe a significant difference in apical tuft protrusion density between adult (P60) control and C4 conditions. However, in human SCZ postmortem tissue, spine loss of PFC cortical L3 neurons persists into adulthood (Glantz & Lewis 2000). Notably, our genetic manipulation targeted a single gene, C4, whereas SCZ results from polygenetic mechanisms (Salleh 2004), implicating a multitude of genes. It is possible that the mechanisms that allow for the compensation of spine density in P60 mice are also impaired in SCZ. Therefore, our data suggest that the C4-induced connectivity changes observed during the third week of development could

stimulate compensatory plasticity mechanisms not present in SCZ. Additionally, there may be differences in how human and mouse pyramidal neurons respond to increased levels of C4, which could explain the discrepancy in adult dendritic spine density between mice and humans. Importantly, our qPCR and western blot data show that C4 levels at P60 were not increased in the mC4 condition mice. Therefore, the fact that spine density in C4 conditions recovered to control levels by P60 could simply be due to the lack of C4 overexpression at P60. Although spine density in C4-overexpressing neurons returned to control levels by P60, our behavioral data in adult mice suggest that the underlying circuitry remains aberrant in mice overexpressing C4 in the frontal cortex. It remains to be determined whether increased expression of C4 can lead to other abnormal changes in circuitry (i.e., L2/3 output to deeper cortical layers or PFC network properties) that were not measured in this study that persist into adulthood.

Our electrophysiological data strengthen our morphological findings and provide additional insight into the functional abnormalities caused by C4 overexpression. Previous studies have shown that microglia are able to trogocytose—or “nibble” and phagocytose—small volumes of neurons and synapses (Weinhard et al. 2018). It is possible that microglia trogocytose some of the PSD without fully eliminating synapses, thus causing a reduction in synaptic strength due to a loss of glutamate receptors. In our experiments, the decrease in excitatory synaptic drive caused by C4 overexpression could be the result of an increase in phagocytosis of synapses by microglia. Alternatively, microglia trogocytosis of synaptic material could trigger synaptic elimination mediated through conventional synaptic mechanisms such as long-term depression (Sheng &

Ertürk 2014). On the other hand, C4 did not induce a change in the frequency or amplitude of mIPSCs, which is in line with previous observations showing that complement does not target GABAergic synapses in mouse and cellular models of Alzheimer's disease (Dejanovic et al. 2018). The slowed kinetics of inhibitory transmission could be mediated through a loss of excitatory dendritic spines, which has been shown to alter inhibitory synapse location since there is local coordination of excitatory and inhibitory synaptic localization (Chen et al. 2012). It is possible that the loss of excitatory synapses of distal apical dendrites could alter the localization of inhibitory synapse localization, leading to changes in the kinetics of inhibitory transmission, however future work is required to understand how C4 overexpression might alter inhibitory connectivity.

In addition to being the brain's resident macrophage, microglia can influence brain development by playing roles in synapse formation, elimination, and maintenance (Schafer et al. 2015, Wu et al. 2015, Bohlen et al 2019). Our data show that increased C4 expression led to morphological changes in lysosomes and enhanced phagocytic activity. Since microglia are the only cells in the brain parenchyma that express CR3 and are poised to engulf synapses (as opposed to brain border macrophages which express CR3 but are not positioned for synapse engulfment) (Schafer et al. 2015), they are equipped to recognize material that has been tagged by the complement cascade to initiate phagocytosis. Indeed, previous work has shown that in normal brain development, microglia phagocytose synaptic material and that this process of synapse elimination is necessary for normal brain wiring (Paolicelli et al. 2011). Our data in the PFC are

consistent with and expand upon previous studies in the retinogeniculate pathway that show microglia engulf synapses in a complement-dependent manner (Schafer et al. 2012, Bialas et al. 2013), which suggests that complement-dependent circuit wiring is necessary for normal development and contributes to pathology when mis-regulated.

Importantly, the mechanisms of microglia-mediated synaptic pruning is still not well-understood. It remains to be determined whether microglia target the pre- or post-synapse, or both. There is evidence suggesting that microglia target and engulf pre-synaptic material (Schafer et al. 2012, Weinhard et al. 2018, Lehrman et al. 2018, Vasek et al. 2016). However, there is also evidence for microglial engulfment of post-synaptic material (Comer et al. 2020, Hong et al. 2016, He et al. 2019, Vainchtein et al. 2018) and evidence suggesting that microglia interact with and engulf both pre- and post-synaptic material (Paolicelli et al. 2011, Wake et al. 2009, Tremblay 2012, Tremblay et al. 2010, Sellgren et al. 2019). One study isolated synaptosomes and found that C1q, the initiator of the complement cascade, tagged a subset of synapses that were positive for apoptotic-like markers such as cleaved caspase-3 (Györfy et al. 2018). In this study, C1q was present in both pre- and post-synaptic fractions but was greater localized to the pre-synaptic element (Györfy et al. 2018). Another study suggested that rather than phagocytosing synaptic material, microglia engulf smaller volumes of synaptic material ($< 1 \mu\text{m}^3$), termed trogocytosis (Weinhard et al. 2018). This study used EM and imaging in organotypic hippocampal cultures and found evidence for complete microglial inclusions of synaptic material (Weinhard et al. 2018). The authors concluded that microglia specifically engulfed presynaptic boutons, however of the 17 inclusions found

in microglia using electron microscopy, only 2 of these inclusions were identified as presynaptic by the presence of vesicles. The remaining 15 inclusions were not able to be characterized as pre or post-synaptic material (Weinhard et al. 2018). This study highlights the need to conduct real-time imaging experiments *in vivo* to better understand microglial interactions at the synapse. Since there is evidence for both pre- and post-synaptic elimination, there are likely circumstances where either the pre or post-synapse, or both are targeted. This could be disease specific in which in some instances either the pre- or post-synaptic element is differentially targeted. *In vivo* time-lapse imaging will likely be necessary, as opposed to *in vitro* methods, to gain further insight into the mechanisms of microglial-dependent synapse removal, with the possibility for different mechanisms in different contexts (homeostatic vs pathological pruning, differences between different disease states, etc.).

It is important to note that other immune pathways, outside of the complement system, have been implicated in synaptic pruning. For example, the chemokine fractalkine receptor CX3CR1 expressed by microglia is critical and its neuronal ligand CX3CL1 is critical for proper synaptic pruning (Zhan et al. 2014, Paolicelli et al. 2011). Mice that are deficient for CX3CR1 prune less synapses than typically developing mice and this lack of sufficient pruning causes functional connectivity alterations and behavioral deficits (Zhan et al. 2014, Paolicelli et al. 2011). Additionally, the protective immune molecule CD47 and its receptor SIRP α are expressed in synapses, are activity dependent, and protect synapses from microglia-mediated engulfment (Lehrman et al. 2018). Additionally, the microglial innate immune receptor TREM2, which plays a role

in phagocytosis, is necessary for homeostatic synaptic elimination and contributes to disease states when misregulated (Jay et al. 2019, Filipello et al. 2018, Zheng et al. 2018, Konishi et al. 2018). Other immune molecules, such as TGF- β , interact with complement proteins and play a role in synaptic refinement that occurs during development (Bialas et al. 2013). The role of the immune system in synapse development has only recently been explored, and likely many factors of the immune system regulate processes such as synaptic pruning through the coordination of both pro- and anti-inflammatory regulators that are able to finely orchestrate synapse removal based on activity-dependent mechanisms.

Social deficits in individuals with SCZ are an early feature of this disease, and poorer social functioning is associated with worse functional outcome in adults with SCZ (Green 2016, Velthorst et al. 2017). Therefore, investigating the causes of early social deficits could reveal potential targets for early therapeutic interventions in SCZ. In L1, the apical dendrites of pyramidal cells in multiple cortical layers interact with projections from higher-order areas (Douglas & Martin 2007). It is thought that cortical “feedback” that inputs to L1 exerts “top-down” control that is important for higher-order cognitive processes (Sjöström & Häusser 2006); therefore, the vulnerability of this layer to C4 overexpression could provide a cellular substrate for social dysfunction. The changes that we observed in connectivity and behavior parallel known SCZ phenotypes in humans (Green 2006, Velthorst et al. 2017, Vita et al. 2012, Glantz & Lewis 2000, Thompson et al. 2001) and provide evidence that the PFC regulates social behavior. Future studies

could interrogate the role of C4 in other SCZ-relevant phenotypes such as deficits in memory function (Donohoe et al. 2018).

Previous work has shown that mice deficient for various complement proteins, including C3R, C1q, C3, and C4, have a reduced pruning of synaptic terminals in the visual system during development (Sekar et al. 2016, Stevens et al. 2007, Schafer et al. 2012). Since it has been shown that other complement proteins play a role in developmental pruning, it is possible that C4 exerts its effects through the activation of the complement cascade. However, C4 might act on other pathways in neurons to alter connectivity, independent of the complement cascade. Future work could aim to elucidate noncanonical pathways that C4 could interact with by performing proteomics or transcriptomics in neurons.

Although polygenetic mechanisms underlie SCZ (Schizophrenia Working Group of the Psychiatric Genomics Consortium 2014), we provide evidence that altering expression of a single gene, C4, in mPFC neurons is sufficient to cause cellular and behavioral phenotypes that resemble SCZ pathology. We propose that mPFC neurons express low levels of C4 during normal brain development, which makes them especially susceptible to genetic and environmental risk factors that increase C4 expression, which are associated with SCZ. In summary, we have identified a critical developmental window during which prefrontal cortical circuits are susceptible to alterations in C4 expression, thus opening the possibility for therapeutic intervention to either alter the developmental trajectory of SCZ or reduce its progression.

This work is compelling when considering that complement proteins are not just relevant to schizophrenia, but have also been implicated in synapse remodeling in other diseases including multiple neurodegenerative disorders, spinal cord and brain injuries, autism spectrum disorder and in normal aging (Magdalon et al. 2020). Additionally, complement system dysregulation is associated with multiple environmental risk factors, such as MIA and exposure to pollution, which contribute to the risk of developing multiple nervous system disorders (Magdalon et al. 2020). Therefore, the studies presented here (Comer et al. 2020) have the potential to be useful in understanding the pathogenesis in multiple diseases. Interestingly, evidence suggests that SCZ has both neurodevelopmental and neurodegenerative components (Gupta et al. 2010). Our method for experimentally overexpressing C4 did not stably increase C4 levels throughout adulthood (Comer et al. 2020), therefore methods that allow stable overexpression, such as transgenic mouse models, could allow for greater understanding of how complement proteins contribute to both developmental and degeneration-associated synaptic over-pruning.

BIBLIOGRAPHY

- Abbott, N. J., Patabendige, A. A., Dolman, D. E., Yusof, S. R., & Begley, D. J. (2010). Structure and function of the blood-brain barrier. *Neurobiology of Disease*, 37(1), 13-25.
- Agarwal, A., Zhang, M., Trembak-Duff, I., Unterbarnscheidt, T., Radyushkin, K., Dibaj, P., et al. (2014). Dysregulated expression of neuregulin-1 by cortical pyramidal neurons disrupts synaptic plasticity. *Cell Reports*, 8(4), 1130-1145.
- Akiyoshi, R., Wake, H., Kato, D., Horiuchi, H., Ono, R., Ikegami, A., et al. (2018). Microglia Enhance Synapse Activity to Promote Local Network Synchronization. *eNeuro*, 5(5).
- Allen, J. L., Liu, X., Pelkowski, S., Palmer, B., Conrad, K., Oberdörster, G., et al. (2014). Early postnatal exposure to ultrafine particulate matter air pollution: persistent ventriculomegaly, neurochemical disruption, and glial activation preferentially in male mice. *Environmental Health Perspectives*, 122(9), 939-945.
- Allen, J. L., Oberdorster, G., Morris-Schaffer, K., Wong, C., Klocke, C., Sobolewski, M., et al. (2017). Developmental neurotoxicity of inhaled ambient ultrafine particle air pollution: Parallels with neuropathological and behavioral features of autism and other neurodevelopmental disorders. *Neurotoxicology*, 59, 140-154.
- Allswede, D. M., Yolken, R. H., Buka, S. L., & Cannon, T. D. (2020). Cytokine concentrations throughout pregnancy and risk for psychosis in adult offspring: a longitudinal case-control study. *Lancet Psychiatry*, 7(3), 254-261.
- American Psychiatric Association. (2013). Diagnostic and statistical manual of mental disorders : DSM-5pp. 1 online resource (xlv, 947 pages)).
- Amoli, M. M., Khatami, F., Arzaghi, S. M., Enayati, S., & Nejatisafa, A. A. (2019). Over-expression of TGF- β 1 gene in medication free Schizophrenia. *Psychoneuroendocrinology*, 99, 265-270.
- Andreasen, N. C., O'Leary, D. S., Flaum, M., Nopoulos, P., Watkins, G. L., Boles Ponto, L. L., et al. (1997). Hypofrontality in schizophrenia: distributed dysfunctional circuits in neuroleptic-naïve patients. *Lancet*, 349(9067), 1730-1734.
- Anticevic A, Schleifer C, Youngsun TC. (2015). Emotional and cognitive dysregulation in schizophrenia and depression: understanding common and distinct behavioral and neural mechanisms. *Dialogues in Clinical Neuroscience*. 17(4), 421-34.

- Arellano, J. I., Benavides-Piccione, R., Defelipe, J., & Yuste, R. (2007). Ultrastructure of dendritic spines: correlation between synaptic and spine morphologies. *Frontiers in Neuroscience*, *1*(1), 131-143.
- Athanasiau, L., Giddaluru, S., Fernandes, C., Christoforou, A., Reinvang, I., Lundervold, A. J., et al. (2017). A genetic association study of CSMD1 and CSMD2 with cognitive function. *Brain, Behavior, and Immunity*, *61*, 209-216.
- Ayata, P., Badimon, A., Strasburger, H. J., Duff, M. K., Montgomery, S. E., Loh, Y. E., et al. (2018). Epigenetic regulation of brain region-specific microglia clearance activity. *Nature Neuroscience*, *21*(8), 1049-1060.
- Babadjouni, R., Patel, A., Liu, Q., Shkirkova, K., Lamorie-Foote, K., Connor, M., et al. (2018). Nanoparticulate matter exposure results in neuroinflammatory changes in the corpus callosum. *PLoS One*, *13*(11), e0206934.
- Bachiller, S., Jiménez-Ferrer, I., Paulus, A., Yang, Y., Swanberg, M., Deierborg, T., et al. (2018). Microglia in Neurological Diseases: A Road Map to Brain-Disease Dependent-Inflammatory Response. *Frontiers in Cellular Neuroscience*, *12*, 488.
- Bai, K. J., Chuang, K. J., Chen, C. L., Jhan, M. K., Hsiao, T. C., Cheng, T. J., et al. (2019). Microglial activation and inflammation caused by traffic-related particulate matter. *Chemico-Biological Interactions*, *311*, 108762.
- Bale, T. L., Baram, T. Z., Brown, A. S., Goldstein, J. M., Insel, T. R., McCarthy, M. M., et al. (2010). Early life programming and neurodevelopmental disorders. *Biological Psychiatry*, *68*(4), 314-319.
- Balu, D. T. (2016). The NMDA Receptor and Schizophrenia: From Pathophysiology to Treatment. *Advances in Pharmacology*, *76*, 351-382.
- Banaj, N., Piras, F., Ciullo, V., Iorio, M., Battaglia, C., Pantoli, D., et al. (2018). Cognitive and psychopathology correlates of brain white/grey matter structure in severely psychotic schizophrenic inpatients. *Schizophrenia Research Cognition*, *12*, 29-36.
- Banks, W. A., Kovac, A., & Morofuji, Y. (2018). Neurovascular unit crosstalk: Pericytes and astrocytes modify cytokine secretion patterns of brain endothelial cells. *Journal of Cerebral Blood Flow & Metabolism*, *38*(6), 1104-1118.
- Banqueri, M., Méndez, M., Gómez-Lázaro, E., & Arias, J. L. (2019). Early life stress by repeated maternal separation induces long-term neuroinflammatory response in glial cells of male rats. *Stress*, *22*(5), 563-570.

- Barak, B., Feldman, N., & Okun, E. (2014). Toll-like receptors as developmental tools that regulate neurogenesis during development: an update. *Frontiers in Neuroscience*, 8, 272.
- Barch, D. M., Braver, T. S., Akbudak, E., Conturo, T., Ollinger, J., & Snyder, A. (2001). Anterior cingulate cortex and response conflict: effects of response modality and processing domain. *Cerebral Cortex*, 11(9), 837-848.
- Barnes, P. J. (1998). Anti-inflammatory actions of glucocorticoids: molecular mechanisms. *Clin Sci (Lond)*, 94(6), 557-572.
- Batista-Brito, R., Vinck, M., Ferguson, K. A., Chang, J. T., Laubender, D., Lur, G., et al. (2017). Developmental Dysfunction of VIP Interneurons Impairs Cortical Circuits. *Neuron*, 95(4), 884-895.e889.
- Bayer, T. A., Buslei, R., Havas, L., & Falkai, P. (1999). Evidence for activation of microglia in patients with psychiatric illnesses. *Neuroscience Letters*, 271(2), 126-128.
- Bechter, K., Reiber, H., Herzog, S., Fuchs, D., Tumani, H., & Maxeiner, H. G. (2010). Cerebrospinal fluid analysis in affective and schizophrenic spectrum disorders: identification of subgroups with immune responses and blood-CSF barrier dysfunction. *Journal of Psychiatric Research*, 44(5), 321-330.
- Becker, Y., Marcoux, G., Allaey, I., Julien, A. S., Loignon, R. C., Benk-Fortin, H., et al. (2019). Autoantibodies in Systemic Lupus Erythematosus Target Mitochondrial RNA. *Frontiers in Immunology*, 10, 1026.
- Belt, K. T., Yu, C. Y., Carroll, M. C., & Porter, R. R. (1985). Polymorphism of human complement component C4. *Immunogenetics*, 21(2), 173-180.
- Benes, F. M. (2010). Amygdalocortical circuitry in schizophrenia: from circuits to molecules. *Neuropsychopharmacology*, 35(1), 239-257.
- Beneyto, M., & Lewis, D. A. (2011). Insights into the neurodevelopmental origin of schizophrenia from postmortem studies of prefrontal cortical circuitry. *International Journal of Developmental Neuroscience*, 29(3), 295-304.
- Berdenis van Berlekom, A., Muflihah, C. H., Snijders, G. J. L. J., MacGillavry, H. D., Middeldorp, J., Hol, E. M., et al. (2020). Synapse Pathology in Schizophrenia: A Meta-analysis of Postsynaptic Elements in Postmortem Brain Studies. *Schizophrenia Bulletin*, 46(2), 374-386.

- Bergdolt, L., & Dunaevsky, A. (2019). Brain changes in a maternal immune activation model of neurodevelopmental brain disorders. *Search Results*, 175, 1-19.
- Bernardo, A., & Minghetti, L. (2006). PPAR-gamma agonists as regulators of microglial activation and brain inflammation. *Current Pharmaceutical Design*, 12(1), 93-109.
- Bialas, A. R., & Stevens, B. (2013). TGF- β signaling regulates neuronal C1q expression and developmental synaptic refinement. *Nature Neuroscience*, 16(12), 1773-1782.
- Bicks, L. K., Koike, H., Akbarian, S., & Morishita, H. (2015). Prefrontal Cortex and Social Cognition in Mouse and Man. *Frontiers in Psychology*, 6, 1805.
- Bilbo, S. D., & Schwarz, J. M. (2009). Early-life programming of later-life brain and behavior: a critical role for the immune system. *Frontiers in Behavioral Neuroscience*, 3, 14.
- Bisht, K., Sharma, K. P., Lecours, C., Sánchez, M. G., El Hajj, H., Milior, G., et al. (2016). Dark microglia: A new phenotype predominantly associated with pathological states. *Glia*, 64(5), 826-839.
- Blessing, E. M., Murty, V. P., Zeng, B., Wang, J., Davachi, L., & Goff, D. C. (2019). Anterior Hippocampal-Cortical Functional Connectivity Distinguishes Antipsychotic Naïve First-Episode Psychosis Patients From Controls and May Predict Response to Second-Generation Antipsychotic Treatment. *Schizophrenia Bulletin*.
- Block, M. L., & Calderón-Garcidueñas, L. (2009). Air pollution: mechanisms of neuroinflammation and CNS disease. *Trends in Neuroscience*, 32(9), 506-516.
- Bloomfield, P. S., Selvaraj, S., Veronese, M., Rizzo, G., Bertoldo, A., Owen, D. R., et al. (2016). Microglial Activity in People at Ultra High Risk of Psychosis and in Schizophrenia: An [(11)C]PBR28 PET Brain Imaging Study. *American Journal of Psychiatry*, 173(1), 44-52.
- Boerrigter, D., Weickert, T. W., Lenroot, R., O'Donnell, M., Galletly, C., Liu, D., et al. (2017). Using blood cytokine measures to define high inflammatory biotype of schizophrenia and schizoaffective disorder. *Journal of Neuroinflammation*, 14(1), 188.
- Bohlen, C. J., Friedman, B. A., Dejanovic, B., & Sheng, M. (2019). Microglia in Brain Development, Homeostasis, and Neurodegeneration. *Annual Review of Genetics*.

- Boido, D., Rungta, R. L., Osmanski, B. F., Roche, M., Tsurugizawa, T., Le Bihan, D., et al. (2019). Mesoscopic and microscopic imaging of sensory responses in the same animal. *Nature Communications*, 10(1), 1110.
- Bollinger, J. L., Collins, K. E., Patel, R., & Wellman, C. L. (2017). Behavioral stress alters corticolimbic microglia in a sex- and brain region-specific manner. *PLoS One*, 12(12), e0187631.
- Bolton, J. L., Huff, N. C., Smith, S. H., Mason, S. N., Foster, W. M., Auten, R. L., et al. (2013). Maternal stress and effects of prenatal air pollution on offspring mental health outcomes in mice. *Environmental Health Perspectives*, 121(9), 1075-1082.
- Bolton, J. L., Marinero, S., Hassanzadeh, T., Natesan, D., Le, D., Belliveau, C., et al. (2017). Gestational Exposure to Air Pollution Alters Cortical Volume, Microglial Morphology, and Microglia-Neuron Interactions in a Sex-Specific Manner. *Frontiers in Synaptic Neuroscience*, 9, 10.
- Bolton, J. L., Smith, S. H., Huff, N. C., Gilmour, M. I., Foster, W. M., Auten, R. L., et al. (2012). Prenatal air pollution exposure induces neuroinflammation and predisposes offspring to weight gain in adulthood in a sex-specific manner. *The FASEB Journal*, 26(11), 4743-4754.
- Bonhoeffer, T., & Yuste, R. (2002). Spine motility. Phenomenology, mechanisms, and function. *Neuron*, 35(6), 1019-1027.
- Bordeleau, M., Carrier, M., Luheshi, G. N., & Tremblay, M. (2019). Microglia along sex lines: From brain colonization, maturation and function, to implication in neurodevelopmental disorders. *Seminars in Cell and Developmental Biology*, 94, 152-163.
- Borjini, N., Paouri, E., Tognatta, R., Akassoglou, K., & Davalos, D. (2019). Imaging the dynamic interactions between immune cells and the neurovascular interface in the spinal cord. *Experimental Neurology*, 322, 113046.
- Borrell, V., & Marín, O. (2006). Meninges control tangential migration of hem-derived Cajal-Retzius cells via CXCL12/CXCR4 signaling. *Nature Neuroscience*, 9(10), 1284-1293.
- Borrell, V., Yoshimura, Y., & Callaway, E. M. (2005). Targeted gene delivery to telencephalic inhibitory neurons by directional in utero electroporation. *Journal of Neuroscience Methods* 143(2), 151-158.

- Bos, I., De Boever, P., Emmerechts, J., Buekers, J., Vanoirbeek, J., Meeusen, R., et al. (2012). Changed gene expression in brains of mice exposed to traffic in a highway tunnel. *Inhalation Toxicology*, 24(10), 676-686.
- Bossù, P., Piras, F., Palladino, I., Iorio, M., Salani, F., Ciaramella, A., et al. (2015). Hippocampal volume and depressive symptoms are linked to serum IL-18 in schizophrenia. *Neurology Neuroimmunology & Neuroinflammation*, 2(4), e111.
- Boyle, C. A., Boulet, S., Schieve, L. A., Cohen, R. A., Blumberg, S. J., Yeargin-Allsopp, M., et al. (2011). Trends in the prevalence of developmental disabilities in US children, 1997-2008. *Pediatrics*, 127(6), 1034-1042.
- Brandon, N. J., Millar, J. K., Korth, C., Sive, H., Singh, K. K., & Sawa, A. (2009). Understanding the role of DISC1 in psychiatric disease and during normal development. *Journal of Neuroscience*, 29(41), 12768-12775.
- Braniste, V., Al-Asmakh, M., Kowal, C., Anuar, F., Abbaspour, A., Tóth, M., et al. (2014). The gut microbiota influences blood-brain barrier permeability in mice. *Science Translational Medicine*, 6(263), 263ra158.
- Brannigan, R., Cannon, M., Tanskanen, A., Huttunen, M. O., Leacy, F. P., & Clarke, M. C. (2019). The association between subjective maternal stress during pregnancy and offspring clinically diagnosed psychiatric disorders. *Acta Psychiatrica Scandinavica*, 139(4), 304-310.
- Brenhouse, H. C., & Andersen, S. L. (2011). Nonsteroidal anti-inflammatory treatment prevents delayed effects of early life stress in rats. *Biological Psychiatry*, 70(5), 434-440.
- Brenhouse, H. C., Danese, A., & Grassi-Oliveira, R. (2019). Neuroimmune Impacts of Early-Life Stress on Development and Psychopathology. *Current Topics in Behavioral Neuroscience*, 43, 423-447.
- Brent, B. K., Thermenos, H. W., Keshavan, M. S., & Seidman, L. J. (2013). Gray matter alterations in schizophrenia high-risk youth and early-onset schizophrenia: a review of structural MRI findings. *Child and Adolescent Psychiatric Clinics of North America*, 22(4), 689-714.
- Bronson, S. L., & Bale, T. L. (2014). Prenatal stress-induced increases in placental inflammation and offspring hyperactivity are male-specific and ameliorated by maternal antiinflammatory treatment. *Endocrinology*, 155(7), 2635-2646.

- Brown, A. S., & Derkits, E. J. (2010). Prenatal infection and schizophrenia: a review of epidemiologic and translational studies. *American Journal of Psychiatry*, *167*(3), 261-280.
- Brumback, A. C., Ellwood, I. T., Kjaerby, C., Iafrati, J., Robinson, S., Lee, A. T., et al. (2018). Identifying specific prefrontal neurons that contribute to autism-associated abnormalities in physiology and social behavior. *Molecular Psychiatry*, *23*(10), 2078-2089.
- Bullmann, T., Arendt, T., Frey, U., & Hanashima, C. (2015). A transportable, inexpensive electroporator for in utero electroporation. *Dev Growth Differ*, *57*(5), 369-377.
- Burghardt, K., Grove, T., & Ellingrod, V. (2014). Endothelial nitric oxide synthetase genetic variants, metabolic syndrome and endothelial function in schizophrenia. *J Psychopharmacol*, *28*(4), 349-356.
- Bustillo J.R., Chen H., Jones T., Lemke N., Abbott C., Qualls C., et al. (2014). Increased glutamine in patients undergoing long-term treatment for schizophrenia: a proton magnetic resonance spectroscopy study at 3 T. *JAMA Psychiatry*, *71*(3), 265-72.
- Cai, H. Q., Catts, V. S., Webster, M. J., Galletly, C., Liu, D., O'Donnell, M., et al. (2018). Increased macrophages and changed brain endothelial cell gene expression in the frontal cortex of people with schizophrenia displaying inflammation. *Molecular Psychiatry*.
- Calderón-Garcidueñas, L., Franco-Lira, M., D'Angiulli, A., Rodríguez-Díaz, J., Blaurock-Busch, E., Busch, Y., et al. (2015). Mexico City normal weight children exposed to high concentrations of ambient PM2.5 show high blood leptin and endothelin-1, vitamin D deficiency, and food reward hormone dysregulation versus low pollution controls. Relevance for obesity and Alzheimer disease. *Environmental Research*, *140*, 579-592.
- Calderón-Garcidueñas, L., Solt, A. C., Henríquez-Roldán, C., Torres-Jardón, R., Nuse, B., Herritt, L., et al. (2008). Long-term air pollution exposure is associated with neuroinflammation, an altered innate immune response, disruption of the blood-brain barrier, ultrafine particulate deposition, and accumulation of amyloid beta-42 and alpha-synuclein in children and young adults. *Toxicologic Pathology*, *36*(2), 289-310.
- Callaway, E. M., & Luo, L. (2015). Monosynaptic Circuit Tracing with Glycoprotein-Deleted Rabies Viruses. *Journal of Neuroscience*, *35*(24), 8979-8985.

- Cannon, M., Jones, P., Gilvarry, C., Rifkin, L., McKenzie, K., Foerster, A., et al. (1997). Premorbid social functioning in schizophrenia and bipolar disorder: similarities and differences. *American Journal of Psychiatry*, *154*(11), 1544-1550.
- Cannon, T. D., Chung, Y., He, G., Sun, D., Jacobson, A., van Erp, T. G., et al. (2015). Progressive reduction in cortical thickness as psychosis develops: a multisite longitudinal neuroimaging study of youth at elevated clinical risk. *Biological Psychiatry*, *77*(2), 147-157.
- Cao, H., McEwen, S. C., Chung, Y., Chén, O. Y., Bearden, C. E., Addington, J., et al. (2018). Altered Brain Activation During Memory Retrieval Precedes and Predicts Conversion to Psychosis in Individuals at Clinical High Risk. *Schizophrenia Bulletin*.
- Cardno, A. G., & Gottesman, I. I. (2000). Twin studies of schizophrenia: from bow-and-arrow concordances to star wars Mx and functional genomics. *American Journal of Medical Genetics*, *97*(1), 12-17.
- Careaga, M., Taylor, S. L., Chang, C., Chiang, A., Ku, K. M., Berman, R. F., et al. (2018). Variability in PolyIC induced immune response: Implications for preclinical maternal immune activation models. *Journal of Neuroimmunology*, *323*, 87-93.
- Carroll, M. C., Belt, T., Palsdottir, A., & Porter, R. R. (1984). Structure and organization of the C4 genes. *Philosophical Transactions of the Royal Society B: Biological Sciences*, *306*(1129), 379-388.
- Castro-Nallar, E., Bendall, M. L., Pérez-Losada, M., Sabuncyan, S., Severance, E. G., Dickerson, F. B., et al. (2015). Composition, taxonomy and functional diversity of the oropharynx microbiome in individuals with schizophrenia and controls. *PeerJ*, *3*, e1140.
- Catale, C., Gironda, S., Lo Iacono, L., & Carola, V. (2020). Microglial Function in the Effects of Early-Life Stress on Brain and Behavioral Development. *Journal of Clinical Medicine*, *9*(2).
- Chase, K. A., Rosen, C., Gin, H., Bjorkquist, O., Feiner, B., Marvin, R., et al. (2015). Metabolic and inflammatory genes in schizophrenia. *Psychiatry Research*, *225*(1-2), 208-211.
- Chechik, G., Meilijson, I., & Ruppin, E. (1999). Neuronal regulation: A mechanism for synaptic pruning during brain maturation. *Neural Computation*, *11*(8), 2061-2080.

- Chen, B., & Kan, H. (2008). Air pollution and population health: a global challenge. *Environmental Health and Preventive Medicine, 13*(2), 94-101.
- Chen, C. Y., Shih, Y. C., Hung, Y. F., & Hsueh, Y. P. (2019). Beyond defense: regulation of neuronal morphogenesis and brain functions via Toll-like receptors. *Journal of Biomedical Science, 26*(1), 90.
- Chen, J., Luo, Y., Hui, H., Cai, T., Huang, H., Yang, F., et al. (2017). CD146 coordinates brain endothelial cell-pericyte communication for blood-brain barrier development. *Proceedings of the National Academy of Sciences of the United States of America, 114*(36), E7622-E7631.
- Chen, J. L., Villa, K. L., Cha, J. W., So, P. T., Kubota, Y., & Nedivi, E. (2012). Clustered dynamics of inhibitory synapses and dendritic spines in the adult neocortex. *Neuron, 74*(2), 361-373.
- Cheng, H., Saffari, A., Sioutas, C., Forman, H. J., Morgan, T. E., & Finch, C. E. (2016). Nanoscale Particulate Matter from Urban Traffic Rapidly Induces Oxidative Stress and Inflammation in Olfactory Epithelium with Concomitant Effects on Brain. *Environmental Health Perspectives, 124*(10), 1537-1546.
- Chiappelli, J., Shi, Q., Kodi, P., Savransky, A., Kochunov, P., Rowland, L. M., et al. (2016). Disrupted glucocorticoid--Immune interactions during stress response in schizophrenia. *Psychoneuroendocrinology, 63*, 86-93.
- Chini, M., Pöpplau, J. A., Lindemann, C., Carol-Perdiguer, L., Hnida, M., Oberländer, V., et al. (2020). Resolving and Rescuing Developmental Miswiring in a Mouse Model of Cognitive Impairment. *Neuron, 105*(1), 60-74.e67.
- Cho RY, Konecky RO, Carter CS. (2006). Impairments in frontal cortical gamma synchrony and cognitive control in schizophrenia. *Proceedings of the National Academy of Sciences. 103*(52), 19878-83.
- Chrousos, G. P. (2009). Stress and disorders of the stress system. *Nature Reviews Endocrinology, 5*(7), 374-381.
- Chubb, J. E., Bradshaw, N. J., Soares, D. C., Porteous, D. J., & Millar, J. K. (2008). The DISC locus in psychiatric illness. *Molecular Psychiatry, 13*(1), 36-64.
- Cipollini, V., Anrather, J., Orzi, F., & Iadecola, C. (2019). Th17 and Cognitive Impairment: Possible Mechanisms of Action. *Frontiers in Neuroanatomy, 13*, 95.
- Ciufolini, S., Dazzan, P., Kempton, M. J., Pariante, C., & Mondelli, V. (2014). HPA axis response to social stress is attenuated in schizophrenia but normal in depression:

evidence from a meta-analysis of existing studies. *Neuroscience & Biobehavioral Reviews*, 47, 359-368.

Clifton, N. E., Hannon, E., Harwood, J. C., Di Florio, A., Thomas, K. L., Holmans, P. A., et al. (2019). Dynamic expression of genes associated with schizophrenia and bipolar disorder across development. *Translational Psychiatry*, 9(1), 74.

Cohen, S., Ke, X., Liu, Q., Fu, Q., Majnik, A., & Lane, R. (2016). Adverse early life environment increases hippocampal microglia abundance in conjunction with decreased neural stem cells in juvenile mice. *International Journal of Developmental Neuroscience*, 55, 56-65.

Cohen-Cory, S. (2002). The developing synapse: construction and modulation of synaptic structures and circuits. *Science*, 298(5594), 770-776.

Cole, T. B., Coburn, J., Dao, K., Roqué, P., Chang, Y. C., Kalia, V., et al. (2016). Sex and genetic differences in the effects of acute diesel exhaust exposure on inflammation and oxidative stress in mouse brain. *Toxicology*, 374, 1-9.

Collin, G., Derks, E. M., van Haren, N. E., Schnack, H. G., Hulshoff Pol, H. E., Kahn, R. S., et al. (2012). Symptom dimensions are associated with progressive brain volume changes in schizophrenia. *Schizophrenia Research*, 138(2-3), 171-176.

Comer AL, Carrier M, Tremblay ME, Cruz-Martín A. The inflamed brain in schizophrenia: the convergence of genetic and environmental risk factors that lead to uncontrolled neuroinflammation. (Submitted). Invited review article.

Comer, A. L.*, Jinadasa, T.*, Sriram, B., Phadke, R. A., Kretsge, L. N., Nguyen, T. P. H., et al. (2020). Increased expression of schizophrenia-associated gene C4 leads to hypoconnectivity of prefrontal cortex and reduced social interaction. *PLoS Biology*, 18(1), e3000604.

Comer AL, Sriram B, Yen WW, Cruz-Martín A. A pipeline using bilateral in utero electroporation to interrogate genetic influences on rodent behavior. 2020. *Journal of Visual Experiments*, (159), 10.3791/61350.

Connor, J. R., & Menzies, S. L. (1996). Relationship of iron to oligodendrocytes and myelination. *Glia*, 17(2), 83-93.

Consortium, S. P. G.-W. A. S. G. (2011). Genome-wide association study identifies five new schizophrenia loci. *Nature Genetics*, 43(10), 969-976.

Consortium, S. W. G. o. t. P. G. (2014). Biological insights from 108 schizophrenia-associated genetic loci. *Nature*, 511(7510), 421-427.

- Corcoran, C., Mujica-Parodi, L., Yale, S., Leitman, D., & Malaspina, D. (2002). Could stress cause psychosis in individuals vulnerable to schizophrenia? *CNS Spectrums*, 7(1), 33-38, 41-32.
- Cruz-Martín, A., Crespo, M., & Portera-Cailliau, C. (2010). Delayed stabilization of dendritic spines in fragile X mice. *Journal of Neuroscience*, 30(23), 7793-7803.
- Cruz-Martín, A., Crespo, M., & Portera-Cailliau, C. (2012). Glutamate induces the elongation of early dendritic protrusions via mGluRs in wild type mice, but not in fragile X mice. *PLoS One*, 7(2), e32446.
- Cruz-Martín, A., El-Danaf, R. N., Osakada, F., Sriram, B., Dhande, O. S., Nguyen, P. L., et al. (2014). A dedicated circuit links direction-selective retinal ganglion cells to the primary visual cortex. *Nature*, 507(7492), 358-361.
- Culmsee, C., Michels, S., Scheu, S., Arolt, V., Dannlowski, U., & Alferink, J. (2018). Mitochondria, Microglia, and the Immune System-How Are They Linked in Affective Disorders? *Frontiers in Psychiatry*, 9, 739.
- da Fonseca, A. C., Matias, D., Garcia, C., Amaral, R., Geraldo, L. H., Freitas, C., et al. (2014). The impact of microglial activation on blood-brain barrier in brain diseases. *Frontiers in Cellular Neuroscience*, 8, 362.
- Da Mesquita, S., Louveau, A., Vaccari, A., Smirnov, I., Cornelison, R. C., Kingsmore, K. M., et al. (2018). Functional aspects of meningeal lymphatics in ageing and Alzheimer's disease. *Nature*, 560(7717), 185-191.
- Dahlgren, J., Samuelsson, A. M., Jansson, T., & Holmäng, A. (2006). Interleukin-6 in the maternal circulation reaches the rat fetus in mid-gestation. *Pediatric Research*, 60(2), 147-151.
- Dai, J., Sheetz, M. P., Wan, X., & Morris, C. E. (1998). Membrane tension in swelling and shrinking molluscan neurons. *Journal of Neuroscience*, 18(17), 6681-6692.
- dal Maschio, M., Ghezzi, D., Bony, G., Alabastri, A., Deidda, G., Brondi, M., et al. (2012). High-performance and site-directed in utero electroporation by a triple-electrode probe. *Nature Communications*, 3, 960.
- Dandi, E., Kalamari, A., Touloumi, O., Lagoudaki, R., Nousiopoulou, E., Simeonidou, C., et al. (2018). Beneficial effects of environmental enrichment on behavior, stress reactivity and synaptophysin/BDNF expression in hippocampus following early life stress. *International Journal of Developmental Neuroscience*, 67, 19-32.

- Davis, D. A., Bortolato, M., Godar, S. C., Sander, T. K., Iwata, N., Pakbin, P., et al. (2013). Prenatal exposure to urban air nanoparticles in mice causes altered neuronal differentiation and depression-like responses. *PLoS One*, 8(5), e64128.
- Dazzan P, Soulsby B, Mechelli A, Wood SJ, Velakoulis D, Phillips LJ, et al. (2012). Volumetric abnormalities predating the onset of schizophrenia and affective psychoses: an MRI study in subjects at ultrahigh risk of psychosis. *Schizophrenia Bulletin*. 38(5), 1083-91.
- De Marco Garcia, N. V., & Fishell, G. (2014). Subtype-selective electroporation of cortical interneurons. *Journal of Visualized Experiments*, (90), e51518.
- De Picker, L., Fransen, E., Coppens, V., Timmers, M., de Boer, P., Oberacher, H., et al. (2019). Immune and Neuroendocrine Trait and State Markers in Psychotic Illness: Decreased Kynurenines Marking Psychotic Exacerbations. *Frontiers in Immunology*, 10, 2971.
- De Picker, L. J., Morrens, M., Chance, S. A., & Boche, D. (2017). Microglia and Brain Plasticity in Acute Psychosis and Schizophrenia Illness Course: A Meta-Review. *Frontiers in Psychiatry*, 8, 238.
- De Vadder, F., Kovatcheva-Datchary, P., Goncalves, D., Vinera, J., Zitoun, C., Duchamp, A., et al. (2014). Microbiota-generated metabolites promote metabolic benefits via gut-brain neural circuits. *Cell*, 156(1-2), 84-96.
- Deczkowska, A., Keren-Shaul, H., Weiner, A., Colonna, M., Schwartz, M., & Amit, I. (2018). Disease-Associated Microglia: A Universal Immune Sensor of Neurodegeneration. *Cell*, 173(5), 1073-1081.
- Dejanovic, B., Huntley, M. A., De Mazière, A., Meilandt, W. J., Wu, T., Srinivasan, K., et al. (2018). Changes in the Synaptic Proteome in Tauopathy and Rescue of Tau-Induced Synapse Loss by C1q Antibodies. *Neuron*, 100(6), 1322-1336.e1327.
- Del Pino, I., Rico, B., & Marín, O. (2018). Neural circuit dysfunction in mouse models of neurodevelopmental disorders. *Current Opinions in Neurobiology*, 48, 174-182.
- DeLisi, L. E. (2008). The concept of progressive brain change in schizophrenia: implications for understanding schizophrenia. *Schizophrenia Bulletin*, 34(2), 312-321.
- DeLisi C., Wiegel F.W. (1983). Membrane fluidity and the probability of complement fixation. *Journal of Theoretical Biology*, 102(2):307-22.

- Delpech, J. C., Wei, L., Hao, J., Yu, X., Madore, C., Butovsky, O., et al. (2016). Early life stress perturbs the maturation of microglia in the developing hippocampus. *Brain, Behavior, and Immunity*, *57*, 79-93.
- Delvecchio, G., Sugranyes, G., & Frangou, S. (2013). Evidence of diagnostic specificity in the neural correlates of facial affect processing in bipolar disorder and schizophrenia: a meta-analysis of functional imaging studies. *Psychological Medicine*, *43*(3), 553-569.
- DeNardo, L., & Luo, L. (2017). Genetic strategies to access activated neurons. *Current Opinions in Neurobiology*, *45*, 121-129.
- Dennison, C. A., Legge, S. E., Pardiñas, A. F., & Walters, J. T. R. (2019). Genome-wide association studies in schizophrenia: Recent advances, challenges and future perspective. *Schizophrenia Research*.
- Derecki, N. C., Cardani, A. N., Yang, C. H., Quinnes, K. M., Cihfield, A., Lynch, K. R., et al. (2010). Regulation of learning and memory by meningeal immunity: a key role for IL-4. *Journal of Experimental Medicine*, *207*(5), 1067-1080.
- Desbonnet, L., Clarke, G., Shanahan, F., Dinan, T. G., & Cryan, J. F. (2014). Microbiota is essential for social development in the mouse. *Molecular Psychiatry*, *19*(2), 146-148.
- Desbonnet, L., Clarke, G., Shanahan, F., Dinan, T. G., & Cryan, J. F. (2014c). Microbiota is essential for social development in the mouse. *Molecular Psychiatry*, *19*(2), 146-148.
- Di Biase, M. A., Zalesky, A., O'keefe, G., Laskaris, L., Baune, B. T., Weickert, C. S., et al. (2017). PET imaging of putative microglial activation in individuals at ultra-high risk for psychosis, recently diagnosed and chronically ill with schizophrenia. *Translational Psychiatry*, *7*(8), e1225.
- Di Liberto, G., Pantelyushin, S., Kreutzfeldt, M., Page, N., Musardo, S., Coras, R., et al. (2018). Neurons under T Cell Attack Coordinate Phagocyte-Mediated Synaptic Stripping. *Cell*, *175*(2), 458-471.e419.
- Diaz Heijtz, R., Wang, S., Anuar, F., Qian, Y., Björkholm, B., Samuelsson, A., et al. (2011). Normal gut microbiota modulates brain development and behavior. *Proceedings of the National Academy of Sciences of the United States of America*, *108*(7), 3047-3052.
- Dienel, S. J., & Lewis, D. A. (2019). Alterations in cortical interneurons and cognitive function in schizophrenia. *Neurobiology of Disease*, *131*, 104208.

- do Prado, C. H., Grassi-Oliveira, R., Daruy-Filho, L., Wieck, A., & Bauer, M. E. (2017). Evidence for Immune Activation and Resistance to Glucocorticoids Following Childhood Maltreatment in Adolescents Without Psychopathology. *Neuropsychopharmacology*, *42*(11), 2272-2282.
- do Prado, C. H., Narahari, T., Holland, F. H., Lee, H. N., Murthy, S. K., & Brenhouse, H. C. (2016). Effects of early adolescent environmental enrichment on cognitive dysfunction, prefrontal cortex development, and inflammatory cytokines after early life stress. *Developmental Psychobiology*, *58*(4), 482-491.
- Dong Y, Benveniste EN. (2001). Immune function of astrocytes. *Glia*. (2):180-90.
- Donohoe, G., Holland, J., Mothersill, D., McCarthy-Jones, S., Cosgrove, D., Harold, D., et al. (2018). Genetically predicted complement component 4A expression: effects on memory function and middle temporal lobe activation. *Psychological Medicine*, *48*(10), 1608-1615.
- Doorduyn, J., de Vries, E. F., Willemsen, A. T., de Groot, J. C., Dierckx, R. A., & Klein, H. C. (2009). Neuroinflammation in schizophrenia-related psychosis: a PET study. *Journal of Nuclear Medicine*, *50*(11), 1801-1807.
- Douglas, R. J., & Martin, K. A. (2007). Mapping the matrix: the ways of neocortex. *Neuron*, *56*(2), 226-238.
- Dunkelberger, J. R., & Song, W. C. (2010). Complement and its role in innate and adaptive immune responses. *Cellular Research*, *20*(1), 34-50.
- Duque, E. e. A., & Munhoz, C. D. (2016). The Pro-inflammatory Effects of Glucocorticoids in the Brain. *Frontiers in Endocrinology* (Lausanne), *7*, 78.
- Elmer, B. M., & McAllister, A. K. (2012). Major histocompatibility complex class I proteins in brain development and plasticity. *Trends in Neuroscience*, *35*(11), 660-670.
- Elvevåg, B., & Goldberg, T. E. (2000). Cognitive impairment in schizophrenia is the core of the disorder. *Critical Reviews in Neurobiology*, *14*(1), 1-21.
- Elward, K., & Gasque, P. (2003). "Eat me" and "don't eat me" signals govern the Innate Immunity response and tissue repair in the CNS: emphasis on the critical role of the complement system. *Molecular Immunology*, *40*(2-4), 85-94.
- Entringer, S., Kumsta, R., Hellhammer, D. H., Wadhwa, P. D., & Wüst, S. (2009). Prenatal exposure to maternal psychosocial stress and HPA axis regulation in young adults. *Hormones and Behavior*, *55*(2), 292-298.

- Erny, D., Hrabě de Angelis, A. L., Jaitin, D., Wieghofer, P., Staszewski, O., David, E., et al. (2015). Host microbiota constantly control maturation and function of microglia in the CNS. *Nature Neuroscience*, *18*(7), 965-977.
- Estes, M. L., Farrelly, K., Cameron, S., Aboubechara, J. P., Haapanen, L., Schauer, J. D., et al. (2019). Enhancing rigor and reproducibility in maternal immune activation models: practical considerations and predicting resilience and susceptibility using baseline immune responsiveness before pregnancy. bioRxiv: bioRxiv.
- Estes, M. L., & McAllister, A. K. (2014). Alterations in immune cells and mediators in the brain: it's not always neuroinflammation! *Brain Pathology*, *24*(6), 623-630.
- Estes, M. L., & McAllister, A. K. (2016). Maternal immune activation: Implications for neuropsychiatric disorders. *Science*, *353*(6301), 772-777.
- Fabry, Z., Fitzsimmons, K. M., Herlein, J. A., Moninger, T. O., Dobbs, M. B., & Hart, M. N. (1993). Production of the cytokines interleukin 1 and 6 by murine brain microvessel endothelium and smooth muscle pericytes. *Journal of Neuroimmunology*, *47*(1), 23-34.
- Fagan, K., Crider, A., Ahmed, A. O., & Pillai, A. (2017). Complement C3 Expression Is Decreased in Autism Spectrum Disorder Subjects and Contributes to Behavioral Deficits in Rodents. *Molecular Neuropsychiatry*, *3*(1), 19-27.
- Fauci, A. S., Lane, H. C., & Redfield, R. R. (2020). Covid-19 - Navigating the Uncharted. *The New England Journal of Medicine*, *382*(13), 1268-1269.
- Fernández de Cossío, L., Guzmán, A., van der Veldt, S., & Luheshi, G. N. (2017). Prenatal infection leads to ASD-like behavior and altered synaptic pruning in the mouse offspring. *Brain, Behavior, and Immunity*, *63*, 88-98.
- Fiksinski, A. M., Schneider, M., Murphy, C. M., Armando, M., Vicari, S., Canyelles, J. M., et al. (2018). Understanding the pediatric psychiatric phenotype of 22q11.2 deletion syndrome. *American Journal of Medical Genetics*, *176*(10), 2182-2191.
- Filiano, A. J., Xu, Y., Tustison, N. J., Marsh, R. L., Baker, W., Smirnov, I., et al. (2016). Unexpected role of interferon- γ in regulating neuronal connectivity and social behaviour. *Nature*, *535*(7612), 425-429.
- Filipello, F., Morini, R., Corradini, I., Zerbi, V., Canzi, A., Michalski, B., et al. (2018). The Microglial Innate Immunity Receptor TREM2 Is Required for Synapse Elimination and Normal Brain Connectivity. *Immunity*, *48*(5), 979-991.e978.

- Fillman, S. G., Weickert, T. W., Lenroot, R. K., Catts, S. V., Bruggemann, J. M., Catts, V. S., et al. (2016). Elevated peripheral cytokines characterize a subgroup of people with schizophrenia displaying poor verbal fluency and reduced Broca's area volume. *Molecular Psychiatry*, *21*(8), 1090-1098.
- Flippo, K. H., & Strack, S. (2017). An emerging role for mitochondrial dynamics in schizophrenia. *Schizophrenia Research*, *187*, 26-32.
- Forrest, M. P., Parnell, E., & Penzes, P. (2018). Dendritic structural plasticity and neuropsychiatric disease. *Nature Reviews Neuroscience*, *19*(4), 215-234.
- Franklin, C. L., & Ericsson, A. C. (2017). Microbiota and reproducibility of rodent models. *Lab Animal* (NY), *46*(4), 114-122.
- Frost, G., Sleeth, M. L., Sahuri-Arisoylu, M., Lizarbe, B., Cerdan, S., Brody, L., et al. (2014). The short-chain fatty acid acetate reduces appetite via a central homeostatic mechanism. *Nature Communications*, *5*, 3611.
- Frydecka, D., Misiak, B., Pawlak-Adamska, E., Karabon, L., Tomkiewicz, A., Sedlaczek, P., et al. (2015). Interleukin-6: the missing element of the neurocognitive deterioration in schizophrenia? The focus on genetic underpinnings, cognitive impairment and clinical manifestation. *European Archives of Psychiatry and Clinical Neuroscience*, *265*(6), 449-459.
- Galloway, D. A., Phillips, A. E. M., Owen, D. R. J., & Moore, C. S. (2019). Phagocytosis in the Brain: Homeostasis and Disease. *Frontiers in Immunology*, *10*, 790.
- Gambino, F., & Holtmaat, A. (2012). Synapses let loose for a change: inhibitory synapse pruning throughout experience-dependent cortical plasticity. *Neuron*, *74*(2), 214-217.
- Gao, L., Li, Z., Chang, S., & Wang, J. (2014). Association of interleukin-10 polymorphisms with schizophrenia: a meta-analysis. *PLoS One*, *9*(3), e90407.
- Garay, P. A., Hsiao, E. Y., Patterson, P. H., & McAllister, A. K. (2013). Maternal immune activation causes age- and region-specific changes in brain cytokines in offspring throughout development. *Brain, Behavior, and Immunity*, *31*, 54-68.
- García-Bueno, B., Gassó, P., MacDowell, K. S., Callado, L. F., Mas, S., Bernardo, M., et al. (2016). Evidence of activation of the Toll-like receptor-4 proinflammatory pathway in patients with schizophrenia. *Journal of Psychiatry & Neuroscience*, *41*(3), E46-55.

- Gareau, M. G., Wine, E., Rodrigues, D. M., Cho, J. H., Whary, M. T., Philpott, D. J., et al. (2011). Bacterial infection causes stress-induced memory dysfunction in mice. *Gut*, 60(3), 307-317.
- Gasque, P., Fontaine, M., & Morgan, B. P. (1995). Complement expression in human brain. Biosynthesis of terminal pathway components and regulators in human glial cells and cell lines. *Journal of Immunology*, 154(9), 4726-4733.
- Genc, S., Zadeoglulari, Z., Fuss, S. H., & Genc, K. (2012). The adverse effects of air pollution on the nervous system. *Journal of Toxicology*, 2012, 782462.
- Giedd JN, Rapoport JL. (2010). Structural MRI of pediatric brain development: what have we learned and where are we going? *Neuron*. 67(5), 728-34.
- Girgis, R. R., Kumar, S. S., & Brown, A. S. (2014). The cytokine model of schizophrenia: emerging therapeutic strategies. *Biological Psychiatry*, 75(4), 292-299.
- Glantz, L. A., & Lewis, D. A. (1997). Reduction of synaptophysin immunoreactivity in the prefrontal cortex of subjects with schizophrenia. Regional and diagnostic specificity. *Archives of General Psychiatry*, 54(10), 943-952.
- Glantz, L. A., & Lewis, D. A. (2000). Decreased dendritic spine density on prefrontal cortical pyramidal neurons in schizophrenia. *Archives of General Psychiatry*, 57(1), 65-73.
- Glantz, L. A., & Lewis, D. A. (2001). Dendritic spine density in schizophrenia and depression. *Archives of General Psychiatry*, 58(2), 203.
- Glassman, M., Wehring, H. J., Pociavsek, A., Sullivan, K. M., Rowland, L. M., McMahon, R. P., et al. (2018). Peripheral Cortisol and Inflammatory Response to a Psychosocial Stressor in People with Schizophrenia. *Journal of Neuropsychiatry (Foster City)*, 2(2).
- Glausier, J. R., & Lewis, D. A. (2013). Dendritic spine pathology in schizophrenia. *Neuroscience*, 251, 90-107.
- Goldsmith, D. R., & Rapaport, M. H. (2020). Inflammation and Negative Symptoms of Schizophrenia: Implications for Reward Processing and Motivational Deficits. *Frontiers in Psychiatry*, 11, 46.
- Golshani, P., Gonçalves, J. T., Khoshkhoo, S., Mostany, R., Smirnakis, S., & Portera-Cailliau, C. (2009). Internally mediated developmental desynchronization of neocortical network activity. *Journal of Neuroscience*, 29(35), 10890-10899.

- Gomes, F. V., Zhu, X., & Grace, A. A. (2019). Stress during critical periods of development and risk for schizophrenia. *Schizophrenia Research*, 213, 107-113.
- González-Pardo, H., Arias, J. L., Vallejo, G., & Conejo, N. M. (2019). Environmental enrichment effects after early stress on behavior and functional brain networks in adult rats. *PLoS One*, 14(12), e0226377.
- Goodwill, H. L., Manzano-Nieves, G., LaChance, P., Teramoto, S., Lin, S., Lopez, C., et al. (2018). Early Life Stress Drives Sex-Selective Impairment in Reversal Learning by Affecting Parvalbumin Interneurons in Orbitofrontal Cortex of Mice. *Cell Reports*, 25(9), 2299-2307.e2294.
- Gorelik A, Sapir T, Haffner-Krausz R, Olender T, Woodruff TM, Reiner O. (2007). Developmental activities of the complement pathway in migrating neurons. *Nature Communications*. 8, 15096.
- Gottesman II, Shields J. (1976). A critical review of recent adoption, twin, and family studies of schizophrenia: behavioral genetics perspectives. *Schizophrenia Bulletin*. 2(3):360-401.
- Grandjean, J., Canella, C., Anckaerts, C., Ayrancı, G., Bougacha, S., Bienert, T., et al. (2020). Common functional networks in the mouse brain revealed by multi-centre resting-state fMRI analysis. *Neuroimage*, 205, 116278.
- Gray, N. W., Weimer, R. M., Bureau, I., & Svoboda, K. (2006). Rapid redistribution of synaptic PSD-95 in the neocortex in vivo. *PLoS Biology*, 4(11), e370.
- Green, M. F. (2006). Cognitive impairment and functional outcome in schizophrenia and bipolar disorder. *Journal of Clinical Psychiatry*, 67(10), e12.
- Green, M. F. (2016). Impact of cognitive and social cognitive impairment on functional outcomes in patients with schizophrenia. *Journal of Clinical Psychiatry*, 77 Suppl 2, 8-11.
- Green, M. F., Horan, W. P., & Lee, J. (2015). Social cognition in schizophrenia. *Nature Reviews Neuroscience*, 16(10), 620-631.
- Greene, C., Hanley, N., & Campbell, M. (2019). Claudin-5: gatekeeper of neurological function. *Fluids and Barriers of the CNS*, 16(1), 3.
- Greene, C., Kealy, J., Humphries, M. M., Gong, Y., Hou, J., Hudson, N., et al. (2018). Dose-dependent expression of claudin-5 is a modifying factor in schizophrenia. *Molecular Psychiatry*, 23(11), 2156-2166.

- Gretebeck, L. M., & Subbarao, K. (2015). Animal models for SARS and MERS coronaviruses. *Current Opinions in Virology*, *13*, 123-129.
- Gross, G. G., Junge, J. A., Mora, R. J., Kwon, H. B., Olson, C. A., Takahashi, T. T., et al. (2013). Recombinant probes for visualizing endogenous synaptic proteins in living neurons. *Neuron*, *78*(6), 971-985.
- Grossmann, T. (2013). The role of medial prefrontal cortex in early social cognition. *Frontiers in Human Neuroscience*, *7*, 340.
- Grove, J., Ripke, S., Als, T. D., Mattheisen, M., Walters, R. K., Won, H., et al. (2019). Identification of common genetic risk variants for autism spectrum disorder. *Nature Genetics*, *51*(3), 431-444.
- Gruol, D. L. (2015). IL-6 regulation of synaptic function in the CNS. *Neuropharmacology*, *96*(Pt A), 42-54.
- Gruzieva, O., Merid, S. K., Gref, A., Gajulapuri, A., Lemonnier, N., Ballereau, S., et al. (2017). Exposure to Traffic-Related Air Pollution and Serum Inflammatory Cytokines in Children. *Environmental Health Perspectives*, *125*(6), 067007.
- Gumusoglu, S. B., Fine, R. S., Murray, S. J., Bittle, J. L., & Stevens, H. E. (2017). The role of IL-6 in neurodevelopment after prenatal stress. *Brain, Behavior, and Immunity*, *65*, 274-283.
- Gunner, G., Cheadle, L., Johnson, K. M., Ayata, P., Badimon, A., Mondo, E., et al. (2019). Sensory lesioning induces microglial synapse elimination via ADAM10 and fractalkine signaling. *Nature Neuroscience*, *22*(7), 1075-1088.
- Gupta, S., & Kulhara, P. (2010). What is schizophrenia: A neurodevelopmental or neurodegenerative disorder or a combination of both? A critical analysis. *Indian Journal of Psychiatry*, *52*(1), 21-27.
- Gupta, S., Masand, P. S., Kaplan, D., Bhandary, A., & Hendricks, S. (1997). The relationship between schizophrenia and irritable bowel syndrome (IBS). *Schizophrenia Research*, *23*(3), 265-268.
- Györfy, B. A., Kun, J., Török, G., Bulyáki, É., Borhegyi, Z., Gulyácssy, P., et al. (2018). Local apoptotic-like mechanisms underlie complement-mediated synaptic pruning. *Proceedings of the National Academy of Sciences of the United States of America*, *115*(24), 6303-6308.
- Hadar, R., Dong, L., Del-Valle-Anton, L., Guneykaya, D., Voget, M., Edemann-Callesen, H., et al. (2017). Deep brain stimulation during early adolescence prevents

- microglial alterations in a model of maternal immune activation. *Brain, Behavior, and Immunity*, 63, 71-80.
- Haida, O., Al Sagheer, T., Balbous, A., Francheteau, M., Matas, E., Soria, F., et al. (2019). Sex-dependent behavioral deficits and neuropathology in a maternal immune activation model of autism. *Translational Psychiatry*, 9(1), 124.
- Halden, R. U. (2010). Plastics and health risks. *Annual Review of Public Health*, 31, 179-194.
- Hammond, T. R., Dufort, C., Dissing-Olesen, L., Giera, S., Young, A., Wysoker, A., et al. (2019). Single-Cell RNA Sequencing of Microglia throughout the Mouse Lifespan and in the Injured Brain Reveals Complex Cell-State Changes. *Immunity*, 50(1), 253-271.e256.
- Hammond, T. R., Robinton, D., & Stevens, B. (2018). Microglia and the Brain: Complementary Partners in Development and Disease. *Annual Review of Cell and Developmental Biology*, 34, 523-544.
- Harrisberger, F., Smieskova, R., Vogler, C., Egli, T., Schmidt, A., Lenz, C., et al. (2016). Impact of polygenic schizophrenia-related risk and hippocampal volumes on the onset of psychosis. *Translational Psychiatry*, 6(8), e868.
- Hartz, A. M., Bauer, B., Block, M. L., Hong, J. S., & Miller, D. S. (2008). Diesel exhaust particles induce oxidative stress, proinflammatory signaling, and P-glycoprotein up-regulation at the blood-brain barrier. *The FASEB Journal*, 22(8), 2723-2733.
- Haruwaka, K., Ikegami, A., Tachibana, Y., Ohno, N., Konishi, H., Hashimoto, A., et al. (2019). Dual microglia effects on blood brain barrier permeability induced by systemic inflammation. *Nature Communications*, 10(1), 5816.
- Hayashi-Takagi, A., Takaki, M., Graziane, N., Seshadri, S., Murdoch, H., Dunlop, A. J., et al. (2010). Disrupted-in-Schizophrenia 1 (DISC1) regulates spines of the glutamate synapse via Rac1. *Nature Neuroscience*, 13(3), 327-332.
- He, J., Zhao, C., Dai, J., Weng, C. H., Bian, B. S. J., Gong, Y., et al. (2019). Microglia Mediate Synaptic Material Clearance at the Early Stage of Rats With Retinitis Pigmentosa. *Frontiers in Immunology*, 10, 912.
- Hepgul, N., Pariante, C. M., Dipasquale, S., DiForti, M., Taylor, H., Marques, T. R., et al. (2012). Childhood maltreatment is associated with increased body mass index and increased C-reactive protein levels in first-episode psychosis patients. *Psychological Medicine*, 42(9), 1893-1901.

- Hercher, C., Chopra, V., & Beasley, C. L. (2014). Evidence for morphological alterations in prefrontal white matter glia in schizophrenia and bipolar disorder. *Journal of Psychiatry & Neuroscience*, 39(6), 376-385.
- Herland, P., Huet, M., Callebaut, I., Gane, P., Ihanus, E., Gahmberg, C. G., et al. (2000). Binding sites of leukocyte beta 2 integrins (LFA-1, Mac-1) on the human ICAM-4/LW blood group protein. *The Journal of Biological Chemistry*, 275(34), 26002-26010.
- Hess, C., & Kemper, C. (2016). Complement-Mediated Regulation of Metabolism and Basic Cellular Processes. *Immunity*, 45(2), 240-254.
- Hill, J. J., Hashimoto, T., & Lewis, D. A. (2006). Molecular mechanisms contributing to dendritic spine alterations in the prefrontal cortex of subjects with schizophrenia. *Molecular Psychiatry*, 11(6), 557-566.
- Hill, K., Mann, L., Laws, K. R., Stephenson, C. M., Nimmo-Smith, I., & McKenna, P. J. (2004). Hypofrontality in schizophrenia: a meta-analysis of functional imaging studies. *Acta Psychiatrica Scandinavica*, 110(4), 243-256.
- Holland, F. H., Ganguly, P., Potter, D. N., Chartoff, E. H., & Brenhouse, H. C. (2014). Early life stress disrupts social behavior and prefrontal cortex parvalbumin interneurons at an earlier time-point in females than in males. *Neuroscience Letters*, 566, 131-136.
- Holtmaat, A., & Svoboda, K. (2009). Experience-dependent structural synaptic plasticity in the mammalian brain. *Nature Reviews Neuroscience*, 10(9), 647-658.
- Holtmaat, A. J., Trachtenberg, J. T., Wilbrecht, L., Shepherd, G. M., Zhang, X., Knott, G. W., et al. (2005). Transient and persistent dendritic spines in the neocortex in vivo. *Neuron*, 45(2), 279-291.
- Holtzman, C. W., Trotman, H. D., Goulding, S. M., Ryan, A. T., Macdonald, A. N., Shapiro, D. I., et al. (2013). Stress and neurodevelopmental processes in the emergence of psychosis. *Neuroscience*, 249, 172-191.
- Hong, S., Beja-Glasser, V. F., Nfonoyim, B. M., Frouin, A., Li, S., Ramakrishnan, S., et al. (2016). Complement and microglia mediate early synapse loss in Alzheimer mouse models. *Science*, 352(6286), 712-716.
- Hong, S., Dissing-Olesen, L., & Stevens, B. (2016). New insights on the role of microglia in synaptic pruning in health and disease. *Current Opinions in Neurobiology*, 36, 128-134.

- Horsdal, H. T., Agerbo, E., McGrath, J. J., Vilhjálmsson, B. J., Antonsen, S., Closter, A. M., et al. (2019). Association of Childhood Exposure to Nitrogen Dioxide and Polygenic Risk Score for Schizophrenia With the Risk of Developing Schizophrenia. *JAMA Network Open*, 2(11), e1914401.
- Hoshiko, M., Arnoux, I., Avignone, E., Yamamoto, N., & Audinat, E. (2012). Deficiency of the microglial receptor CX3CR1 impairs postnatal functional development of thalamocortical synapses in the barrel cortex. *Journal of Neuroscience*, 32(43), 15106-15111.
- Horton R, Wilming L, Rand V. (2004). Gene map of the extended human MHC. *Nature Reviews Genetics*. 5(12), 889–899.
- Houtepen, L. C., Boks, M. P., Kahn, R. S., Joëls, M., & Vinkers, C. H. (2015). Antipsychotic use is associated with a blunted cortisol stress response: a study in euthymic bipolar disorder patients and their unaffected siblings. *European Neuropsychopharmacology*, 25(1), 77-84.
- Howard, D. M., Adams, M. J., Clarke, T. K., Hafferty, J. D., Gibson, J., Shirali, M., et al. (2019). Genome-wide meta-analysis of depression identifies 102 independent variants and highlights the importance of the prefrontal brain regions. *Nature Neuroscience*, 22(3), 343-352.
- Howes, O. D., McCutcheon, R., Owen, M. J., & Murray, R. M. (2017). The Role of Genes, Stress, and Dopamine in the Development of Schizophrenia. *Biological Psychiatry*, 81(1), 9-20.
- Hoyles, L., Snelling, T., Umlai, U. K., Nicholson, J. K., Carding, S. R., Glen, R. C., et al. (2018). Microbiome-host systems interactions: protective effects of propionate upon the blood-brain barrier. *Microbiome*, 6(1), 55.
- Hsiao, E. Y., McBride, S. W., Hsien, S., Sharon, G., Hyde, E. R., McCue, T., et al. (2013). Microbiota modulate behavioral and physiological abnormalities associated with neurodevelopmental disorders. *Cell*, 155(7), 1451-1463.
- Hsiao, E. Y., & Patterson, P. H. (2012). Placental regulation of maternal-fetal interactions and brain development. *Developmental Neurobiology*, 72(10), 1317-1326.
- Huang, Z. J., & Zeng, H. (2013). Genetic approaches to neural circuits in the mouse. *Annual Review of Neuroscience*, 36, 183-215.
- Hudson, Z. D., & Miller, B. J. (2018). Meta-Analysis of Cytokine and Chemokine Genes in Schizophrenia. *Clinical Schizophrenia & Related Psychoses*, 12(3), 121-129B.

- Hui, C. W., Bhardwaj, S. K., Sharma, K., Joseph, A. T., Bisht, K., Picard, K., et al. (2019). Microglia in the developing prefrontal cortex of rats show dynamic changes following neonatal disconnection of the ventral hippocampus. *Neuropharmacology*, *146*, 264-275.
- Hui, C. W., St-Pierre, A., El Hajj, H., Remy, Y., Hébert, S. S., Luheshi, G. N., et al. (2018). Prenatal Immune Challenge in Mice Leads to Partly Sex-Dependent Behavioral, Microglial, and Molecular Abnormalities Associated with Schizophrenia. *Frontiers in Molecular Neuroscience*, *11*, 13.
- Hulme, H., Meikle, L. M., Strittmatter, N., van der Hooft, J. J. J., Swales, J., Bragg, R. A., et al. (2020). Microbiome-derived carnitine mimics as previously unknown mediators of gut-brain axis communication. *Science Advances*, *6*(11), eaax6328.
- Hunt, C. A., Schenker, L. J., & Kennedy, M. B. (1996). PSD-95 is associated with the postsynaptic density and not with the presynaptic membrane at forebrain synapses. *Journal of Neuroscience*, *16*(4), 1380-1388.
- Huttenlocher, P. R., & Dabholkar, A. S. (1997). Regional differences in synaptogenesis in human cerebral cortex. *Journal of Comparative Neurology*, *387*(2), 167-178.
- Håvik, B., Le Hellard, S., Rietschel, M., Lybæk, H., Djurovic, S., Mattheisen, M., et al. (2011). The complement control-related genes CSMD1 and CSMD2 associate to schizophrenia. *Biological Psychiatry*, *70*(1), 35-42.
- Ikezu, S., Yeh, H., Delpech, J. C., Woodbury, M. E., Van Enoo, A. A., Ruan, Z., et al. (2020). Inhibition of colony stimulating factor 1 receptor corrects maternal inflammation-induced microglial and synaptic dysfunction and behavioral abnormalities. *Molecular Psychiatry*.
- Inoue, K., Takano, H., Sakurai, M., Oda, T., Tamura, H., Yanagisawa, R., et al. (2006). Pulmonary exposure to diesel exhaust particles enhances coagulatory disturbance with endothelial damage and systemic inflammation related to lung inflammation. *Experimental Biology and Medicine*(Maywood), *231*(10), 1626-1632.
- Irwin, S. A., Galvez, R., & Greenough, W. T. (2000). Dendritic spine structural anomalies in fragile-X mental retardation syndrome. *Cerebral Cortex*, *10*(10), 1038-1044.
- Israel, A. K., Seeck, A., Boettger, M. K., Rachow, T., Berger, S., Voss, A., et al. (2011). Peripheral endothelial dysfunction in patients suffering from acute schizophrenia: a potential marker for cardiovascular morbidity? *Schizophrenia Research*, *128*(1-3), 44-50.

- Jacomb, I., Stanton, C., Vasudevan, R., Powell, H., O'Donnell, M., Lenroot, R., et al. (2018). C-Reactive Protein: Higher During Acute Psychotic Episodes and Related to Cortical Thickness in Schizophrenia and Healthy Controls. *Frontiers in Immunology*, 9, 2230.
- Jay, T. R., von Saucken, V. E., Muñoz, B., Codocedo, J. F., Atwood, B. K., Lamb, B. T., et al. (2019). TREM2 is required for microglial instruction of astrocytic synaptic engulfment in neurodevelopment. *Glia*, 67(10), 1873-1892.
- Jézéquel, J., Johansson, E. M., Dupuis, J. P., Rogemond, V., Gréa, H., Kellermayer, B., et al. (2017). Dynamic disorganization of synaptic NMDA receptors triggered by autoantibodies from psychotic patients. *Nature Communications*, 8(1), 1791.
- Johnson, F. K., & Kaffman, A. (2018). Early life stress perturbs the function of microglia in the developing rodent brain: New insights and future challenges. *Brain, Behavior, and Immunity*, 69, 18-27.
- Joost, E., Jordão, M. J. C., Mages, B., Prinz, M., Bechmann, I., & Krueger, M. (2019). Microglia contribute to the glia limitans around arteries, capillaries and veins under physiological conditions, in a model of neuroinflammation and in human brain tissue. *Brain Structure and Function*, 224(3), 1301-1314.
- Joseph, A. T., Bhardwaj, S. K., & Srivastava, L. K. (2018). Role of prefrontal cortex anti- and pro-inflammatory cytokines in the development of abnormal behaviors induced by disconnection of the ventral hippocampus in neonate rats. *Frontiers in Behavioral Neuroscience*, 12, 244.
- Ju, F., Ran, Y., Zhu, L., Cheng, X., Gao, H., Xi, X., et al. (2018). Increased BBB permeability enhances activation of microglia and exacerbates loss of dendritic spines after transient global cerebral ischemia. *Frontiers in Cellular Neuroscience*, 12, 236.
- Jézéquel, J., Johansson, E. M., Dupuis, J. P., Rogemond, V., Gréa, H., Kellermayer, B., et al. (2017). Dynamic disorganization of synaptic NMDA receptors triggered by autoantibodies from psychotic patients. *Nature Communications*, 8(1), 1791.
- Kaar, S. J., Angelescu, I., Marques, T. R., & Howes, O. D. (2019). Pre-frontal parvalbumin interneurons in schizophrenia: a meta-analysis of post-mortem studies. *Journal of Neural Transmission*, 126(12), 1637-1651.
- Kahn, R. S., Sommer, I. E., Murray, R. M., Meyer-Lindenberg, A., Weinberger, D. R., Cannon, T. D., et al. (2015). Schizophrenia. *Nature Reviews Disease Primers*, 1, 15067.

- Kalmady, S. V., Venkatasubramanian, G., Shivakumar, V., Gautham, S., Subramaniam, A., Jose, D. A., et al. (2014). Relationship between Interleukin-6 gene polymorphism and hippocampal volume in antipsychotic-naïve schizophrenia: evidence for differential susceptibility? *PLoS One*, 9(5), e96021.
- Kang, W. S., Park, J. K., Lee, S. M., Kim, S. K., Park, H. J., & Kim, J. W. (2013). Association between genetic polymorphisms of Toll-like receptor 2 (TLR2) and schizophrenia in the Korean population. *Gene*, 526(2), 182-186.
- Kannan, G., Gressitt, K. L., Yang, S., Stallings, C. R., Katsafanas, E., Schweinfurth, L. A., et al. (2017). Pathogen-mediated NMDA receptor autoimmunity and cellular barrier dysfunction in schizophrenia. *Translational Psychiatry*, 7(8), e1186.
- Katila, H., Hänninen, K., & Hurme, M. (1999). Polymorphisms of the interleukin-1 gene complex in schizophrenia. *Molecular Psychiatry*, 4(2), 179-181.
- Kavzoglu, S. O., & Hariri, A. G. (2013). Intracellular Adhesion Molecule (ICAM-1), Vascular Cell Adhesion Molecule (VCAM-1) and E-Selectin Levels in First Episode Schizophrenic Patients. *Klinik Psikofarmakoloji Bülteni-Bulletin of Clinical Psychopharmacology* 23(3), 205-214.
- Kayser, M. S., & Dalmau, J. (2016). Anti-NMDA receptor encephalitis, autoimmunity, and psychosis. *Schizophrenia Research*, 176(1), 36-40.
- Kentner, A. C., Bilbo, S. D., Brown, A. S., Hsiao, E. Y., McAllister, A. K., Meyer, U., et al. (2019). Maternal immune activation: reporting guidelines to improve the rigor, reproducibility, and transparency of the model. *Neuropsychopharmacology*, 44(2), 245-258.
- Kesby, J. P., Eyles, D. W., McGrath, J. J., & Scott, J. G. (2018). Dopamine, psychosis and schizophrenia: the widening gap between basic and clinical neuroscience. *Translational Psychiatry*, 8(1), 30.
- Kessler, R. C., McLaughlin, K. A., Green, J. G., Gruber, M. J., Sampson, N. A., Zaslavsky, A. M., et al. (2010). Childhood adversities and adult psychopathology in the WHO World Mental Health Surveys. *The British Journal of Psychiatry*, 197(5), 378-385.
- Kim, M., Haney, J. R., Zhang, P., Hernandez, L. M., Wang, L.-k., Perez-Cano, L., et al. (2020). Network signature of complement component 4 variation in the human brain identifies convergent molecular risk for schizophrenia. bioRxiv: bioRxiv.

- Kim, S., Kim, H., Yim, Y. S., Ha, S., Atarashi, K., Tan, T. G., et al. (2017). Maternal gut bacteria promote neurodevelopmental abnormalities in mouse offspring. *Nature*, *549*(7673), 528-532.
- Kim Y, Zerwas S, Trace SE, Sullivan PF. (2011). Schizophrenia genetics: where next? *Schizophrenia Bulletin*. *37*(3), 456-63.
- Klocke, C., Sherina, V., Graham, U. M., Gunderson, J., Allen, J. L., Sobolewski, M., et al. (2018). Enhanced cerebellar myelination with concomitant iron elevation and ultrastructural irregularities following prenatal exposure to ambient particulate matter in the mouse. *Inhalation Toxicology*, *30*(9-10), 381-396.
- Kneeland, R. E., & Fatemi, S. H. (2013). Viral infection, inflammation and schizophrenia. *Progress in Neuro-Psychopharmacology & Biological Psychiatry*, *42*, 35-48.
- Knuesel, I., Chicha, L., Britschgi, M., Schobel, S. A., Bodmer, M., Hellings, J. A., et al. (2014a). Maternal immune activation and abnormal brain development across CNS disorders. *Nature Reviews Neurology*, *10*(11), 643-660.
- Ko, J. (2017). Neuroanatomical Substrates of Rodent Social Behavior: The Medial Prefrontal Cortex and Its Projection Patterns. *Frontiers in Neural Circuits*, *11*, 41.
- Kofman, O. (2002). The role of prenatal stress in the etiology of developmental behavioural disorders. *Neuroscience & Biobehavioral Reviews*, *26*(4), 457-470.
- Kolk, S. M., de Mooij-Malsen, A. J., & Martens, G. J. (2011). Spatiotemporal Molecular Approach of in utero Electroporation to Functionally Decipher Endophenotypes in Neurodevelopmental Disorders. *Frontiers in Molecular Neuroscience*, *4*, 37.
- Konishi, H., & Kiyama, H. (2018). Microglial TREM2/DAP12 Signaling: A Double-Edged Sword in Neural Diseases. *Frontiers in Cellular Neuroscience*, *12*, 206.
- Konturek, S. J., Konturek, J. W., Pawlik, T., & Brzozowski, T. (2004). Brain-gut axis and its role in the control of food intake. *Journal of Physiology and Pharmacology*, *55*(1 Pt 2), 137-154.
- Konur, S., & Yuste, R. (2004). Developmental regulation of spine and filopodial motility in primary visual cortex: reduced effects of activity and sensory deprivation. *Journal of Neurobiology*, *59*(2), 236-246.
- Kowash, H. M., Potter, H. G., Edye, M. E., Prinssen, E. P., Bandinelli, S., Neill, J. C., et al. (2019). Poly(I:C) source, molecular weight and endotoxin contamination affect

dam and prenatal outcomes, implications for models of maternal immune activation. *Brain, Behavior, and Immunity*, 82, 160-166.

Kraus, D. M., Elliott, G. S., Chute, H., Horan, T., Pfenninger, K. H., Sanford, S. D., et al. (2006). CSMD1 is a novel multiple domain complement-regulatory protein highly expressed in the central nervous system and epithelial tissues. *Journal of Immunology*, 176(7), 4419-4430.

Kroken, R. A., Sommer, I. E., Steen, V. M., Dieset, I., & Johnsen, E. (2018). Constructing the Immune Signature of Schizophrenia for Clinical Use and Research; An Integrative Review Translating Descriptives Into Diagnostics. *Frontiers in Psychiatry*, 9, 753.

Kubicki, M., Park, H., Westin, C. F., Nestor, P. G., Mulkern, R. V., Maier, S. E., et al. (2005). DTI and MTR abnormalities in schizophrenia: analysis of white matter integrity. *Neuroimage*, 26(4), 1109-1118.

Kulas, J. A., Hettwer, J. V., Sohrabi, M., Melvin, J. E., Manocha, G. D., Puig, K. L., et al. (2018). In utero exposure to fine particulate matter results in an altered neuroimmune phenotype in adult mice. *Environmental Pollution*, 241, 279-288.

Kur, I. M., Prouvot, P. H., Fu, T., Fan, W., Müller-Braun, F., Das, A., et al. (2020). Neuronal activity triggers uptake of hematopoietic extracellular vesicles in vivo. *PLoS Biology*, 18(3), e3000643.

Lange, C., Huber, C. G., Fröhlich, D., Borgwardt, S., Lang, U. E., & Walter, M. (2017). Modulation of HPA axis response to social stress in schizophrenia by childhood trauma. *Psychoneuroendocrinology*, 82, 126-132.

Lassmann, H., Zimprich, F., Vass, K., & Hickey, W. F. (1991). Microglial cells are a component of the perivascular glia limitans. *Journal of Neuroscience Research*, 28(2), 236-243.

Law SK, Minich TM, Levine RP. (1984). Covalent binding efficiency of the third and fourth complement proteins in relation to pH, nucleophilicity, and availability of hydroxyl groups. *Biochemistry*. 23(14), 3267-72.

Lawrie SM, Abukmeil SS. Brain abnormality in schizophrenia. (1998). A systematic and quantitative review of volumetric magnetic resonance imaging studies. *The British Journal of Psychiatry*. 172, 110-20.

Lee, E., Rhim, I., Lee, J. W., Ghim, J. W., Lee, S., Kim, E., et al. (2016). Enhanced Neuronal Activity in the Medial Prefrontal Cortex during Social Approach Behavior. *Journal of Neuroscience*, 36(26), 6926-6936.

- Lee, J. D., Coulthard, L. G., & Woodruff, T. M. (2019). Complement dysregulation in the central nervous system during development and disease. *Seminars in Immunology*, 45, 101340.
- Lehmann, M. L., Weigel, T. K., Cooper, H. A., Elkahloun, A. G., Kigar, S. L., & Herkenham, M. (2018). Decoding microglia responses to psychosocial stress reveals blood-brain barrier breakdown that may drive stress susceptibility. *Scientific Reports*, 8(1), 11240.
- Lehmann, M. L., Weigel, T. K., Poffenberger, C. N., & Herkenham, M. (2019). The Behavioral Sequelae of Social Defeat Require Microglia and Are Driven by Oxidative Stress in Mice. *Journal of Neuroscience*, 39(28), 5594-5605.
- Lehner, T. (2012). The genes in the major histocompatibility complex as risk factors for schizophrenia: de omnibus dubitandum. *Biological Psychiatry*, 72(8), 615-616.
- Lehrman, E. K., Wilton, D. K., Litvina, E. Y., Welsh, C. A., Chang, S. T., Frouin, A., et al. (2018). CD47 Protects Synapses from Excess Microglia-Mediated Pruning during Development. *Neuron*, 100(1), 120-134.e126.
- Lertxundi, A., Baccini, M., Lertxundi, N., Fano, E., Aranbarri, A., Martínez, M. D., et al. (2015). Exposure to fine particle matter, nitrogen dioxide and benzene during pregnancy and cognitive and psychomotor developments in children at 15 months of age. *Environment International*, 80, 33-40.
- Levitt JJ, Bobrow L, Lucia D, Srinivasan P. (2010). A selective review of volumetric and morphometric imaging in schizophrenia. *Current Topics in Behavioral Neuroscience*. 4, 243-81.
- Lesh, T. A., Careaga, M., Rose, D. R., McAllister, A. K., Van de Water, J., Carter, C. S., et al. (2018). Cytokine alterations in first-episode schizophrenia and bipolar disorder: relationships to brain structure and symptoms. *Journal of Neuroinflammation*, 15(1), 165.
- Levy, A. D., Omar, M. H., & Koleske, A. J. (2014). Extracellular matrix control of dendritic spine and synapse structure and plasticity in adulthood. *Frontiers in Neuroanatomy*, 8, 116.
- Lewis, D. A., Glantz, L. A., Pierri, J. N., & Sweet, R. A. (2003). Altered cortical glutamate neurotransmission in schizophrenia: evidence from morphological studies of pyramidal neurons. *Annals of the New York Academy of Sciences*, 1003, 102-112.

- Li, M., van Esch, B. C. A. M., Wagenaar, G. T. M., Garssen, J., Folkerts, G., & Henricks, P. A. J. (2018). Pro- and anti-inflammatory effects of short chain fatty acids on immune and endothelial cells. *European Journal of Pharmacology*, *831*, 52-59.
- Li, Q., & Barres, B. A. (2018). Microglia and macrophages in brain homeostasis and disease. *Nature Reviews Immunology*, *18*(4), 225-242.
- Li, X., Zhang, W., Lencz, T., Darvasi, A., Alkelai, A., Lerer, B., et al. (2015). Common variants of IRF3 conferring risk of schizophrenia. *Journal of Psychiatric Research*, *64*, 67-73.
- Li, Y., Missig, G., Finger, B. C., Landino, S. M., Alexander, A. J., Mokler, E. L., et al. (2018). Maternal and Early Postnatal Immune Activation Produce Dissociable Effects on Neurotransmission in mPFC-Amygdala Circuits. *Journal of Neuroscience*, *38*(13), 3358-3372.
- Li, Z., Chen, J., Yu, H., He, L., Xu, Y., Zhang, D., et al. (2017). Genome-wide association analysis identifies 30 new susceptibility loci for schizophrenia. *Nature Genetics*, *49*(11), 1576-1583.
- Liang, B., Zhang, L., Barbera, G., Fang, W., Zhang, J., Chen, X., et al. (2018). Distinct and Dynamic ON and OFF Neural Ensembles in the Prefrontal Cortex Code Social Exploration. *Neuron*, *100*(3), 700-714.e709.
- Lieberman, J. A., Stroup, T. S., McEvoy, J. P., Swartz, M. S., Rosenheck, R. A., Perkins, D. O., et al. (2005). Effectiveness of antipsychotic drugs in patients with chronic schizophrenia. *The New England Journal of Medicine*, *353*(12), 1209-1223.
- Liu, Y., Fu, X., Tang, Z., Li, C., Xu, Y., Zhang, F., et al. (2019). Altered expression of the CSMD1 gene in the peripheral blood of schizophrenia patients. *BMC Psychiatry*, *19*(1), 113.
- Liu, Y. U., Ying, Y., Li, Y., Eyo, U. B., Chen, T., Zheng, J., et al. (2019). Neuronal network activity controls microglial process surveillance in awake mice via norepinephrine signaling. *Nature Neuroscience*, *22*(11), 1771-1781.
- Lobsiger, C. S., Boillée, S., Pozniak, C., Khan, A. M., McAlonis-Downes, M., Lewcock, J. W., et al. (2013). C1q induction and global complement pathway activation do not contribute to ALS toxicity in mutant SOD1 mice. *Proceedings of the National Academy of Sciences of the USA*, *110*(46), E4385-4392.
- LoTurco, J., Manent, J. B., & Sidiqi, F. (2009). New and improved tools for in utero electroporation studies of developing cerebral cortex. *Cerebral Cortex*, *19 Suppl 1*, i120-125.

- Louveau, A., Herz, J., Alme, M. N., Salvador, A. F., Dong, M. Q., Viar, K. E., et al. (2018). CNS lymphatic drainage and neuroinflammation are regulated by meningeal lymphatic vasculature. *Nature Neuroscience*, 21(10), 1380-1391.
- Louveau, A., Smirnov, I., Keyes, T. J., Eccles, J. D., Rouhani, S. J., Peske, J. D., et al. (2015). Structural and functional features of central nervous system lymphatic vessels. *Nature*, 523(7560), 337-341.
- Lu, Y. C., Yeh, W. C., & Ohashi, P. S. (2008). LPS/TLR4 signal transduction pathway. *Cytokine*, 42(2), 145-151.
- Luchicchi, A., Lecca, S., Melis, M., De Felice, M., Cadeddu, F., Frau, R., et al. (2016). Maternal Immune Activation Disrupts Dopamine System in the Offspring. *International Journal of Neuropsychopharmacology*, 19(7).
- Lui, H., Zhang, J., Makinson, S. R., Cahill, M. K., Kelley, K. W., Huang, H. Y., et al. (2016). Progranulin Deficiency Promotes Circuit-Specific Synaptic Pruning by Microglia via Complement Activation. *Cell*, 165(4), 921-935.
- Luo, L., Callaway, E. M., & Svoboda, K. (2018). Genetic Dissection of Neural Circuits: A Decade of Progress. *Neuron*, 98(2), 256-281.
- Lévi-Strauss, M., & Mallat, M. (1987). Primary cultures of murine astrocytes produce C3 and factor B, two components of the alternative pathway of complement activation. *Journal of Immunology*, 139(7), 2361-2366.
- MacDonald, M. L., Alhassan, J., Newman, J. T., Richard, M., Gu, H., Kelly, R. M., et al. (2017). Selective Loss of Smaller Spines in Schizophrenia. *American Journal of Psychiatry*, 174(6), 586-594.
- MacDowell, K. S., Pinacho, R., Leza, J. C., Costa, J., Ramos, B., & García-Bueno, B. (2017). Differential regulation of the TLR4 signalling pathway in post-mortem prefrontal cortex and cerebellum in chronic schizophrenia: Relationship with SP transcription factors. *Progress in Neuro-Psychopharmacology & Biological Psychiatry*, 79(Pt B), 481-492.
- Mackes, N. K., Golm, D., Sarkar, S., Kumsta, R., Rutter, M., Fairchild, G., et al. (2020). Early childhood deprivation is associated with alterations in adult brain structure despite subsequent environmental enrichment. *Proceedings of the National Academy of Sciences of the United States of America*, 117(1), 641-649.
- Magdalon, J., Mansur, F., Teles E Silva, A. L., de Goes, V. A., Reiner, O., & Sertié, A. L. (2020). Complement System in Brain Architecture and Neurodevelopmental Disorders. *Frontiers in Neuroscience* 14, 23.

- Mallard, C. (2012). Innate Immunity regulation by toll-like receptors in the brain. *ISRN Neurology*, 2012, 701950.
- Manent, J. B., Wang, Y., Chang, Y., Paramasivam, M., & LoTurco, J. J. (2009). Dcx reexpression reduces subcortical band heterotopia and seizure threshold in an animal model of neuronal migration disorder. *Nature Medicine*, 15(1), 84-90.
- Manoach, D. S., Press, D. Z., Thangaraj, V., Searl, M. M., Goff, D. C., Halpern, E., et al. (1999). Schizophrenic subjects activate dorsolateral prefrontal cortex during a working memory task, as measured by fMRI. *Biological Psychiatry*, 45(9), 1128-1137.
- Marín O. (2016). Developmental timing and critical windows for the treatment of psychiatric disorders. *Nature Medicine*, (11):1229-1238.
- Marsland, A. L., Walsh, C., Lockwood, K., & John-Henderson, N. A. (2017). The effects of acute psychological stress on circulating and stimulated inflammatory markers: A systematic review and meta-analysis. *Brain, Behavior, and Immunity*, 64, 208-219.
- Martinelli, D. C., Chew, K. S., Rohlmann, A., Lum, M. Y., Ressler, S., Hattar, S., et al. (2016). Expression of C1ql3 in Discrete Neuronal Populations Controls Efferent Synapse Numbers and Diverse Behaviors. *Neuron*, 91(5), 1034-1051.
- Mathis, A., Mamidanna, P., Cury, K. M., Abe, T., Murthy, V. N., Mathis, M. W., et al. (2018). DeepLabCut: markerless pose estimation of user-defined body parts with deep learning. *Nature Neuroscience*, 21(9), 1281-1289.
- Matsuda, T., & Cepko, C. L. (2004). Electroporation and RNA interference in the rodent retina in vivo and in vitro. *Proceedings of the National Academy of Sciences of the United States of America*, 101(1), 16-22.
- Mattei, D., Ivanov, A., Ferrai, C., Jordan, P., Guneykaya, D., Buonfiglioli, A., et al. (2017). Maternal immune activation results in complex microglial transcriptome signature in the adult offspring that is reversed by minocycline treatment. *Translational Psychiatry*, 7(5), e1120.
- Małkiewicz, M. A., Szarmach, A., Sabisz, A., Cubała, W. J., Szurowska, E., & Winklewski, P. J. (2019). Blood-brain barrier permeability and physical exercise. *Journal of Neuroinflammation*, 16(1), 15.
- McCreary, J. K., & Metz, G. A. S. (2016). Environmental enrichment as an intervention for adverse health outcomes of prenatal stress. *Environmental Epigenetics*, 2(3), dvw013.

- McGrath, J., Saha, S., Welham, J., El Saadi, O., MacCauley, C., & Chant, D. (2004). A systematic review of the incidence of schizophrenia: the distribution of rates and the influence of sex, urbanicity, migrant status and methodology. *BMC Medicine*, 2, 13.
- McIntosh AM, Owens DC, Moorhead WJ, Whalley HC, Stanfield AC, Hall J, et al. (2011). Longitudinal volume reductions in people at high genetic risk of schizophrenia as they develop psychosis. *Biological Psychiatry*. 69(10), 953-8.
- McKernan, D. P., Dennison, U., Gaszner, G., Cryan, J. F., & Dinan, T. G. (2011). Enhanced peripheral toll-like receptor responses in psychosis: further evidence of a pro-inflammatory phenotype. *Translational Psychiatry*, 1, e36.
- Meredith, R. M. (2015). Sensitive and critical periods during neurotypical and aberrant neurodevelopment: a framework for neurodevelopmental disorders. *Neuroscience & Biobehavioral Reviews*, 50, 180-188.
- Merlini, M., Davalos, D., & Akassoglou, K. (2012). In vivo imaging of the neurovascular unit in CNS disease. *Intravital*, 1(2), 87-94.
- Meyer, U. (2019). Neurodevelopmental Resilience and Susceptibility to Maternal Immune Activation. *Trends in Neuroscience*, 42(11), 793-806.
- Micheva, K. D., & Beaulieu, C. (1996). Quantitative aspects of synaptogenesis in the rat barrel field cortex with special reference to GABA circuitry. *Journal of Comparative Neurology*, 373(3), 340-354.
- Millan, M. J., Andrieux, A., Bartzokis, G., Cadenhead, K., Dazzan, P., Fusar-Poli, P., et al. Altering the course of schizophrenia: progress and perspectives. *Nature Reviews Drug Discovery*, 15(7), 485-515
- Millan, M. J., Andrieux, A., Bartzokis, G., Cadenhead, K., Dazzan, P., Fusar-Poli, P., et al. (2016). Altering the course of schizophrenia: progress and perspectives. *Nature Reviews Drug Discovery*, 15(7), 485-515.
- Miller, G. E., & Chen, E. (2010). Harsh family climate in early life presages the emergence of a proinflammatory phenotype in adolescence. *Psychological Science*, 21(6), 848-856.
- Miyamoto, A., Wake, H., Ishikawa, A. W., Eto, K., Shibata, K., Murakoshi, H., et al. (2016). Microglia contact induces synapse formation in developing somatosensory cortex. *Nature Communications*, 7, 12540.

- Mnif, W., Hassine, A. I., Bouaziz, A., Bartegi, A., Thomas, O., & Roig, B. (2011). Effect of endocrine disruptor pesticides: a review. *International Journal of Environmental Research and Public Health*, 8(6), 2265-2303.
- Molina, V., Sanz, J., Reig, S., Martínez, R., Sarramea, F., Luque, R., et al. (2005). Hypofrontality in men with first-episode psychosis. *The British Journal of Psychiatry*, 186, 203-208.
- Mondelli, V., Dazzan, P., Hepgul, N., Di Forti, M., Aas, M., D'Albenzio, A., et al. (2010). Abnormal cortisol levels during the day and cortisol awakening response in first-episode psychosis: the role of stress and of antipsychotic treatment. *Schizophrenia Research*, 116(2-3), 234-242.
- Mondelli, V., Di Forti, M., Morgan, B. P., Murray, R. M., Pariante, C. M., & Dazzan, P. (2020). Baseline high levels of complement component 4 predict worse clinical outcome at 1-year follow-up in first-episode psychosis. *Brain, Behavior, and Immunity*.
- Mondelli, V., Pariante, C. M., Navari, S., Aas, M., D'Albenzio, A., Di Forti, M., et al. (2010). Higher cortisol levels are associated with smaller left hippocampal volume in first-episode psychosis. *Schizophrenia Research*, 119(1-3), 75-78.
- Morgan BP, Gasque P. (1997). Extrahepatic complement biosynthesis: where, when and why? *Clinical & Experimental Immunology*. 107(1), 1-7.
- Morita, K., Sasaki, H., Furuse, M., & Tsukita, S. (1999). Endothelial claudin: claudin-5/TMVCF constitutes tight junction strands in endothelial cells. *Journal of Cell Biology*, 147(1), 185-194.
- Morris, R. W., Sparks, A., Mitchell, P. B., Weickert, C. S., & Green, M. J. (2012). Lack of cortico-limbic coupling in bipolar disorder and schizophrenia during emotion regulation. *Translational Psychiatry*, 2, e90.
- Morris-Schaffer, K., Merrill, A., Jew, K., Wong, C., Conrad, K., Harvey, K., et al. (2019). Effects of neonatal inhalation exposure to ultrafine carbon particles on pathology and behavioral outcomes in C57BL/6J mice. *Particle and Fibre Toxicology*, 16(1), 10.
- Motahari, Z., Moody, S. A., Maynard, T. M., & LaMantia, A. S. (2019). In the line-up: deleted genes associated with DiGeorge/22q11.2 deletion syndrome: are they all suspects? *Journal of Neurodevelopmental Disorders*, 11(1), 7.
- Mueller, B. R., & Bale, T. L. (2008). Sex-specific programming of offspring emotionality after stress early in pregnancy. *Journal of Neuroscience*, 28(36), 9055-9065.

- Mumaw, C. L., Levesque, S., McGraw, C., Robertson, S., Lucas, S., Stafflinger, J. E., et al. (2016). Microglial priming through the lung-brain axis: the role of air pollution-induced circulating factors. *The FASEB Journal*, *30*(5), 1880-1891.
- Munji, R. N., Soung, A. L., Weiner, G. A., Sohet, F., Semple, B. D., Trivedi, A., et al. (2019). Profiling the mouse brain endothelial transcriptome in health and disease models reveals a core blood-brain barrier dysfunction module. *Nature Neuroscience*, *22*(11), 1892-1902.
- Murphy, K. C. (2002). Schizophrenia and velo-cardio-facial syndrome. *Lancet*, *359*(9304), 426-430.
- Müller, N., & Schwarz, M. J. (2010). Immune System and Schizophrenia. *Current Immunology Reviews*, *6*(3), 213-220.
- Na, K. S., Jung, H. Y., & Kim, Y. K. (2014). The role of pro-inflammatory cytokines in the neuroinflammation and neurogenesis of schizophrenia. *Progress in Neuro-Psychopharmacology & Biological Psychiatry*, *48*, 277-286.
- Najjar, S., Pahlajani, S., De Sanctis, V., Stern, J. N. H., Najjar, A., & Chong, D. (2017). Neurovascular Unit Dysfunction and Blood-Brain Barrier Hyperpermeability Contribute to Schizophrenia Neurobiology: A Theoretical Integration of Clinical and Experimental Evidence. *Frontiers in Psychiatry*, *8*, 83.
- Nair, A., & Bonneau, R. H. (2006). Stress-induced elevation of glucocorticoids increases microglia proliferation through NMDA receptor activation. *Journal of Neuroimmunology*, *171*(1-2), 72-85.
- Negrón-Oyarzo, I., Dagnino-Subiabre, A., & Muñoz Carvajal, P. (2015). Synaptic Impairment in Layer 1 of the Prefrontal Cortex Induced by Repeated Stress During Adolescence is Reversed in Adulthood. *Frontiers in Cellular Neuroscience*, *9*, 442.
- Nesargikar, P. N., Spiller, B., & Chavez, R. (2012). The complement system: history, pathways, cascade and inhibitors. *European Journal of Microbiology and Immunology*, *2*(2), 103-111.
- Neufeld, K. M., Kang, N., Bienenstock, J., & Foster, J. A. (2011). Reduced anxiety-like behavior and central neurochemical change in germ-free mice. *Neurogastroenterology & Motility*, *23*(3), 255-264, e119.
- Newbury, J. B., Arseneault, L., Beevers, S., Kitwiroon, N., Roberts, S., Pariante, C. M., et al. (2019). Association of Air Pollution Exposure With Psychotic Experiences During Adolescence. *JAMA Psychiatry*, *76*(6), 614-623.

- Newman, N. C., Ryan, P., Lemasters, G., Levin, L., Bernstein, D., Hershey, G. K., et al. (2013). Traffic-related air pollution exposure in the first year of life and behavioral scores at 7 years of age. *Environmental Health Perspectives*, 121(6), 731-736.
- Nguyen, T. T., Dev, S. I., Chen, G., Liou, S. C., Martin, A. S., Irwin, M. R., et al. (2018). Abnormal levels of vascular endothelial biomarkers in schizophrenia. *European Archives of Psychiatry and Clinical Neuroscience*, 268(8), 849-860.
- Nicolson, R., & Szatmari, P. (2003). Genetic and neurodevelopmental influences in autistic disorder. *The Canadian Journal of Psychiatry*, 48(8), 526-537.
- Nimmerjahn, A., Kirchhoff, F., & Helmchen, F. (2005). Resting microglial cells are highly dynamic surveillants of brain parenchyma in vivo. *Science*, 308(5726), 1314-1318.
- Nishioku, T., Dohgu, S., Takata, F., Eto, T., Ishikawa, N., Kodama, K. B., et al. (2009). Detachment of brain pericytes from the basal lamina is involved in disruption of the blood-brain barrier caused by lipopolysaccharide-induced sepsis in mice. *Cellular and Molecular Neurobiology*, 29(3), 309-316.
- Nishiura, K., Ichikawa-Tomikawa, N., Sugimoto, K., Kunii, Y., Kashiwagi, K., Tanaka, M., et al. (2017). PKA activation and endothelial claudin-5 breakdown in the schizophrenic prefrontal cortex. *Oncotarget*, 8(55), 93382-93391.
- Nonaka, M., Nakayama, K., Yeul, Y. D., & Takahashi, M. (1985). Complete nucleotide and derived amino acid sequences of the fourth component of mouse complement (C4). Evolutionary aspects. *The Journal of Biological Chemistry*, 260(20), 10936-10943.
- Notter, T., Coughlin, J. M., Gschwind, T., Weber-Stadlbauer, U., Wang, Y., Kassiou, M., et al. (2018). Translational evaluation of translocator protein as a marker of neuroinflammation in schizophrenia. *Molecular Psychiatry*, 23(2), 323-334.
- Notter, T., Schalbeter, S. M., Clifton, N. E., Mattei, D., Richetto, J., Thomas, K., et al. (2020). Neuronal activity increases translocator protein (TSPO) levels. *Molecular Psychiatry*. <https://doi.org/10.1038/s41380-020-0745-1>
- Oberlander, V. C., Xu, X., Chini, M., & Hanganu-Opatz, I. L. (2019). Developmental dysfunction of prefrontal-hippocampal networks in mouse models of mental illness. *European Journal of Neuroscience*, 50(6), 3072-3084.

- Ochoa, S., Usall, J., Cobo, J., Labad, X., & Kulkarni, J. (2012). Gender differences in schizophrenia and first-episode psychosis: a comprehensive literature review. *Schizophrenia Research Treatment*, 2012, 916198.
- Ohta, K. I., Suzuki, S., Warita, K., Sumitani, K., Tenkumo, C., Ozawa, T., et al. (2020). The effects of early life stress on the excitatory/inhibitory balance of the medial prefrontal cortex. *Behavioural Brain Research*, 379, 112306.
- Okabe, S. (2017). Fluorescence imaging of synapse dynamics in normal circuit maturation and in developmental disorders. *Proceedings of the Japan Academy Series B Physical and Biological Sciences*, 93(7), 483-497.
- Okano, H., Sasaki, E., Yamamori, T., Iriki, A., Shimogori, T., Yamaguchi, Y., et al. (2016). Brain/MINDS: A Japanese National Brain Project for Marmoset Neuroscience. *Neuron*, 92(3), 582-590.
- Olinicy, A., House, R., Gao, B., Recksiek, P., Phang, T. L., Sullivan, B., et al. (2011). Elevated DISC1 transcript levels in PBMCs during acute psychosis in patients with schizophrenia. *Translational Biomedicine Journal*, 2(1).
- Onwordi, E. C., Halff, E. F., Whitehurst, T., Mansur, A., Cotel, M. C., Wells, L., et al. (2020). Synaptic density marker SV2A is reduced in schizophrenia patients and unaffected by antipsychotics in rats. *Nature Communications*, 11(1), 246.
- Orešič, M., Tang, J., Seppänen-Laakso, T., Mattila, I., Saarni, S. E., Saarni, S. I., et al. (2011). Metabolome in schizophrenia and other psychotic disorders: a general population-based study. *Genome Medicine*, 3(3), 19.
- Ozcan, A. S. (2017). Filopodia: A Rapid Structural Plasticity Substrate for Fast Learning. *Frontiers in Synaptic Neuroscience*, 9, 12.
- Pagani, F., Paolicelli, R. C., Murana, E., Cortese, B., Di Angelantonio, S., Zurolo, E., et al. (2015). Defective microglial development in the hippocampus of Cx3cr1 deficient mice. *Frontiers in Cellular Neuroscience*, 9, 111.
- Pagliaccio, D., Herbstman, J. B., Perera, F., Tang, D., Goldsmith, J., Peterson, B. S., et al. (2020). Prenatal exposure to polycyclic aromatic hydrocarbons modifies the effects of early life stress on attention and Thought Problems in late childhood. *Journal of Child Psychology and Psychiatry*.
- Pan, Y., Chen, X. Y., Zhang, Q. Y., & Kong, L. D. (2014). Microglial NLRP3 inflammasome activation mediates IL-1 β -related inflammation in prefrontal cortex of depressive rats. *Brain, Behavior, and Immunity*, 41, 90-100.

- Paolicelli, R. C., Bergamini, G., & Rajendran, L. (2018). Cell-to-cell Communication by Extracellular Vesicles: Focus on Microglia. *Neuroscience*.
- Paolicelli, R. C., Bisht, K., & Tremblay, M. (2014). Fractalkine regulation of microglial physiology and consequences on the brain and behavior. *Frontiers in Cellular Neuroscience*, 8, 129.
- Paolicelli, R. C., Bolasco, G., Pagani, F., Maggi, L., Scianni, M., Panzanelli, P., et al. (2011). Synaptic pruning by microglia is necessary for normal brain development. *Science*, 333(6048), 1456-1458.
- Paolicelli, R. C., & Ferretti, M. T. (2017). Function and Dysfunction of Microglia during Brain Development: Consequences for Synapses and Neural Circuits. *Frontiers in Synaptic Neuroscience*, 9, 9.
- Paolicelli, R. C., Jawaid, A., Henstridge, C. M., Valeri, A., Merlini, M., Robinson, J. L., et al. (2017). TDP-43 Depletion in Microglia Promotes Amyloid Clearance but Also Induces Synapse Loss. *Neuron*, 95(2), 297-308.e296.
- Park, J., Chun, J. W., Park, H. J., Kim, E., & Kim, J. J. (2018). Involvement of amygdala-prefrontal dysfunction in the influence of negative emotion on the resolution of cognitive conflict in patients with schizophrenia. *Brain and Behavior*, 8(8), e01064.
- Parkhurst, C. N., Yang, G., Ninan, I., Savas, J. N., Yates, J. R., Lafaille, J. J., et al. (2013). Microglia promote learning-dependent synapse formation through brain-derived neurotrophic factor. *Cell*, 155(7), 1596-1609.
- Paul-Samojedny, M., Owczarek, A., Suchanek, R., Kowalczyk, M., Fila-Danilow, A., Borkowska, P., et al. (2011a). Association study of interferon gamma (IFN- γ) +874T/A gene polymorphism in patients with paranoid schizophrenia. *Journal of Molecular Neuroscience*, 43(3), 309-315.
- Paul-Samojedny, M., Owczarek, A., Suchanek, R., Kowalczyk, M., Fila-Danilow, A., Borkowska, P., et al. (2011b). Association study of interferon gamma (IFN- γ) +874T/A gene polymorphism in patients with paranoid schizophrenia. *Journal of Molecular Neuroscience*, 43(3), 309-315.
- Paxinos, G., & Franklin, K. B. J. (2001). *The mouse brain in stereotaxic coordinates* (2nd ed.). San Diego, Calif. London: Academic.
- Pearce, B. D. (2001). Schizophrenia and viral infection during neurodevelopment: a focus on mechanisms. *Molecular Psychiatry*, 6(6), 634-646.

- Pedersen, C. B., Raaschou-Nielsen, O., Hertel, O., & Mortensen, P. B. (2004). Air pollution from traffic and schizophrenia risk. *Schizophrenia Research*, 66(1), 83-85.
- Pedersen, J. M., Mortensen, E. L., Christensen, D. S., Rosing, M., Brunsgaard, H., Meincke, R. H., et al. (2018). Prenatal and early postnatal stress and later life inflammation. *Psychoneuroendocrinology*, 88, 158-166.
- Pedraz-Petrozzi, B., Elyamany, O., Rummel, C., & Mulert, C. (2020). Effects of inflammation on the kynurenine pathway in schizophrenia - a systematic review. *Journal of Neuroinflammation*, 17(1), 56.
- Pendyala, G., Chou, S., Jung, Y., Coiro, P., Spartz, E., Padmashri, R., et al. (2017). Maternal Immune Activation Causes Behavioral Impairments and Altered Cerebellar Cytokine and Synaptic Protein Expression. *Neuropsychopharmacology*, 42(7), 1435-1446.
- Penzes, P., Cahill, M. E., Jones, K. A., VanLeeuwen, J. E., & Woolfrey, K. M. (2011). Dendritic spine pathology in neuropsychiatric disorders. *Nature Neuroscience*, 14(3), 285-293.
- Peters, A., Veronesi, B., Calderón-Garcidueñas, L., Gehr, P., Chen, L. C., Geiser, M., et al. (2006). Translocation and potential neurological effects of fine and ultrafine particles a critical update. *Particle and Fibre Toxicology*, 3, 13.
- Peterson, S. L., Nguyen, H. X., Mendez, O. A., & Anderson, A. J. (2015). Complement protein C1q modulates neurite outgrowth in vitro and spinal cord axon regeneration in vivo. *Journal of Neuroscience*, 35(10), 4332-4349.
- Piskulic D, Olver JS, Norman TR, Mruff P. (2007). Behavioural studies of spatial working memory dysfunction in schizophrenia: a quantitative literature review. *Psychiatry Research*. 150(2):111-21.
- Pope, C. A., Bhatnagar, A., McCracken, J. P., Abplanalp, W., Conklin, D. J., & O'Toole, T. (2016). Exposure to Fine Particulate Air Pollution Is Associated With Endothelial Injury and Systemic Inflammation. *Circulation Research*, 119(11), 1204-1214.
- Popovic, D., Schmitt, A., Kaurani, L., Senner, F., Papiol, S., Malchow, B., et al. (2019). Childhood Trauma in Schizophrenia: Current Findings and Research Perspectives. *Frontiers in Neuroscience*, 13, 274.

- Portera-Cailliau, C., Pan, D. T., & Yuste, R. (2003). Activity-regulated dynamic behavior of early dendritic protrusions: evidence for different types of dendritic filopodia. *Journal of Neuroscience*, *23*(18), 7129-7142.
- Pouget, J. G. (2018). The Emerging Immunogenetic Architecture of Schizophrenia. *Schizophrenia Bulletin*, *44*(5), 993-1004.
- Pouget, J. G., Gonçalves, V. F., Spain, S. L., Finucane, H. K., Raychaudhuri, S., Kennedy, J. L., et al. (2016). Genome-Wide Association Studies Suggest Limited Immune Gene Enrichment in Schizophrenia Compared to 5 Autoimmune Diseases. *Schizophrenia Bulletin*, *42*(5), 1176-1184.
- Pouget, J. G., Han, B., Wu, Y., Mignot, E., Ollila, H. M., Barker, J., et al. (2019). Cross-disorder analysis of schizophrenia and 19 immune-mediated diseases identifies shared genetic risk. *Human Molecular Genetics*, *28*(20), 3498-3513.
- Pratt, L., Ni, L., Ponzio, N. M., & Jonakait, G. M. (2013). Maternal inflammation promotes fetal microglial activation and increased cholinergic expression in the fetal basal forebrain: role of interleukin-6. *Pediatric Research*, *74*(4), 393-401.
- Priller, J., & Prinz, M. (2019). Targeting microglia in brain disorders. *Science*, *365*(6448), 32-33.
- Pugliese, V., Bruni, A., Carbone, E. A., Calabrò, G., Cerminara, G., Sampogna, G., et al. (2019). Maternal stress, prenatal medical illnesses and obstetric complications: Risk factors for schizophrenia spectrum disorder, bipolar disorder and major depressive disorder. *Psychiatry Research*, *271*, 23-30.
- Purcell, S. M., Wray, N. R., Stone, J. L., Visscher, P. M., O'Donovan, M. C., Sullivan, P. F., et al. (2009). Common polygenic variation contributes to risk of schizophrenia and bipolar disorder. *Nature*, *460*(7256), 748-752.
- Purves-Tyson, T. D., Weber-Stadlbauer, U., Richetto, J., Rothmond, D. A., Labouesse, M. A., Polesel, M., et al. (2019). Increased levels of midbrain immune-related transcripts in schizophrenia and in murine offspring after maternal immune activation. *Molecular Psychiatry*. <https://doi.org/10.1038/s41380-019-0434-0>
- Quidé, Y., Ong, X. H., Mohnke, S., Schnell, K., Walter, H., Carr, V. J., et al. (2017). Childhood trauma-related alterations in brain function during a Theory-of-Mind task in schizophrenia. *Schizophrenia Research*, *189*, 162-168.
- Quirk, G. J., & Beer, J. S. (2006). Prefrontal involvement in the regulation of emotion: convergence of rat and human studies. *Current Opinions in Neurobiology*, *16*(6), 723-727.

- Raison, C. L., Rutherford, R. E., Woolwine, B. J., Shuo, C., Schettler, P., Drake, D. F., et al. (2013). A randomized controlled trial of the tumor necrosis factor antagonist infliximab for treatment-resistant depression: the role of baseline inflammatory biomarkers. *JAMA Psychiatry*, *70*(1), 31-41.
- Rajendran, L., & Paolicelli, R. C. (2018). Microglia-Mediated Synapse Loss in Alzheimer's Disease. *Journal of Neuroscience*, *38*(12), 2911-2919.
- Read, J., Bentall, R. P., & Fosse, R. (2009). Time to abandon the bio-bio-bio model of psychosis: Exploring the epigenetic and psychological mechanisms by which adverse life events lead to psychotic symptoms. *Epidemiologia e psichiatria sociale*, *18*(4), 299-310.
- Reed, M. D., Yim, Y. S., Wimmer, R. D., Kim, H., Ryu, C., Welch, G. M., et al. (2020). IL-17a promotes sociability in mouse models of neurodevelopmental disorders. *Nature*, *577*(7789), 249-253.
- Remington, G., Foussias, G., Fervaha, G., Agid, O., Takeuchi, H., Lee, J., et al. (2016). Treating Negative Symptoms in Schizophrenia: an Update. *Current Treatment Options in Psychiatry*, *3*, 133-150.
- Ribeiro, M., Brigas, H. C., Temido-Ferreira, M., Pousinha, P. A., Regen, T., Santa, C., et al. (2019). Meningeal $\gamma\delta$ T cell-derived IL-17 controls synaptic plasticity and short-term memory. *Science Immunology*, *4*(40).
- Riga, D., Matos, M. R., Glas, A., Smit, A. B., Spijker, S., & Van den Oever, M. C. (2014). Optogenetic dissection of medial prefrontal cortex circuitry. *Frontiers in Systems Neuroscience*, *8*, 230.
- Ripke, S., O'Dushlaine, C., Chambert, K., Moran, J. L., Kähler, A. K., Akterin, S., et al. (2013). Genome-wide association analysis identifies 13 new risk loci for schizophrenia. *Nature Genetics*, *45*(10), 1150-1159.
- Roberts, R. C. (2017). Postmortem studies on mitochondria in schizophrenia. *Schizophrenia Research*, *187*, 17-25.
- Rocheffort, N. L., Garaschuk, O., Milos, R. I., Narushima, M., Marandi, N., Pichler, B., et al. (2009). Sparsification of neuronal activity in the visual cortex at eye-opening. *Proceedings of the National Academy of Sciences of the United States of America*, *106*(35), 15049-15054.
- Rocheffort, N. L., & Konnerth, A. (2012). Dendritic spines: from structure to in vivo function. *EMBO Reports*, *13*(8), 699-708.

- Rogers, G. B., Keating, D. J., Young, R. L., Wong, M. L., Licinio, J., & Wesselingh, S. (2016). From gut dysbiosis to altered brain function and mental illness: mechanisms and pathways. *Molecular Psychiatry*, *21*(6), 738-748.
- Rose, T., & Bonhoeffer, T. (2018). Experience-dependent plasticity in the lateral geniculate nucleus. *Current Opinions in Neurobiology*, *53*, 22-28.
- Rothhammer, V., Borucki, D. M., Tjon, E. C., Takenaka, M. C., Chao, C. C., Ardura-Fabregat, A., et al. (2018). Microglial control of astrocytes in response to microbial metabolites. *Nature*, *557*(7707), 724-728.
- Rua, R., Lee, J. Y., Silva, A. B., Swafford, I. S., Maric, D., Johnson, K. R., et al. (2019). Infection drives meningeal engraftment by inflammatory monocytes that impairs CNS immunity. *Nature Immunology*, *20*(4), 407-419.
- Rustenhoven, J., & Kipnis, J. (2019). Bypassing the blood-brain barrier. *Science*, *366*(6472), 1448-1449.
- Ryan, M. C., Sharifi, N., Condren, R., & Thakore, J. H. (2004). Evidence of basal pituitary-adrenal overactivity in first episode, drug naïve patients with schizophrenia. *Psychoneuroendocrinology*, *29*(8), 1065-1070.
- Réus, G. Z., Fernandes, G. C., de Moura, A. B., Silva, R. H., Darabas, A. C., de Souza, T. G., et al. (2017). Early life experience contributes to the developmental programming of depressive-like behaviour, neuroinflammation and oxidative stress. *Journal of Psychiatric Research*, *95*, 196-207.
- Réus, G. Z., Silva, R. H., de Moura, A. B., Presa, J. F., Abelaira, H. M., Abatti, M., et al. (2019). Early Maternal Deprivation Induces Microglial Activation, Alters Glial Fibrillary Acidic Protein Immunoreactivity and Indoleamine 2,3-Dioxygenase during the Development of Offspring Rats. *Molecular Neurobiology*, *56*(2), 1096-1108.
- Saito, T. (2006). In vivo electroporation in the embryonic mouse central nervous system. *Nature Protocols*, *1*(3), 1552-1558.
- Salleh, M. R. (2004). The genetics of schizophrenia. *Malaysian Journal of Medical Sciences*, *11*(2), 3-11.
- Salter, M. W., & Beggs, S. (2014). Sublime microglia: expanding roles for the guardians of the CNS. *Cell*, *158*(1), 15-24.
- Salter, M. W., & Stevens, B. (2017). Microglia emerge as central players in brain disease. *Nature Medicine*, *23*(9), 1018-1027.

- Sampson, T. R., Debelius, J. W., Thron, T., Janssen, S., Shastri, G. G., Ilhan, Z. E., et al. (2016). Gut Microbiota Regulate Motor Deficits and Neuroinflammation in a Model of Parkinson's Disease. *Cell*, *167*(6), 1469-1480.e1412.
- Sanes, J. R., & Lichtman, J. W. (1999). Development of the vertebrate neuromuscular junction. *Annual Review of Neuroscience*, *22*, 389-442.
- Sankowski, R., Böttcher, C., Masuda, T., Geirsdottir, L., Sagar, Sindram, E., et al. (2019). Mapping microglia states in the human brain through the integration of high-dimensional techniques. *Nature Neuroscience*, *22*(12), 2098-2110.
- Sarma, J. V., & Ward, P. A. (2011). The complement system. *Cell and Tissue Research*, *343*(1), 227-235.
- Sasayama, D., Hori, H., Teraishi, T., Hattori, K., Ota, M., Iijima, Y., et al. (2011). Possible association between interleukin-1 β gene and schizophrenia in a Japanese population. *Behavioral and Brain Functions*, *7*, 35.
- Sass, V., Kravitz-Wirtz, N., Karceski, S. M., Hajat, A., Crowder, K., & Takeuchi, D. (2017). The effects of air pollution on individual psychological distress. *Health Place*, *48*, 72-79.
- Schaafsma, W., Basterra, L. B., Jacobs, S., Brouwer, N., Meerlo, P., Schaafsma, A., et al. (2017). Maternal inflammation induces immune activation of fetal microglia and leads to disrupted microglia immune responses, behavior, and learning performance in adulthood. *Neurobiology of Disease*, *106*, 291-300.
- Schafer, D. P., Lehrman, E. K., Kautzman, A. G., Koyama, R., Mardinly, A. R., Yamasaki, R., et al. (2012). Microglia sculpt postnatal neural circuits in an activity and complement-dependent manner. *Neuron*, *74*(4), 691-705.
- Schafer, D. P., & Stevens, B. (2015). Microglia Function in Central Nervous System Development and Plasticity. *Cold Spring Harbor Perspectives in Biology*, *7*(10), a020545.
- Schifani, C., Tseng, H. H., Kenk, M., Tagore, A., Kiang, M., Wilson, A. A., et al. (2018). Cortical stress regulation is disrupted in schizophrenia but not in clinical high risk for psychosis. *Brain*, *141*(7), 2213-2224.
- Schizophrenia Working Group of the Psychiatric Genomics Consortium. (2014). Biological insights from 108 schizophrenia-associated genetic loci. *Nature*, *511*(7510), 421-427.

- Schwartzter, J. J., Careaga, M., Onore, C. E., Rushakoff, J. A., Berman, R. F., & Ashwood, P. (2013). Maternal immune activation and strain specific interactions in the development of autism-like behaviors in mice. *Translational Psychiatry*, 3, e240.
- Schwarz, E., Maukonen, J., Hyytiäinen, T., Kieseppä, T., Orešič, M., Sabunciyan, S., et al. (2018). Analysis of microbiota in first episode psychosis identifies preliminary associations with symptom severity and treatment response. *Schizophrenia Research*, 192, 398-403.
- Sekar, A., Bialas, A. R., de Rivera, H., Davis, A., Hammond, T. R., Kamitaki, N., et al. (2016). Schizophrenia risk from complex variation of complement component 4. *Nature*, 530(7589), 177-183.
- Selemon LD, Goldman-Rakic PS. (1999). The reduced neuropil hypothesis: a circuit based model of schizophrenia. *Biological Psychiatry*. 45(1), 17-25.
- Sellgren, C. M., Gracias, J., Watmuff, B., Biag, J. D., Thanos, J. M., Whittredge, P. B., et al. (2019). Increased synapse elimination by microglia in schizophrenia patient-derived models of synaptic pruning. *Nature Neuroscience*, 22(3), 374-385.
- Selvaraj, S., Bloomfield, P. S., Cao, B., Veronese, M., Turkheimer, F., & Howes, O. D. (2018). Brain TSPO imaging and gray matter volume in schizophrenia patients and in people at ultra high risk of psychosis: An [11C]PBR28 study. *Schizophrenia Research*, 195, 206-214.
- Senatorov, V. V., Friedman, A. R., Milikovsky, D. Z., Ofer, J., Saar-Ashkenazy, R., Charbash, A., et al. (2019). Blood-brain barrier dysfunction in aging induces hyperactivation of TGF β signaling and chronic yet reversible neural dysfunction. *Science Translational Medicine*, 11(521).
- Servick, K. (2018). U.S. labs clamor for marmosets. *Science*, 362(6413), 383-384.
- Shen, Y., Li, R., McGeer, E. G., & McGeer, P. L. (1997). Neuronal expression of mRNAs for complement proteins of the classical pathway in Alzheimer brain. *Brain Research*, 769(2), 391-395.
- Sheng, M., & Ertürk, A. (2014). Long-term depression: a cell biological view. *Philosophical Transactions of the Royal Society B: Biological Sciences*, 369(1633), 20130138.
- Sherwin, E., Bordenstein, S. R., Quinn, J. L., Dinan, T. G., & Cryan, J. F. (2019). Microbiota and the social brain. *Science*, 366(6465).

- Shi, J., Levinson, D. F., Duan, J., Sanders, A. R., Zheng, Y., Pe'er, I., et al. (2009). Common variants on chromosome 6p22.1 are associated with schizophrenia. *Nature*, 460(7256), 753-757.
- Shi, Q., Chowdhury, S., Ma, R., Le, K. X., Hong, S., Caldarone, B. J., et al. (2017). Complement C3 deficiency protects against neurodegeneration in aged plaque-rich APP/PS1 mice. *Science Translational Medicine*, 9(392).
- Shigemoto-Mogami, Y., Hoshikawa, K., & Sato, K. (2018). Activated Microglia Disrupt the Blood-Brain Barrier and Induce Chemokines and Cytokines in a Rat. *Frontiers in Cellular Neuroscience*, 12, 494.
- Shin Yim, Y., Park, A., Berrios, J., Lafourcade, M., Pascual, L. M., Soares, N., et al. (2017). Reversing behavioural abnormalities in mice exposed to maternal inflammation. *Nature*, 549(7673), 482-487.
- Sierra, A., Gottfried-Blackmore, A., Milner, T. A., McEwen, B. S., & Bulloch, K. (2008). Steroid hormone receptor expression and function in microglia. *Glia*, 56(6), 659-674.
- Sigurdsson, T. (2016). Neural circuit dysfunction in schizophrenia: Insights from animal models. *Neuroscience*, 321, 42-65.
- Sigurdsson, T., & Duvarci, S. (2015). Hippocampal-Prefrontal Interactions in Cognition, Behavior and Psychiatric Disease. *Frontiers in Systems Neuroscience*, 9, 190.
- Sigurdsson T, Stark KL, Karayiorgou M, Gogos JA, Gordon JA. (2010). Impaired hippocampal-prefrontal synchrony in a genetic mouse model of schizophrenia. *Nature*. 464(7289), 763-7.
- Simões, L. R., Sangiogo, G., Tashiro, M. H., Generoso, J. S., Faller, C. J., Domingui, D., et al. (2018). Maternal immune activation induced by lipopolysaccharide triggers immune response in pregnant mother and fetus, and induces behavioral impairment in adult rats. *Journal of Psychiatric Research*, 100, 71-83.
- Sinclair, D., Webster, M. J., Fullerton, J. M., & Weickert, C. S. (2012). Glucocorticoid receptor mRNA and protein isoform alterations in the orbitofrontal cortex in schizophrenia and bipolar disorder. *BMC Psychiatry*, 12, 84.
- Singh, V., Roth, S., Llovera, G., Sadler, R., Garzetti, D., Stecher, B., et al. (2016). Microbiota Dysbiosis Controls the Neuroinflammatory Response after Stroke. *Journal of Neuroscience*, 36(28), 7428-7440.

- Sjöström, P. J., & Häusser, M. (2006). A cooperative switch determines the sign of synaptic plasticity in distal dendrites of neocortical pyramidal neurons. *Neuron*, *51*(2), 227-238.
- Sneeboer, M. A. M., van der Doef, T., Litjens, M., Psy, N. B. B., Melief, J., Hol, E. M., et al. (2020). Microglial activation in schizophrenia: Is translocator 18 kDa protein (TSPO) the right marker? *Schizophrenia Research*, *215*, 167-172.
- Sofroniew, N. J., Flickinger, D., King, J., & Svoboda, K. (2016). A large field of view two-photon mesoscope with subcellular resolution for in vivo imaging. *Elife*, *5*.
- Solaimani, P., Saffari, A., Sioutas, C., Bondy, S. C., & Campbell, A. (2017). Exposure to ambient ultrafine particulate matter alters the expression of genes in primary human neurons. *Neurotoxicology*, *58*, 50-57.
- Soma, M., Aizawa, H., Ito, Y., Maekawa, M., Osumi, N., Nakahira, E., et al. (2009). Development of the mouse amygdala as revealed by enhanced green fluorescent protein gene transfer by means of in utero electroporation. *Journal of Comparative Neurology*, *513*(1), 113-128.
- Sommer, I. E., van Westrhenen, R., Begemann, M. J., de Witte, L. D., Leucht, S., & Kahn, R. S. (2014). Efficacy of anti-inflammatory agents to improve symptoms in patients with schizophrenia: an update. *Schizophrenia Bulletin*, *40*(1), 181-191.
- St Clair, D., Blackwood, D., Muir, W., Carothers, A., Walker, M., Spowart, G., et al. (1990). Association within a family of a balanced autosomal translocation with major mental illness. *Lancet*, *336*(8706), 13-16.
- Stankiewicz, A. M., Goscik, J., Majewska, A., Swiergiel, A. H., & Juszczak, G. R. (2015). The Effect of Acute and Chronic Social Stress on the Hippocampal Transcriptome in Mice. *PLoS One*, *10*(11), e0142195.
- Steen RG, Mull C, McClure R, Hamer RM, Lieberman JA. (2006). Brain volume in first-episode schizophrenia: systematic review and meta-analysis of magnetic resonance imaging studies. *The British Journal of Psychiatry*. *188*, 510-8.
- Stephan, A. H., Madison, D. V., Mateos, J. M., Fraser, D. A., Lovelett, E. A., Coutellier, L., et al. (2013). A dramatic increase of C1q protein in the CNS during normal aging. *Journal of Neuroscience*, *33*(33), 13460-13474.
- Stefansson, H., Ophoff, R. A., Steinberg, S., Andreassen, O. A., Cichon, S., Rujescu, D., et al. (2009). Common variants conferring risk of schizophrenia. *Nature*, *460*(7256), 744-747.

- Steiner, J., Bogerts, B., Sarnyai, Z., Walter, M., Gos, T., Bernstein, H. G., et al. (2012). Bridging the gap between the immune and glutamate hypotheses of schizophrenia and major depression: Potential role of glial NMDA receptor modulators and impaired blood-brain barrier integrity. *The World Journal of Biological Psychiatry*, *13*(7), 482-492.
- Steiner, J., Frodl, T., Schiltz, K., Dobrowolny, H., Jacobs, R., Fernandes, B. S., et al. (2020). Innate Immunity Cells and C-Reactive Protein in Acute First-Episode Psychosis and Schizophrenia: Relationship to Psychopathology and Treatment. *Schizophrenia Bulletin*, *46*(2), 363-373.
- Stephan, A. H., Barres, B. A., & Stevens, B. (2012). The complement system: an unexpected role in synaptic pruning during development and disease. *Annual Review of Neuroscience*, *35*, 369-389.
- Stephens, C. L., & Henkart, P. A. (1979). Electrical measurements of complement-mediated membrane damage in cultured nerve and muscle cells. *Journal of Immunology*, *122*(2), 455-458.
- Stevens, B., Allen, N. J., Vazquez, L. E., Howell, G. R., Christopherson, K. S., Nouri, N., et al. (2007). The classical complement cascade mediates CNS synapse elimination. *Cell*, *131*(6), 1164-1178.
- Stevens, R. D., & Puybasset, L. (2011). The brain-lung-brain axis. *Intensive Care Medicine*, *37*(7), 1054-1056.
- Strandwitz, P. (2018). Neurotransmitter modulation by the gut microbiota. *Brain Research*, *1693*(Pt B), 128-133.
- Stratoulas, V., Venero, J. L., Tremblay, M., & Joseph, B. (2019). Microglial subtypes: diversity within the microglial community. *EMBO Journal*, *38*(17), e101997.
- Strecker, J., Ladha, A., Gardner, Z., Schmid-Burgk, J. L., Makarova, K. S., Koonin, E. V., et al. (2019). RNA-guided DNA insertion with CRISPR-associated transposases. *Science*, *365*(6448), 48-53.
- Sudo, N., Chida, Y., Aiba, Y., Sonoda, J., Oyama, N., Yu, X. N., et al. (2004). Postnatal microbial colonization programs the hypothalamic-pituitary-adrenal system for stress response in mice. *The Journal of Physiology*, *558*(Pt 1), 263-275.
- Supekar, K., Uddin, L. Q., Khouzam, A., Phillips, J., Gaillard, W. D., Kenworthy, L. E., et al. (2013). Brain hyperconnectivity in children with autism and its links to social deficits. *Cell Reports*, *5*(3), 738-747.

- Swanwick, C. C., Murthy, N. R., Mchedlishvili, Z., Sieghart, W., & Kapur, J. (2006). Development of gamma-aminobutyric acidergic synapses in cultured hippocampal neurons. *Journal of Comparative Neurology*, *495*(5), 497-510.
- Szczurkowska, J., Cwetsch, A. W., dal Maschio, M., Ghezzi, D., Ratto, G. M., & Cancedda, L. (2016). Targeted in vivo genetic manipulation of the mouse or rat brain by in utero electroporation with a triple-electrode probe. *Nature Protocols*, *11*(3), 399-412.
- Sørensen, H. J., Mortensen, E. L., Reinisch, J. M., & Mednick, S. A. (2009). Association between prenatal exposure to bacterial infection and risk of schizophrenia. *Schizophrenia Bulletin*, *35*(3), 631-637.
- Tan, Y. L., Yuan, Y., & Tian, L. (2020). Microglial regional heterogeneity and its role in the brain. *Molecular Psychiatry*, *25*(2), 351-367.
- Tang, A. T., Choi, J. P., Kotzin, J. J., Yang, Y., Hong, C. C., Hobson, N., et al. (2017). Endothelial TLR4 and the microbiome drive cerebral cavernous malformations. *Nature*, *545*(7654), 305-310.
- Tas, C., Brown, E. C., Eskikurt, G., Irmak, S., Aydın, O., Esen-Danaci, A., et al. (2018). Cortisol response to stress in schizophrenia: Associations with oxytocin, social support and social functioning. *Psychiatry Research*, *270*, 1047-1052.
- Tay, T. L., Mai, D., Dautzenberg, J., Fernández-Klett, F., Lin, G., Sagar, et al. (2017). A new fate mapping system reveals context-dependent random or clonal expansion of microglia. *Nature Neuroscience*, *20*(6), 793-803.
- Tay, T. L., Savage, J. C., Hui, C. W., Bisht, K., & Tremblay, M. (2017). Microglia across the lifespan: from origin to function in brain development, plasticity and cognition. *The Journal of Physiology*, *595*(6), 1929-1945.
- Taylor, S. F., Kang, J., Brege, I. S., Tso, I. F., Hosanagar, A., & Johnson, T. D. (2012). Meta-analysis of functional neuroimaging studies of emotion perception and experience in schizophrenia. *Biological Psychiatry*, *71*(2), 136-145.
- Thion, M. S., Low, D., Silvin, A., Chen, J., Grisel, P., Schulte-Schrepping, J., et al. (2018). Microbiome Influences Prenatal and Adult Microglia in a Sex-Specific Manner. *Cell*, *172*(3), 500-516.e516.
- Thion, M. S., Mosser, C. A., Férézou, I., Grisel, P., Baptista, S., Low, D., et al. (2019). Biphasic Impact of Prenatal Inflammation and Macrophage Depletion on the Wiring of Neocortical Inhibitory Circuits. *Cell Reports*, *28*(5), 1119-1126.e1114.

- Thune JJ, Uylings HB, Pakkenberg B. (2001). No deficit in total number of neurons in the prefrontal cortex in schizophrenics. *Journal of Psychiatric Research*, 35(1), 15-21.
- Thompson, P. M., Vidal, C., Giedd, J. N., Gochman, P., Blumenthal, J., Nicolson, R., et al. (2001). Mapping adolescent brain change reveals dynamic wave of accelerated gray matter loss in very early-onset schizophrenia. *Proceedings of the National Academy of Sciences of the United States of America*, 98(20), 11650-11655.
- Tillberg, P. W., Chen, F., Piatkevich, K. D., Zhao, Y., Yu, C. C., English, B. P., et al. (2016). Protein-retention expansion microscopy of cells and tissues labeled using standard fluorescent proteins and antibodies. *Nature Biotechnology*, 34(9), 987-992.
- Trachtenberg, J. T., Chen, B. E., Knott, G. W., Feng, G., Sanes, J. R., Welker, E., et al. (2002). Long-term in vivo imaging of experience-dependent synaptic plasticity in adult cortex. *Nature*, 420(6917), 788-794.
- Tremblay, M., Lowery, R. L., & Majewska, A. K. (2010). Microglial interactions with synapses are modulated by visual experience. *PLoS Biology*, 8(11), e1000527.
- Trépanier, M. O., Hopperton, K. E., Mizrahi, R., Mechawar, N., & Bazinet, R. P. (2016). Postmortem evidence of cerebral inflammation in schizophrenia: a systematic review. *Molecular Psychiatry*, 21(8), 1009-1026.
- Trossbach, S. V., Hecher, L., Schafflick, D., Deenen, R., Popa, O., Lautwein, T., et al. (2019). Dysregulation of a specific immune-related network of genes biologically defines a subset of schizophrenia. *Translational Psychiatry*, 9(1), 156.
- Trépanier, M. O., Hopperton, K. E., Mizrahi, R., Mechawar, N., & Bazinet, R. P. (2016). Postmortem evidence of cerebral inflammation in schizophrenia: a systematic review. *Molecular Psychiatry*, 21(8), 1009-1026.
- Uhlhaas, P. J. (2013). Dysconnectivity, large-scale networks and neuronal dynamics in schizophrenia. *Current Opinions in Neurobiology*, 23(2), 283-290.
- Uno, Y., & Coyle, J. T. (2019). Glutamate hypothesis in schizophrenia. *Psychiatry and Clinical Neurosciences*, 73(5), 204-215.
- Uranova, N. A., Vikhрева, O. V., Rakhmanova, V. I., & Orlovskaya, D. D. (2018). Ultrastructural pathology of oligodendrocytes adjacent to microglia in prefrontal white matter in schizophrenia. *NPJ Schizophrenia*, 4(1), 26.

- Uranova, N. A., Vikhрева, O. V., Rakhmanova, V. I., & Orlovskaya, D. D. (2020). Dystrophy of Oligodendrocytes and Adjacent Microglia in Prefrontal Gray Matter in Schizophrenia. *Frontiers in Psychiatry*, 11, 204.
- Uranova, N. A., Zimina, I. S., Vikhрева, O. V., Krukov, N. O., Rachmanova, V. I., & Orlovskaya, D. D. (2010). Ultrastructural damage of capillaries in the neocortex in schizophrenia. *The World Journal of Biological Psychiatry*, 11(3), 567-578.
- Vainchtein, I. D., Chin, G., Cho, F. S., Kelley, K. W., Miller, J. G., Chien, E. C., et al. (2018). Astrocyte-derived interleukin-33 promotes microglial synapse engulfment and neural circuit development. *Science*, 359(6381), 1269-1273.
- van Berckel, B. N., Bossong, M. G., Boellaard, R., Kloet, R., Schuitemaker, A., Caspers, E., et al. (2008). Microglia activation in recent-onset schizophrenia: a quantitative (R)-[11C]PK11195 positron emission tomography study. *Biological Psychiatry*, 64(9), 820-822.
- van Beveren, N. J., Buitendijk, G. H., Swagemakers, S., Krab, L. C., Röder, C., de Haan, L., et al. (2012). Marked reduction of AKT1 expression and deregulation of AKT1-associated pathways in peripheral blood mononuclear cells of schizophrenia patients. *PLoS One*, 7(2), e32618.
- van Kesteren, C. F., Gremmels, H., de Witte, L. D., Hol, E. M., Van Gool, A. R., Falkai, P. G., et al. (2017). Immune involvement in the pathogenesis of schizophrenia: a meta-analysis on postmortem brain studies. *Translational Psychiatry*, 7(3), e1075.
- van Leeuwen, J. M. C., Vink, M., Fernández, G., Hermans, E. J., Joëls, M., Kahn, R. S., et al. (2018). At-risk individuals display altered brain activity following stress. *Neuropsychopharmacology*, 43(9), 1954-1960.
- van Venrooij, J. A., Fluitman, S. B., Lijmer, J. G., Kavelaars, A., Heijnen, C. J., Westenberg, H. G., et al. (2012). Impaired neuroendocrine and immune response to acute stress in medication-naïve patients with a first episode of psychosis. *Schizophrenia Bulletin*, 38(2), 272-279.
- Vancampfort, D., De Hert, M., Knapen, J., Wampers, M., Demunter, H., Deckx, S., et al. (2011). State anxiety, psychological stress and positive well-being responses to yoga and aerobic exercise in people with schizophrenia: a pilot study. *Disability and Rehabilitation*, 33(8), 684-689.
- Vasek, M. J., Garber, C., Dorsey, D., Durrant, D. M., Bollman, B., Soung, A., et al. (2016). A complement-microglial axis drives synapse loss during virus-induced memory impairment. *Nature*, 534(7608), 538-543.

- Veerhuis R, Janssen I, De Groot CJ, Van Muiswinkel FL, Hack CE, Eikelenboom P. (1999). Cytokines associated with amyloid plaques in Alzheimer's disease brain stimulate human glial and neuronal cell cultures to secrete early complement proteins, but not C1-inhibitor. *Experimental Neurology*. 160(1), 289-99.
- Veerhuis, R., Janssen, I., Hoozemans, J. J., De Groot, C. J., Hack, C. E., & Eikelenboom, P. (1998). Complement C1-inhibitor expression in Alzheimer's disease. *Acta Neuropathologica*, 96(3), 287-296.
- Veerhuis, R., Nielsen, H. M., & Tenner, A. J. (2011). Complement in the brain. *Molecular Immunology*, 48(14), 1592-1603.
- Velthorst, E., Fett, A. J., Reichenberg, A., Perlman, G., van Os, J., Bromet, E. J., et al. (2017). The 20-year longitudinal trajectories of social functioning in individuals with psychotic disorders. *American Journal of Psychiatry*, 174(11), 1075-1085.
- Volk DW, Lewis DA. (2010). Prefrontal cortical circuits in schizophrenia. *Current Topics in Behavioral Neuroscience*. 4, 485- 508 (2010).
- Vinolo, M. A., Rodrigues, H. G., Nachbar, R. T., & Curi, R. (2011). Regulation of inflammation by short chain fatty acids. *Nutrients*, 3(10), 858-876.
- Vita, A., De Peri, L., Deste, G., & Sacchetti, E. (2012). Progressive loss of cortical gray matter in schizophrenia: a meta-analysis and meta-regression of longitudinal MRI studies. *Translational Psychiatry*, 2, e190.
- Wake, H., Moorhouse, A. J., Jinno, S., Kohsaka, S., & Nabekura, J. (2009). Resting microglia directly monitor the functional state of synapses in vivo and determine the fate of ischemic terminals. *Journal of Neuroscience*, 29(13), 3974-3980.
- Walder, D. J., Walker, E. F., & Lewine, R. J. (2000). Cognitive functioning, cortisol release, and symptom severity in patients with schizophrenia. *Biological Psychiatry*, 48(12), 1121-1132.
- Walker DG, Kim SU, McGeer PL. (1995). Complement and cytokine gene expression in cultured microglial derived from postmortem human brains. *Journal of Neuroscience Research*. 40(4), 478-93.
- Wang, H. T., Huang, F. L., Hu, Z. L., Zhang, W. J., Qiao, X. Q., Huang, Y. Q., et al. (2017). Early-Life Social Isolation-Induced Depressive-Like Behavior in Rats Results in Microglial Activation and Neuronal Histone Methylation that Are Mitigated by Minocycline. *Neurotoxicity Research*, 31(4), 505-520.

- Wang, Y. L., Han, Q. Q., Gong, W. Q., Pan, D. H., Wang, L. Z., Hu, W., et al. (2018). Microglial activation mediates chronic mild stress-induced depressive- and anxiety-like behavior in adult rats. *Journal of Neuroinflammation*, *15*(1), 21.
- Wassie, A. T., Zhao, Y., & Boyden, E. S. (2019). Expansion microscopy: principles and uses in biological research. *Nature Methods*, *16*(1), 33-41.
- Webster, M. J., Knable, M. B., O'Grady, J., Orthmann, J., & Weickert, C. S. (2002). Regional specificity of brain glucocorticoid receptor mRNA alterations in subjects with schizophrenia and mood disorders. *Molecular Psychiatry*, *7*(9), 985-994, 924.
- Weickert, C. S., Fung, S. J., Catts, V. S., Schofield, P. R., Allen, K. M., Moore, L. T., et al. (2013). Molecular evidence of N-methyl-D-aspartate receptor hypofunction in schizophrenia. *Molecular Psychiatry*, *18*(11), 1185-1192.
- Weinberger, J. F., Raison, C. L., Rye, D. B., Montague, A. R., Woolwine, B. J., Felger, J. C., et al. (2015). Inhibition of tumor necrosis factor improves sleep continuity in patients with treatment resistant depression and high inflammation. *Brain, Behavior, and Immunity*, *47*, 193-200.
- Weinhard, L., di Bartolomei, G., Bolasco, G., Machado, P., Schieber, N. L., Neniskyte, U., et al. (2018). Microglia remodel synapses by presynaptic trogocytosis and spine head filopodia induction. *Nature Communications*, *9*(1), 1228.
- Weinstock, M. (2008a). The long-term behavioural consequences of prenatal stress. *Neuroscience & Biobehavioral Reviews*, *32*(6), 1073-1086.
- Welsh, C. A., Stephany, C., Sapp, R. W., & Stevens, B. (2020). Ocular Dominance Plasticity in Binocular Primary Visual Cortex Does Not Require C1q. *Journal of Neuroscience*, *40*(4), 769-783.
- Whiteford, H. A., Degenhardt, L., Rehm, J., Baxter, A. J., Ferrari, A. J., Erskine, H. E., et al. (2013). Global burden of disease attributable to mental and substance use disorders: findings from the Global Burden of Disease Study 2010. *Lancet*, *382*(9904), 1575-1586.
- Williams, M. E., de Wit, J., & Ghosh, A. (2010). Molecular mechanisms of synaptic specificity in developing neural circuits. *Neuron*, *68*(1), 9-18.
- Wolkin, A., Sanfilippo, M., Wolf, A. P., Angrist, B., Brodie, J. D., & Rotrosen, J. (1992). Negative symptoms and hypofrontality in chronic schizophrenia. *Archives of General Psychiatry*, *49*(12), 959-965.

- Woodruff TM, Ager RR, Tenner AJ, Noakes PG, Taylor SM. (2010). The role of the complement system and the activation fragment C5a in the central nervous system. *Neuromolecular Medicine*, 12(2), 179-92.
- Woodward, N., Finch, C. E., & Morgan, T. E. (2015). Traffic-related air pollution and brain development. *AIMS Environmental Science*, 2(2), 353-373.
- Woodward, N. C., Haghani, A., Johnson, R. G., Hsu, T. M., Saffari, A., Sioutas, C., et al. (2018). Prenatal and early life exposure to air pollution induced hippocampal vascular leakage and impaired neurogenesis in association with behavioral deficits. *Translational Psychiatry*, 8(1), 261.
- Woodward, N. C., Levine, M. C., Haghani, A., Shirmohammadi, F., Saffari, A., Sioutas, C., et al. (2017). Toll-like receptor 4 in glial inflammatory responses to air pollution in vitro and in vivo. *Journal of Neuroinflammation*, 14(1), 84.
- Wright, P., Nimgaonkar, V. L., Donaldson, P. T., & Murray, R. M. (2001). Schizophrenia and HLA: a review. *Schizophrenia Research*, 47(1), 1-12.
- Wu, T., Dejanovic, B., Gandham, V. D., Gogineni, A., Edmonds, R., Schauer, S., et al. (2019). Complement C3 Is Activated in Human AD Brain and Is Required for Neurodegeneration in Mouse Models of Amyloidosis and Tauopathy. *Cell Reports*, 28(8), 2111-2123.e2116.
- Wu, W. L., Hsiao, E. Y., Yan, Z., Mazmanian, S. K., & Patterson, P. H. (2017). The placental interleukin-6 signaling controls fetal brain development and behavior. *Brain, Behavior, and Immunity*, 62, 11-23.
- Wu, Y., Dissing-Olesen, L., MacVicar, B. A., & Stevens, B. (2015). Microglia: Dynamic Mediators of Synapse Development and Plasticity. *Trends in Immunology*, 36(10), 605-613.
- Wu, Z., Yang, H., & Colosi, P. (2010). Effect of genome size on AAV vector packaging. *Mol Ther*, 18(1), 80-86.
- Xuan, J., Pan, G., Qiu, Y., Yang, L., Su, M., Liu, Y., et al. (2011). Metabolomic profiling to identify potential serum biomarkers for schizophrenia and risperidone action. *Journal of Proteome Research*, 10(12), 5433-5443.
- Yang I, Han SJ, Kaur G, Crane C, Parsa AT. (2010). The role of microglia in central nervous system immunity and glioma immunology. *Journal of Clinical Neuroscience*. 17(1), 6-10.

- Yang, Y., Wang, L., Li, L., Li, W., Zhang, Y., Chang, H., et al. (2018). Genetic association and meta-analysis of a schizophrenia GWAS variant rs10489202 in East Asian populations. *Translational Psychiatry*, 8(1), 144.
- Yano, J. M., Yu, K., Donaldson, G. P., Shastri, G. G., Ann, P., Ma, L., et al. (2015). Indigenous bacteria from the gut microbiota regulate host serotonin biosynthesis. *Cell*, 161(2), 264-276.
- Yenari, M. A., Xu, L., Tang, X. N., Qiao, Y., & Giffard, R. G. (2006). Microglia potentiate damage to blood-brain barrier constituents: improvement by minocycline in vivo and in vitro. *Stroke*, 37(4), 1087-1093.
- Yizhar, O. (2012). Optogenetic insights into social behavior function. *Biological Psychiatry*, 71(12), 1075-1080.
- Yolken, R. H., Severance, E. G., Sabunciyani, S., Gressitt, K. L., Chen, O., Stallings, C., et al. (2015). Metagenomic Sequencing Indicates That the Oropharyngeal Phageome of Individuals With Schizophrenia Differs From That of Controls. *Schizophrenia Bulletin*, 41(5), 1153-1161.
- Yue, N., Huang, H., Zhu, X., Han, Q., Wang, Y., Li, B., et al. (2017). Activation of P2X7 receptor and NLRP3 inflammasome assembly in hippocampal glial cells mediates chronic stress-induced depressive-like behaviors. *Journal of Neuroinflammation*, 14(1), 102.
- Yüksel, R. N., Titiz, A. P., Yaylacı, E. T., Ünal, K., Turhan, T., Erzin, G., et al. (2019). Serum PGE2, 15d-PGJ, PPAR γ and CRP levels in patients with schizophrenia. *Asian J Psychiatr*, 46, 24-28.
- Zabel, M. K., & Kirsch, W. M. (2013). From development to dysfunction: microglia and the complement cascade in CNS homeostasis. *Ageing Research Reviews*, 12(3), 749-756.
- Zeng, H., Xu, C., Fan, J., Tang, Y., Deng, Q., Zhang, W., et al. (2020). Antibodies in Infants Born to Mothers With COVID-19 Pneumonia. *JAMA*, 323(18):1848-1849.
- Zhan, Y., Paolicelli, R. C., Sforzini, F., Weinhard, L., Bolasco, G., Pagani, F., et al. (2014). Deficient neuron-microglia signaling results in impaired functional brain connectivity and social behavior. *Nature Neuroscience*, 17(3), 400-406.
- Zhang, J., Jing, Y., Zhang, H., Bilkey, D. K., & Liu, P. (2018). Maternal immune activation altered microglial immunoreactivity in the brain of postnatal day 2 rat offspring. *Synapse*, e22072.

- Zhang, J. H., Adikaram, P., Pandey, M., Genis, A., & Simonds, W. F. (2016). Optimization of genome editing through CRISPR-Cas9 engineering. *Bioengineered*, 7(3), 166-174.
- Zhang, Y., Catts, V. S., Sheedy, D., McCrossin, T., Kril, J. J., & Shannon Weickert, C. (2016). Cortical grey matter volume reduction in people with schizophrenia is associated with neuro-inflammation. *Translational Psychiatry*, 6(12), e982.
- Zhang XY, Zhou DF, Cao LY, Wu GY, Shen YC. (2005). Cortisol and cytokines in chronic and treatment-resistant patients with schizophrenia: association with psychopathology and response to antipsychotics. *Neuropsychopharmacology*. 30(8), 1532-8.
- Zhao, Q., Wang, Q., Wang, J., Tang, M., Huang, S., Peng, K., et al. (2019). Maternal immune activation-induced PPAR γ -dependent dysfunction of microglia associated with neurogenic impairment and aberrant postnatal behaviors in offspring. *Neurobiology of Disease*, 125, 1-13.
- Zheng, H., Cheng, B., Li, Y., Li, X., Chen, X., & Zhang, Y. W. (2018). TREM2 in Alzheimer's Disease: Microglial Survival and Energy Metabolism. *Frontiers in Aging Neuroscience*, 10, 395.
- Zheng, P., Zeng, B., Liu, M., Chen, J., Pan, J., Han, Y., et al. (2019). The gut microbiome from patients with schizophrenia modulates the glutamate-glutamine-GABA cycle and schizophrenia-relevant behaviors in mice. *Science Advances*, 5(2), eaau8317.
- Zhou, Y., Guo, M., Wang, X., Li, J., Wang, Y., Ye, L., et al. (2013). TLR3 activation efficiency by high or low molecular mass poly I:C. *Innate Immunity*, 19(2), 184-192.
- Zhu, F., Guo, R., Wang, W., Ju, Y., Wang, Q., Ma, Q., et al. (2019). Transplantation of microbiota from drug-free patients with schizophrenia causes schizophrenia-like abnormal behaviors and dysregulated kynurenine metabolism in mice. *Molecular Psychiatry*.
- Ziv, N. E., & Smith, S. J. (1996). Evidence for a role of dendritic filopodia in synaptogenesis and spine formation. *Neuron*, 17(1), 91-102.
- Zoghbi, H. Y., & Bear, M. F. (2012). Synaptic dysfunction in neurodevelopmental disorders associated with autism and intellectual disabilities. *Cold Spring Harbor Perspectives in Biology*, 4(3).

CURRICULUM VITAE

